AWARD NUMBER: W81XWH-14-1-0448

TITLE: Characterizing the Hypermutated Subtype of Advanced Prostate Cancer as a Predictive Biomarker for Precision Medicine

PRINCIPAL INVESTIGATOR: Colin Pritchard

CONTRACTING ORGANIZATION: University of Washington
Seattle, WA 98195-9472

REPORT DATE: October 2016

TYPE OF REPORT: Annual

PREPARED FOR: U.S. Army Medical Research and Materiel Command
Fort Detrick, Maryland 21702-5012

REPORT DOCUMENTATION PAGE

Form Approved
OMB No. 0704-0188

1. REPORT DATE	**2. REPORT TYPE**	**3. DATES COVERED**
October 2016	Annual	15 Sept 2015 - 14 Sept 2016

4. TITLE AND SUBTITLE

Characterizing the Hypermutated Subtype of Advanced Prostate Cancer as a Predictive Biomarker for Precision Medicine

5a. CONTRACT NUMBER

5b. GRANT NUMBER
W81XWH-14-1-0448

5c. PROGRAM ELEMENT NUMBER

6. AUTHOR(S)
Colin Pritchard

E-mail: cpritch@uw.edu

5d. PROJECT NUMBER

5e. TASK NUMBER

5f. WORK UNIT NUMBER

7. PERFORMING ORGANIZATION NAME(S) AND ADDRESS(ES)

University of Washington
4333 Brooklyn Ave NE
Seattle, WA 98195-0001

8. PERFORMING ORGANIZATION REPORT NUMBER

9. SPONSORING / MONITORING AGENCY NAME(S) AND ADDRESS(ES)

U.S. Army Medical Research and Materiel Command
Fort Detrick, Maryland 21702-5012

10. SPONSOR/MONITOR'S ACRONYM(S)

11. SPONSOR/MONITOR'S REPORT NUMBER(S)

12. DISTRIBUTION / AVAILABILITY STATEMENT

Approved for Public Release; Distribution Unlimited

13. SUPPLEMENTARY NOTES

14. ABSTRACT
The goal of this research is to characterize the mechanisms leading to hypermutated prostate cancer and to integrate tumor hypermutation status with clinical decision making and therapy to improve the care of men with advanced prostate cancer. We identified 10/103 patients (10% of men) with hypermutated advanced prostate cancers. Using a targeted deep sequencing assay that includes intronic and flanking regions we discovered DNA mismatch repair (MMR) gene mutations in all hypermutated tumors. Mutations were commonly complex genomic rearrangements in the *MSH2* and *MSH6* mismatch repair genes. There was loss of the corresponding MMR protein expression in tumor tissue and phenotypic microsatellite instability in every hypermutated tumor. Our results support that microsatellite instability resulting from loss of function mutations in DNA mismatch repair genes is the major mechanism leading to hypermutation in prostate cancer. We have developed the mSINGS method to detect phenotype microsatellite instability from next-generation sequencing data. This method accurately classified all hypermutated prostate cancers. We have successfully applied mSINGS to targeted capture assays (and to exome data. We have developed a clinical assay termed MSIplus based on the mSINGS method. We have begun work on PDX models to test responsiveness to specific therapies and have begun to recruit men with prostate cancer in a pilot study to test for MSI and hypermutation. We and others have observed that prostate cancer patients with hypermutated MSI tumors may be responsive to checkpoint blockade immunoterhapy. During the next year we plan to focus work on aim 4, which will involve testing MMR gene mutations using UW-OncoPlex and MSI status using the MSIplus test to identify men with prostate cancer for checkpoint blockage immunotherapy trials.

15. SUBJECT TERMS
Prostate cancer, hypermutation, hyper-mutation, microsatellite instability, MSI, MLH1, MSH2, MSH6, PMS2, metastasis, precision medicine

16. SECURITY CLASSIFICATION OF:			**17. LIMITATION OF ABSTRACT**	**18. NUMBER OF PAGES**	**19a. NAME OF RESPONSIBLE PERSON**
a. REPORT	**b. ABSTRACT**	**c. THIS PAGE**			USAMRMC
U	U	U	UU	121	**19b. TELEPHONE NUMBER** *(include area code)*

Table of Contents

Page

1. INTRODUCTION

The goal of this project is to characterize the mechanisms leading to hypermutated prostate cancer and to integrate tumor hypermutation status with clinical decision making and therapy to improve the care of men with advanced prostate cancer. Using Next-Gen sequencing approaches my colleagues at the University of Washington recently identified a hypermutated phenotype/genotype in 10-20% of advanced prostate cancers. This phenotype was subsequently observed in primary prostate cancer. Prostate cancer hypermutation is a promising target for precision therapy, but the mechanisms leading to hypermutation, optimal methods to measure hypermutation status in the clinic, and clinical implications for prostate cancer patients are not yet understood. Our hypothesis is that hypermutated advanced prostate cancer is caused by defects in genes regulating DNA repair pathways, which can be accurately identified using existing clinical diagnostics, and that hypermutation status can predict responses to therapy.

2. KEYWORDS

Prostate cancer, hypermutation, hyper-mutation, microsatellite instability, MSI, MLH1, MSH2, MSH6, PMS2, metastasis, precision medicine

3. ACCOMPLISHMENTS

Accomplishments in the first and second years for research-specific tasks are reported according to major goals of the project in the approved SOW, and organized by specific aim.

3.1 What were the major goals of the project?

Specific Aim 1: Identify mechanisms that drive the hypermutated phenotype in advanced prostate cancer.	**Months**	**Completed?**
Major Task: Sequence DNA repair pathway genes in advanced prostate cancer tumor samples	**1-12**	**Yes**
Subtask 1: Examine hypermutated and non-hypermutated UW prostate cancer rapid autopsy samples using BROCA and UW-OncoPlex assays	1-6	**Yes**
Subtask 2: Assess for functional loss of DNA repair pathway gene expression by IHC, and MSI PCR	3-12	**Yes**
Milestone(s) Achieved: identification of specific mutated DNA repair pathway genes in hypermutated prostate cancer	12	**Yes**

Specific Aim 2: Determine unique vulnerabilities of hypermutated prostate cancer to therapy in xenograft models.	**Months**	**Completed?**
Major Task: Assess differential responses to chemotherapy and targeted therapy in LuCaP tumor cell lines xenografted in mice	12-36	Partially
Subtask 1: Use xenograft LuCaP hypermutated prostate cancer cells lines 58, 73, and 147 and 3 non-hypermutated control cell lines. Assess xenograft tumor responses to chemotherapy and targeted therapy agents	12-36	Partially
Milestone(s) Achieved: Identification of differential efficacy of targeted therapies in hypermutated prostate cancer	24-36	Partially

Specific Aim 3: Develop and validate a clinical diagnostic approach to determine hypermutation status in advanced prostate cancer.	**Months**	**Completed?**
Major Task: Establish a clinical assay(s) to detect tumor hypermutation	1-24	Yes
Subtask 1: Develop bioinformatics methods to accurately detect hypermutation and microsatellite instability using the UW-OncoPlex assay	1-12	Yes
Subtask 2: Establish the performance characteristics of MSI-PCR and IHC-based approaches to detect hypermutation compared to the UW-OncoPlex genomic sequencing	12-24	Yes
Milestone(s) Achieved: Clinically validated approach to detect the hypermutated subtype of advanced prostate cancer established	24	Yes
Milestone(s) Achieved: Original manuscript on bioinformatics method on detected MSI by next-generation sequencing	12-24	Yes

Specific Aim 4: Implement diagnostic testing for hypermutation status in the UW-OncoPlex program for precision cancer medicine.	**Months**	**Completed?**
Major Task: Clinical trial of UW-OncoPlex testing in advanced prostate cancer that includes assessment of hypermutation status	24-36	Partially
Subtask 1: Establish a clinical trial that includes hypermutation testing by UW-OncoPlex with or without additional MSI-PCR/MSI-IHC tests depending on results of Aim 3	24-36	Yes
Subtask 2: Report hypermutation status results to medical oncologists in prostate cancer precision tumor board meetings and document treatment decisions and short-term outcomes.	24-36	Partially
Milestone(s) Achieved: Hypermutation status is used in clinical decision making for men with advanced prostate cancer with feedback on outcomes	36	Partially
Milestone(s) Achieved: Manuscript describing the clinical role of tumor hypermutation status as a predictive biomarker for advanced prostate cancer	36	Partially

3.12 What was accomplished under these goals?

Specific Aim 1: Identify mechanisms that drive the hypermutated phenotype in advanced prostate cancer

Work on Specific Aim 1 was largely completed in Year 1 and 2 and is summarized below. We published a manuscript in *Nature Communications* based on the work accomplished in Aim 1 (Pritchard et al. *Nat Commun.* 2014 5:4988, see Appendix 1). In Year 2 we completed sequencing of all available patient samples from the UW rapid autopsy cohort.

Specific Aim 1, Subtask 1: *Examine hypermutated and non-hypermutated UW prostate cancer rapid autopsy samples using BROCA and UW-OncoPlex assays*

We hypothesized that mutations in key DNA repair pathway genes lead to the hypermutated subtype of advanced prostate cancer, most likely mutations in DNA mismatch repair genes. To test this hypothesis we performed targeted deep sequencing of DNA repair genes in hypermutated and non-hypermutated advanced prostate cancer samples from two sources: LuCaP xenograft lines and tumors from the UWMC rapid autopsy program. Both tumor sources consisted primarily of castration resistant prostate cancer (CRPC). Using exome sequencing we identified 3 hypermutated patient-derived xenograft (PDX) lines (LuCaP 58, LuCaP 73, and LuCaP 147) and 8 of 91 rapid autopsy patients with hypermutated tumors (05-165, 03-130, 06-134, 00-010, 05-123, 01-002, 04-108, 99-111). There was partial overlap between the PDX and the autopsy cases because some LuCaP lines had been derived from the autopsy patients. There were a total of 10 out of 103 unique patients who had hypermutated tumors, for an overall prevalence of 9.7% in our cohort.

We performed the BROCA targeted DNA capture and massively parallel sequencing assay that assesses single nucleotide variants (SNVs), small insertions and deletions (indels), copy number variants (CNVs), and structural variants (SVs) in DNA repair genes simultaneously. Importantly, the BROCA assay includes capture of complete genes including introns and flanking sequences, which is in contract to exome sequencing which captures exons only. This detail proved to be crucial to our success in this research aim. We sequenced samples to an average of ~800x depth, multiplexing 24 samples per lane on a HiSeq2500. The BROCA assay uses the Agilent SureSelect enrichment system to capture the coding exons and flanking splice sites of genes listed in **Table 1**.

Table 1: BROCA genes (assay version 6)

DNA Repair Pathways	*ATM*	*ATR*	*BAP1*	*BARD1*	*BRCA1*	*BRCA2*	*BRCC3*	*BRIP1*
	CHEK1	*CHEK2*	*FAM175A*	***MLH1***	*MRE11A*	***MSH2***	***MSH6***	*NBN*
	PALB2	***PMS2***	*PRSS1*	*PTEN*	*RAD50*	*RAD51B*	*RAD51C*	*RAD51D*
	RBBP8	*TP53*	*TP53BP1*	*XRCC2*				
Additional Cancer-Related	*AKT1*	*APC*	*BMPR1A*	*CDH1*	*CDK4*	*CDKN2A*	*CTNNA1*	*GALNT12*
	GEN1	*GREM1*	*HOXB13*	*MEN1*	*MUTYH*	*PIK3CA*	***POLD1***	***POLE***
	PPM1D	*RET*	*SDHB*	*SDHC*	*SDHD*	*SMAD4*	*STK11*	*VHL*

To assess within-patient tumor mutation heterogeneity we tested up to 4 different metastatic sites in a subset of patients. For each patient we also tested matched normal (non-tumor) tissue to determine if mutations were inherited or somatic.

All three PDX hypermutated tumors had complex structural rearrangements in *MSH2*, *MSH6* or both genes (**Table 2**), while only 1 of 20 non-hypermutated xenografts had mutations in these genes (LuCaP 145, derived from a patient with neuroendocrine prostate cancer, Supplementary Fig. 4). A second loss-of-function mutation in *MSH2* or *MSH6* was detected in the three hypermutated PDX tumors, but not in LuCaP 145, supporting a requirement for bi-allelic gene inactivation underlying the hypermutated genome.

We performed the BROCA targeted DNA capture and massively parallel sequencing assays that assesses single nucleotide variants (SNVs), small insertions and deletions (indels), copy number variants (CNVs), and structural variants (SVs) in DNA repair genes simultaneously.

All three PDX hypermutated tumors had complex structural rearrangements in *MSH2*, *MSH6* or both genes (**Table 2**), while only 1 of 20 non-hypermutated xenografts had mutations in these genes (LuCaP 145, derived from a patient with neuroendocrine prostate cancer). A second loss-of-function mutation in *MSH2* or *MSH6* was detected in the three hypermutated PDX tumors, but not in LuCaP 145, supporting a requirement for bi-allelic gene inactivation underlying the hypermutated genome.

Table 2: Mismatch Repair (MMR) Gene Mutations Detected in All Hypermutated Prostate Cancers

Patient**	Hypermutated	MSI	MMR Gene Mutation(s)*
05-165 (LuCaP 147)	Yes	Yes	MSH2-C2orf61 inversion, MSH2-KCNK12 inversion
00-010	Yes	Yes	MSH2 frameshift
05-123	Yes	Yes	MSH2 frameshift
03-130	Yes	Yes	MSH2 translocation t(2;18)
06-134	Yes	Yes	MLH1 homozygous copy loss
LuCaP 58	Yes	Yes	MSH6 del exon 8 to 3'UTR, MSH6 frameshift
LuCaP 73	Yes	Yes	MSH6 3Mb inversion + frameshift, MSH2 440kb inversion
01-002	Yes	Yes	MSH2 exon 1-8 del (germline with LOH)
04-108	Yes	Yes	MSH2 rearrangement
99-111	Yes	Yes	MSH2 exon 1-8 del (no matched germline)

*Mosaic *MSH6* frameshift mutations observed in a poly G tract in exon 5 (c.3261dup/del) and poly A tract in exon 7 (c.3573del) were detected in several hypermutated samples and are not included in the table because they are presumed to be due to MSI.
**LuCaP 147 is derived from patient 05-165

We detected mutations with predicted loss-of-function in *MSH2*, *MSH6*, or both genes in 7 of 8 rapid autopsy patients with hypermutated tumors. Mutations included complex structural

rearrangements, copy losses, and frameshift mutations (**Table 2**). One hypermutated patient had mutations in the MMR gene *MLH1*. In all patients where multiple sites were tested hypermutation status and MMR mutations were concordant at different metastatic sites tested in the same patient. MMR mutations were somatic except for patient 01-002, who had a germline *MSH2* deletion and Lynch syndrome.

.

A) *MSH2* Structural Rearrangement in Hypermutated Autopsy Tumor 05-165 and LuCaP 147

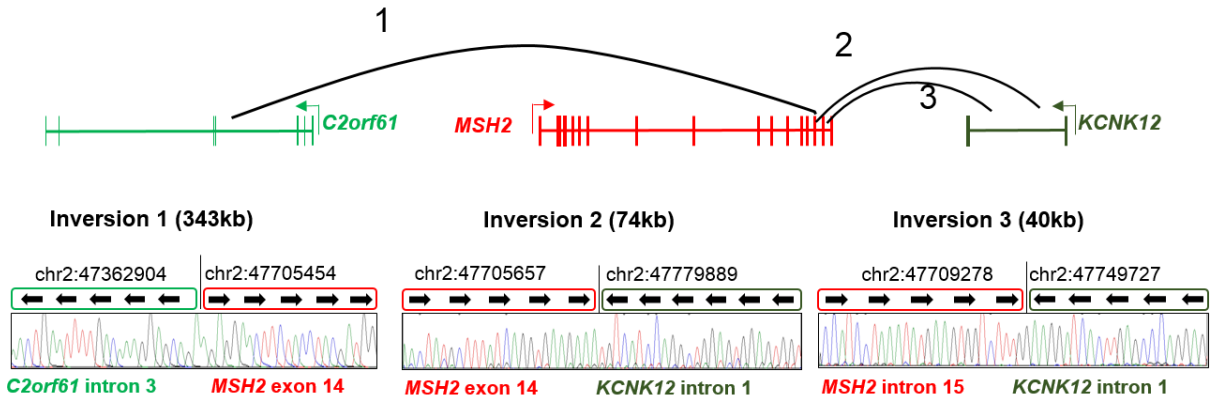

B) *MSH2* Structural Rearrangement in Hypermutated Autopsy Tumor 03-130

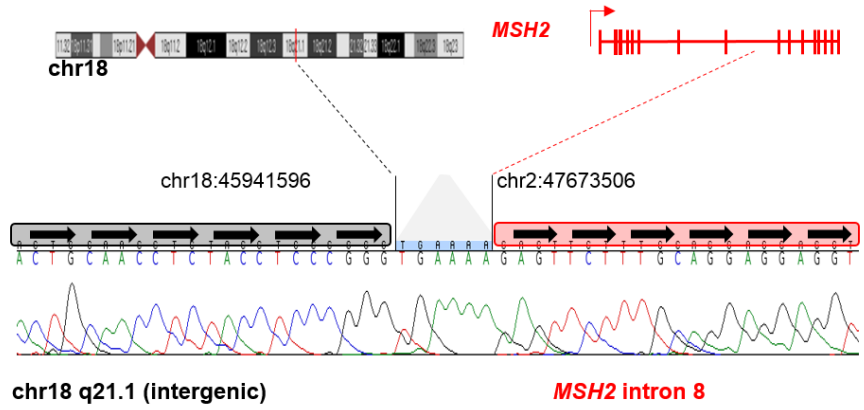

Figure 1: Examples of complex *MSH2* structural rearrangement detected in hypermutated prostate tumors. A) In autopsy sample 05-165 and patient-derived xenograft LuCaP 147 is a representative complex *MSH2* rearrangement (LuCaP 147 was derived from autopsy patient 05-165). B) *MSH2* structural rearrangement in hypermutated autopsy tumor 03-130. Breakpoints were confirmed by Sanger sequencing. Genomic coordinates are build hg19. A total of 4 or 7 hypermutated cases had complex rearrangements in *MSH2* and *MSH6* or both genes.

To cross-validate mutation calling for our UW-OncoPlex targeted sequencing platform that is the focus of clinical sequencing work for precision medicine we tested one hypermutated rapid autopsy prostate cancer case (00-010) and two non-hypermutated autopsy cases (00-029 and 00-090) using UW-OncoPlex. We also tested one LuCaP line (LuCaP 23.1). Among the genes that overlap the two panels there was 100% concordance of somatic coding mutation calls that were present at >5% variant allele fraction between the two platforms.

Specific Aim 1, Subtask 2: *Assess for functional loss of DNA repair pathway gene expression by IHC, and MSI PCR*

MSH2 and *MSH6* are mismatch DNA repair genes that act together as a heterodimer, and bi-allelic inactivating mutations of either gene are predicted to result in microsatellite instability (MSI). PCR of microsatellite loci revealed MSI in all hypermutated tumors, from both PDX and autopsy patients (**Figure 2**, **Table 2**). IHC for DNA mismatch repair proteins in hypermutated tumors demonstrated complete loss of MSH2 and/or MSH6 in a pattern consistent with the inactivating mutations detected by sequencing (**Figure 3**). Non-hypermutated tumors were microsatellite stable and had intact MSH2 and MSH6 protein.

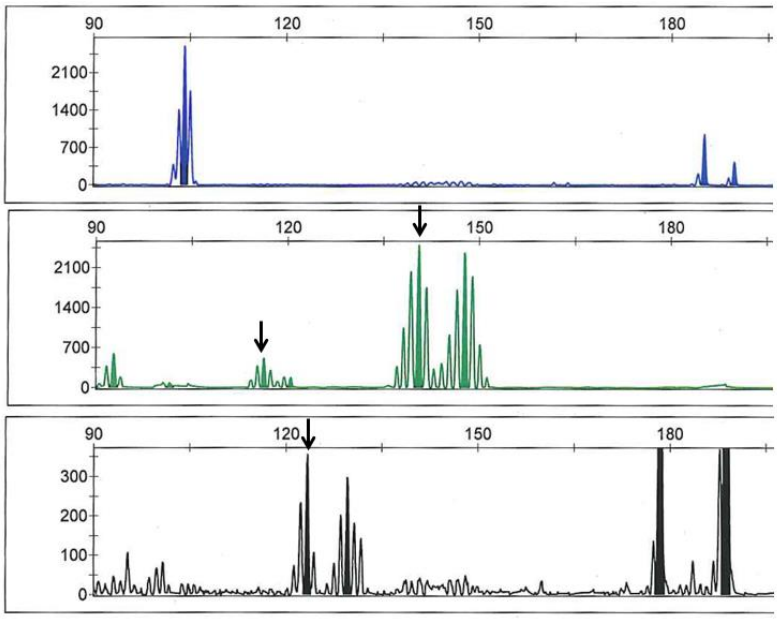

Figure 2: Hypermutated tumors are MSI-High. Hypermutated tumors exhibited microsatellite instability by PCR. Shown is representative data for LuCaP 58 which is positive for MSI in 3/5 mononucleotide marker systems (BAT25, MONO27, NR26, arrows). All hypermutated tumors were MSI-PCR positive in at least 2/5 loci.

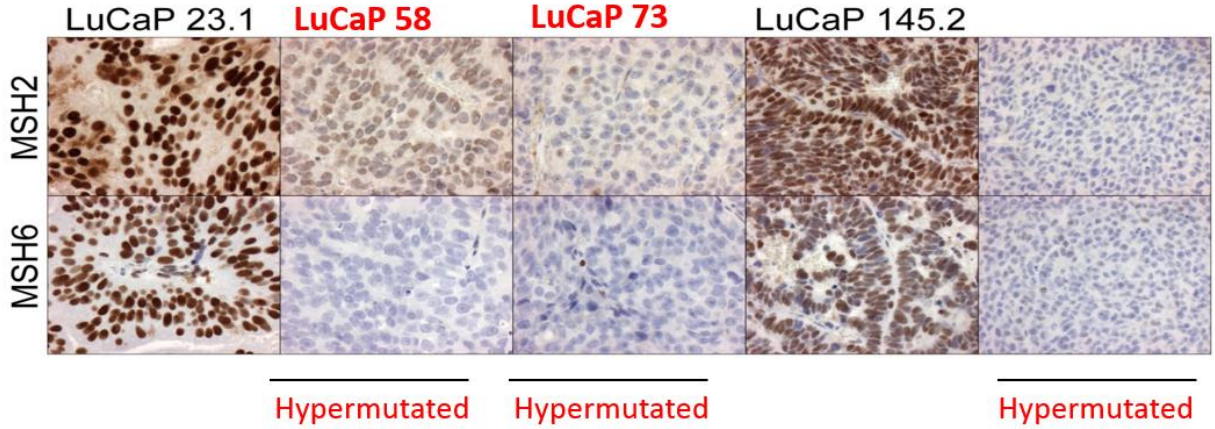

Figure 3: Hypermutated have loss of MSH2 and MSH6 protein by IHC. Similar results were observed in hypermutated tumors from rapid autopsy patients (see Appendix 1).

The findings support the conclusion that the hypermutated subtype of prostate cancer is chiefly due to loss-of-function mutations in *MSH2* and *MSH6* that result in MSI. Most interestingly, 6 of 10 hypermutated cases had complex structural rearrangements in *MSH2* and *MSH6* that were not detected by exome sequencing in the same samples, and would also not be expected to be detected by traditional exon-based Sanger sequencing methods. Previous studies have reported MMR protein loss and MSI in both primary and advanced prostate cancers, but very few MMR mutations have been identified. We speculate that technical limitations have led to an underestimation of MMR gene mutations in prostate cancer.

Specific Aim 2: Determine unique vulnerabilities of hypermutated prostate cancer to therapy in xenograft models.

Aim 2, Subtask 1: *Use xenograft LuCaP hypermutated prostate cancer cells lines 58, 73, and 147 and 3 non-hypermutated control cell lines. Assess xenograft tumor responses to chemotherapy and targeted therapy agents*

Work on aim 2 has been started in year 2 and will be completed in year 3. Note that no funding for animal studies is provided by this award. The goal of this aim is to carry out a pilot study using patient-derived xenograft (PDX) preclinical models as 'tumor avatars' to test anti-cancer therapies in comparison to responses in non-hypermutated LuCaP xenograft lines. We are assessing responses to currently used and approved chemotherapeutics including docetaxel, carboplatin and 5-fluorouricil, to determine if the hypermutated subtype is more or less susceptible to drugs that can be immediately used in clinical practice. We have identified 3 hypermutated PDX lines (LuCaP 58, 73, and 147) that we are using to assess selective responses of these therapies, in collaboration with Drs. Colm Morrissey, Robert Vessella, and Eva Corey at the University of Washington GU Cancer Research Laboratory.

For hypermutated PDX tumor LuCaP 147 we obtained 4 different metastatic sites from the patient from whom the xenograft line was derived and found that the same complex *MSH2* structural rearrangements were present in all metastatic sites in the pre-xenografted tumors, demonstrating that the MMR gene structural rearrangements are not an artifact of xenografting.

In collaboration with Drs. Corey, Vessella, Morrissey, and Nelson, we evaluated the efficacy of docetaxel, carboplatin, and 5-FU in hypermutated LuCaP xenografts (LuCaP 58, 73 and 147) and non–hypermutated LuCaP xenografts (LuCaP 70, 96CR, 141, 70, 35, and 35CR). LuCaP tumors were subcutaneously implanted into SCID male mice. When tumor exceeded 100mm^3, animals were randomized and enrolled into following groups: 1) Docetaxel treatment at 10 mg/kg, 2) Docetaxel treatment at 20 mg/kg, 3) Carboplatin at 50 mg/kg twice weekly, 4) 5-FU at 50mg/kg qweek, 5) Vehicle controls/no treatment animals, and 6) Castration animals. Tumor volumes and body weight were measured once weekly.

Treatment responses for the two different docetaxel dosages (10 mg/kg and 20 mg/kg) varied across the hypermutated and non-hypermutated tumor models. For hypermutated models, 10 mg/kg treatment responses ranged from major tumor growth inhibition in LuCaP 58 to mostly unimpeded tumor progression in LuCaP 147. At 20 mg/kg, LuCaP 73 exhibited maximal

responsiveness as opposed to LuCaP 58 and 147 (**Figure 4**). We also assessed single animal response to docetaxel (20 mg/kg) within the hypermutated LuCaP PDX and found heterogeneity in responses. Similar to hypermutated LuCaP PDX, the non–hypermutated LuCaP PDX exhibited a broad range of susceptibility to docetaxel. Comparing the responses of hypermutated and non–hypermutated LuCaP PDX, we did not find a significant difference in susceptibility to docetaxel, or a differential survival benefit. Our results suggest a range of docetaxel responsiveness among LuCaP PDX lines that is not strongly predicted by hypermutation status.

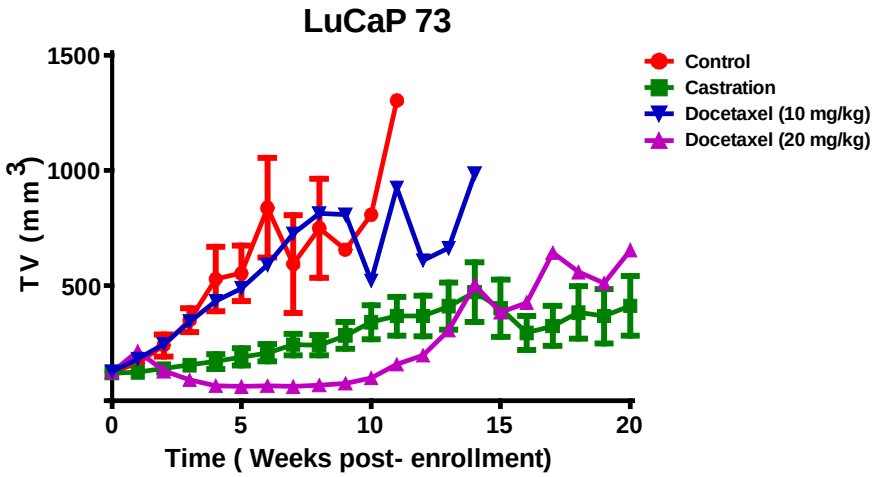

Figure 4. Responses to docetaxel in hypermutated prostate cancer PDX LuCaP 73.

In year 2 we focused on carboplatin and 5-FU. We have nearly completed similar experiments in the hypermutated and non-hypermuated LuCaP lines using carboplatin and 5-FU. 5-FU at 50mg/kg did not have a significant impact on tumor inhibition in either hypermutated or non-hypermutated lines. Carboplatin at 50mg/kg twice weekly dosing was high effective in halting tumor growth in hypermutated lines **(Figure 5**). Carboplatin response data is not yet complete for the non-hypermutated lines. Because recent data supports that carboplatin is expected to be effective in PDX with homologous recombination DNA repair deficiency, a subgroup analysis of the non-hypermutated lines is planned to evaluate and compare responses in lines with or without HR DNA repair deficiency.

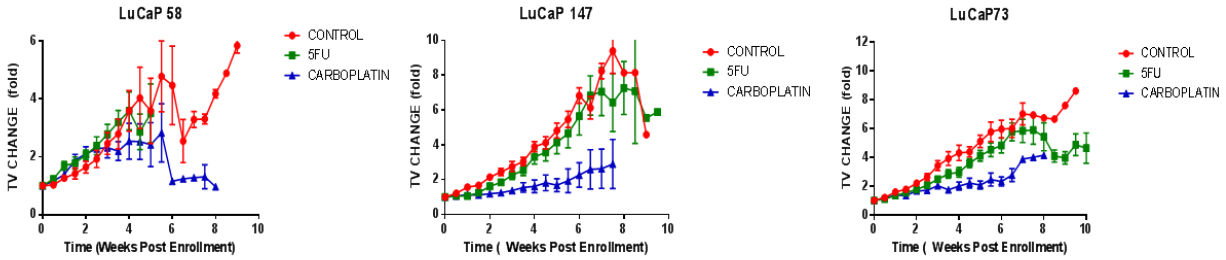

Figure 5: Carboplatin and 5-FU responses in hypermutated LuCaP PDX lines.

Specific Aim 3: Develop and validate a clinical diagnostic approach to determine hypermutation status in advanced prostate cancer.

Aim 3, Subtask 1: *Develop bioinformatics methods to accurately detect hypermutation and microsatellite instability using the UW-OncoPlex assay*

Work on Aim 3, has been a focus of work in Year 1 and will continue in Year 2. We developed a novel method for inferring MSI and hypermutation from next-generation sequencing data that we call "mSINGS". We recently published a manuscript on this method for which Dr. Pritchard was the senior and corresponding author (Salipante et al. *Clin Chem.* 2014 60:1192-9). A graphical depiction of how the mSINGS method works is given in **Figure 5**.

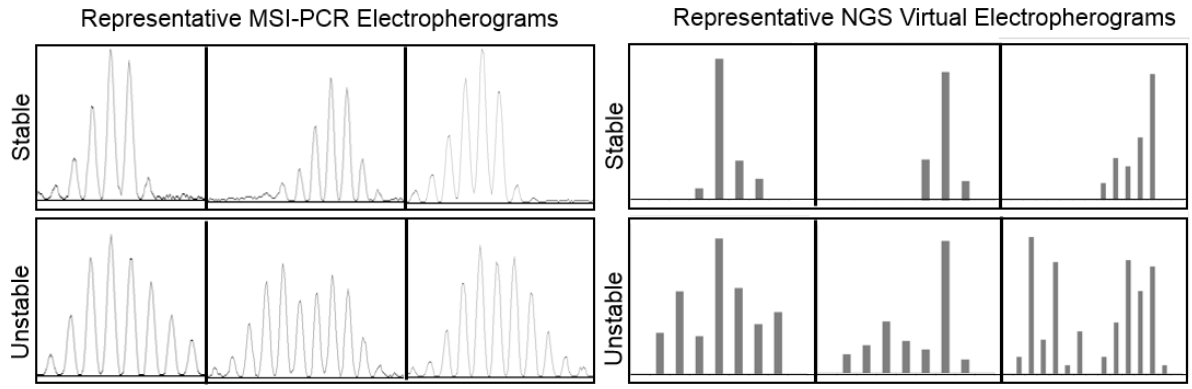

Figure 5: Detection of microsatellite instability by MSI-PCR and next-generation DNA sequencing using "mSINGS". Representative capillary electrophoresis results from MSI-PCR (top panels) and "virtual electropherograms" of next-generation DNA sequencing data (bottom panels), where the length (x-axis) and relative abundance (Y-axis) of variant repeats are plotted. Loci in top and bottom panels are not equivalent, and are from different genomic locations.

We have adapted the mSINGS method to both the BROCA and UW-OncoPlex genomic deep sequencing platforms to accurately detect both phenotypic MSI and hypermutation status, even when matched non-tumor tissue is not available (**Figure 6**). UW-OncoPlex is a clinically-validated diagnostic platform for precision cancer medicine developed by Dr. Pritchard that has been used to test over 1,000 cancer patients to date (for details on the assay see http://tests.labmed.washington.edu/UW-OncoPlex, or Google: "UW-OncoPlex"). We have identified 65 mononucleotide microsatellite loci that are captured in the current UW-OncoPlex assay version (version 4). We established parameters for each locus to be called unstable based on the SD of peak distribution and defined MSI-High as having at 20% unstable loci. Using the mSINGS informatics approach, we correctly identified all known MSI-High cancer samples (7/7) including one hypermutated prostate cancer sample which had 24/65 (37%) loci unstable (autopsy sample 00-010, liver metastasis). MSI-High samples had 35 +/- 12 unstable loci (n=7, mean +/- SD), while known microsatellite stable samples had only 2 +/- 1.5 unstable loci (n=10).

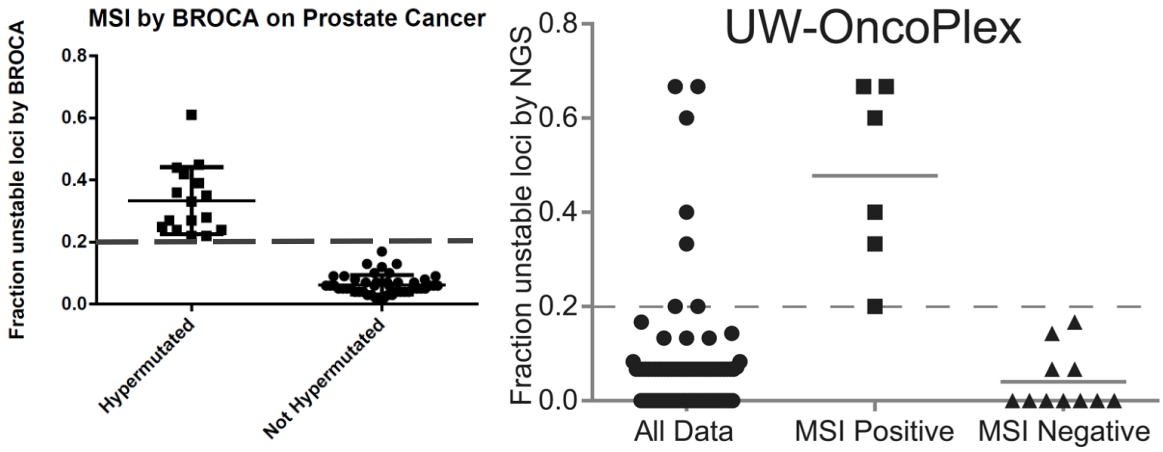

Figure 6: Detection of MSI in prostate cancer samples using mSINGS applied to BROCA and UW-OncoPlex targeted gene sequencing panels. (Left panel) The fraction of unstable microsatellite loci are shown for BROCA (left) and UW-OncoPlex (right) targeted sequencing. Results are stratified by hypermutation or MSI status. The threshold used for interpreting MSI status is indicated by a dashed line, set at a fraction of 0.2 (20% unstable loci). This threshold perfectly separated hypermutated (MSI positive) and not hypermutated (MSI negative) tumors.

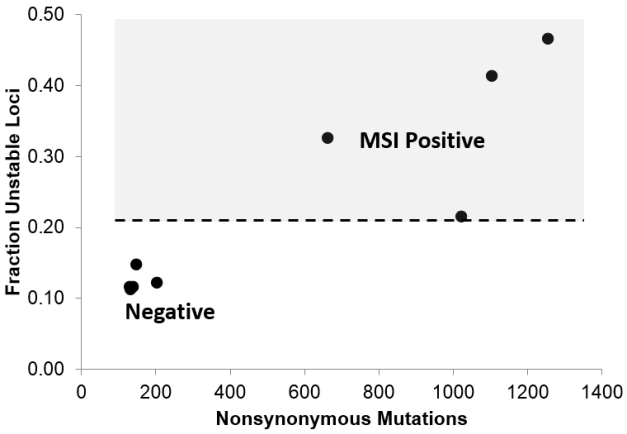

Figure 7. Hypermutated CRPC cases from SU2C international dream team have phenotypic microsatellite instability (MSI) detected by mSINGS. We applied an approach to measure microsatellite instability directly from next-generation sequencing data (mSINGS) to four hypermutated cases, defined as >300 nonsynonymous mutations in exome sequencing. A threshold fraction of 0.2 (20%) unstable loci is the cutoff for microsatellite instability using the mSINGS method (dashed line). All four hypermutated cases were MSI positive and had somatic mutations in mismatch repair genes (*MLH1, MSH2*, or *MSH6*). Selected cases with less than 300 nonsynonymous mutations were MSI negative (bottom).

In collaboration with Stephen Salipante and Jay Shendure we applied the mSINGS method to exome data from 18 available TCGA datasets comprising a total of 5,930 cancer samples. This work led to important mechanistic insights of MSI and was published in *Nature Medicine* (Hause et al. 2016, see Appendix).

We next developed a simple and rapid clinical diagnostic assay based on the mSINGS method that we call "MSIplus". This method using amplicon sequencing of 18 microsatellite loci, following by NGS. We validated this method on 81 tumor specimens with known MSI status, including prostate cancer samples (**Figure 8**). This work has led to a manuscript which is currently in press in the *Journal of Molecular Diagnostics* (see Appendix). In collaboration with Dr. Michael Schweizer, another CDMRP Physician Scientist Training Award recipient, the MSIplus assay will be used to prescreen patients in a clinical trial of the PD-L1 inhibitor durvalumab in Year 3.

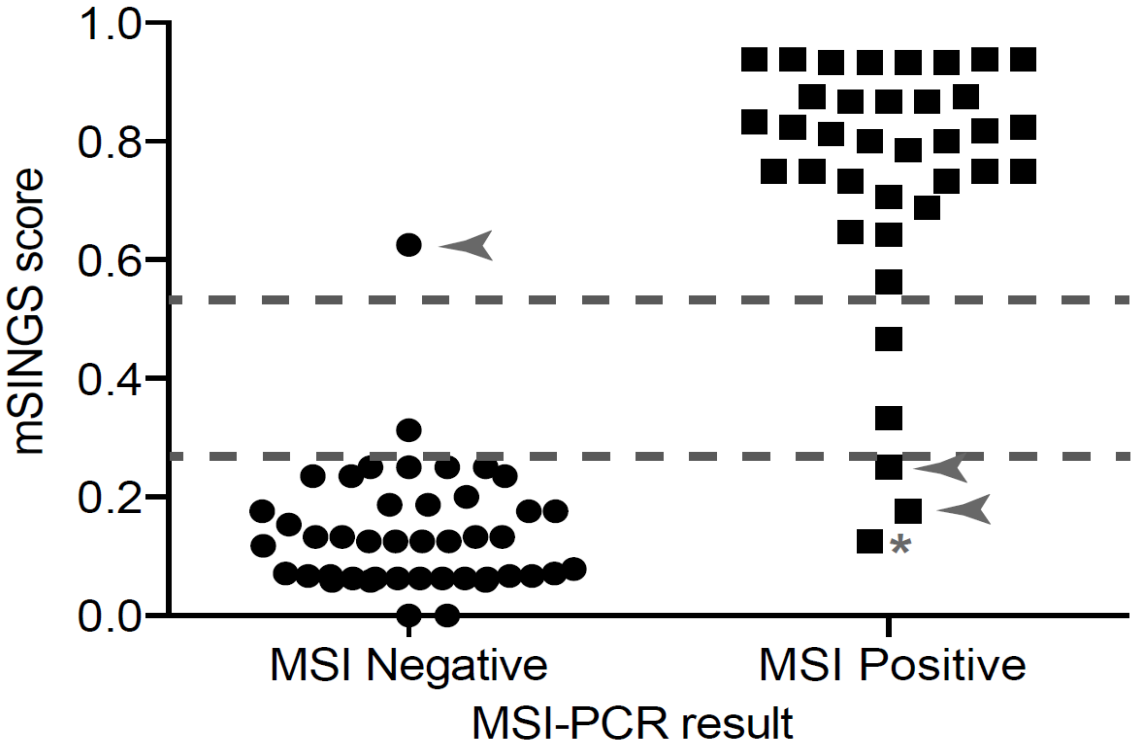

Figure 8: "MSIplus": A rapid and cost-effective stand-alone 18-loci MSI test based on the mSINGS method. 81 tumor samples with known MSI status. Arrows represent potentially discrepant cases in which the original MSI result used as the gold standard was likely to be in error.

Aim 3, Subtask 2: *Establish the performance characteristics of MSI-PCR and IHC-based approaches to detect hypermutation compared to the UW-OncoPlex genomic sequencing*

We have identified and evaluated MSI using MSIplus and UW-OncoPlex in 4 MSI high hypermutated cases and 6 MSS non-hypermutated cases with 100% concordance. Although we have already shown that MSI can be detected in hypermutated prostate cancer samples using MSIplus, we anticipate that a subset of microsatellite loci will be optimal for detection of MSI in prostate cancer. Through our study of the landscape of MSI in cancer (Hause et al. 2016 *Nature Medicine*) we have discovered several additional microsatellite loci that perform especially well for discriminating MSI in prostate cancer. In collaboration with Dr. Stephen

Salipante we plan to adapt the MSIplus assay to evaluate these loci for prostate cancer samples. In year 3 we plan to add these additional loci to expand the MSIplus panel, and will perform a validation study.

With help from mentor Dr. Larry True, we have identified a histologic correlate to hypermutation and MSI status. We found that hypermutated prostate cancer was associated with ductal histology, a rare histologic variant. Ductal prostatic adenocarcinomas (dPC) are an aggressive histopathologic variant of prostate cancer, characterized by large glands lined by tall, pseudostratified, columnar neoplastic epithelial cells (**Figure 9**). Approximately 3% of all prostate cancers have at least a component of ductal histology, with only 0.2% having pure ductal histology. Clinically, dPCs tend to have a more aggressive course – behaving similarly to Gleason 4+4=8 carcinomas. Tumors with >10% ductal component are associated with a higher stage, are more likely to present with metastatic disease, and may be less responsive to androgen deprivation.

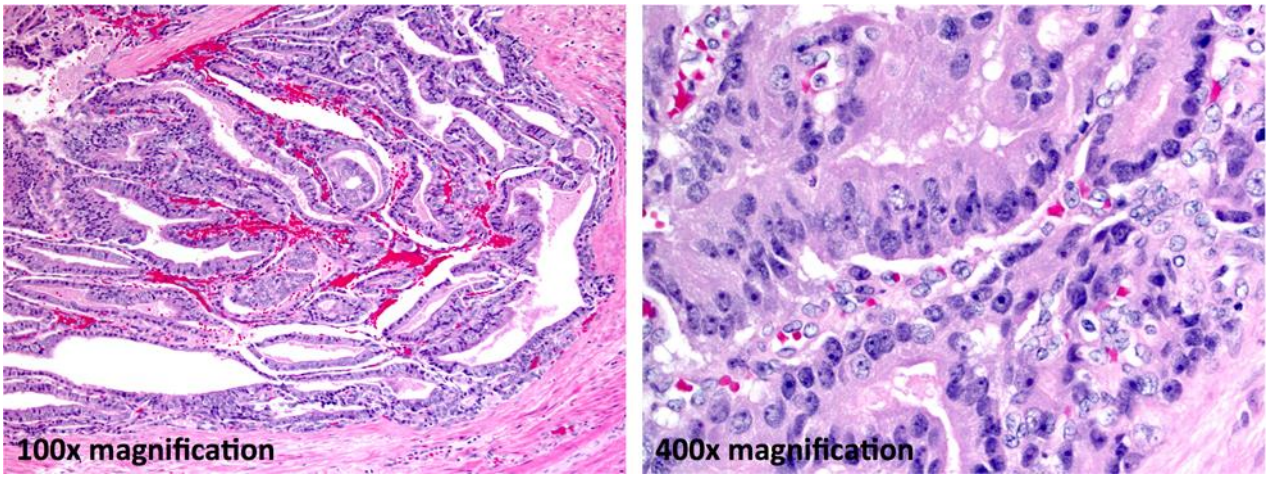

Figure 9: Ductal adenocarcinoma component of a hypermutated prostate cancer case. In this case, approximately 65% of the carcinoma is ductal. Large tumor cell aggregates have a tubulopapillary architecture (100x final magnification). Forming a pseudostratified columnar epithelium the tumor cells have markedly atypical nuclei with clumped chromatin and prominent nucleoli (400x final magnification).

We applied UW-OncoPlex targeted deep sequencing to tumors from 10 consecutive patients with known dPC. Nine of 10 samples had sufficient material for tumor sequencing. Four (40%) patients' tumors had a mismatch repair (MMR) gene alteration (N=2, *MSH2*; N=1, *MSH6*; and N=1, *MLH1*), of which 3 (75%) had evidence of MSI using mSINGS and hypermutation **(Table 3).** The three hypermutated cases with MSI had clear evidence of bi-allelic MMR mutation, while the one case without MSI or hypermutated had only on MMR mutation (subject 2). Similar to what we observed in the rapid autopsy series, MMR mutations were structural rearrangements in 3 of 4 cases. Sections of the primary carcinomas from two of the rapid autopsy patients were available of review; remarkable—both of these tumors had dPC. MMR mutations associated with hypermutation were common in our cohort of dPC patients. The presence of dPC may be a rapid means to enrich populations for further screening for hypermutation and MSI. Given our small sample size, we plan to evaluate additional dPC cases. This work has led to a manuscript that is currently in review.

Table 3: Summary of DNA repair mutations identified in ductal prostate cancer cases.

Subject number	Ductal component of sample used for NGS	MMR gene alteration	HR gene alteration	MSI by mSINGS	Hyper-mutated	Total Coding Mutations (per 1.2Mb sequenced)
1	71%	No	*CHEK2* c.1100delC +LOH	No	No	4
2	**45%**	***MSH2* inversion**	**No**	**No**	**No**	**4**
3	65%	No	No	No	No	4
4	**30%**	***MSH6* c.1900_1901del+LOH**	**No**	**Yes (low)**	**Yes**	**29**
5	**97%**	***MSH2-GRHL2* rearrangement +LOH**	**No**	**Yes**	**Yes**	**34**
6	99%	No	No	50%	No	5
7	25%	-	-	0%	-	-
8	31%	No	No	70%	No	5
9	35%	No	*BRCA2* c.5946delT +likely LOH	10%	No	3
10	**-**	***MLH1* exon 19+ 3'UTR homozygous deletion**	**No**	**Yes**	**Yes**	**32**

In year 3 we plan to evaluate IHC patterns in hypermutated tumors to determine if IHC may be a reliable screening assay to identify hypermutation.

Specific Aim 4: Implement diagnostic testing for hypermutation status in the UW-OncoPlex program for precision cancer medicine.

Aim 4, Subtask 1: *Establish a clinical trial that includes hypermutation testing by UW-OncoPlex with or without additional MSI-PCR/MSI-IHC tests depending on results of Aim 3*

Work on Aim 4 is currently is in progress and will be a focus in year 3. In year 1 we obtained IRB human subjects approval for this work. We have begun to offer clinical UW-OncoPlex testing (**Table 3**) for prostate cancer patients with a total of 96 patients tested to date. Clinical reports are provided and results discussed directly with treating oncologists and urologists at a monthly precision tumor board led by Dr. Pritchard (**Figure 10**). We are evaluating treatment decision making in prostate cancer patients who have undergone UW-OncoPlex testing. We have published a manuscript describing our findings in the first 45 patients (see Appendix, Cheng et al. 2016 *Prostate*.

Table 3: UW-OncoPlex™ genes (assay version 5)

Tier 1: Currently actionable	ABL1	AKT1	ALK	AR	***ARAF***	ASXL1	ATM	AURKA	BCR	BRAF
	BRCA1	BRCA2	CALR	CCND1	CEBPA	***CSF3R***	***DDR2***	DNAJB1	DNMT3A	EGFR
	EML4	ERBB2	***ERCC2***	***ESR1***	FGFR2	FGFR3	FGFR4	FLT3	HIF1A	IDH1
	IDH2	JAK2	KIT	KRAS	MAP2K1	MET	MLL	MPL	***MTOR***	***MYD88***
	NOTCH1	NOTCH2	NPM1	NRAS	NTRK1	***NTRK2***	***NTRK3***	PALB2	PDGFRA	PIK3CA
	PML	PTEN	RARA	RET	ROS1	***SETBP1***	SMO	STK11	TP53	VHL
Tier 2: Actionable in the near future	ABL2	AKT2	AKT3	ARID1A	ATRX	AURKB	AXL	BAP1	BARD1	BCL2L11
	BCOR	***BCORL1***	BRIP1	CBL	CBLB	CCNE1	CDK4	CDK6	CDK8	CHEK1
	CHEK2	DAXX	ERBB3	ERBB4	FAM175A	***FANCA***	FBXW7	FGFR1	FLT1	FLT4
	GATA2	GATA3	GLI1	GNA11	GNAQ	GRM3	H3F3A	HDAC4	HRAS	IGF1R
	IKZF1	JAK3	KDM6A	KDR	KIF5B	MAP2K2	MAPK1	MC1R	MCL1	MDM2
	MDM4	MEN1	MITF	MLH1	MRE11A	MSH2	MSH6	MYC	MYCN	NBN
	NF1	NF2	NKX2-1	PAX5	PDGFRB	PHF6	PIK3R1	PMS2	POLD1	POLE
	RAD51C	RAD51D	RAF1	RB1	***RSPO2***	***RSPO3***	RUNX1	SHH	SMAD4	SMARCA4
	SRSF2	SUFU	SUZ12	TACSTD2	TET2	TMPRSS2	TSC1	TSC2	WT1	
Tier 3: Frequently mutated	APC	BAK1	BCL2	CBLC	***CBLC***	CDH1	***CDK12***	***CDK9***	CDKN1A	CDKN2A
	CHD1	CREBBP	CRLF2	CSF1R	CTNNB1	***CUX1***	DEPDC5	DOCK7	EPHA3	EPHA5
	EPHB2	EPHB6	ETV6	EZH2	***FKBP1A***	FOXA1	GAB2	GATA1	GNAS	GRIN2A
	HNF1A	IL7R	JAK1	MAP2K4	MED12	MIOS	MLH3	MTAP	MUTYH	MYCL1
	NPRL2	NPRL3	PAK1	PBRM1	PLK1	PLK3	PLK4	PRPF40B	PTCH1	PTPN11
	PTPRD	***RAC1***	***RAD21***	***RHEB***	RICTOR	RPS14	***RPTOR***	SF1	SF3B1	SMAD2
	SMAD3	SMARCB1	***SMC1A***	***SMC3***	SPOP	SPRY4	SRC	TACC3	***TET1***	***TET3***
	TFG	TGFBR2	TRRAP	U2AF1	U2AF65	ZBTB16	ZRSR2			
Germline pharmaco-genomics	ABCB1	ABCC4	ABCG2	CYP1B1	CYP2C19	CYP2C8	CYP2D6	CYP3A4	CYP3A5	DPYD
	EIF3A	ESR2	FCGR1A	FCGR2A	FCGR3A	GSTP1	ITPA	LRP2	MAN1B1	MTHFR
	NQO1	NRP2	SLC19A1	SLC22A2	SLCO1B3	SOD2	SULT1A1	TPMT	TYMS	TYR
	UGT1A1	UMPS								

*New genes on v5 in **BOLD**

http://tests.labmed.washington.edu/UW-OncoPlex
This is a clinically-available comprehensive gene sequencing platform co-developed and offered clinically by Dr. Pritchard's CLIA-certified genetics and solid tumors laboratory.

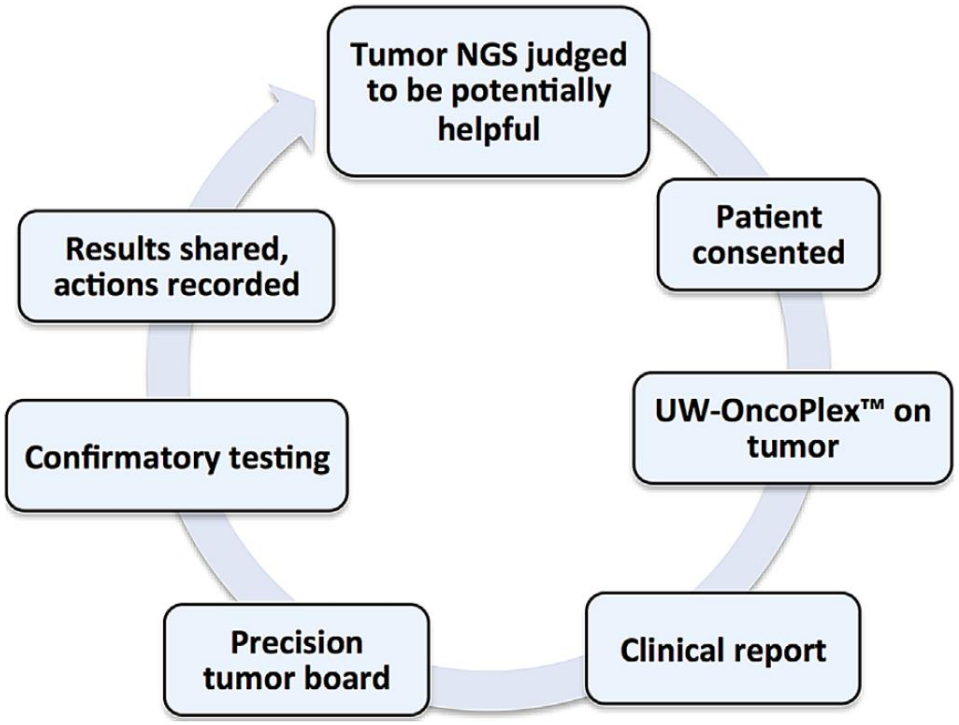

Figure 10: UW-OncoPlex Prostate Pilot Study Schema.

We plan to use this established assay and tumor board framework to formally test the role of hypermutation status as a precision biomarker in a clinical trial in Year 2 and 3 of this research. Recent work suggests that hypermutation and MSI due to DNA mismatch repair deficiency is a predictive biomarker for anti-programmed cell death 1 (PD-1) immunotherapy in several cancers (Le et al. N Engl J Med. 2015 372:2509-20). In collaboration with Dr. Michael Schweizer, we have established a protocol to screen men with prostate cancer for MSI using MSIplus as a qualifying test for enrollment on an anti-PD-1 therapeutic trial (durvalumab). Men who screen positive by MSIplus will have UW-OncoPlex testing done on tumor to determine hypermutation and MMR gene mutation status, as well as to confirm MSI.

Aim 4, Subtask 2: *Report hypermutation status results to medical oncologists in prostate cancer precision tumor board meetings and document treatment decisions and short-term outcomes.*

Work on this subtask was a focus in year 2 and will continue in year 3. We have already identified 4 of 96 patients with hypermutated prostate cancer at precision tumor board. All 4 patients had MSI detected by our mSINGS method using UW-OncoPlex and an underlying tumor *MMR* mutation with associated loss of heterozygosity or homozygous deletion, meaning bi-allelic inactivation (**Table 4**). One patient had Lynch syndrome with a germline *MSH2* mutation; the other three patients had double somatic MMR mutations. The discussion at precision tumor board suggested that the patient may be eligible for an anti-PD-1 checkpoint inhibitor immunotherapy trial. Recent work on MSI-high cancers indicates that hypermutation may predict response to anti-PD1 therapy. One patient with an MSH6 mutation and

hypermutated MSI cancer received the PD-1 inhibitor pembrolizumab and achieved a partial PSA response before the drug needed to be discontinued due to side effects (**Figure 11**). In year 3 we anticipate identifying additional hypermutated patients through our pilot study.

Table 4: Summary of hypermutated patients identified by UW-OncoPlex

MMR gene alteration	MSI Status by OncoPlex (using mSINGS)	Coding Mutations (per 1.2Mb)	Ductal Histology?
MSH6 frameshift + LOH	8/63 (13% unstable)	29	Yes
MSH2-GRHL2 rearrangement + LOH	21/65 (32% unstable)	34	Yes
MLH1 focal homozygous deletion	18/65 (28% unstable)	32	Yes
MSH2 p.Q61X germline + LOH	9/61 (15% unstable)	17	Unknown

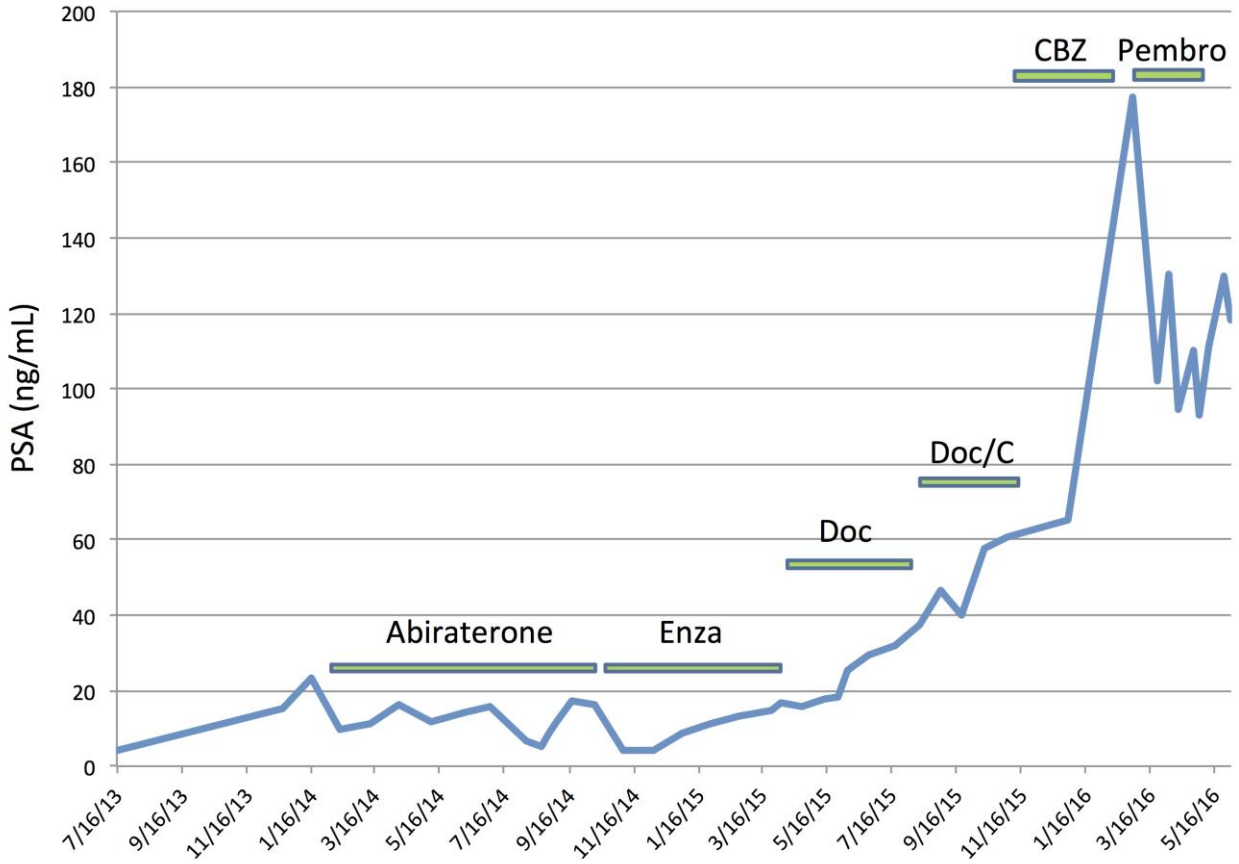

Figure 11: PSA response to checkpoint blockade immunotherapy in a patient with hypermutated prostate cancer. Prior to initiating pembrolizumab, patient had bone, adrenal and lymph node metastases, and a baseline PSA of 177.35 (ng/mL). A total of 3 cycles of pembrolizumab were administered before stopping due to an immune related adverse event requiring corticosteroids. Enza, enzalutamide; Doc, docetaxel; C, carboplatin; CBZ, cabazitaxel; Pembro, pembrolizumab.

3.3 What opportunities for training and professional development has the project provided?

Training-specific tasks from the approved SOW are given below. Detail related to training goals in the first year is provided in the section that follows.

Major Task: Training and educational development in prostate cancer research	**Months**	**Completed in Year 1-2?**
Subtask 1: Attend the Prostate Cancer Foundation Annual Retreat and the Association of Molecular Pathology Annual Conference	1-36	Yes, see *National Conferences and Committees section below*
Subtask 2: Present research at the monthly mentor group meetings, and at least once per year at Pacific Northwest Prostate Cancer SPORE research conferences	1-36	Yes, *Seminars* and *Interaction with Mentors sections below*
Subtask 3: Lead local prostate cancer precision tumor board, including review of genomic sequencing data and preparation of presentations that integrate prostate cancer patient clinical histories with genomic findings	1-36	Yes, see *Prostate Precision Tumor Board section* below
Subtask 4: Attend face-to-face meetings as part of the Stand-Up-To-Cancer (SU2C) prostate cancer dream team 2 to 3 times/year. Attend monthly conference calls for the SU2C prostate cancer dream team sequencing and analysis group	1-24	Yes, see *National Conferences and Committees section below*
Subtask 5: Lead local “pipeline” journal club focused on application of new genomic technologies in the clinic	1-36	Yes*, see Journal Club section below*
Subtask 6: Train senior pathology residents and fellows in the interpretation and clinical reporting of prostate-cancer focused precision diagnostics	1-36	Yes*, see Teaching section below*
Subtask 7: Serve as PI for the prostate cancer precision medicine component of the local “ACT-SMART” initiative as part of the institute for prostate cancer research	1-36	Yes
Subtask 8: Clinical reporting of UW-OncoPlex testing applied to advanced prostate cancer	12-36	Yes, *see prostate cancer precision tumor board and clinical duties below*
Subtask 9: Hands-on training in prostate cancer with Dr. True in pathology/immunohistochemistry and exposure to preclinical	1-36	Yes, see *Hand’s-on training*

prostate cancer models with Drs. Vessella and Morrissey.		section below
Milestone(s) Achieved: Publication of original research	24-36	Yes, *see appendices for publications in the first year*
Milestone(s) Achieved: Presentation of project data at a national meeting	12-36	Yes, see *National Conferences and Committees section below*

National Conferences and Committees: In year 1 and 2 I attended the Prostate Cancer Foundation annual retreat where I presented work on mechanisms of hypermutation in advanced prostate cancer both years. I also attended the Prostate Cancer Foundation Coffey-Holden Prostate Cancer Academy Meeting both in Year 1 and in Year 2. This 3-day invite-only meeting was a think tank of leading prostate cancer researchers focused on the question of oligo-metastatic disease. I was part of the program organizing committee for the 2016 Coffey-Holden Prostate Cancer Academy meeting in year 2, where I organized a session on DNA repair deficiency in advanced prostate cancer. This session in included talks from international experts that invited for my moderated session, including Dr. Rob Bristow and Dr. Joaquin Mateo, and Dr. Heather Cheng. I attended the Association of Molecular Pathology Annual Conference, which is my primary professional society. I was invited to give an opening plenary session at the 2015 Association of Molecular Pathology Annual Conference on the topic of bioinformatics as a new area for the clinical laboratory. I also attended Stand Up to Cancer (SU2C) Prostate Cancer International Dream Team face-to-face meetings and participated in monthly SU2C sequencing and analysis conference calls. In Year 2 I was invited to present in Chicago as part of the SU2C/PCF international dream team site visit on my work in DNA repair mutations in advanced prostate cancer. As part of my involvement with the SU2C Prostate Cancer International Dream Team I analyzed genomic data, prepared figures for publication, and gave a formal presentation to the SU2C team members. In Year 2 I also attended the DOD IMPACT meeting in Baltimore where a presented a poster on the work achieved to date through this award. My poster was one of only 4 selected for a video interview that was posted on the CDMRP website and on YouTube to highlight the work of the CDMRP PCRP program. Finally, I have been invited to be on the Advanced Prostate Cancer Consensus Conference (APCCC) committee. This is a prestigious international committee that meets in Switzerland annually to vote on practice recommendations for advanced prostate cancer.

Seminars: I continue to attend and present at the weekly Pacific Northwest Prostate Cancer SPORE conference series. For example, in Year 1 I presented a SPORE talk my work on Aim 1 of this research was presented in addition to my collaborative with the SU2C international dream team. In September of Year 2 I presented at SPORE again with an updated on the work completed to date as part of this project. I also attend weekly Laboratory Medicine grand rounds and Laboratory Medicine research rounds which include a wide range of topics related to clinical diagnostic medicine. Finally, I attend weekly genetics seminars hosted by our division.

Teaching: In year 1 and 2 of funding I have trained a total of 6 senior clinical pathology residents, 3 molecular genetic pathology fellows, and 2 junior molecular pathology faculty (Dr. Eric Konnick and Dr. Tina Lockwood) in the clinical interpretation and reporting of genomic testing for prostate cancer. I have continued to be an active mentor to our molecular genetic pathology (MGP) fellowship director, MGP fellows, and chief resident in prostate cancer-related molecular diagnostics. In addition, I have mentored 3 medical genetics senior residents in molecular oncology diagnostics, including one resident (Dr. Mari Tokita) who spent 9 months of dedicated time in my research laboratory developing circulating tumor DNA diagnostics methods. As part of this work she helped to assemble ctDNA samples for clinical assay validation from patients with metastatic prostate cancer. As associate director of the genetics and solid tumors laboratory at the UW I have also mentored 12 junior clinical pathology residents in 4-week basic genetics training rotations.

Journal Club: I continue to lead the "pipeline" monthly journal club at UW which is attended by about 20-30 faculty and senior trainees and is focused on genomic technologies applied in the clinic. I have recruited several speakers in year 1 of funding. Examples include a speaker (Mary Goldman) who works for the UCSC genome browser and outlined new tools for cancer data visualization, and a speaker who discussed new methods for gene fusion analysis in cancer, including *TMPRSS2-ERG* fusion detection in prostate cancer (David Wu). This is a forum where the Molecular Genetic Pathology fellows I mentor are required to present at least once per year.

Prostate Precision Tumor Board**:** I lead the local prostate precision tumor board at the University of Washington where we review genome sequencing data from advanced prostate cancer patients and make treatment recommendations to treating oncologists. This activity is a substantial effort in which I prepare detailed PowerPoint presentations for each patient and do a thorough literature review to identify potential or actual therapeutic implications for genomic findings. This monthly tumor board is attended by GU medical oncologists, pathologists (including co-mentor Dr. Larry True), urologists, research coordinators, genetic counselors, and trainees including our junior faculty and molecular genetic pathology fellows. This forum continues to grow in popularity as molecular findings in prostate cancer begin to be using in practice and it is very well-attended

Clinical Duties**:** I am a primary faculty member responsible for clinical reporting of BROCA and UW-OncoPlex tests that are available through my CLIA-certified laboratory. I have already trained 2 other junior molecular pathology faculty to assist me, and will continue to mentor and train new junior faculty to assist with these clinical duties. My clinical work includes close mentorship from Dr. Mary-Claire King, who personally consults on all BROCA cases. We have weekly "signout" meetings that last 1 to 2 hours. I interpret and write clinical reports for approximately 1,000 genomic sequencing cases per year. As part of my clinical work I interpret and report on UW-OncoPlex clinical testing for all prostate cancer patients tested.

Grant Writing**:** In collaboration with Dr. Peter Nelson and Dr. Eli Van Allen, I am a partnering PI for a DOD IMPACT proposal focused on DNA repair defects as a predictive biomarker for advanced prostate cancer. I have a submitted an R01 application in collaboration with Heather Hampel at The Ohio State University focused on genomic sequencing as a tool for Lynch syndrome screening. This application benefits from the work we have done to develop robust

methods to detect hypermutation and MSI in cancer. Finally, I am key collaborator on a prostate cancer foundation challenge award application focused on MMR deficiency and immunotherapy.

***Hand's-on training*:** With Dr. True I have received personal tutorials in prostate cancer pathology, including one-on-one formal lectures followed by teaching slide review. In addition, Dr. True provides helpful feedback on prostate pathology-related issues at the monthly prostate precision tumor board that I lead. I also receive 'hand's on' exposure to preclinical prostate cancer models with Drs. Eva Corey, Robert Vessella and Colm Morrissey in the University of Washington GU Cancer Research Laboratory.

Interaction with Mentors: I am **co-mentored by Dr. Larry True and Dr. Mary-Claire King** for this training award. Dr. True is an internationally prominent genitourinary pathologist with over 30 years-experience mentoring junior academic researchers. He and I have worked together since 2000, and he has effectively mentored me in aspects of prostate cancer pathology, and molecular biomarker development. For example, I served on the NCI Tissue-Based biomarker subcommittee of the Investigational Drug Steering Committee that Dr. True chaired. Dr. King is an internationally famous geneticist who discovered the *BRCA1* locus, and has mentored dozens of highly successful faculty in the area of cancer genetics. She has mentored me since 1998 as part of the medical scientist training program and has been an even closer ongoing mentor to me over the past 3 years in the clinical implementation of the BROCA assay that was developed in her laboratory by Dr. Tom Walsh. I meet more than once a month at length with Dr. King to discuss BROCA test results and discuss research directions, and I meet with Dr. True at the monthly prostate cancer precision tumor board. In addition, I meet with Dr. True for formal prostate cancer pathology training.

3.4 How were the results disseminated to communities of interest?

Through the Institute for Prostate Cancer Research (IPCR) we have reached out to patient advocates in the region. This has included a formal presentation on prostate cancer precision medicine that I gave to a lay audience for the IPCR on the topic of the UW-OncoPlex program for prostate cancer precision medicine. In year 2 we aired a segment on TV that highlights the prostate cancer precision tumor board that I lead. Also, in year 2 at the Innovative Minds in Prostate Cancer Today (IMPACT) meeting I was filmed at my poster for segment to be posted for patients and researcher on the CDMRP website.

3.5 What do you plan to do during the next reporting period to accomplish the goals?

Plans in Year 3

Research-specific tasks

- Complete work in Aim 2 evaluating carboplatin and 5-FU therapies in hypermutated PDX tumors (no funds from this award used for animal studies).
- Evaluate performance characteristics of MSIplus for prostate cancer and determine the optimal loci.
- Test additional SU2C international dream team CRPC cases by mSINGS and correlate with MMR mutation status.

- Continue prostate cancer pilot project using clinical UW-OncoPlex for men with prostate cancer. Use experience gained from clinical testing to inform a future clinical trial for men with hypermutated prostate cancer.
- Incorporate circulating tumor DNA testing (ctDNA) into the UW-OncoPlex pilot study and evaluate the performance of ctDNA compared to matched tumor tissue testing as the second phase of the pilot study.
- Continue to evaluate treatment decision making in prostate cancer patients who have undergone UW-OncoPlex testing through review with treating oncologists at the precision tumor board. The primary measured outcome will be treatment decisions specifically influenced by hypermutation status results. We will use this data to plan future clinical trials to more formally test the role of hypermutation status as a precision biomarker.
- Continue to evaluate histologic correlates that may be predictive of hypermutation status and MMR deficiency including ductal histology.
- Begin enrolling patients on clinical trial of PD-L1 inhibitor durvalumab using MSIplus and UW-OncoPlex to pre-screen patients that have hypermutated prostate tumors harboring MSI.

Training-specific tasks

- Attend PCF annual meeting and AMP annual meetings as well as SU2C prostate international dream team face-to-face meetings.
- Continue to present data at SPORE conference and at national conferences.
- Continue resident and fellow training of genomic testing in prostate cancer
- Continue hand's on training meetings with Dr. True in prostate cancer pathology
- Continue frequent genomic sequencing signout sessions in cancer genetics with Dr. Mary-Claire King (about 2 to 3 times per month).
- Continue to lead monthly Prostate Precision Tumor Board
- Continue to lead monthly pipeline journal club
- Continue grant writing activities
- Continue activity on national and international prostate cancer committees

4. IMPACT

4.1 What was the impact on the development of the principal discipline(s) of the project?

This research has led to the discovery of the mechanism of hypermutation in advanced prostate cancer. We found that complex somatic *MSH2* and *MSH6* mismatch DNA repair mutations resulting in microsatellite instability are the chief cause of hypermutation. We also found that hypermutation is more common in advanced prostate cancer than previously expected, with 10/103 (10%) patients identified in our series. Our discovery identifies parallels and differences in the mechanisms of hypermutation in prostate cancer compared with other microsatellite instability-associated cancers. Our findings have important implications for prognosis and treatment. If hypermutation can be targeted, a substantial minority of patients with advanced prostate cancer may benefit. For example, cancers with mismatch DNA repair deficiency have recently been shown to be responsive to anti-PD-1 immunotherapy. Our research has also facilitated microsatellite instability and immunohistochemistry-based testing as screening tools

for hypermutation in advanced prostate cancer, as well as identified an important histologic correlate that may facilitate identification of hypermutated cancers..

Our work has also led to the development of highly innovative and robust methods to detect microsatellite instability (MSI) that is associated with hypermutation. We recently developed the "mSINGS" method for detection of MSI directly from NGS. This has facilitated MSI analysis of exome data from the SU2C prostate cancer international dream team consortium, proving that all hypermutated prostate cancer cases in that series also have MSI associated with underlying mismatch DNA repair mutations. Importantly, our work as part of this award has led to the approval of a clinical trial of the PD-L1 inhibitor durvalumab in men with hypermutated MSI prostate cancer. This trial will use MSIplus and UW-OncoPlex to identify eligible men with hypermutated prostate cancers.

4.2 What was the impact on other disciplines?

Our work builds bridges between research in colorectal and endometrial cancer and research in prostate cancer. Hypermutation and MSI are well-studied in colorectal and endometrial cancer. We have applied the mSINGS method we developed to both colorectal and endometrial cancer, resulting in the first ever tumor-based DNA sequencing test for Lynch syndrome, ColoSeq Tumor. We collaborate closely with colleagues at the Ohio State University on Lynch syndrome screening research (Heather Hampel and Albert de la Chapelle), resulting in a recent NIH R01 grant submission that harnesses the mSINGS method. We are currently working on tumor sequencing via UW-OncoPlex of nearly 500 colorectal cancer cases prospectively collected in Ohio state to evaluate if tumor sequencing can be effectively used a screening test for MMR mutation, MSI status, hypermutation, and other predictive biomarkers.

Our work also builds bridges with basic science disciplines. The mSINGS method we developed was recently used to profile the landscape of microsatellite instability across 18 different cancer types, providing important insights into the biology of MSI.

4.3 What was the impact on technology transfer?

Nothing to Report

4.4 What was the impact on society beyond science and technology?

Nothing to Report

5. CHANGES/PROBLEMS

5.1 Changes in approach and reasons for change

Due to cost constraints we were required to slightly modify our planned experimental design for aim 2 to evaluate only 3 different therapies in the hypermutated and non-hypermutated LuCaP xenograft models. The three therapies chosen are docetaxel, carboplatin, and 5-FU. Note that

this change does not affect the budget of this award because no vertebrate animal work is funded through this training award.

5.2 Actual or anticipated problems or delays and actions or plans to resolve them

Based on prior experience by the GU cancer research laboratory we anticipate potential problems with carboplatin toxicity in future LuCaP xenograft animal studies. This is particularly a problem for the LuCaP 58 hypermutated line in which frequent ulceration may occur. To address this, we lowered the dose and dosing frequency of carboplatin for this arm of the study.

5.3 Changes that had a significant impact on expenditures

Nothing to report.

5.4 Significant changes in use or care of human subjects, vertebrate animals, biohazards, and/or select agents

Nothing to report.

6. PRODUCTS

6.1 Publications, conference papers, and presentations

6.11 Journal publications

Pritchard CC (corresponding author), Morrissey C, Kumar A, Zhang X, Smith C, Coleman I, Salipante SJ, Milbank J, Tait JF, Corey E, Vessella RL, Walsh T, Shendure J, Nelson PS; Complex *MSH2* and *MSH6* Mutations in Hypermutated Microsatellite Unstable Advanced Prostate Cancer; *Nature Communications*; 5: 2014; 4988; published; acknowledgement of federal support (yes).
See Appendix 1 and 2

Robinson D, Van Allen EM, Wu Y, Schultz N., Lonigro RJ, Mosquera J, Montgomery R, Taplin ME, **Pritchard CC (co-second author)**, Attard G, Beltran H, Abida WM, Bradley RK, Vinson J, Cao X, Vats P, Kunju LP, Hussain M, Feng FY, Tomlins SA, Cooney KA, Smith DC, Brennan C, Siddiqui J, Mehra R, Scher HI, Chen Y, Rathkopf DE, Morris MJ, Solomon SB, Durack JC, Reuter VE, Gopalan A, Gao J, Loda M, Lis RT, Bowden M, Balk SP, Gaviola G, Sougnez C, Gupta M, Yu EY, Mostaghel EA, Cheng HH, Chew FS, True LD, Plymate SR, Dvinge H, Ferraldeschi R, Flohr P, Miranda S, Zafeiriou Z, Tunariu N, Mateo J, Demichelis F, Elemento O, Robinson BD, Sboner A, Schiffman MA, Nanus DM, Tagawa ST, Sigaras A, Eng KW, Heath E, Pienta KJ, Kantoff P, de Bono JS, Rubin MA, Nelson PS, Garraway LA, Sawyers CL, Chinnaiyan AM; Integrative clinical sequencing analysis of metastatic castration resistant prostate cancer reveals a high frequency of clinical actionability; *Cell*. 161: 2015; 1215–1228; published; acknowledgement of federal support (yes).
See Appendix 3

Hempelmann JA, Scroggins SM, **Pritchard CC**, Salipante SJ; MSIplus: integrated colorectal cancer molecular testing by next-generation sequencing; *Journal of Molecular Diagnostics*. 17: 2015; 705-14; published; acknowledgement of federal support (yes).
See Appendix 4

Cheng HH, **Pritchard CC**, Boyd T, Nelson PS, Montgomery B. Biallelic Inactivation of BRCA2 in Platinum-sensitive Metastatic Castration-resistant Prostate Cancer. *European Journal of Urology*. 69: 2016; 992-5. published; acknowledgement of federal support (yes).
See Appendix 5

Van Allen EM, Robinson D, Morrissey C, **Pritchard C**, Carter SL, Rosenberg M, McKenna A, Chinnaiyan A, Garraway L, Nelson PS. A Comparative Assessment of Clinical Whole Exome and Transcrip-tome Profiling Across Sequencing Centers: Implications for Precision Cancer Medicine. *Oncotarget*. 2016: Epub ahead of print. PMID:27167109. published; acknowledgement of federal support (yes).

Cowen (Shiovitz) S, Turner EH, Beightol MB, Jacobson A, Gooley TA, Salipante SJ, Haraldsdottir S, Smith C, Scroggins S, Tait JF, Grady WHM, Lin EH, Cohn, DE, Goodfellow PJ, Arnold MW, Chapelle Adl, Pearlman R, Hampel H, **and Pritchard CC (senior author)**. Frequent PIK3CA Mutations in Colorectal and Endometrial Tumors with 2 or More Somatic Mutations in Mismatch Repair Genes. *Gastroenterology* 151: 2016; 440-447. published; acknowledgement of federal support (yes).

Cheng HH, Klemfuss N, Montgomery B, Higano CS, Schweizer MT, Mostaghel EA, McFerrin LG, Yu EY, Nelson PS, **and Pritchard CC (senior author)**. Pilot study of clinical targeted next generation sequencing for prostate cancer: consequences for treatment and genetic counseling. *Prostate*. 76: 2016; 1303-11. published; acknowledgement of federal support (yes).
See Appendix 6

Mateo J, Boysen G, Barbieri CE, Bryant HE, Castro E, Nelson PS, Olmos D, **Pritchard CC**, Rubin MA, de Bono JS. DNA Repair in Prostate Cancer: Biology and Clinical Implications. *European Journal of Urology*. Epub ahead of print: 2016; PMID:27590317. published; acknowledgement of federal support (yes).
See Appendix 7

Pritchard CC (first author), Mateo J, Walsh MF, De Sarkar N, Abida W, Beltran H, Garofalo A, Gulati R, Carreira S, Eeles R, Elemento O, Rubin MA, Robinson D, Lonigro R, Hussein M, Chinnaiyan A, Vinson J, Filipenko J, Garraway L, Taplin M-E, AlDubayan S, Han GC, Beightol M, Morrissey C, Noteboom J, Nghiem B, Cheng HH, Montgomery B, Walsh T, Casadei S, Vijai J, Scher HI, Sawyers C, Schultz N, Kantoff P, Solit D, Robson M, Van Allen EM, Offit K, DeBono J, and Nelson PS. Inherited DNA-Repair Gene Mutations in Men with Metastatic Prostate Cancer. *New England Journal of Medicine*. 375: 2016; 443-53. published; acknowledgement of federal support (yes).
See Appendix 8

Hause RJ, **Pritchard CC**, Shendure J, Salipante SJ. Classification and characterization of microsatellite instability across 18 cancer types. *Nature Medicine*. 2016: Epub ahead of print; PMID:27694933. published; acknowledgement of federal support (yes).

See Appendix 9

6.12 Books or other non-periodical, one-time publications.

Nothing to report

6.13 Other publications, conference papers, and presentations.

Pritchard CC, Morrissey C, Kumar A, Zhang X, Smith C, Coleman I, Salipante S, Grady WM, Tait JF, Vessella R, Walsh T, Shendure J, and Nelson PS. Mechanisms of Microsatellite Instability in Hypermutated Advanced Prostate Cancer. (2014) Prostate Cancer Foundation Annual Scientific Retreat.

Salipante S, Scroggins S, Hampel HL, Turner EH, and **Pritchard CC**. Microsatellite Instability Detection By Next-Generation Sequencing. (2014) Academy of Clinical Laboratory and Physician Scientists Annual Meeting.

Cheng HC, Klemfuss N, Montgomery B, Higano CS, Schweizer MT, Mostaghel E, Yu EY, Nelson PS, **and Pritchard CC**. Pilot study of clinical targeted next generation sequencing for prostate cancer: treatment and genetic counseling actionability. (2015) Prostate Cancer Foundation Annual Scientific Retreat.

Shiovitz S, Turner EH, Beightol MB, Jacobson A, Gooley TA, Salipante SJ, Haraldsdottir S, Smith C, Scroggins S, Tait JF, Grady WHM, Lin EH, Cohn, DE, Goodfellow PJ, Arnold MW, Chapelle Adl, Pearlman R, Hampel H, **and Pritchard CC**. *PIK3CA* mutations in colorectal and endometrial cancer with double somatic mismatch repair mutations compared to Lynch syndrome. (2015) American Society of Clinical Oncology Annual Meeting.

Cheng HH, **Pritchard CC**, Boyd T, Nelson PS, and Montgomery B. Biallelic Inactivation of *BRCA2* in Platinum-sensitive, Metastatic Castration Resistant Prostate Cancer. (2016). American Society of Clinical Oncology Genitourinary Cancers Symposium Meeting.

Nelson PS, Mateo J, Beltran H, De Sarkar N, Elemento O, Rubin MA, Vinson J, Filipenko J, Robinson DR, Chinnaiyan A, Garraway L, Van Allen EM, Garofalo A, Taplin M-E, Garraway LA, Carreira S, Montgomery RB, Morrissey C, Cheng HH, DeBono JS, **and Pritchard CC**. (2016). American Society of Clinical Oncology (ASCO) Annual Meeting. [Selected for oral platform presentation with discussant as ASCO]

Pritchard CC, Morrissey C, Cheng HH, Salipante S, True L, Schweizer M, Klemfuss N, Montgomery RB, Corey E, Nelson PS. Hypermutation in Advanced Prostate Cancer: From Mechanism to Implementation of Genomic Testing for Precision Therapy. (2016) DOD Prostate Cancer Young Investigators IMPACT meeting, Baltimore MD.

Shirts BH, Konnick EQ, Jacobson A, Garrett L, Hampel H, Pearlman R, King MC, Walsh T, **and Pritchard CC**. Using somatic mutations to classify pathogenic Lynch syndrome variants (2016) Association for Molecular Pathology annual meeting.

De Sarkar N, **Pritchard CC**, Nelson P. "Inherited Deleterious Germline Variants in Men with Prostate Cancer Identified by Whole Exome Sequencing" (2016) American Society for Human Genetics (ASHG) annual meeting. [Selected for oral platform presentation at ASHG]

6.2 Website(s) or other Internet site(s)

Nothing to report.

6.3 Technologies or techniques

We have developed the mSINGS method for detection of microsatellite instability from targeted next-generation sequencing data. The source code for this bioinformatics method is freely available for academic users and can be found at: https://bitbucket.org/uwlabmed/msings. This source code has already been shared with multiple national and international researchers.

6.4 Inventions, patent applications, and/or licenses

Nothing to report.

6.5 Other Products

The genomic sequencing dataset we generated as part of the research on aim 1 to identify mechanisms of hypermutation is publically available at GenBank/EMBL/DDBJ under the accession code SRP044943.

7. PARTICIPANTS & OTHER COLLABORATING ORGANIZATIONS

7.1 What individuals have worked on the project?

Name: Colin C. Pritchard
Project Role: PI
Researcher Identifier: ORCID ID: 0000-0002-7424-2956)
Nearest person month worked: 5
Contribution to Project: Dr. Pritchard has obtained funding support, designed experiments, and written manuscripts related to this work
Funding Support: (this award)

Name: Robert Livingston
Project Role: Senior Research Scientist
Nearest person month worked: 1
Contribution to Project: Dr. Livingston has coordinated coordinating genomic sequencing library preparation and assisted in data analysis.
Funding Support: (this award)

Name: Mallory Beightol
Project Role: Research Technician

Nearest person month worked: 1
Contribution to Project: Ms. Beightol has helped perform genomic sequencing assays including BROCA and UW-OncoPlex.
Funding Support: Institutional, PNW Prostate Cancer SPORE pilot funds

7.2 Has there been a change in the active other support of the PD/PI(s) or senior/key personnel since the last reporting period?

Colin Pritchard: Changes in current support since last reporting period:

PC141019P2

Title: Noninvasive Detection of AR-FL/AR-V7 as a Predictive Biomarker for Therapeutic Resistance in Men with Metastatic Castration-Resistant Prostate Cancer

Time Commitment: .6 calendar months (5% effort)

Supporting Agency: Department of Defense

Name of Procuring Contracting/Grants Officer: TBD

Address of Funding Agency: USAMRAA, Branch A4, 820 Chandler Street, Ft. Detrick, MD 21702-5014

Performance Period: 9/15/15-6/30/17

Level of Funding: $927,000

Project Goal: The goal of this project is to develop AR-V7 as a clinical biomarker for therapeutic decision making to improve the care of men with advanced prostate cancer. The specific aims are Aim1: To perform cross-institutional analytical validation of a blood-based assay in a certified environment (CLIA or international equivalent). Aim 2: To expand existing prospective clinical correlation studies to enable assay qualification and clinical validation. Aim 3: To plan, coordinate, and facilitate multi-institutional clinical trials integrating AR biomarkers.

Project overlap or parallel: None

7.3 What other organizations were involved as partners?

Nothing to report.

8. SPECIAL REPORTING REQUIREMENTS

Nothing to report.

9. APPENDICES

Appendix 1: Reprint of Pritchard CC et al.; Complex *MSH2* and *MSH6* Mutations in Hypermutated Microsatellite Unstable Advanced Prostate Cancer; *Nature Communications*; 5: 2014; 4988.

Appendix 2: Supplemental Figures from Pritchard CC et al.; Complex *MSH2* and *MSH6* Mutations in Hypermutated Microsatellite Unstable Advanced Prostate Cancer; *Nature Communications*; 5: 2014; 4988.

Appendix 3: Reprint of Robinson D et al.; Integrative clinical sequencing analysis of metastatic castration resistant prostate cancer reveals a high frequency of clinical actionability; *Cell*. 161: 2015; 1215–1228.

Appendix 4: Reprint of Hempelmann JA et al.; MSIplus: integrated colorectal cancer molecular testing by next-generation sequencing; *Journal of Molecular Diagnostics*. 17: 2015; 705-14.

Appendix 5: Cheng HH et al. Biallelic Inactivation of BRCA2 in Platinum-sensitive Metastatic Castration-resistant Prostate Cancer. *European Journal of Urology*. 69: 2016; 992-5.

Appendix 6: Reprint of Cheng HH et al. Pilot study of clinical targeted next generation sequencing for prostate cancer: consequences for treatment and genetic counseling. *Prostate*. 76: 2016; 1303-11.

Appendix 7: Reprint of Mateo J et al. DNA Repair in Prostate Cancer: Biology and Clinical Implications. *European Journal of Urology*. Epub ahead of print: 2016; PMID:27590317.

Appendix 8: Reprint of Pritchard CC et al. Inherited DNA-Repair Gene Mutations in Men with Metastatic Prostate Cancer. *New England Journal of Medicine*. 375: 2016; 443-53.

Appendix 9: Reprint of Hause RJ et al. Classification and characterization of microsatellite instability across 18 cancer types. *Nature Medicine*. 2016: Epub ahead of print; PMID:27694933.

nature COMMUNICATIONS

ARTICLE

Received 13 Mar 2014 | Accepted 14 Aug 2014 | Published 25 Sep 2014

DOI: 10.1038/ncomms5988 OPEN

Complex *MSH2* and *MSH6* mutations in hypermutated microsatellite unstable advanced prostate cancer

Colin C. Pritchard[1], Colm Morrissey[2], Akash Kumar[3], Xiaotun Zhang[2], Christina Smith[1], Ilsa Coleman[4], Stephen J. Salipante[1,3], Jennifer Milbank[3], Ming Yu[5], William M. Grady[5], Jonathan F. Tait[1], Eva Corey[2], Robert L. Vessella[2], Tom Walsh[6], Jay Shendure[3] & Peter S. Nelson[4]

A hypermutated subtype of advanced prostate cancer was recently described, but prevalence and mechanisms have not been well-characterized. Here we find that 12% (7 of 60) of advanced prostate cancers are hypermutated, and that all hypermutated cancers have mismatch repair gene mutations and microsatellite instability (MSI). Mutations are frequently complex *MSH2* or *MSH6* structural rearrangements rather than *MLH1* epigenetic silencing. Our findings identify parallels and differences in the mechanisms of hypermutation in prostate cancer compared with other MSI-associated cancers.

[1] Department of Laboratory Medicine, University of Washington, Seattle, Washington 98195, USA. [2] Department of Urology, University of Washington, Seattle, Washington 98195, USA. [3] Department of Genome Sciences, University of Washington, Seattle, Washington 98195, USA. [4] Division of Human Biology, Fred Hutchinson Cancer Research Center, Seattle, Washington 98109, USA. [5] Division of Clinical Research, Fred Hutchinson Cancer Research Center, Seattle, Washington 98109, USA. [6] Division of Medical Genetics, Department of Medicine, University of Washington, Seattle, Washington 98195, USA. Correspondence and requests for materials should be addressed to C.C.P. (email: cpritch@uw.edu).

Recently exome sequencing of metastatic prostate cancers revealed that a subset of patients harboured tumors with markedly elevated single-nucleotide mutation rates, defining a new hypermutated subtype[1]. This phenotype was subsequently observed in primary prostate cancer in a tumour that harboured an *MSH6* mutation[2]. However, mechanisms that lead to hypermutation and the prevalence of this distinct subtype have not been completely defined. Comprehensive cancer genomics efforts recently published by The Cancer Genome Atlas Research Network (TCGA) reported that 16% of colon cancers and up to 35% of endometrial cancers exhibit hypermutation[3,4]. For both colon and endometrial cancers, about three quarters of hypermutated tumors were associated with phenotypic microsatellite instability (MSI) and loss-of-function DNA mismatch repair genes via mutation or epigenetic silencing. Therefore, we hypothesized that hypermutated prostate cancer may also be associated with DNA mismatch repair (MMR) gene defects and MSI.

In this study we identified hypermutation in 7 of 60 patients with advanced prostate cancer. Using a targeted deep sequencing approach we find that all hypermutated tumors have somatic mutations in MMR genes and associated MSI. In four of seven hypermutated cases MMR mutations were complex structural rearrangements in *MSH2* and *MSH6*. We conclude that somatic rearrangements in *MSH2* and *MSH6* are an important mechanism leading to hypermutation and MSI in advanced prostate cancer.

Results

Prevalence of hypermutation. We identified hypermutated cases in exome sequencing data sets of advanced prostate cancer samples from two sources: a panel of patient-derived xenografts (PDX) and metastatic specimens obtained through a rapid autopsy programme (Supplementary Table 1). Exome data for PDX tumors was from Kumar *et al.*[1], where hypermutation was previously characterized. In the autopsy samples where hypermutation status had not been previously established, we defined hypermutation as >300 somatic protein altering mutations based on the distribution of total mutation burden in metastatic tumors, which had matched normal tissue available (Supplementary Fig. 1; Supplementary Table 1). We identified hypermutation in 3 of 15 PDX tumors (Table 1), and in metastatic tumors from 5 of 50 autopsy patients (Table 2). There was partial overlap between the two patient groups: five of the PDX tumors were derived from autopsy patients, including one with a hypermutated genome (LuCaP 147). Therefore, there were a total of 7/60 unique patients with hypermutated tumors, for an overall prevalence of 11.6%. Hypermutation status was 100% concordant at different metastatic sites, and was also concordant between primary tumour and metastasis in two patients where primary prostate tumors were available (Table 2).

Identification of *MSH2* and *MSH6* rearrangements. Because exome sequencing has limitations in detecting structural rearrangements and larger insertion/deletion (indel) mutations, we investigated alterations in DNA MMR pathway genes in hypermutated and non-hypermutated cases using a targeted deep sequencing approach (BROCA assay) that included capture of intronic and flanking DNA sequences (Supplementary Table 2)[5,6]. We developed a bioinformatics pipeline to accurately detect structural variation, copy number variation and indel mutations of all sizes[7].

All three PDX hypermutated tumors had complex structural rearrangements in *MSH2*, *MSH6* or both genes (Table 1; Fig. 1a; Supplementary Figs 2–4), while only 1 of 20 non-hypermutated xenografts had mutations in these genes (LuCaP 145, derived from a patient with neuroendocrine prostate cancer, Supplementary Fig. 5). A second loss-of-function mutation in *MSH2* or *MSH6* was detected in the three hypermutated PDX tumors, but not in LuCaP 145, supporting a requirement for bi-allelic gene inactivation underlying the hypermutated genome.

We detected mutations with predicted loss-of-function in *MSH2*, *MSH6* or both genes in four of five rapid autopsy patients

Table 1 | MMR gene mutations in prostate cancer PDX.

PDX tumour*	Patient-derived from	Hypermutated?†	MSI	MMR gene mutation(s)‡
LuCaP 58		Yes	Yes	(1) *MSH6* del exon 8 to 3′UTR (2) *MSH6* frameshift (c.3799_3800del)
LuCaP 73		Yes	Yes	(1) *MSH2* and *MSH6* copy loss (del 3 Mb) (2) *MSH2-FBXO11* inversion
LuCaP 147, 147CR	05-165	Yes	Yes	(1) *MSH2-C2orf61* 343 kb inversion (2) *MSH2-KCNK12* 74 kb inversion (3) *MSH2-KCNK12* 40 kb inversion
LuCaP 23.1, 23.1CR		No	No	None
LuCaP 35, 35CR		No	No	None
LuCaP 70, 70CR		No	No	None
LuCaP 77, 77CR		No	No	None
LuCaP 78	98-328	No	No	None
LuCaP 81	98-362	No	No	Chr2 copy losses
LuCaP 86.2, 86.2CR		No	No	None
LuCaP 92	99-069	No	No	None
LuCaP 96, 96CR		No	No	None
LuCaP 105, 105CR		No	No	None
LuCaP 141		No	No	None
LuCaP 145.1, 145.2	05-144	No	No	(1) *MSH2* exon 8-16 del (2) *MSH6-TESC* t(2;12)

MMR, mismatch repair; MSI, microsatellite instability; PDX, patient-derived xenografts.
*Matched pairs of androgen-sensitive and castration-resistant sublines (for example, LuCaP 35 and LuCaP 35CR) and tumour lines derived from the same patient are listed numerically and grouped in the same row.
†Hypermutation status was previously determined in these samples in Kumar *et al.*[1]
‡Mosaic *MSH6* frameshift mutations observed in a poly G tract in exon 5 (c.3261dup/del) and poly A tract in exon 7 (c.3573del) were detected in several hypermutated samples and are not included in the table because they are presumed to be due to MSI.

Table 2 | MMR gene mutations in rapid autopsy patients.

Autopsy patient*	Tumour site(s) tested by BROCA targeted sequencing	Mutation burden† (exome)	Hypermutated?	MSI	MMR gene mutation(s)‡
05-165*	Bone, adrenal, liver and lymph node	855	Yes	Yes	(1) *MSH2-C2orf61* 343 kb inversion (2) *MSH2-KCNK12* 74 kb inversion (3) *MSH2-KCNK12* 40 kb inversion
03-130	Lymph node	647	Yes	Yes	(1) *MSH2* translocation splits the gene t(2;18) (2) *MSH2* copy loss (3) *MSH6* frameshift (c.2690del) (4) *MSH6* copy loss
06-134	Kidney and lymph node	314	Yes	Yes	*MLH1* homozygous copy loss
00-010	Prostate and liver	673	Yes	Yes	*MSH2* frameshift (c.2364_2365insTACA)
05-123	Prostate and lymph node	807	Yes	Yes	(1) *MSH2* frameshift (c.1124_1125insG) (2) *MSH2* frameshift (c.1082del) (3) *MLH1* frameshift (c.1310del), lymph node only
01-095	Liver and lymph node	149	No	No	None
05-144*	Bone, adrenal, liver and lymph node	57	No	No	(1) *MSH2* exon 8-16 del (2) *MSH6-TESC* t(2;12)
05-214	Bone, liver and lymph node (two sites)	46	No	No	None
05-116	Bone, adrenal, liver and lung	47	No	No	None
00-029	Liver	37	No	No	None
00-090	Lymph node	69	No	No	None

MMR, mismatch repair; MSI, microsatellite instability.
*Fifty total unique autopsy patients were assessed by exome sequencing (see Supplementary Table 1). Listed are a subset of cases that were followed up by targeted deep sequencing for MMR genes. Clinical data for this patient subset is provided in Supplementary Table 6. Patient-matched non-cancer tissue was tested in every case and did not exhibit MSI or MMR mutations. LuCaP 147 and 147CR are derived from autopsy patient 05-165. LuCaP 145.1 and 145.2 are derived from autopsy patient 05-144.
†Number of protein altering somatic mutations by exome sequencing with removing of germline variants from matched-non-tumour samples.
‡Mutations were detected at every tumour site unless otherwise indicated. Mosaic *MSH6* frameshift mutations observed in a poly G tract in exon 5 (c.3261dup/del) and poly A tract in exon 7 (c.3573del) were detected in several hypermutated samples and are not included in the table because they are presumed to be due to MSI.

with hypermutated tumors. Mutations included complex structural rearrangements, copy losses and frameshift mutations (Table 2; Supplementary Figs 4 and 6–9). Two hypermutated patients had mutations in the MMR gene *MLH1*. We interrogated a subset of six non-hypermutated patients by deep sequencing and did not detect MMR gene mutations except in patient 05–144 from which the PDX LuCaP 145 was derived (Table 2). Like hypermutation status, MMR mutations were concordant at different metastatic sites in the same patient. MMR mutations were also concordant between primary tumour and metastasis except for a single *MLH1* frameshift mutation in patient 05–123 not found in the primary tumour (Table 2; Supplementary Fig. 9). Patient-matched non-tumour tissues were tested for the autopsy patients (Supplementary Table 1 and Supplementary Data 1). No MMR mutations were detected in patient-matched non-tumour tissue, indicating that none of the MMR mutations were inherited in the germline. Mutations in additional DNA repair genes are given in Supplementary Table 3.

Hypermutated tumors have phenotypic MSI. *MSH2* and *MSH6* are mismatch DNA repair genes that act together as a heterodimer, and bi-allelic inactivating mutations of either gene are predicted to result in MSI. PCR of microsatellite loci revealed MSI in all hypermutated tumors, from both PDX and autopsy patients (Fig. 1b; Supplementary Data 1). Phenotypic MSI was also detected directly from targeted next-generation data for all hypermutated tumors, and not detected in any non-hypermutated tumors (Supplementary Data 1; Supplementary Fig. 10). Immunohistochemistry (IHC) for DNA MMR proteins in hypermutated tumors demonstrated complete loss of MSH2 and/or MSH6 in a pattern consistent with the inactivating mutations detected by sequencing (Fig. 1c; Supplementary Fig. 11). Non-hypermutated tumors were microsatellite stable (Tables 1 and 2; Supplementary Data 1) and had intact MSH2 and MSH6 proteins, except LuCaP 145, which exhibited heterogeneous loss of MSH6 protein (Fig. 1c). *MLH1* methylation was not detected in any of the MSI positive tumors (Supplementary Fig. 12), and MLH1 protein expression was intact by IHC in MSI-positive tumors except in 06–134 that had homozygous *MLH1* gene deletion (Supplementary Fig. 13), arguing that *MLH1* epigenetic silencing was not responsible for MSI in any of the tumors in our series.

Discussion

Our findings support the conclusion that the hypermutated subtype of prostate cancer is chiefly due to loss-of-function mutations in *MSH2* and *MSH6* that result in MSI. Mutations were predicted to be bi-allelic in all cases except 00–010, which may harbour a second undetected mutation. Most interestingly, four of seven hypermutated cases had complex structural rearrangements in *MSH2* and *MSH6* that were not detected by exome sequencing in the same samples, and would also not be expected to be detected by traditional exon-based Sanger sequencing methods. Several previous studies have reported MMR protein loss and MSI in both primary and advanced prostate cancers, but very few MMR mutations have been identified[8–15]. We speculate that technical limitations have led to an underestimation of MMR gene mutations in prostate cancer.

Our finding of predominantly *MSH2* and *MSH6* mutations is in contrast to colon and endometrial cancer, where MSI is most often due to *MLH1* epigenetic silencing[3,4]. This supports an alternate mechanism by which MSI is acquired in prostate cancer. A recent study demonstrated that DNA translocations and deletions in advanced prostate cancer occur in a highly

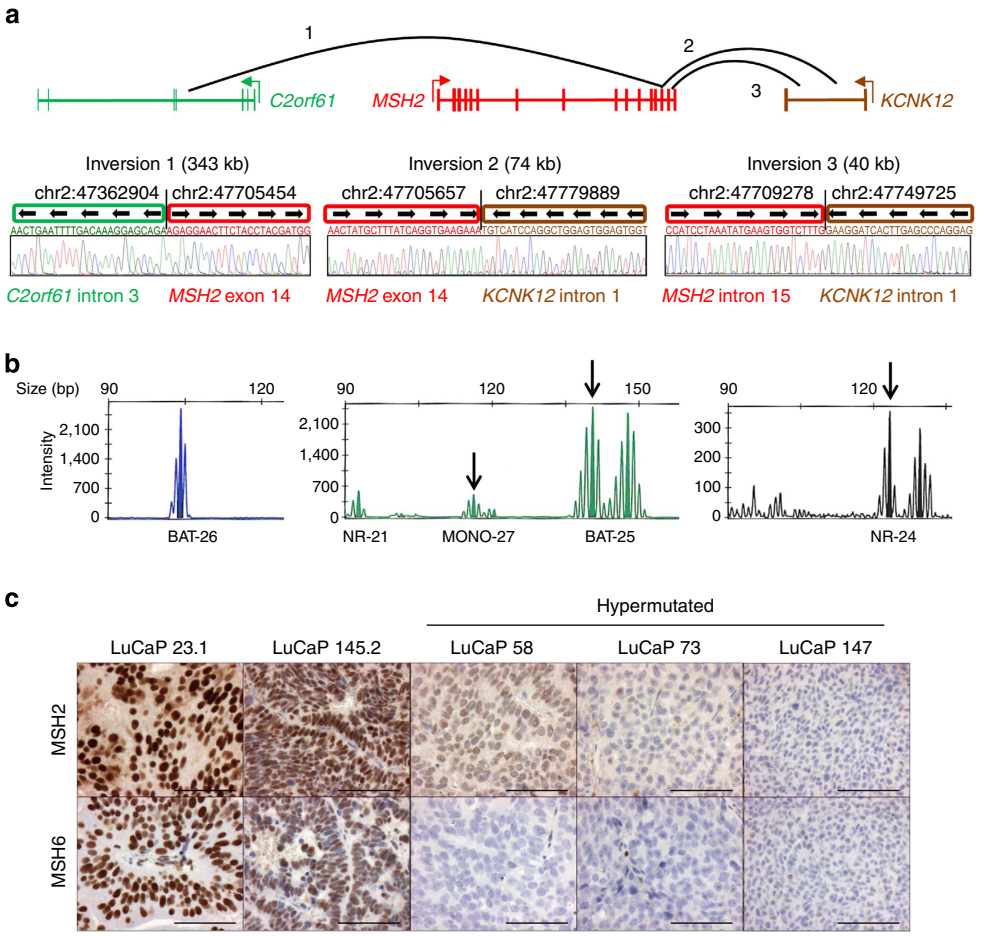

Figure 1 | *MSH2* and *MSH6* rearrangements are associated with loss of protein expression and MSI. (**a**) Four of seven hypermutated cases had complex rearrangements in *MSH2* and *MSH6* or both genes. Shown is a representative complex *MSH2* rearrangement present in hypermutated cases LuCaP 147 and 05-165 (LuCaP 147 was derived from autopsy patient 05-165). Breakpoints were confirmed by Sanger sequencing. Genomic coordinates are hg19. Detail on additional structural rearrangements and other mismatch repair gene mutations is provided in Tables 1 and 2 and Supplementary Figs 2–9. (**b**) Hypermutated tumors exhibited microsatellite instability by PCR. Shown is representative data for LuCaP 58, which is positive for MSI in 3/5 mononucleotide marker systems (MONO-27, BAT-25 and NR-24, arrows). All hypermutated tumors tested were MSI-PCR positive in at least 2/5 loci (Supplementary Data 1). (**c**) Hypermutated tumors LuCaP 58, 73 and 147 have loss of MSH2 and MSH6 proteins by IHC. Similar results were observed in hypermutated tumors from rapid autopsy patients (Supplementary Fig. 11). A representative non-hypermutated tumour (LuCaP 23.1) has intact expression. LuCaP 145 had mono-allelic mutations in *MSH2* and *MSH6* but was not hypermutated. IHC shows loss of MSH6 protein expression in some tumour cells. Scale bars, 0.1 mm.

interdependent manner, a process termed 'chromoplexy'[16]. This process may play a role in the genesis of *MSH2* and *MSH6* structural rearrangements and deserves future study. Androgen receptor (AR) function may also play a role in the formation of *MSH2* and *MSH6* structural alterations. AR has recently been implicated in the genesis of gene rearrangements in prostate cancer by facilitating double-strand DNA breaks and inducing non-homologous end-joining (reviewed in refs 17,18).

In summary, we have shown that complex structural rearrangements in mismatch DNA repair genes *MSH2* and *MSH6* are a major mechanism underlying hypermutation in advanced prostate cancer. Future studies should focus on determining if patients with MMR gene defects exhibit a distinct clinical course and are differentially responsive to genotoxic therapy.

Methods

Patients and specimens. The LuCaP series of prostate cancer xenografts were obtained from the University of Washington Prostate Cancer Biorepository.

Human primary and metastatic prostate cancer tissues were obtained as part of the University of Washington Prostate Cancer Donor Rapid Autopsy Programme. A haematoxylin and eosin slide was reviewed and scrolls from tissue blocks with >50% estimated tumour purity were used. The Institutional Review Board of the University of Washington approved all procedures involving human subjects, and all subjects signed written informed consent. The sample size was chosen based on the number of cases with suitable tissues for exome sequencing.

Genomic DNA was prepared from either formalin-fixed paraffin-embedded tissue or from fresh-frozen tissue (for bone metastases) with the Gentra Puregene DNA Isolation Kit (Qiagen, Catalogue #158489).

Immunohistochemistry. Expression of MMR proteins was determined by IHC using a tissue microarray (UWTMA55), that consisted of 155 metastatic prostate cancer sites from 50 patients, including 77 soft tissue metastases and 83 bone metastases), UWTMA52 consisting of primary prostate cancer obtained at the time of radical prostatectomy from 127 patients, and UWTMA 63 that consisted of prostate cancer tissue from 32 different LuCaP xenograft lines. All the tissue cores were duplicated.

Formalin-fixed paraffin-embedded tissue sections (5 μm) were deparaffinized and rehydrated with three changes of xylene and graded ethanol. Antigen retrieval was performed with heat-induced epitope retrieval for 20 min. Endogenous peroxide and avidin/biotin was blocked and sections were then blocked with 5% normal goat-horse-chicken serum at room temperature for 1 h, and incubated with primary antibody (listed in table below) at 4 °C overnight. After washing three times with 1 × PBS, slides were incubated with biotinylated secondary antibody (Vector Laboratories Inc.), followed by ABC reagent (Vector Laboratories Inc.)

and stable diaminobenzidine (Invitrogen Corp.). All sections were lightly counterstained with haematoxylin and mounted with Cytoseal XYL (Richard Allan Scientific). Mouse or rabbit immunoglobulin-G was used at the same concentration as the primary antibody for negative controls. Antibodies and dilutions used for IHC are given in Supplementary Table 4.

Immunostaining was assessed using a quasi-continuous score system, created by multiplying each intensity level ('0' for no brown colour, '1' for faint and fine brown chromogen deposition and '2' for clear and coarse granular chromogen clumps) with the corresponding percentage of cells expressing the particular intensity, and then summing all values to get a final score for each sample (scores ranging from 0 to 200). Only nuclear staining was evaluated. Samples with damaged tissue core, missing tissue core or poor quality of tissue were excluded from finial analysis.

Microsatellite instability PCR. MSI-PCR testing was performed by the University of Washington (UW) clinical genetics and solid tumors laboratory using the Promega MSI analysis kit (Promega, Madison, WI, USA) following the manufacturer's instructions. Specimens demonstrating instability within two or more of the five mononucleotide markers included in this panel were considered 'MSI positive', others were considered 'MSI negative'. The microsatellite loci tested in the Promega MSI analysis kit were NR-21, BAT-26, BAT-25, NR-24 and MONO-27 (Genbank Accession # XM_033393, U41210, L04143, X60152, AC007684, respectively).

***MLH1* methylation analysis.** Two to four hundred nanograms of DNA from each sample was bisulfite converted using the EZ DNA Methylation Kit (Zymo Research, Irvine, CA, USA) and eluted in 20 µl volume, according to manufacturer's protocol.

SYBR Green qPCR to detect methylated and unmethylated *MLH1* was performed using a CFX 96 Touch Real-Time PCR Detection System (Bio-Rad, Hercules, CA, USA) with a final reaction volume of 20 µl, consisting of 500 nM each primer, 9 ng of bisulfite-converted genomic DNA and iTaq Universal SYBR Green Supermix at the following conditions: 95 °C for 3.5 min, followed by 40 cycles at 95 °C for 5 s and 60 °C for 30 s. The unique primer sequences for methylated *MLH1* were 5′-CGGATAGCGATTTTTAACGC-3′ (forward) and 5′-CCTAAAACGACTACTACCCG-3′ (reverse), and for unmethylated *MLH1* were 5′-AATGAATTAATAGGAAGAGTGGATAGT-3′ (forward) and 5′-TCTCT TCATCCCTCCCTAAAACA-3′ (reverse) (ref. 19). The four primers each also included a 20 bp GC-rich tail (5′-GCGGTCCCAAAAGGGTCAGT-3′) at their 5′ end. Repetitive Alu sequence ('AluC4') was used to normalize for the amount of input DNA2. The absolute quantitation of methylated and unmethylated *MLH1* in each sample was determined by using the Epitect human methylated and unmethylated DNA (Qiagen, Germantown, MD, USA) to create a standard curve. The SYBR Green assay results are expressed as ratios between methyl-*MLH1* or unmethyl-*MLH1* values and the ALUC4 control values. The error bars represent the s.e.m.

Exome sequencing. Exome sequencing for autopsy samples was performed using the Nimblegen EZ SeqCap kit (Roche)[1,20]. Shotgun libraries were constructed by shearing DNA and ligating sequencing adaptors. Libraries were hybridized to either the EZSeqCap V1 or V2 solution-based probe, amplified and sequenced on either the Illumina GAIIx or HiSeq platform. For all metastases, somatic mutations were called using Mutect using default parameters with matched normal (non-tumour) samples. To remove common polymorphisms and other artifacts, we imposed a number of additional requirements, including requiring variants to be observed with a variant allele fraction of at least 10% within a tumour, removing variants present within dbSNP v137 that had first been stripped of all disease-associated variants and removing variants that were present at an allele balance of 40% or more in any germline sample. All exome sequencing was performed on fresh-frozen tissue samples.

Exome data for PDX samples was from Kumar *et al.*[1], where hypermutation status was previously characterized based on the distribution of mutations across samples. For the xenografts, because corresponding normal germline DNA was not available, tumour sequences were compared against a database of common germline variants. The variants remaining were termed novel single-nucleotide variants SNVs ('novSNV') and the estimated the contribution of germline variants was ~200 and sometimes more per individual. novSNV counts from Kumar *et al.*[1] are provided in Supplementary Table 1.

Targeted deep sequencing by BROCA. Targeted deep sequencing of DNA repair pathway genes was performed using the BROCA assay in the UW clinical genetics and solid tumors laboratory[5]. Three micrograms of DNA was sonicated to a peak of 200 bp on a Covaris S2 instrument (Covaris, Woburn, MA, USA). Following sonication, DNA was purified with AMPure XP beads (Beckman Coulter, Brea CA, USA) and subjected to three enzymatic steps: end repair, A-tailing and ligation to Illumina paired-end adaptors as described in the SureSelectXT Target Enrichment for Illumina multiplexed sequencing, which is available for free download. Adapter-ligated library was PCR amplified for five cycles with Illumina primers 1.0 and 2.0 and individual paired-end libraries (500 ng) were hybridized to a custom design of complementary RNA biotinylated oligonucleotides targeting 53 genes in 52 genomic regions (Supplementary Table 2). The 120-mer oligonucleotide baits were designed in Agilent's eArray web portal with the following parameters: centred tiling, 3 × bait overlap and a maximum overlap of 20 bp into repetitive regions. The custom design targets a total of 1.4 Mb of DNA. Following capture, each library was PCR amplified for 13 cycles with primers containing a unique 6 bp index. Equimolar concentrations of 96 libraries were pooled to a final concentration of 10 pM, denatured with 3 N NaOH, and cluster amplified with a cBot instrument on a single lane of an Illumina v3 flowcell. Sequencing was performed with 2 × 101 bp paired-end reads and a 7 bp index read using SBS v3 chemistry on a HiSeq2500 (Illumina, SanDiego, CA, USA).

We used our targeted tumour sequencing bioinformatics pipeline for data analysis[21]. Reads were mapped to human reference genome (hg19/GRCh37) and alignment performed using BWA v0.6.1-r10419 and SAMtools v0.1.1820. SNV and indel calling was performed through the GATK Universal Genotyper using default parameters and using VarScan v2.3.2 and PINDEL version 0.2.42. Structural variants were identified using CREST v1.0 and BreakDancer v1.1. For copy number variant (CNV) analysis, copy number states for individual probes were initially called using CONTRA v2.0.32 with reference to a CNV control comprised of reads from two independent rounds of library preparation and sequencing of HapMap individual NA12878. CNV calls were made at the resolution of individual exons using custom Perl scripts. CNV plots were visualized using the R package ggplot2.

Phenotypic MSI was assessed directly from BROCA next-generation sequencing data using mSINGS (MSI by NGS)[22]. This method evaluated up to 146 mononucleotide microsatellite loci that are captured by BROCA in both matched normal non-tumour and tumour samples. For each specimen, microsatellite loci covered by a read depth of < 30 × were excluded as not passing quality filter. For each microsatellite locus passing quality filter, the distribution of size lengths were compared with a population of normal controls. Loci were considered unstable if the number of repeats is statistically greater than in the control population. A fraction of > 0.20 (20% unstable loci) was considered MSI-high by mSINGS based on validation with 324 tumour specimens, in which 108 cases had MSI-PCR data available as a gold standard[22].

Confirmation of *MSH2* and *MSH6* structural rearrangements. To validate structural rearrangement calls, we designed primers against regions flanking putative breakpoints using either PrimerBlast (http://www.ncbi.nlm.nih.gov/tools/primer-blast/) or Primer3 (http://bioinfo.ut.ee/primer3-0.4.0/primer3/input.htm). We used the iProof High-Fidelity PCR kit (Bio-Rad) to perform PCR under the following conditions: 98 °C for 35 s followed by 30–40 cycles of 55–69 °C for 30 s, 72 °C for 30 s and 72 °C for 10 min. Primers are listed in Supplementary Table 5. We submitted resulting PCR products to Genewiz for Sanger sequencing and aligned fragments to the human genome reference sequence (hg19) using BLAT from the UCSC Genome Browser (http://genome.ucsc.edu/cgi-bin/hgGateway).

Copy number changes were confirmed by genomic microarray. One microgram of high molecular weight genomic DNA from each sample was labelled by random priming using the Agilent Genomic DNA Enzymatic Labelling Kit (Cy3-dUTP.) A pool of reference normal DNA (Promega) was labelled with Cy5-dUTP. Cy3 and Cy5 probes were combined and hybridized to Agilent 2 × 400K SurePrint G3 CGH Microarrays and washed following the manufacturer's specifications. Fluorescent array images were collected using the Agilent DNA microarray scanner G2505C and Agilent Feature Extraction software. Data analysis was performed with Biodiscovery Nexus Copy Number 6.0 software. The FASST2 segmentation algorithm and default Agilent settings for significance, gain and loss thresholds, with at least six probes per segment were used to identify regions of CNV for each sample. Results of copy number analysis by genomic microarray are given in Supplementary Fig. 14.

References

1. Kumar, A. *et al.* Exome sequencing identifies a spectrum of mutation frequencies in advanced and lethal prostate cancers. *Proc. Natl Acad. Sci. USA* **108,** 17087–17092 (2011).
2. Barbieri, C. E. *et al.* Exome sequencing identifies recurrent SPOP, FOXA1 and MED12 mutations in prostate cancer. *Nat. Genet.* **44,** 685–689 (2012).
3. Cancer Genome Atlas Network. Comprehensive molecular characterization of human colon and rectal cancer. *Nature* **487,** 330–337 (2012).
4. Kandoth, C. *et al.* Integrated genomic characterization of endometrial carcinoma. *Nature* **497,** 67–73 (2013).
5. Pritchard, C. C. *et al.* ColoSeq provides comprehensive lynch and polyposis syndrome mutational analysis using massively parallel sequencing. *J. Mol. Diagn.* **14,** 357–366 (2012).
6. Walsh, T. *et al.* Detection of inherited mutations for breast and ovarian cancer using genomic capture and massively parallel sequencing. *Proc. Natl Acad. Sci. USA* **107,** 12629–12633 (2010).
7. Pritchard, C. C. *et al.* Validation and implementation of targeted capture and sequencing for the detection of actionable mutation, copy number variation, and gene rearrangement in clinical cancer specimens. *J. Mol. Diagn.* **16,** 56–67 (2014).

8. Jarzen, J., Diamanduros, A. & Scarpinato, K. D. Mismatch repair proteins in recurrent prostate cancer. *Adv. Clin. Chem.* **60,** 65–84 (2013).
9. Burger, M. *et al.* Elevated microsatellite instability at selected tetranucleotide repeats does not correlate with clinicopathologic features of bladder cancer. *Eur. Urol.* **50,** 770–775 (2006).
10. Chen, Y. *et al.* Defects of DNA mismatch repair in human prostate cancer. *Cancer Res.* **61,** 4112–4121 (2001).
11. Velasco, A. *et al.* Differential expression of the mismatch repair gene hMSH2 in malignant prostate tissue is associated with cancer recurrence. *Cancer* **94,** 690–699 (2002).
12. Sun, X., Chen, C., Vessella, R. L. & Dong, J. T. Microsatellite instability and mismatch repair target gene mutations in cell lines and xenografts of prostate cancer. *Prostate* **66,** 660–666 (2006).
13. Chen, Y. *et al.* Alterations in PMS2, MSH2 and MLH1 expression in human prostate cancer. *Int. J. Oncol.* **22,** 1033–1043 (2003).
14. Dahiya, R. *et al.* High frequency of genetic instability of microsatellites in human prostatic adenocarcinoma. *Int. J. Cancer* **72,** 762–767 (1997).
15. Watanabe, M. *et al.* Microsatellite instability in human prostate cancer. *Br. J. Cancer* **72,** 562–564 (1995).
16. Baca, S. C. *et al.* Punctuated evolution of prostate cancer genomes. *Cell* **153,** 666–677 (2013).
17. White, N. M., Feng, F. Y. & Maher, C. A. Recurrent rearrangements in prostate cancer: causes and therapeutic potential. *Curr. Drug Targets* **14,** 450–459 (2013).
18. Wu, D., Zhang, C., Shen, Y., Nephew, K. P. & Wang, Q. Androgen receptor-driven chromatin looping in prostate cancer. *Trends Endocrinol. Metab.* **22,** 474–480 (2011).
19. Petko, Z. *et al.* Aberrantly methylated CDKN2A, MGMT, and MLH1 in colon polyps and in fecal DNA from patients with colorectal polyps. *Clin. Cancer Res.* **11,** 1203–1209 (2005).
20. O'Roak, B. J. *et al.* Exome sequencing in sporadic autism spectrum disorders identifies severe de novo mutations. *Nat. Genet.* **43,** 585–589 (2011).
21. Pritchard, C. C. *et al.* Validation and implementation of targeted capture and sequencing for the detection of actionable mutation, copy number variation, and gene rearrangement in clinical cancer specimens. *J. Mol. Diagn.* **16,** 56–67 (2014).
22. Salipante, S. J., Scroggins, S. M., Hampel, H. L., Turner, E. H. & Pritchard, C. C. Microsatellite instability detection by next-generation sequencing. *Clin. Chem.* 24987110 (2014).

Acknowledgements

We thank Karen Koehler and Tatyana Marushchak for help with library preparation and sequencing. We thank Deborah Barden, Rachel Slusher, Laura Akagi and Youly Welt for their help in preparing the genomic DNA and with MSI-PCR. We thank Emily Turner for help with data analysis. We thank the University of Washington Rapid Autopsy team members and most importantly the patients and families who participated in research studies. This work was supported by awards P50CA097186, CA085859 and CA163227 from the National Cancer Institute, CDMRP awards PC131820 and PC093372P1 and a 2013 Young Investigator Award from the Prostate Cancer Foundation.

Author contributions

C.C.P. conceived and designed the study, coordinated sample acquisition and processing and performed primary data analyses. C.M., A.K. and P.S.N. assisted with the study design. T.W., J.S., R.L.V., E.C. and J.F.T. assisted with the study design and reviewed the manuscript. R.L.V., C.M. and E.C. were involved in metastasis and PDX tissues collection and selection. A.K., J.M. and S.J.S. performed confirmatory Sanger sequencing studies. C.M. and X.Z. performed and analyzed the IHC studies. C.S., I.C. and A.K. assisted with the genomic sequencing. I.C., S.J.S., C.C.P. and A.K. coordinated informatics analyses. W.M.G. and M.Y. performed *MLH1* methylation studies. C.C.P., P.S.N., R.L.V., T.W. and J.S. directed the research. C.C.P. wrote the manuscript, with contributions from P.S.N., A.K. and C.M.

Additional information

Accession codes: Sequencing data reported in this manuscript have been deposited in GenBank/EMBL/DDBJ under the accession code SRP044943.

Supplementary Information accompanies this paper at http://www.nature.com/naturecommunications

Competing financial interests: The authors declare no competing financial interests.

Reprints and permission information is available online at http://npg.nature.com/reprintsandpermissions/

How to cite this article: Pritchard, C. C. *et al.* Complex *MSH2* and *MSH6* mutations in hypermutated microsatellite unstable advanced prostate cancer. *Nat. Commun.* 5:4988 doi: 10.1038/ncomms5988 (2014).

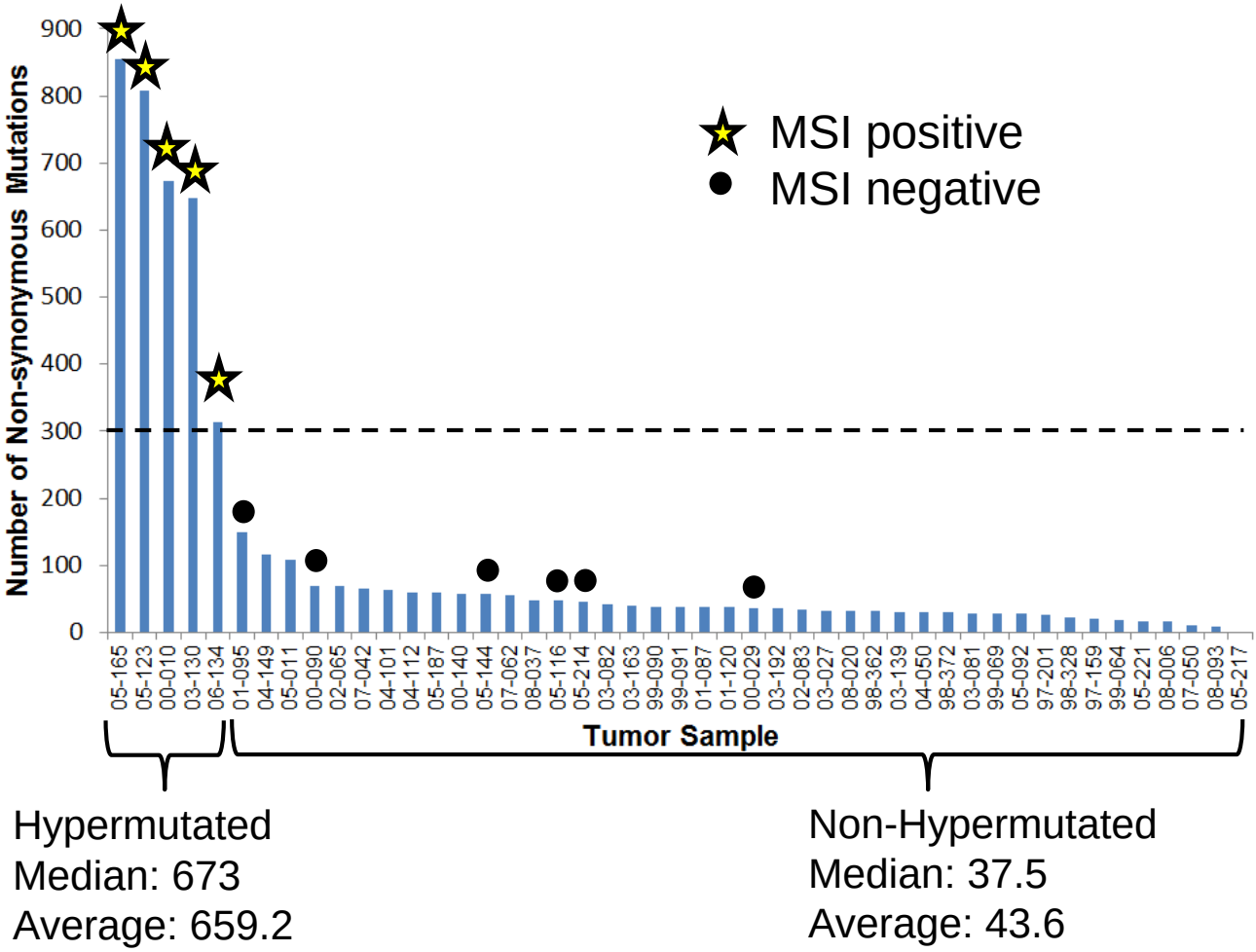

Supplementary Figure 1: Somatic Mutation Burden in Autopsy Cases by Exome Sequencing. Total number of somatic nonsynonymous mutations by exome sequencing for rapid autopsy cases. The threshold of 300 mutations used to determine hypermutation status is shown with the dashed line. Median and average mutation burden is given for both groups. Cases that had microsatellite instability testing are shown with yellow stars (positive) and black circles (negative).

LuCaP 58

1) *MSH6* del exon 8 through 3'UTR

2) *MSH6* frameshift (c.3799_3800del)

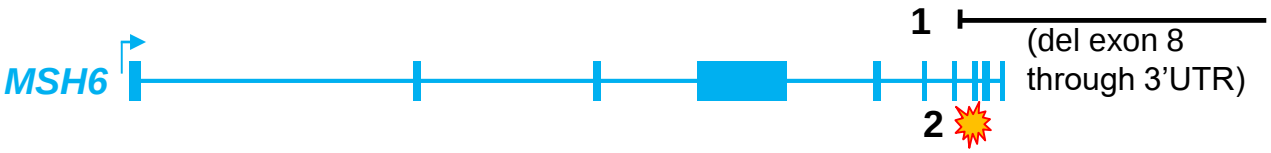

1)

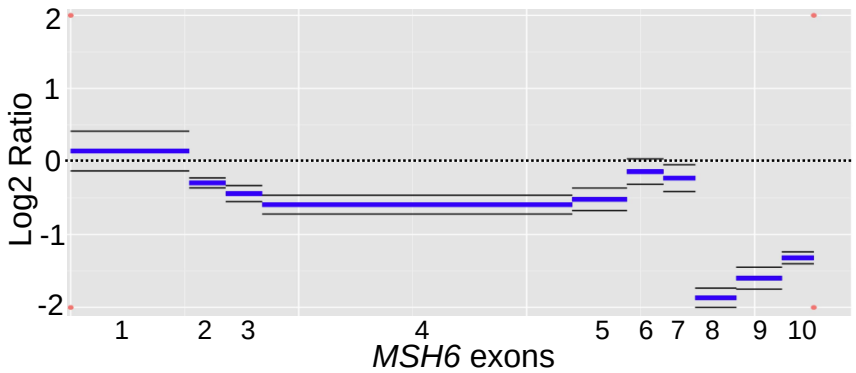

Deletion of exon 8 through 3'UTR

2) *MSH6* c.3799_3800del, p.M1267Gfs*7

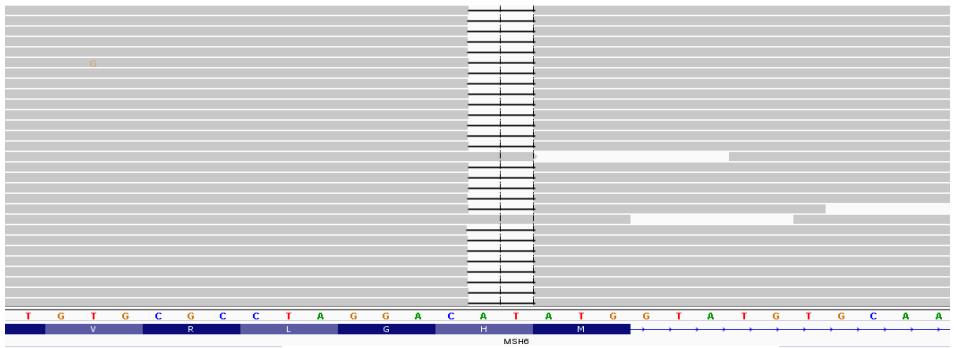

chr2:48033493-48033494delAT

Supplementary Figure 2: Detail on Mismatch Repair Gene Mutations in LuCaP 58. Two inactivating mutations were detected in *MSH6*. The first (1) is a deletion of exon 8 through the 3'UTR (top). Copy number was calculated from normalized depth of coverage of BROCA sequencing data and confirmed by genomic microarray (data not shown). The blue bars indicate exons 1-10 (from left to right) and black bars are the standard deviation of the measurement of Log2 ratio. The second (2) is a 2bp deletion resulting in a frameshift and premature truncation of the MSH6 protein (c.3799_3800del, bottom). Shown is a screenshot from the integrated genomics viewer of representative sequencing reads. The black bars indicated the deleted bases. The frameshift was detected in 314 out of a total of 360 sequencing reads, strongly supporting that there is bi-allelic inactivation of *MSH6*.

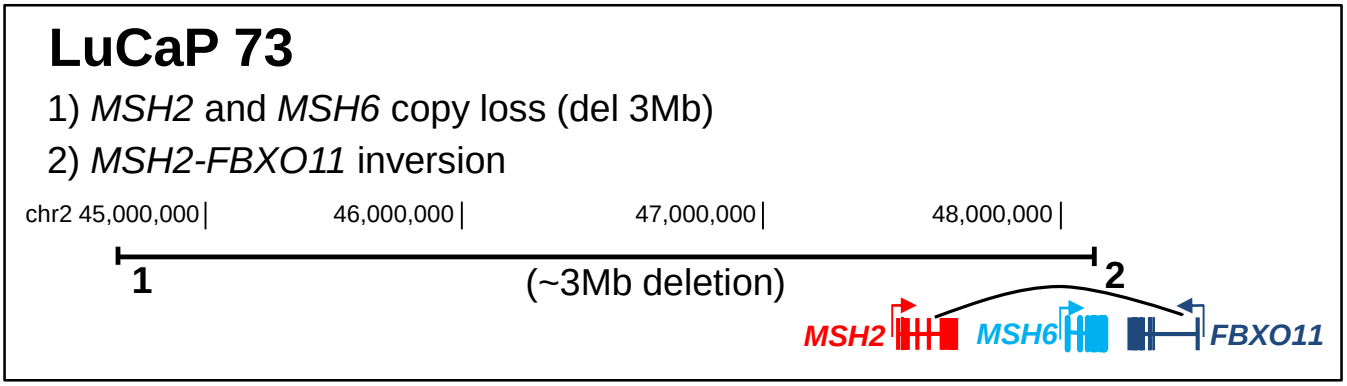

1) ~3MB deletion deletes *MSH2* and most of *MSH6*

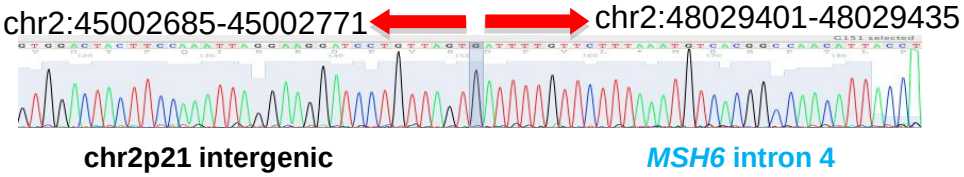

2) 440kb inversion splits the *MSH2* gene

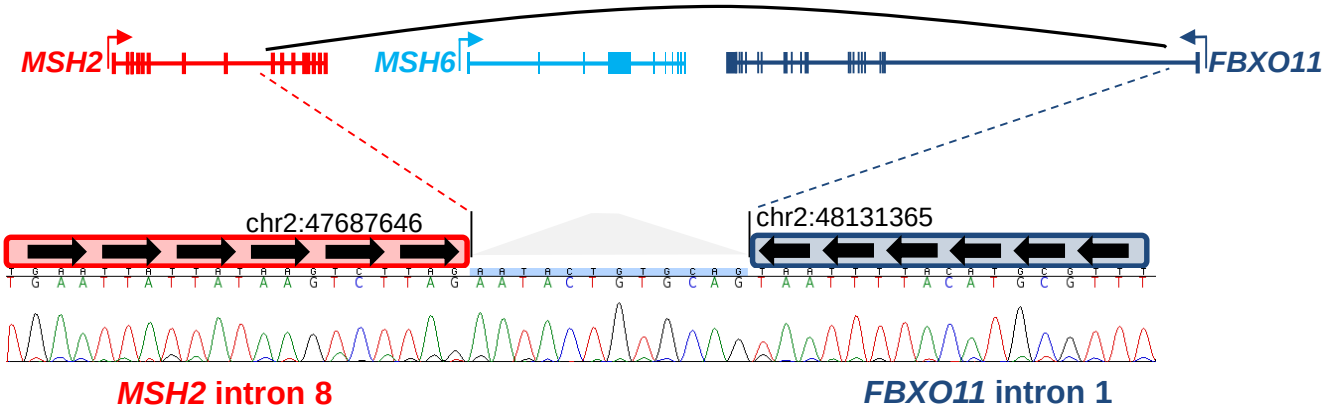

Supplementary Figure 3: Detail on Mismatch Repair Gene Mutations in LuCaP 73. Two large rearrangement mutations were detected at the *MSH2/MSH6* locus on chromosome 2 predicted to result in bi-allelic inactivation of *MSH2*. The first (1) is a 3Mb deletion that deletes both the MSH2 and MSH6 genes. The breakpoints where confirmed by Sanger sequencing as chr2:45,002,771-48,029,401 in hg19 genomic coordinates (top). The second (2) is a 440kb inversion mutation between *MSH2* intron 8 and *FBXO11* intron 1 that splits the *MSH2* gene and is predicted to result in loss of function. The breakpoints of the inversion were confirmed by Sanger sequencing as chr2:47687644-chr2:48131365 (bottom). There is a short inserted sequence between the two breakpoints.

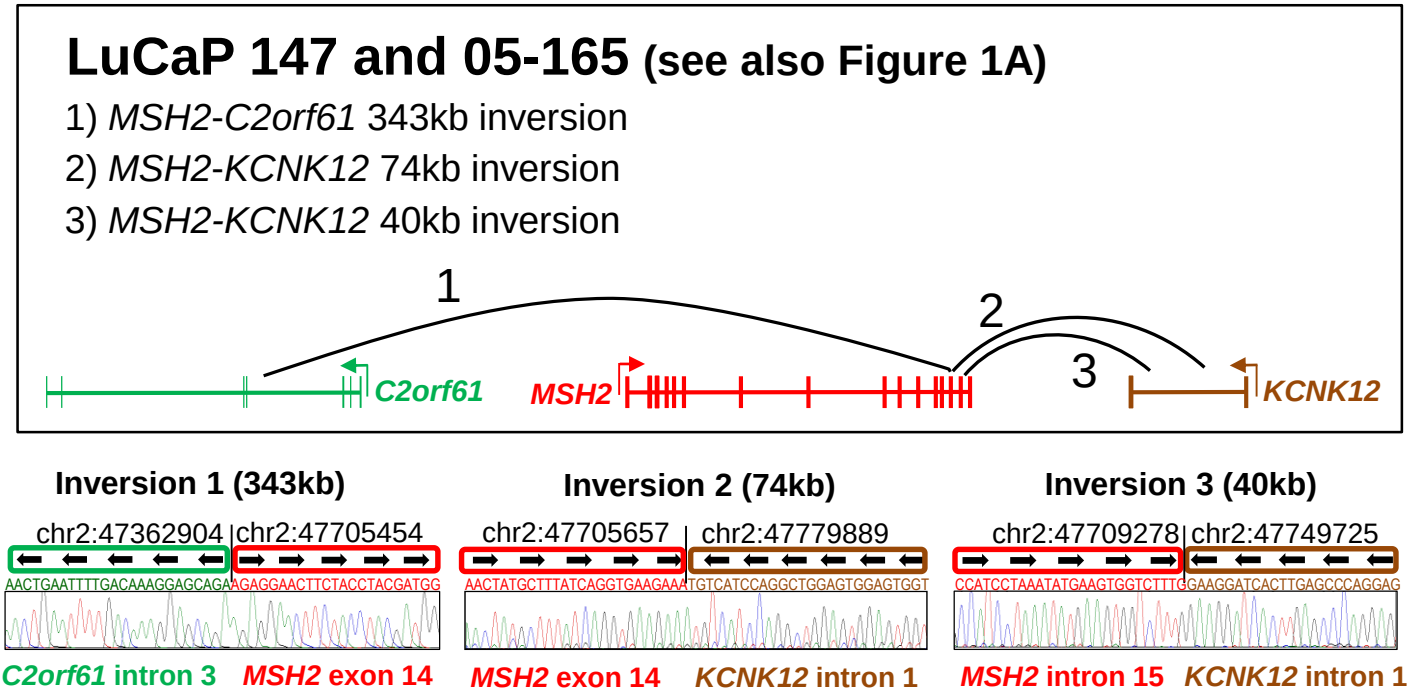

Supplementary Figure 4: Detail on Mismatch Repair Gene Mutations in LuCaP 147 and 05-165. Three different inversion mutations were detected involving the *MSH2* gene that are predicted to result in loss-of-function. The inversions were detected in all metastatic sites (bone, adrenal, liver, and lymph node). Each inversion was confirmed by Sanger sequencing with breakpoints given in hg19 genomic coordinates. LuCaP 147 was derived from autopsy patient 05-165 and the same mutations were detected in both, indicating that the *MSH2* structural rearrangements are not a result of xenografting.

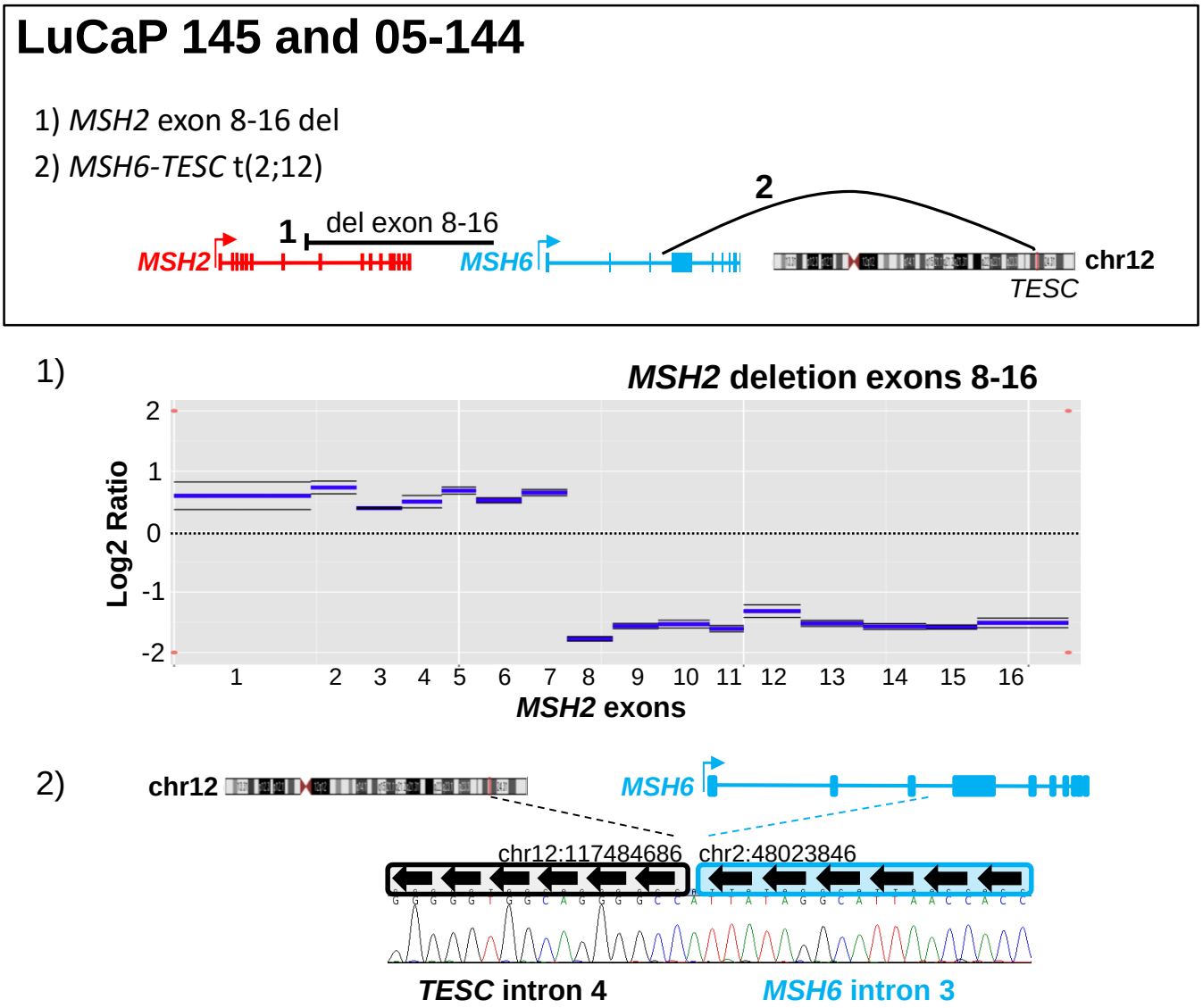

Supplementary Figure 5: Detail on Mismatch Repair Gene Mutations in LuCaP 145 and 05-144. Two mutations were detected. The first (1) is copy loss of exons 8-16 of *MSH2* (top). Copy number was calculated from normalized depth of coverage of BROCA sequencing data and confirmed by genomic microarray (data not shown). The blue bars indicate *MSH2* exons 1-16 (from left to right) and black bars are the standard deviation of the measurement of Log2 ratio. The second (2) is a translocation between *MSH6* intron 3 and *TESC* intron 4 on chromosome 12 q24.22. The breakpoints of the translocation were confirmed by Sanger sequencing. These tumors had neuroendocrine differentiation. Unlike the other tumors *MSH2/MSH6* rearrangements these tumors were not hypermutated and did not demonstrate MSI, most likely because one copy of *MSH2* and *MSH6* remain functionally intact. One hypothesis is that the cancer was 'transitioning' to a hypermutated state when the patient died, with a second hit in the *MSH2* or *MSH6* gene not yet acquired. LuCaP 145 was derived from autopsy patient 05-144 and the same mutations were detected in both, indicating that the structural rearrangements are not a result of xenografting.

Supplementary Figure 6

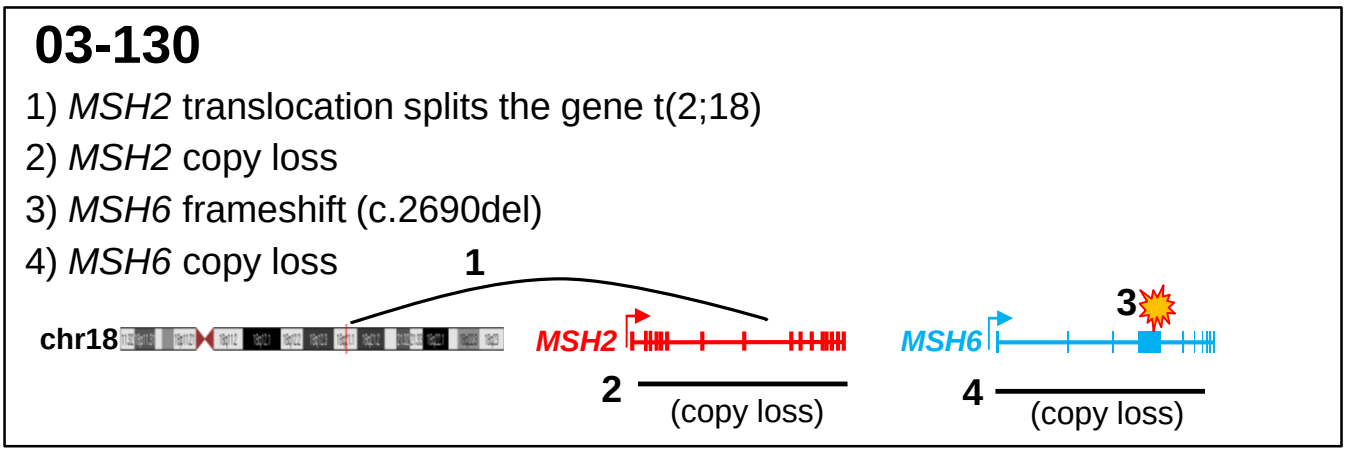

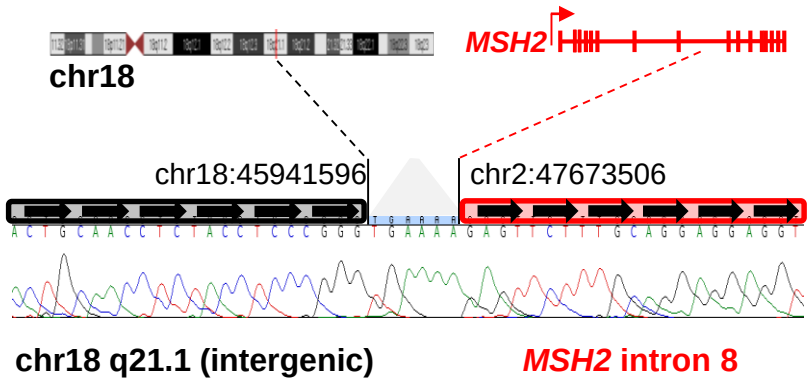

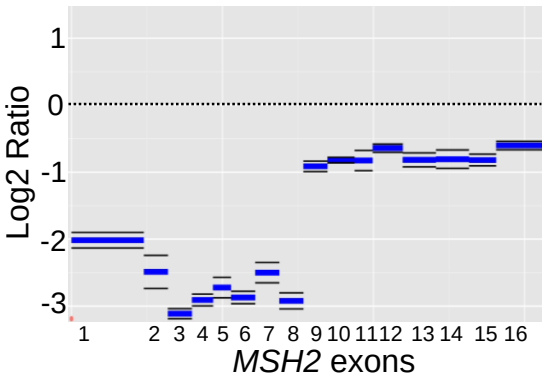

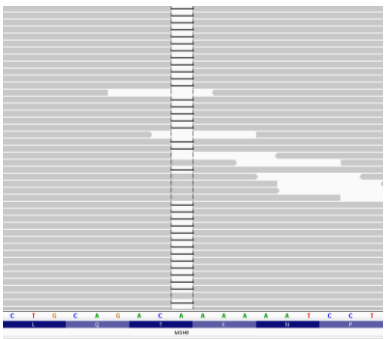

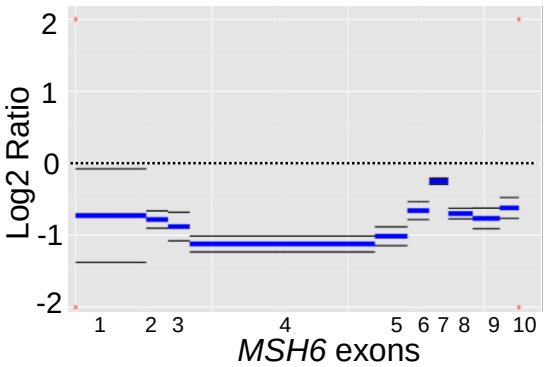

Supplementary Figure 6: Detail on Mismatch Repair Gene Mutations in 03-130. There was evidence of bi-allelic loss-of-function mutations in *MSH2* and *MSH6*. The first mutation (1) is a translocation between *MSH2* intron 8 *and* chr18 q21.1 (top left), in which the breakpoints were confirmed by Sanger sequencing. The second (2) is copy loss of *MSH2* (top right, homozygous in exons 1-8, likely as a result of the *MSH2* translocation). The third (3) is frameshift mutation in exon 4 of MSH6 (c.2690del, p.N897IfsX9). The black bars indicated the deleted bases. The frameshift was detected in 366 out of a total of 547 sequencing reads (67%), despite admixture of tumor with normal cells in the sample tested, supporting that there is bi-allelic inactivation of *MSH6* in tumor. The fourth (4) is copy loss of *MSH6*, probably single copy. In copy number plots blue bars indicate exons and black bars are the standard deviation of the measurement of Log2 ratio. Copy number was calculated by normalized depth of coverage of BROCA sequencing and confirmed by genomic microarray (data not shown)

06-134

MLH1 homozygous copy loss

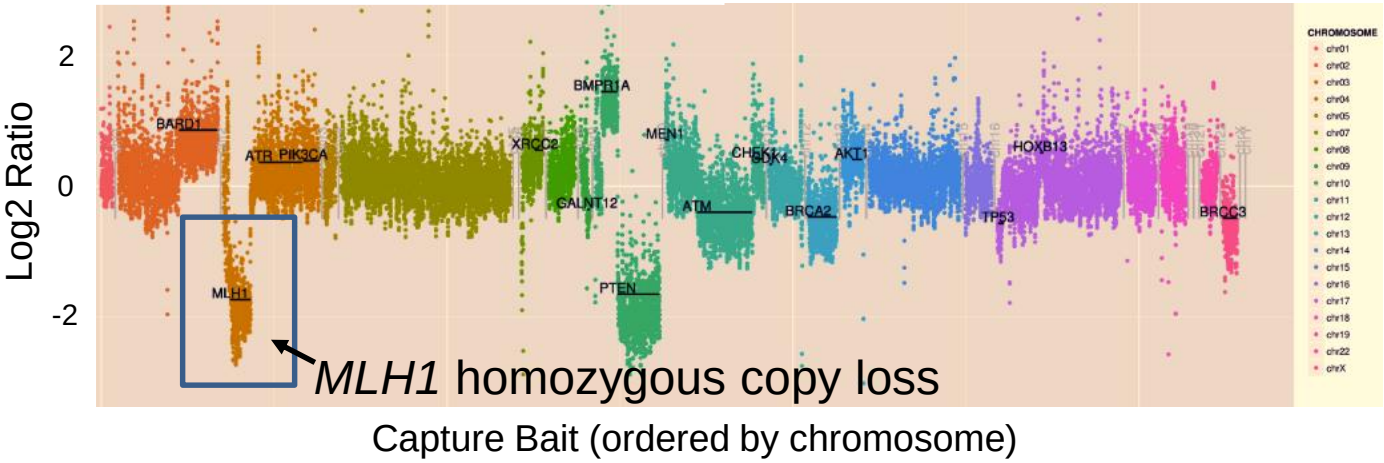

Supplementary Figure 7: Detail on Mismatch Repair Gene Mutations in 06-134. The sample tested had *MLH1* copy loss which is very likely to be homozygous and result in complete loss of MLH1 protein function. Depicted is copy number analysis by BROCA targeted deep sequencing. *MLH1* deletion was confirmed by genomic microarray (data not shown). The Log2 ratio in relationship to a normal female control patient. *BRCC3* (far right) on the X chromosome can be used to calibrate the Log2 ratio expected with heterozygous copy loss because this is a male patient. *PTEN* is also deleted in this patient's tumor, a common event in metastatic prostate cancer.

00-010

MSH2 frameshift (c.2364_2365insTACA, p.A789YfsX11)

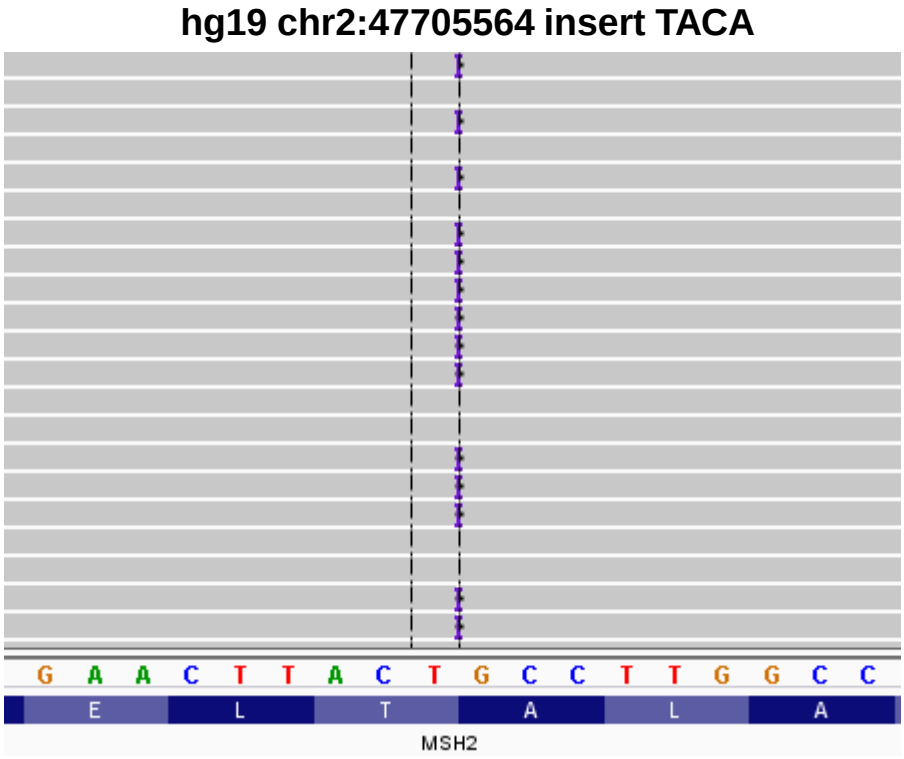

Supplementary Figure 8: Detail on Mismatch Repair Gene Mutations in 00-010. The primary prostate and liver tumor metastasis samples tested had a frameshift loss-of-function mutation in *MSH2* (c.2364_2365insTACA, p.A789YfsX11). The purple "I" indicates the position of the inserted bases, visualized in the integrated genomics viewer. A second loss-of-function mutation was not detected. It is suspected a second *MSH2* loss-of-function mutation is present because the case was MSI high, had loss of MSH2 and MSH6 protein by IHC, was *MLH1* unmethylated, and had intact MLH1 protein IHC (see separate figures).

05-0123

1) *MSH2* frameshift (c.1124_1125insG)
2) *MSH2* frameshift (c.1082del)
3) *MLH1* frameshift (c.1310del), lymph node only

MSH2 c.1082del, p.N361IfsX2
chr2:47656885delA

MSH2 c.1124_1125insG, p.L376FfsX13
chr2:47656928insG

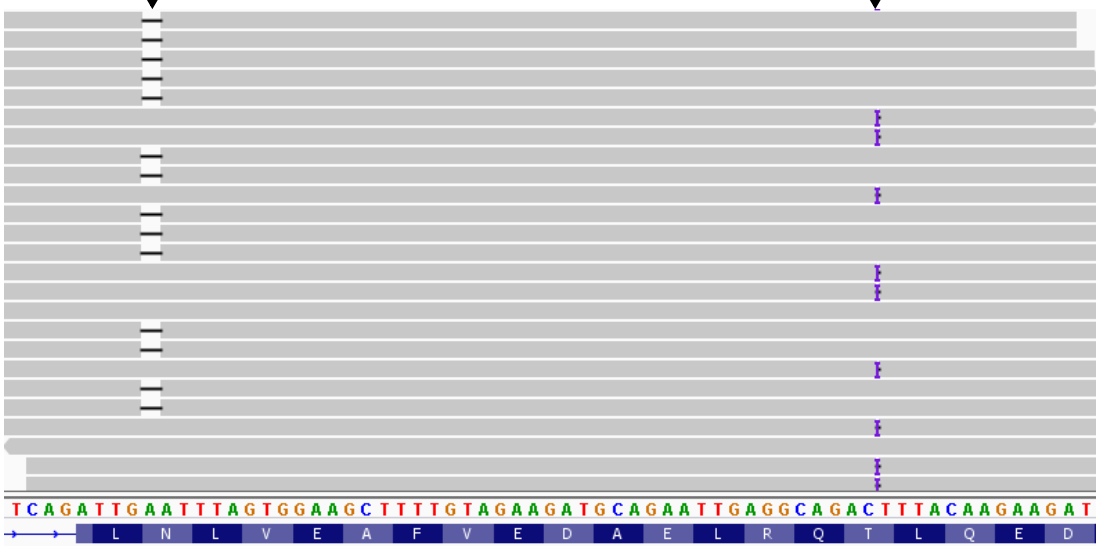

MSH2 exon 7

chr3:37067396delC

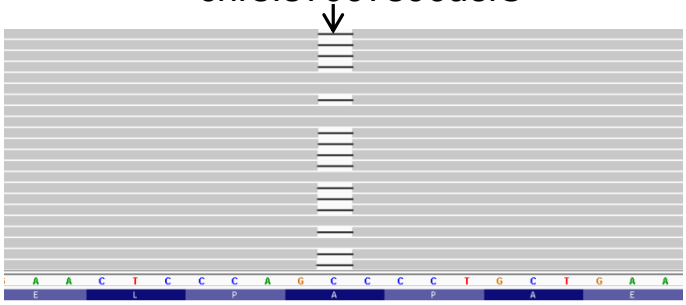

MLH1 exon 12

MLH1 c.1310del, p.P437LfsX54
(Lymph node metastasis only)

Supplementary Figure 9: Detail on Mismatch Repair Gene Mutations in 05-123. The primary prostate and lymph node metastasis tumor samples tested had bi-allelic frameshift loss-of-function mutations in *MSH2* exon 7 (c.1082del and c.1124_1125insG, top). The black bars indicate sequencing reads with the c.1082del deletion; the purple "I" indicates the position of the inserted bases in the c.1124_1125insertion, visualized in the integrated genomics viewer. Note that these two mutations do not occur on sequencing reads from the same allele, strongly supporting that they are *in trans (*bi-allelic). In addition, an *MLH1* frameshift mutation in exon 12 (c.1310delC) was detected in the lymph node metastasis sample only (bottom).

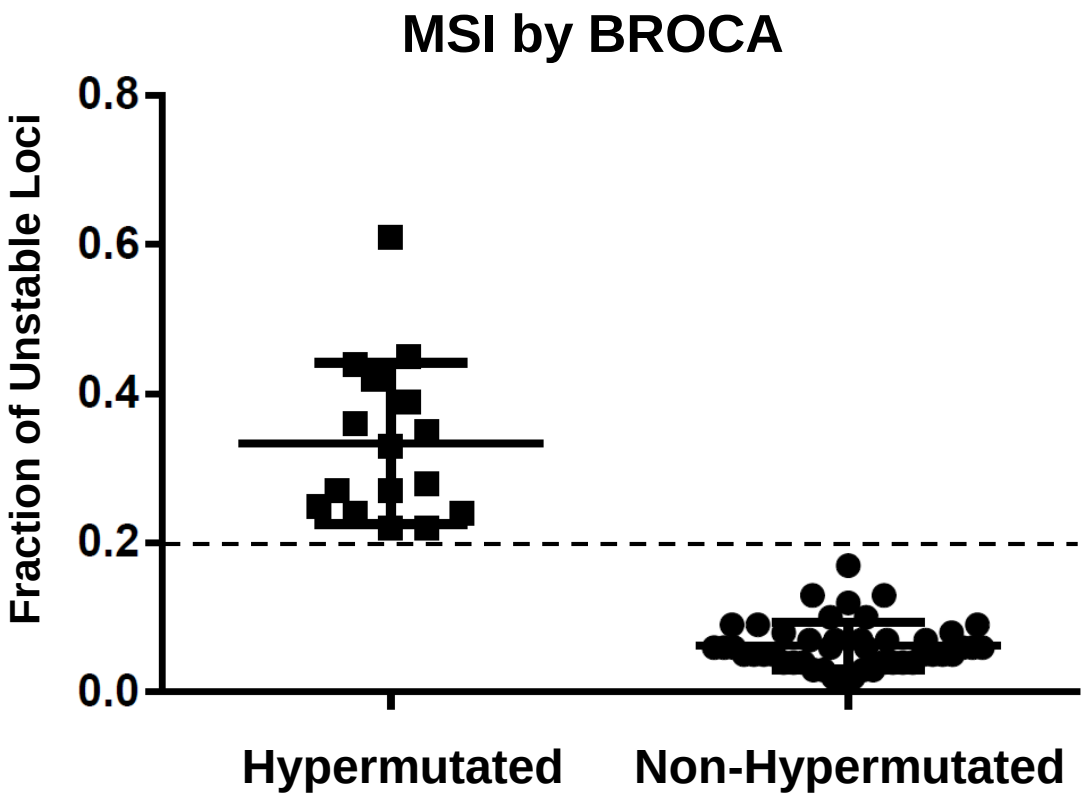

Supplementary Figure 10: Microsatellite Instability Results by BROCA Next-Generation Sequencing. We developed an approach to measure microsatellite instability directly from next-generation sequencing data that we call mSINGS. This method is described in the methods section (Salipante et al. 2014 *Clinical Chemistry*, in press). The fraction of unstable microsatellite loci out of a maximum of 146 mononucleotide microsatellite loci captured by BROCA is given on the y-axis. A threshold of 0.2 (20%) unstable loci was established as a cutoff for microsatellite instability (dashed line). Solid lines represent the median fraction of unstable loci for hypermutated and non-hyermutated cases. The raw data used to generate this summary figure, including which loci were unstable by BROCA in each sample is given in Supplementary Data 3.

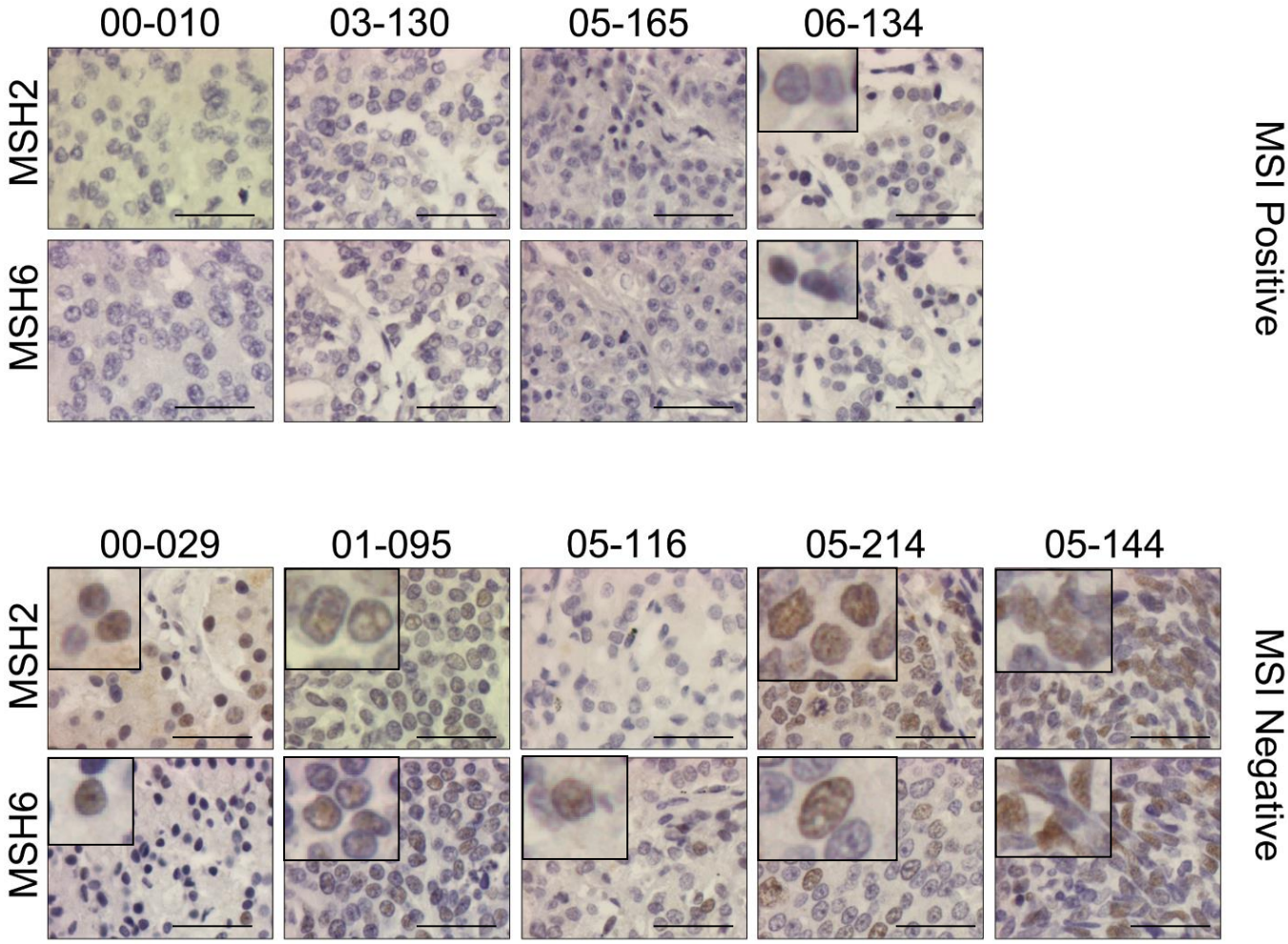

Supplementary Figure 11: IHC results for prostate rapid autopsy metastasis samples. Hypermutated MSI positive autopsy cases 00-010, 03-130, 05-165, which harbored somatic mutations in *MSH2*, *MSH6* or both genes show complete loss of MSH2 and MSH6 expression by IHC using a tissue microarray (top panels). Tissue was not available for IHC studies in hypermutated case 05-123. Hypermutated MSI positive case 06-134, which had somatic deletion of *MLH1*, has focal intact nuclear expression of MSH2 and MSH6 protein (top left, insets). By contrast, MSH2 and MSH6 nuclear staining is intact in MSI-negative autopsy cases 00-029, 01-095, 05-214, and 05-144 (bottom panels, examples of positive nuclear staining in insets). MSH6, but not MSH2 protein expression was detected MSI-negative case 05-116, a case that also had absent MLH1 protein (see separate figure). This could reflect a false negative result due to poor quality tissue for this sample on the tissue microarray. For MSH2 and MSH6, heterogeneity of immunostaining is common in tumor tissue, and protein expression is generally considered intact if any cells display positive nuclear staining. Because MSH2 and MSH6 function as a heterodimer, mutations in one gene frequently result in loss of expression of both proteins, particularly when there are *MSH2* mutations. All samples are from metastases and not primary tumors. Scale bar: 0.1mm.

Supplementary Figure 12

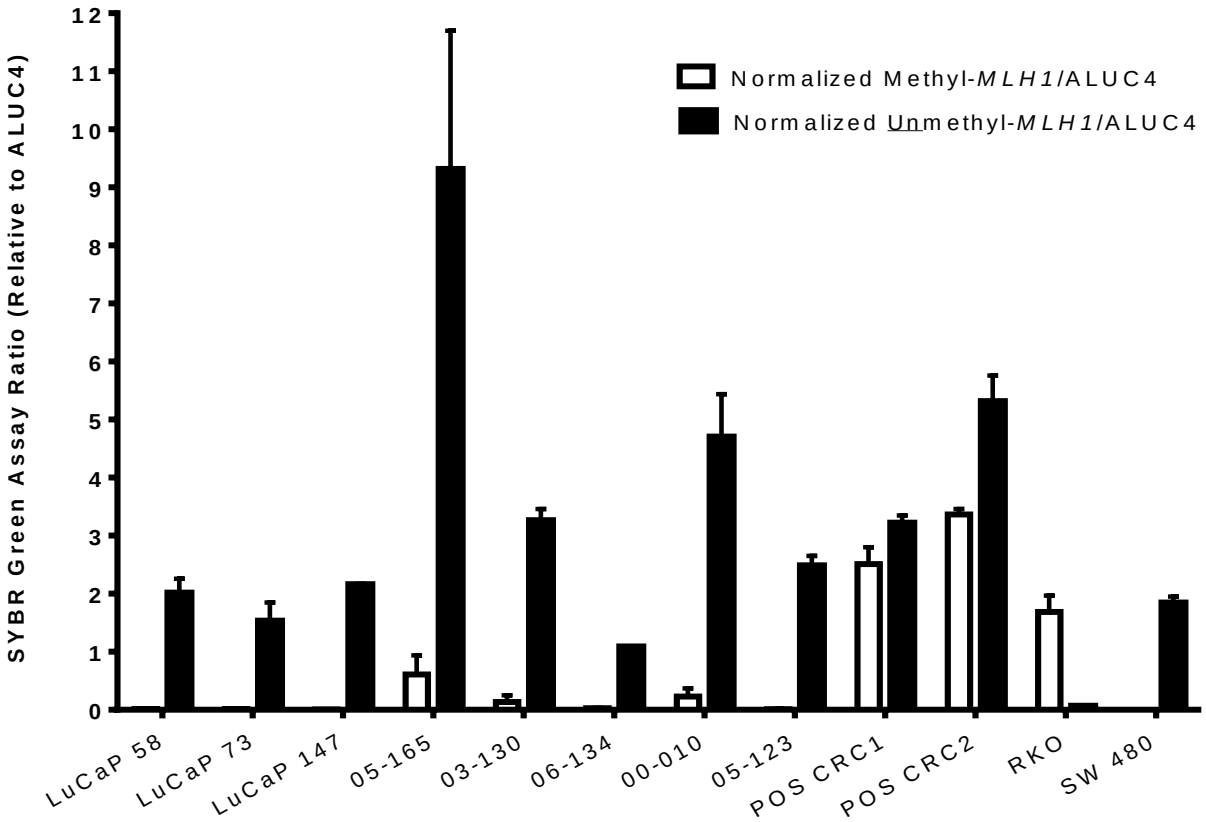

Sample	*MLH1* methylation status
LuCaP 58	Unmethylated
LuCaP 73	Unmethylated
LuCaP 147	Unmethylated
05-165-K3	Unmethylated
03-130-L2	Unmethylated
06-134-P1	Unmethylated
00-010	Unmethylated
05-123-D1	Unmethylated
POS CRC 1 (known methylated colon tumor)	Methylated
POS CRC 2 (known methylated colon tumor)	Methylated
RKO (positive control cell line)	Methylated
SW 480 (negative control cell line)	Unmethylated

Supplementary Figure 12: Hypermutated Prostate Tumors Do Not Exhibit *MLH1* Methylation. Results of a *MLH1* methylation-specific SYBR green assay are expressed as ratios between Methyl-MLH1 or Unmethyl-MLH1 values and the ALUC4 control values. Genomic DNA samples were bisulfite-treated with EZ DNA Methylation Kit (Zymo Research, Irvine, CA) according to manufacturer's protocol. The primers used in the SYBR Green Assay were previously described (see methods). The error bars represent the standard error of the mean. DNA samples from 2 known *MLH1* methylated colon cancer tumors (POS CRC1 and POS CRC2) and cancer cell lines RKO (methylated) and SW480 (unmethylated) are used as controls for the assay.

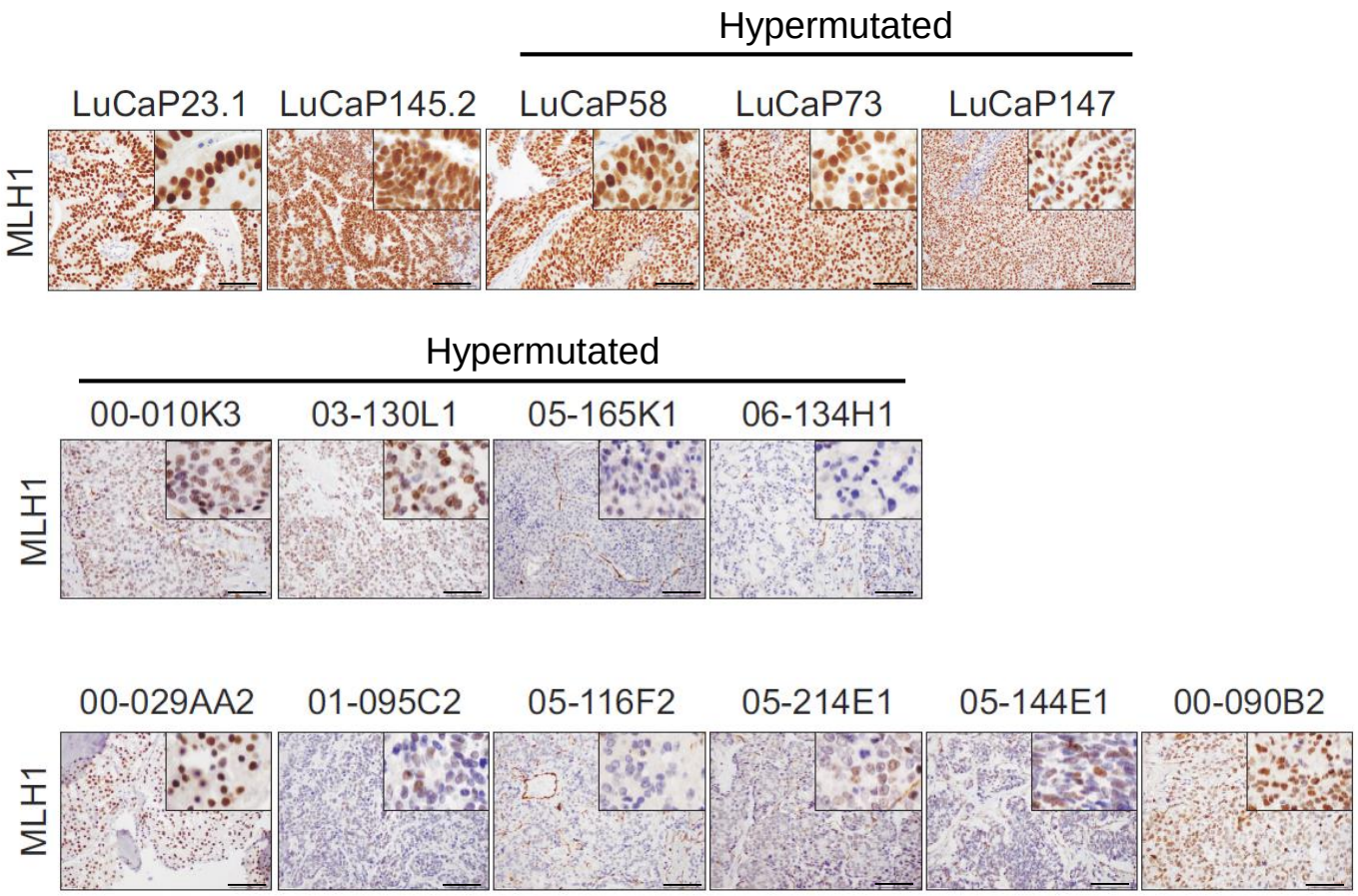

Supplementary Figure 13: Hypermutated MSI Positive Prostate Tumors With *MSH2* or *MSH6* mutations have intact MLH1 protein by IHC. Hypermutated MSI positive cases LuCaP 58, LuCaP 73, LuCaP 147 (top) and autopsy cases 00-010, 03-130, 05-165 (middle), which harbored somatic mutations in *MSH2*, *MSH6* or both have intact MLH1 expression by IHC using a tissue microarray. This corroborates the *MLH1* methylation studies and strongly argues against *MLH1* epigenetic silencing as a mechanism of MSI in these tumors. Hypermutated MSI positive case 06-134 that had homozygous deletion of *MLH1* has absent MLH1 protein. Tissue was not available for IHC studies in hypermutated case 05-123. MLH1 protein expression was not detected MSI-negative case 05-116 (bottom), a case that also had absent MSH2 protein (see separate figure). This could reflect a false negative result due to poor quality tissue for this sample on the tissue microarray. For MLH1, heterogeneity of immunostaining is common in tumor tissue, and protein expression is generally considered intact if any cells display positive nuclear staining. Scale bar: 0.1mm.

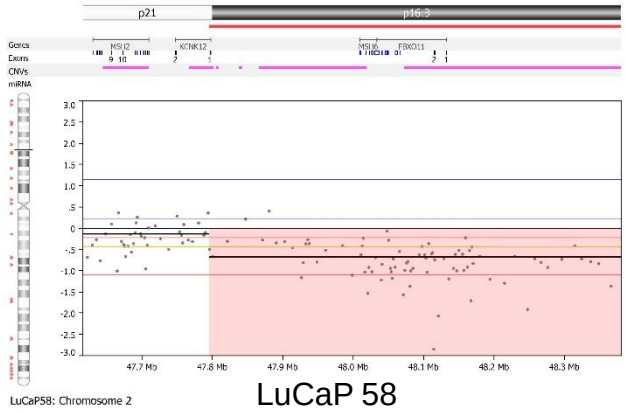

LuCaP 58

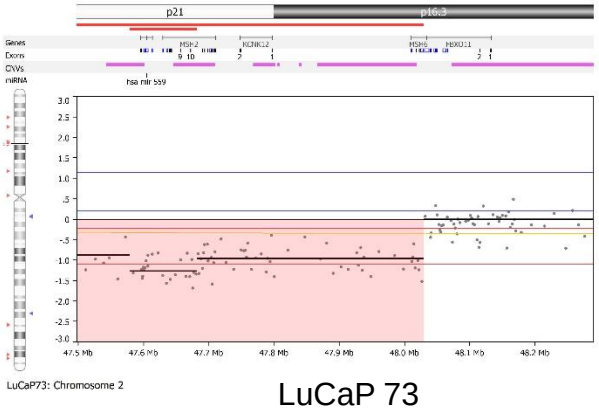

LuCaP 73

LuCaP 147 and 05-165

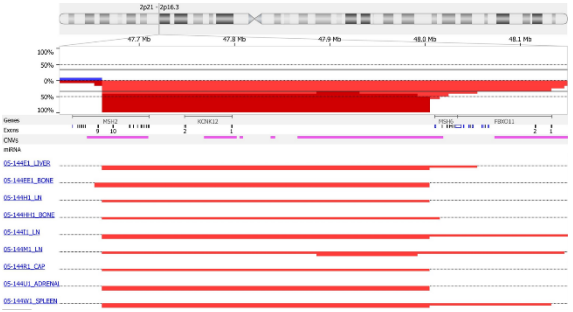

05-144

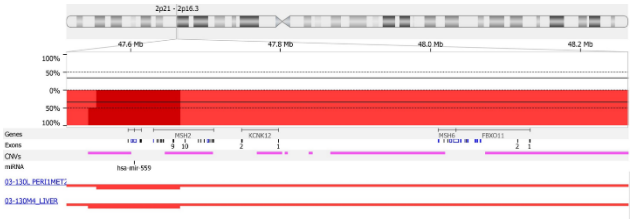

03-130

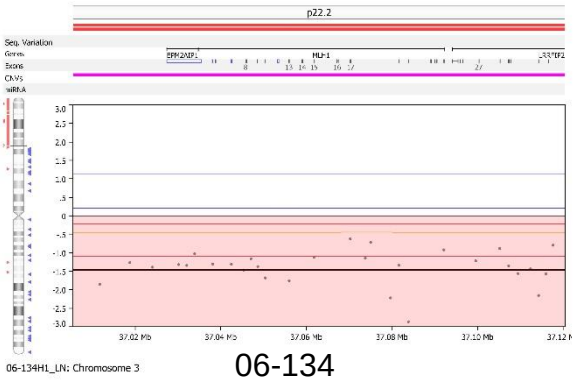

06-134

Supplementary Figure 14: Confirmation of *MSH2*, *MSH6*, and *MLH1* Copy Number Status by Genomic Microarray. Genomic microarray (array CGH) was performed for all cases that had *MSH2* and *MSH6* structural rearrangements and also for case 06-134 with *MLH1* homozygous gene deletion. The genomic loci are given along the top of each panel. Y axes are log2 ratio compared to normal control. Red indicates deletion. The results are concordant with copy number status as assessed by BROCA next-generation sequencing.

Resource

Cell

Integrative Clinical Genomics of Advanced Prostate Cancer

Graphical Abstract

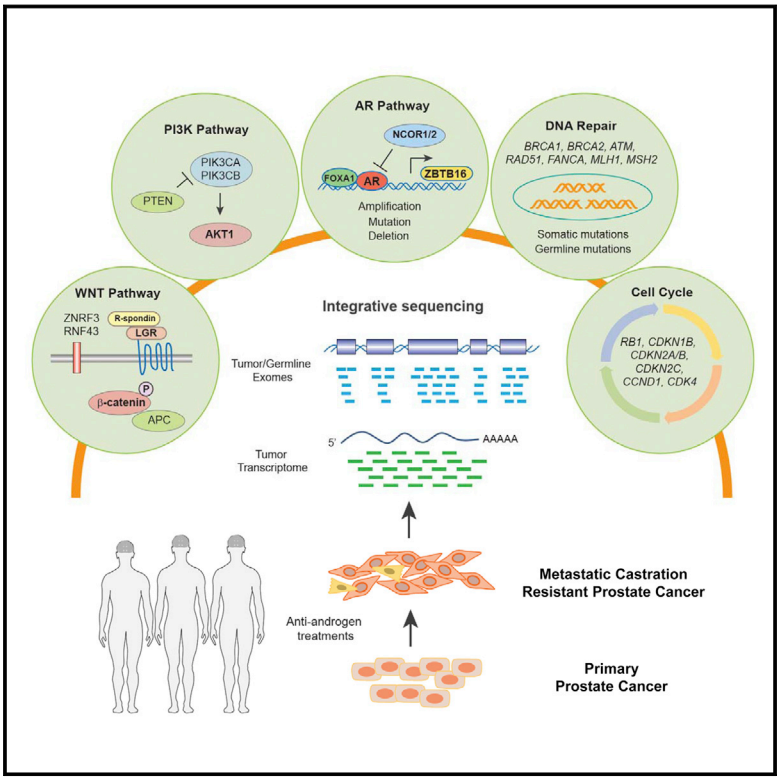

Highlights

- A multi-institutional integrative clinical sequencing of mCRPC
- Approximately 90% of mCRPC harbor clinically actionable molecular alterations
- mCRPC harbors genomic alterations in *PIK3CA/B*, *RSPO*, *RAF*, *APC*, β-catenin, and *ZBTB16*
- 23% of mCRPC harbor DNA repair pathway aberrations, and 8% harbor germline findings

Authors

Dan Robinson, Eliezer M. Van Allen, ..., Charles L. Sawyers, Arul M. Chinnaiyan

Correspondence

sawyersc@mskcc.org (C.L.S.), arul@umich.edu (A.M.C.)

In Brief

A multi-institutional integrative clinical sequencing analysis reveals that the majority of affected individuals with metastatic castration-resistant prostate cancer harbor clinically actionable molecular alterations, highlighting the need for genetic counseling to inform precision medicine in affected individuals with advanced prostate cancer.

Robinson et al., 2015, Cell *161*, 1215–1228
May 21, 2015
http://dx.doi.org/10.1016/j.cell.2015.05.001

CellPress

Cell

Integrative Clinical Genomics of Advanced Prostate Cancer

Dan Robinson,[1,2,43] Eliezer M. Van Allen,[3,4,43] Yi-Mi Wu,[1,2] Nikolaus Schultz,[5,40] Robert J. Lonigro,[1] Juan-Miguel Mosquera,[6,7,8,38] Bruce Montgomery,[9,10] Mary-Ellen Taplin,[3] Colin C. Pritchard,[26] Gerhardt Attard,[11,12] Himisha Beltran,[7,8,13,38] Wassim Abida,[14,20] Robert K. Bradley,[9] Jake Vinson,[15] Xuhong Cao,[1,42] Pankaj Vats,[1] Lakshmi P. Kunju,[1,2,17] Maha Hussain,[16,17,18] Felix Y. Feng,[1,17,19] Scott A. Tomlins,[1,2,17,18] Kathleen A. Cooney,[16,17,18] David C. Smith,[16,17,18] Christine Brennan,[1] Javed Siddiqui,[1] Rohit Mehra,[1,2] Yu Chen,[13,14,20] Dana E. Rathkopf,[13,20] Michael J. Morris,[13,20] Stephen B. Solomon,[21] Jeremy C. Durack,[21] Victor E. Reuter,[22] Anuradha Gopalan,[22] Jianjiong Gao,[40] Massimo Loda,[3,4,23,39] Rosina T. Lis,[3,23] Michaela Bowden,[3,23,39] Stephen P. Balk,[24] Glenn Gaviola,[25] Carrie Sougnez,[4] Manaswi Gupta,[4] Evan Y. Yu,[10] Elahe A. Mostaghel,[9,10] Heather H. Cheng,[9,10] Hyojeong Mulcahy,[27] Lawrence D. True,[28] Stephen R. Plymate,[10] Heidi Dvinge,[9] Roberta Ferraldeschi,[11,12] Penny Flohr,[11,12] Susana Miranda,[11,12] Zafeiris Zafeiriou,[11,12] Nina Tunariu,[11,12] Joaquin Mateo,[11,12] Raquel Perez-Lopez,[11,12] Francesca Demichelis,[7,29] Brian D. Robinson,[6,7,8,38] Marc Schiffman,[7,31,38] David M. Nanus,[7,8,13,38] Scott T. Tagawa,[7,8,13,38] Alexandros Sigaras,[7,30,32] Kenneth W. Eng,[7,30,32] Olivier Elemento,[30] Andrea Sboner,[6,7,30,38] Elisabeth I. Heath,[33,34] Howard I. Scher,[13,20] Kenneth J. Pienta,[35] Philip Kantoff,[3,44] Johann S. de Bono,[11,12,44] Mark A. Rubin,[6,7,8,38,44] Peter S. Nelson,[10,36,37,38,44] Levi A. Garraway,[3,4,44] Charles L. Sawyers,[14,41,44,*] and Arul M. Chinnaiyan[1,2,17,18,42,44,*]

[1]Michigan Center for Translational Pathology, University of Michigan Medical School, Ann Arbor, MI 48109, USA
[2]Department of Pathology, University of Michigan Medical School, Ann Arbor, MI 48109, USA
[3]Department of Medical Oncology, Dana-Farber Cancer Institute, Boston, MA 02215, USA
[4]Broad Institute of Massachusetts Institute of Technology and Harvard, Cambridge, MA 02142, USA
[5]Department of Epidemiology and Biostatistics, Memorial Sloan Kettering Cancer Center, New York, NY 10065, USA
[6]Department of Pathology and Laboratory Medicine, Weill Medical College of Cornell University, New York, NY 10021, USA
[7]Institute for Precision Medicine, Weill Medical College of Cornell University, New York, NY 10021, USA
[8]New York Presbyterian Hospital, New York, NY 10021, USA
[9]Computational Biology Program, Public Health Sciences Division and Basic Science Division, Fred Hutchinson Cancer Center, University of Washington, Seattle, WA 98109, USA
[10]Department of Medicine and VAPSHCS, University of Washington, Seattle, WA 98109, USA
[11]Cancer Biomarkers Team, Division of Clinical Studies, The Institute of Cancer Research, London SM2 5NG, UK
[12]Prostate Cancer Targeted Therapy Group and Drug Development Unit, The Royal Marsden NHS Foundation Trust, London SM2 5NG, UK
[13]Department of Medicine, Weill Medical College of Cornell University, New York, NY 10021, USA
[14]Human Oncology and Pathogenesis Program, Memorial Sloan Kettering Cancer Center, New York, NY 10065, USA
[15]Prostate Cancer Clinical Trials Consortium, Memorial Sloan Kettering Cancer Center, New York, NY 10065, USA
[16]Department of Internal Medicine, Division of Hematology Oncology, University of Michigan Medical School, Ann Arbor, MI 48109, USA
[17]Comprehensive Cancer Center, University of Michigan Medical School, Ann Arbor, MI 48109, USA
[18]Department of Urology, University of Michigan Medical School, Ann Arbor, MI 48109, USA
[19]Department of Radiation Oncology, University of Michigan Medical School, Ann Arbor, MI 48109, USA
[20]Genitourinary Oncology Service, Department of Medicine, Sidney Kimmel Center for Prostate and Urologic Cancers, Memorial Sloan Kettering Cancer Center, New York, NY 10065, USA
[21]Interventional Radiology, Department of Radiology Service, Memorial Sloan Kettering Cancer Center, New York, NY 10065, USA
[22]Department of Pathology, Memorial Sloan Kettering Cancer Center, New York, NY 10065, USA
[23]Center for Molecular Oncologic Pathology, Dana-Farber Cancer Institute, Boston, MA 02215, USA
[24]Division of Hematology-Oncology, Department of Medicine, Beth Israel Deaconess Cancer Center, Beth Israel Deaconess Medical Center, Harvard Medical School, Boston, MA 02215, USA
[25]Department of Musculoskeletal Radiology, Brigham and Women's Hospital, Boston, MA 02115, USA
[26]Department of Laboratory Medicine, University of Washington, Seattle, WA 98195, USA
[27]Department of Radiology, University of Washington, Seattle, WA 98109, USA
[28]Department of Pathology, University of Washington Medical Center, Seattle, WA 98109, USA
[29]Laboratory of Computational Oncology, CIBIO, Centre for Integrative Biology, University of Trento, 38123 Mattarello TN, Italy
[30]Institute for Computational Biomedicine, Department of Physiology and Biophysics, Weill Medical College of Cornell University, New York, NY 10021, USA
[31]Division of Interventional Radiology, Department of Radiology, New York-Presbyterian Hospital/Weill Cornell Medical Center, New York, NY 10021, USA
[32]Department of Physiology & Biophysics, Weill Medical College of Cornell University, New York, NY 10021, USA
[33]Department of Oncology, Wayne State University School of Medicine, Detroit, MI 48201, USA
[34]Molecular Therapeutics Program, Barbara Ann Karmanos Cancer Institute, Detroit, MI 48201, USA
[35]The James Buchanan Brady Urological Institute and Department of Urology, Johns Hopkins School of Medicine, Baltimore, MD 21205, USA
[36]Division of Human Biology, Fred Hutchinson Cancer Research Center, Seattle, WA 98109, USA
[37]Division of Clinical Research, Fred Hutchinson Cancer Research Center, Seattle, WA 98109, USA
[38]Meyer Cancer, Weill Medical College of Cornell University, New York, NY 10021, USA

[39]Department of Pathology, Brigham & Women's Hospital, Boston, MA 02115, USA
[40]Marie-Josée and Henry R. Kravis Center for Molecular Oncology, Memorial Sloan Kettering Cancer Center, New York, NY 10065, USA
[41]Howard Hughes Medical Institute, Memorial Sloan Kettering Cancer Center, New York, NY 10065, USA
[42]Howard Hughes Medical Institute, University of Michigan, Ann Arbor, MI 48109, USA
[43]Co-first author
[44]Co-senior author
*Correspondence: sawyersc@mskcc.org (C.L.S.), arul@umich.edu (A.M.C.)
http://dx.doi.org/10.1016/j.cell.2015.05.001

SUMMARY

Toward development of a precision medicine framework for metastatic, castration-resistant prostate cancer (mCRPC), we established a multi-institutional clinical sequencing infrastructure to conduct prospective whole-exome and transcriptome sequencing of bone or soft tissue tumor biopsies from a cohort of 150 mCRPC affected individuals. Aberrations of *AR*, ETS genes, *TP53*, and *PTEN* were frequent (40%–60% of cases), with *TP53* and *AR* alterations enriched in mCRPC compared to primary prostate cancer. We identified new genomic alterations in *PIK3CA/B*, R-spondin, *BRAF/RAF1*, *APC*, β-catenin, and *ZBTB16/PLZF*. Moreover, aberrations of *BRCA2*, *BRCA1*, and *ATM* were observed at substantially higher frequencies (19.3% overall) compared to those in primary prostate cancers. 89% of affected individuals harbored a clinically actionable aberration, including 62.7% with aberrations in AR, 65% in other cancer-related genes, and 8% with actionable pathogenic germline alterations. This cohort study provides clinically actionable information that could impact treatment decisions for these affected individuals.

INTRODUCTION

Prostate cancer is among the most common adult malignancies, with an estimated 220,000 American men diagnosed yearly (American Cancer Society, 2015). Some men will develop metastatic prostate cancer and receive primary androgen deprivation therapy (ADT). However, nearly all men with metastatic prostate cancer develop resistance to primary ADT, a state known as metastatic castration-resistant prostate cancer (mCRPC). Multiple ''second generation'' ADT treatments, like abiraterone acetate (de Bono et al., 2011; Ryan et al., 2013) and enzalutamide (Beer et al., 2014; Scher et al., 2012), have emerged for mCRPC affected individuals; however, nearly all affected individuals will also develop resistance to these agents. In the U.S., an estimated 30,000 men die of prostate cancer yearly.

Multiple studies have identified recurrent somatic mutations, copy number alterations, and oncogenic structural DNA rearrangements (chromoplexy) in primary prostate cancer (Baca et al., 2013; Barbieri et al., 2012; Berger et al., 2011; Cooper et al., 2015; Pflueger et al., 2011; Taylor et al., 2010; Tomlins et al., 2007; Wang et al., 2011). These include point mutations in *SPOP*, *FOXA1*, and *TP53*; copy number alterations involving *MYC*, *RB1*, *PTEN*, and *CHD1*; and E26 transformation-specific (ETS) fusions, among other biologically relevant genes. Although certain primary prostate cancer alterations or signatures have prognostic clinical significance (Hieronymus et al., 2014; Lalonde et al., 2014), the therapeutic impact of primary prostate cancer genomic events has not yet been realized.

Genomic studies of metastatic prostate cancers demonstrated additional alterations in *AR* (Taplin et al., 1995) and in the androgen signaling pathway (Beltran et al., 2013; Grasso et al., 2012; Gundem et al., 2015; Hong et al., 2015), although these studies were performed predominantly using autopsy samples or preclinical models with limited cohort sizes. Prospective genomic characterization of fresh biopsy samples from living mCRPC affected individuals has been limited due to challenges in obtaining adequate tumor tissue, especially from bone biopsies (Mehra et al., 2011; Van Allen et al., 2014a), which is the most common site of metastatic disease. Thus, the landscape of genomic alterations in mCRPC disease remains incompletely characterized. Moreover, the low frequency of actionable genomic alterations in primary prostate cancer has limited the inclusion of mCRPC among cohorts wherein precision cancer medicine approaches have been piloted to guide treatment or clinical trial enrollment.

We conducted a systematic and multi-institutional study of mCRPC tumors obtained from living affected individuals to determine the landscape of somatic genomic alterations in this cohort, dissect genomic differences between primary prostate cancer and mCRPC, and discover the potential relevance of these findings from a biological and clinical perspective.

RESULTS

Clinical, Biopsy, and Pathology Parameters

An international consortium consisting of eight academic medical center clinical sites was established to capture fresh clinical mCRPC affected individual samples as part of standard-of-care approaches or through a cohort of prospective clinical trials (Figures 1A and 1B). Standard-of-care approaches for mCRPC included abiraterone acetate or enzalutamide. Clinical trials included in this study focused on combination strategies involving abiraterone acetate or enzalutamide, inhibitors of poly ADP ribose polymerase (PARP), or inhibitors of aurora kinase. Here, we report the results of genomic profiling from

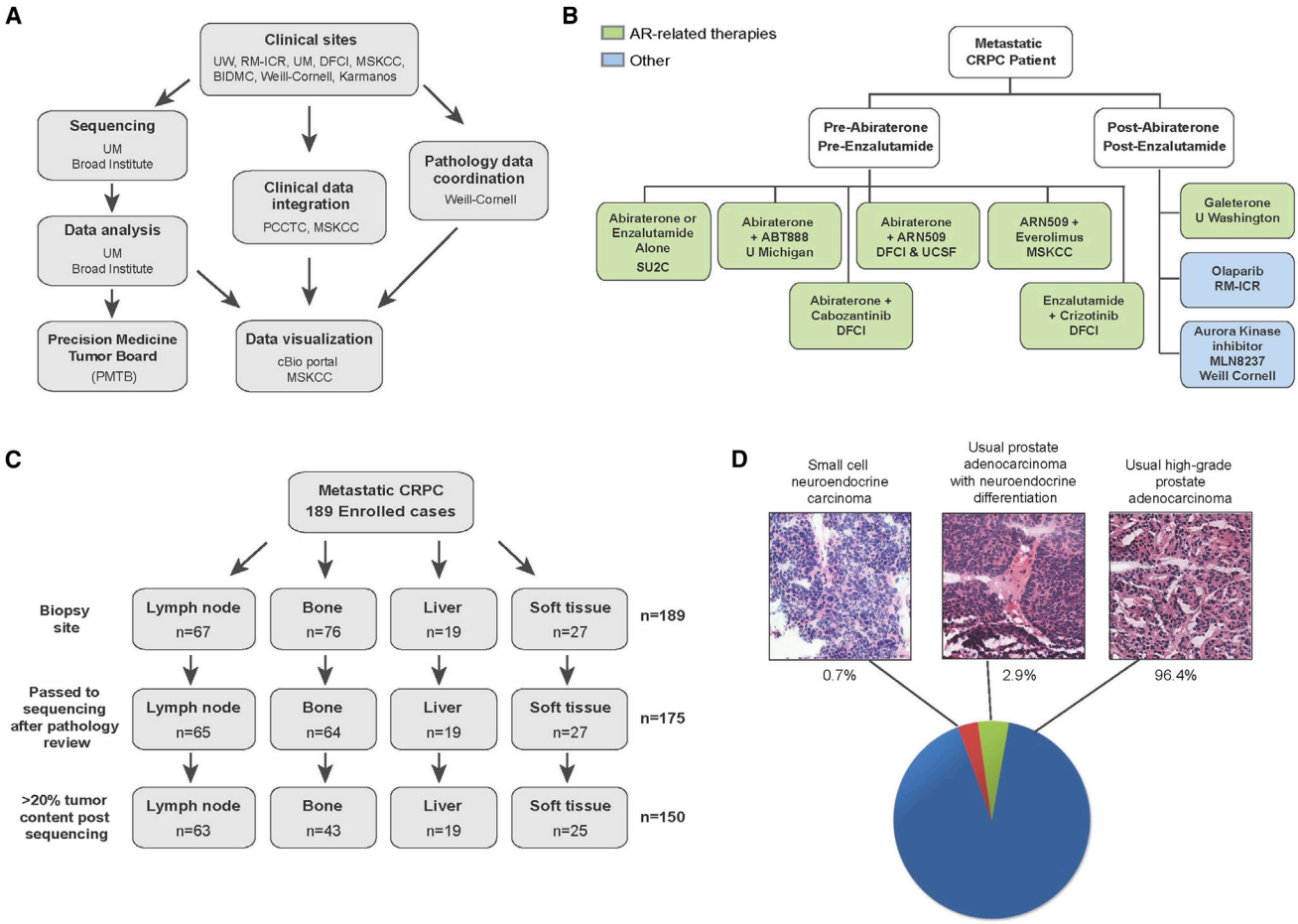

Figure 1. Overview of the SU2C-PCF IDT Multi-Institutional Clinical Sequencing of the mCRPC Project

(A) Schema of multi-institutional clinical sequencing project work flow.

(B) Clinical trials associated with the SU2C-PCF mCRPC project.

(C) Biopsy sites of the samples used for clinical sequencing.

(D) Histopathology of the cohort. Representative images of morphological analysis of mCRPC are shown along with prevalence in our cohort.

mCRPC biopsy samples obtained at time of entry into the cohort study. Future reports will include longitudinal clinical data such as treatment response. The consortium utilized two sequencing and analysis centers, one centralized digital pathology review center, and one centralized data visualization portal (Cerami et al., 2012; Gao et al., 2013; Robinson et al., 2011; Thorvaldsdóttir et al., 2013). Cross-validation of sequencing data from the two original sequencing sites demonstrated comparable variant calls for adequately powered genetic loci (E.M.V.A., D.R., C. Morrissey, C.C.P., S.L. Carter, M. Rosenberg, A. McKenna, A.M.C., L.A.G., and P.S.N., unpublished data).

Here, we describe 150 affected individuals with metastatic disease with complete integrative clinical sequencing results (whole-exome, matched germline, and transcriptome data) (Figure 1C) and summarized in Table S1. 189 affected individuals were enrolled in the study, and 175 cases were sequenced after pathology review and assessment of tumor content. Of these, 150 biopsies had >20% tumor content as defined by computational analysis, based on mutant allele variant fractions and zygosity shifts. The biopsies sequenced were from lymph node (42%), bone (28.7%), liver (12.7%), and other soft tissues (16.7%). Baseline clinical information is available in Table S2. A majority of cases (96.4%) displayed typical high-grade prostate adenocarcinoma features, whereas 2.9% of cases showed neuroendocrine differentiation. One case (0.7%) exhibited small-cell neuroendocrine features (Epstein et al., 2014) (Figure 1D).

Landscape of mCRPC Alterations

Somatic aberrations in a panel of 38 statistically or clinically significant genes are illustrated in Figure 2. Mean target coverage for tumor exomes was 160× and for matched normal exomes was 100×. Although the average mutation rate for mCRPC was 4.4 mutations/Mb, there were four cases that exhibited a mutation rate of nearly 50 per Mb, three of which are likely due to alterations in the mismatch repair genes *MLH1* and *MSH2*, as discussed later.

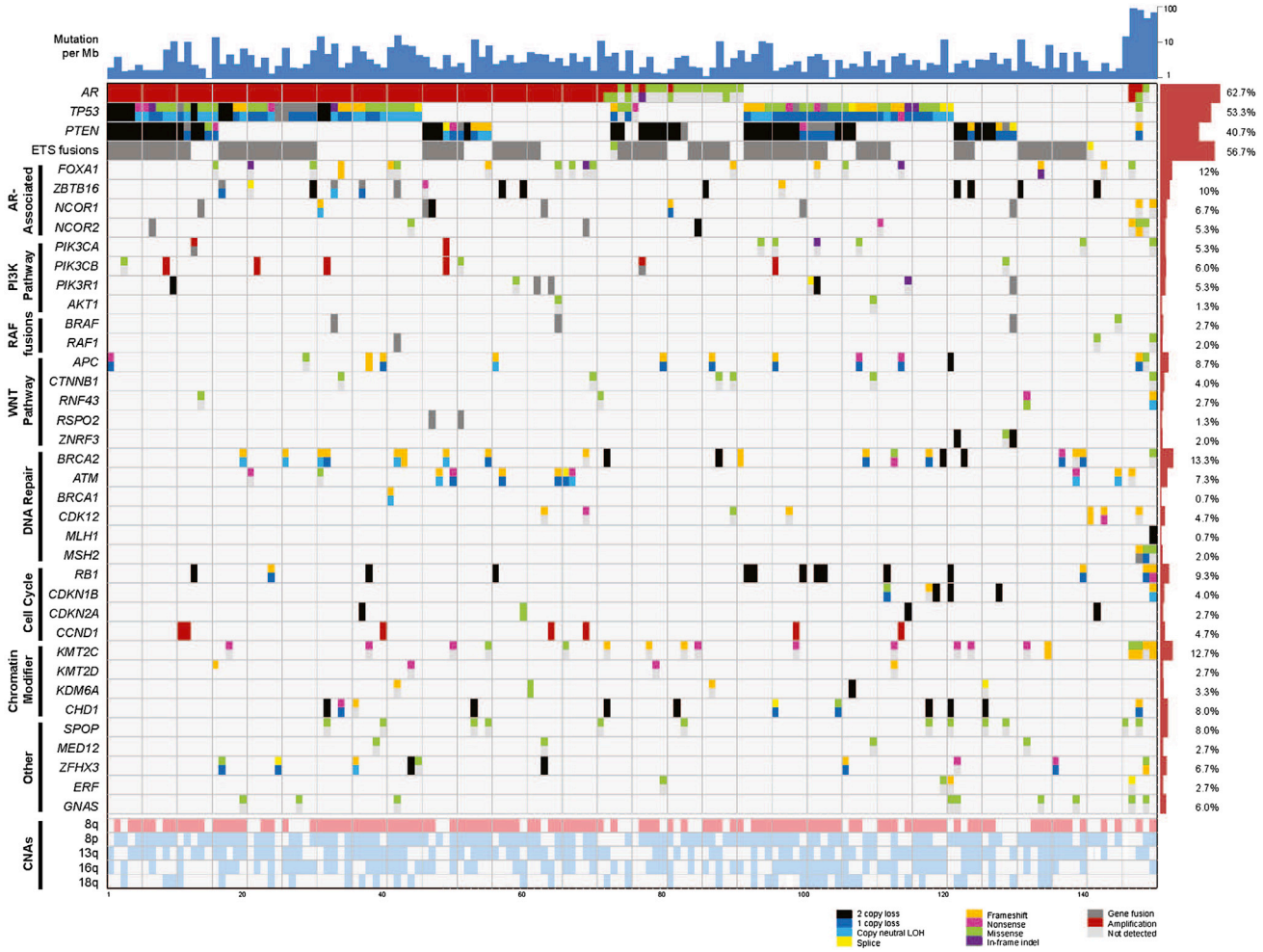

Figure 2. Integrative Landscape Analysis of Somatic and Germline Aberrations in Metastatic CRPC Obtained through DNA and RNA Sequencing of Clinically Obtained Biopsies

Columns represent individual affected individuals, and rows represent specific genes grouped in pathways. Mutations per Mb are shown in the upper histogram, and incidence of aberrations in the cohort is in the right histogram. Copy number variations (CNVs) common to mCRPC are shown in in the lower matrix, with pink representing gain and light blue representing loss. Color legend of the aberrations represented including amplification, two copy loss, one copy loss, copy neutral loss of heterozygosity (LOH), splice site mutation, frameshift mutation, missense mutation, in-frame indel, and gene fusion. Cases with more aberration in a gene are represented by split colors.

Frequent copy number gains of 8q, as well as copy number losses of 8p, 13q, 16q, and 18q, were also observed. The mean number of identified biologically relevant genetic aberrations per case was 7.8 (Figure 2). All mutations identified are presented in Table S3. The landscape of copy number alterations demonstrated expected recurrent amplification peaks (frequent *AR*, 8q gain) and deletion peaks (*CHD1*, *PTEN*, *RB1*, *TP53*) (Figure 3A). Additional frequent focal amplifications were observed in regions encompassing *CCND1* and *PIK3CA* and *PIK3CB*. A new recurrent focal homozygous deletion event was observed in chr11q23, encompassing the transcriptional repressor *ZBTB16*.

To identify gene fusions, analysis of 215 transcriptome libraries derived from the 150 tumor RNAs was performed and identified 4,122 chimeras with at least 4 reads spanning the fusion junction. These fusion junctions resulted from 2,247 gene pairs, an average of 15 gene fusions per tumor (Table S4). Among chimeric fusion transcripts identified, recurrent ETS fusions (Tomlins et al., 2005) were observed in 84 cases (56%), of which the majority were fused to *ERG* and others to *FLI1*, *ETV4*, and *ETV5* (Figure 3B). In addition, potential clinically actionable fusions (involving *BRAF*, *RAF1*, *PIK3CA/B*, or *RSPO2*) were seen in eight cases (Figure S1 and covered subsequently).

To place the mCRPC mutation landscape in the context of primary prostate cancer somatic genomics, we performed a selective enrichment analysis to compare somatic point mutations and short insertion/deletions observed in this cohort with those observed in somatic whole-exome mutation data from 440 primary prostate cancer exomes (Barbieri et al., 2012; The Cancer

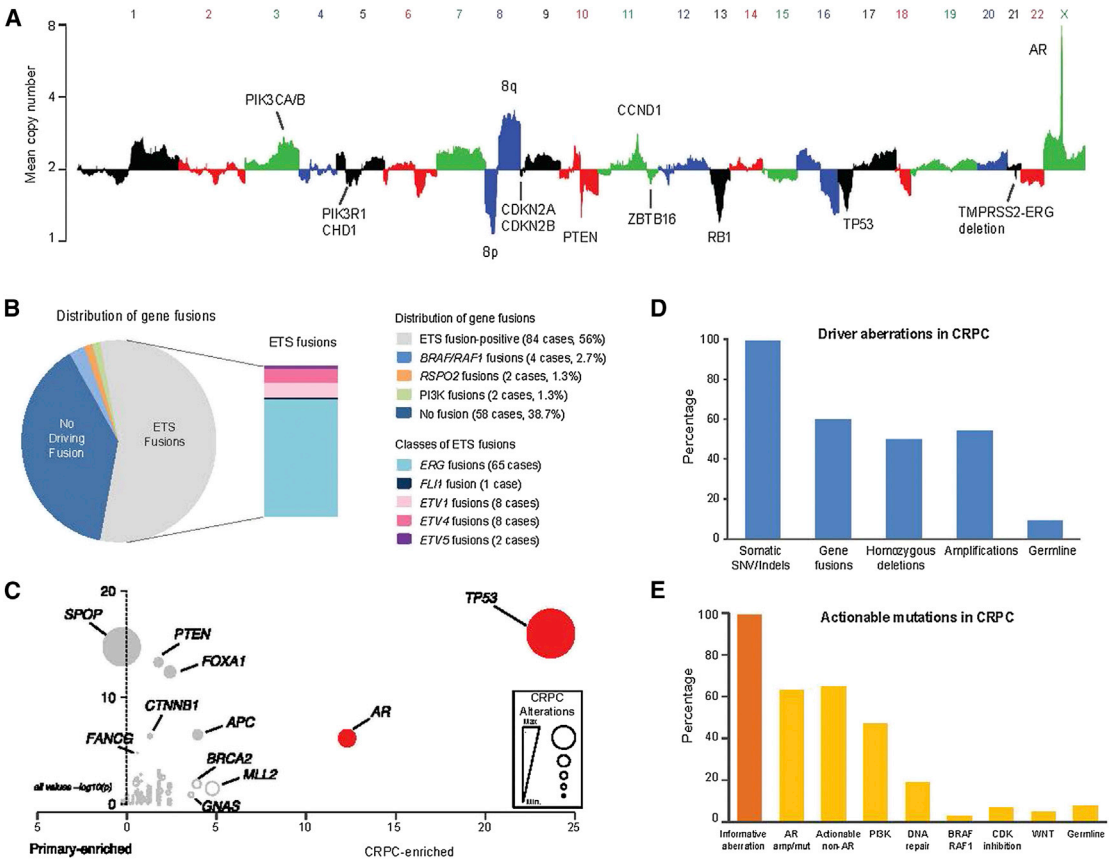

Figure 3. Classes of Genomic Aberrations Seen in mCPRC

(A) Copy number landscape of the SU2C-PCF mCRPC cohort. Individual chromosomes are represented by alternating colors, and key aberrant genes are indicated.

(B) The gene fusion landscape of mCRPC. Pie chart of all driver fusions identified and the box plot represents specific ETS fusions.

(C) Mutations enriched in mCRPC relative to hormone naive primary prostate cancer. Primary prostate cancer data derived from published studies (Barbieri et al., 2012; The Cancer Genome Atlas, 2015). Level of CRPC enrichment is represented by the x axis, and MutSig CRPC significance analysis is provided by the y axis. Diameters are proportional to the number of cases with the specific aberration. Genes of interest are highlighted.

(D) Classes of driver aberrations identified in mCRPC.

(E) Classes of clinically actionable mutations identified in mCRPC.

Genome Atlas, 2015) (Figure 3C and Table S5). Focusing on genes previously implicated in cancer (n = 550), somatic *TP53* mutations were the most selectively mutated ($q < 0.001$; Benjamini-Hochberg), followed by *AR*, *KMT2D*, *APC*, *BRCA2*, and *GNAS* ($q < 0.1$; Benjamini-Hochberg; Table S6). Both *AR* and *GNAS* were mutated exclusively in mCRPC. We found no genes selectively mutated in primary prostate cancer compared to mCRPC.

We identified an established biological "driver" aberration in a cancer-related gene (i.e., known oncogene or tumor suppressor; Table S7) in nearly all the cases (Figure 3D). Although 99% of the mCPRC cases harbored a potential driver single-nucleotide variant (SNV) or indel, other classes of driver aberrations were also highly prevalent. These include driver gene fusions in 60%, driver homozygous deletions in 50% and driver amplifications in 54%. Although informative mutations were present in virtually all mCRPC cases, 63% harbored aberrations in *AR*, an expected finding in castrate-resistant disease but with higher frequency than in prior reports (Figure 3E). Interestingly, even when *AR* was not considered, 65% of cases harbored a putatively clinically actionable alteration (defined as predicting response or resistance to a therapy, having diagnostic or prognostic utility across tumor types) (Table S8) (Roychowdhury et al., 2011; Van Allen et al., 2014c). Non-AR related clinically actionable alterations included aberrations in the PI3K pathway (49%), DNA repair pathway (19%), RAF kinases (3%), CDK inhibitors (7%), and the WNT pathway (5%). In addition to somatic alterations, clinically actionable pathogenic germline variants were seen in 8% of mCRPC affected individuals, potentially emphasizing the need for genetic counseling in affected individuals with prostate cancer.

Genomically Aberrant Pathways in mCRPC

Integrative analysis using both biological and statistical frameworks (Lawrence et al., 2013, 2014) of somatic point mutations,

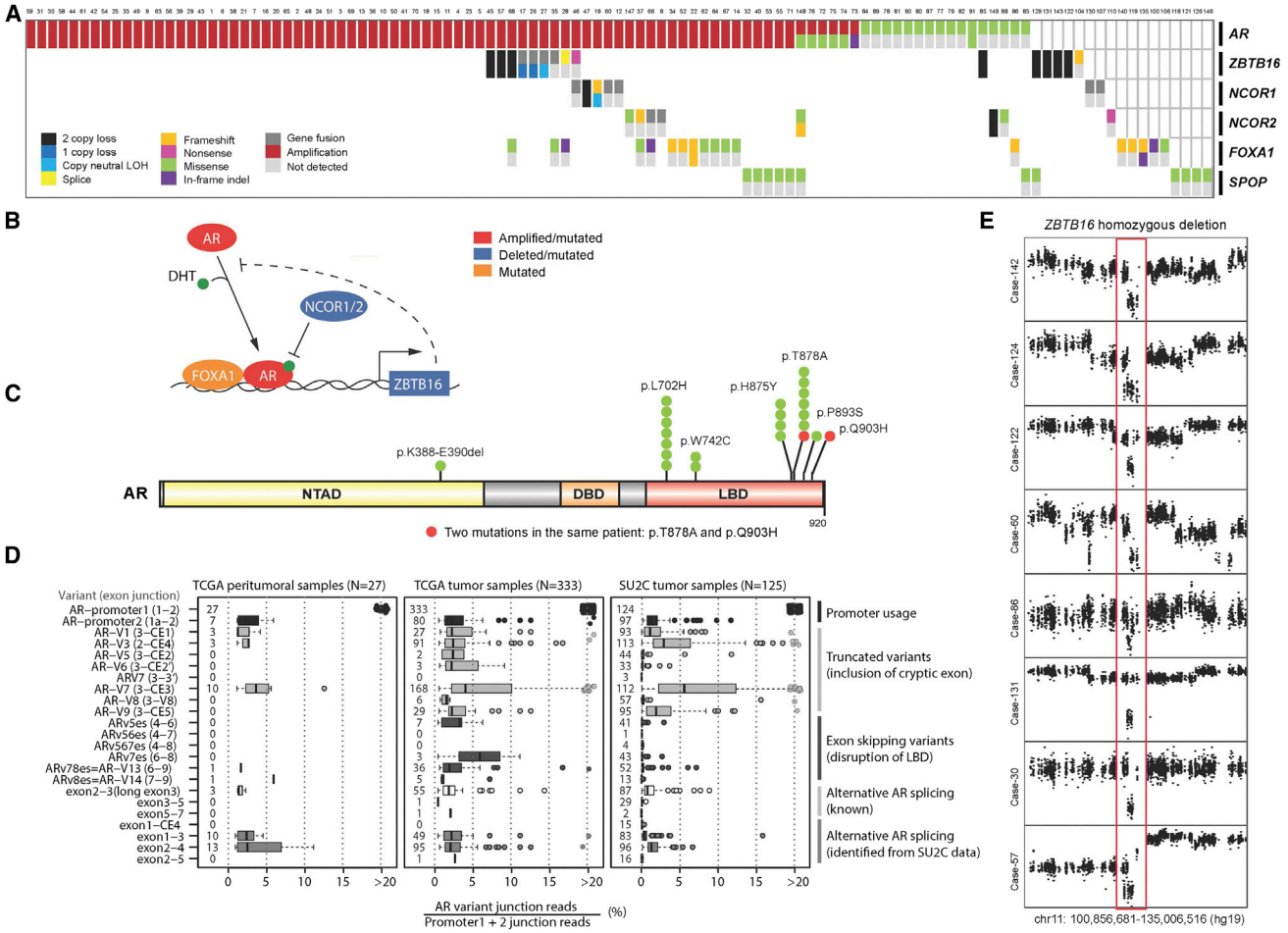

Figure 4. Aberrations in the AR Pathway Found in mCRPC

(A) Cases with aberrations in the AR pathway. Case numbering as in Figure 2.

(B) Key genes found altered in the AR pathway of mCRPC. DHT, dihydrotestosterone.

(C) Point mutations identified in *AR*. Amino acids altered are indicated. NTAD, N-terminal activation. DBD, DNA-binding. LBD, ligand binding.

(D) Splicing landscape of *AR* in mCRPC. Specific splice variants are indicated by exon boundaries, and junction read level is provided. SU2C, this mCRPC cohort. PRAD tumor, primary prostate cancer from the TCGA. PRAD normal, benign prostate from the TCGA.

(E) Homozygous deletion of *ZBTB16*. Copy number plots with x axis representing chromosomal location and the y axis referring to copy number level. Red outline indicates region of *ZBTB16* homozygous loss.

short insertion/deletions, copy number alterations, fusion transcripts, and focused germline variant analysis identified discrete molecular subtypes of mCRPC (Figure 2). These subtypes were classified based on alteration clustering and existing biological pathway knowledge and implicated the *AR* signaling pathway, phosphatidylinositol-4,5-bisphosphate 3-kinase (PI3K), WNT, DNA repair, cell cycle, and chromatin modifier gene sets, among others. The most frequently aberrant genes in mCRPC included *AR* (62.7%), ETS family (56.7%), *TP53* (53.3%), and *PTEN* (40.7%) (Figure 2).

AR Signaling Pathway

In aggregate, 107/150 (71.3%) of cases harbored *AR* pathway aberrations, the majority of which were direct alterations affecting *AR* through amplification and mutation (Figure 4A). Figure 4B summarizes the key genes altered in AR signaling, including *AR* itself, *FOXA1* as a pioneer transcription factor, *NCOR1/2* as negative regulators of AR, *SPOP* as a putative androgen receptor transcriptional regulator (Geng et al., 2013), and *ZBTB16* as an AR inducible target gene that may also negatively regulate *AR*. Recurrent hotspot mutations in *AR* were observed at residues previously reported to confer agonism to AR antagonists such as flutamide (T878A) and bicalutamide (W742C), as well as to glucocorticoids (L702H). Some, but not all, of these affected individuals had documented prior exposures that could explain enrichment for these mutations. Additional clinical data collection is ongoing (Figure 4C). Rare *AR* mutations not previously described were seen in our cohort, although these are of unclear functional significance. Furthermore, one affected individual (Case 89) harbored two putatively

functional *AR* mutations (T878A and Q903H), which may further suggest intra-tumor heterogeneity emerging in the CRPC setting (Carreira et al., 2014). Analysis of *AR* splice variants from RNA-seq data demonstrated a distribution of splice variants observed throughout these mCRPC tumor cases (Figure 4D). Analysis of the TCGA prostate dataset revealed that many of these variants were also present at varying levels in primary prostate cancer and benign prostate tissue. AR-V7, which has been implicated in abiraterone acetate and enzalutamide resistance (Antonarakis et al., 2014), was observed in a majority of pre-abiraterone/enzalutamide cases but at very low ratios relative to full length AR. Implications for treatment response are unknown at this time.

In addition to AR mutations itself, we observed alterations in AR pathway members (Figure 4A). These included known alterations in *NCOR1*, *NCOR2*, and *FOXA1* that have been previously reported in primary prostate cancers and mCRPC (Barbieri et al., 2012; Grasso et al., 2012). In this cohort, truncating and missense mutations in FOXA1 form a cluster near the end of the Forkhead DNA binding domain (Figure S2).

Recurrent homozygous deletions of the androgen-regulated gene *ZBTB16* (also known as PLZF) were seen in 8 (5%) cases (Figure 4E) not previously reported in clinical mCRPC biopsies. Analysis of the minimally deleted region seen in this cohort narrowed the candidate genes in the chr11q23 region to *ZBTB16* (Figure S3). *ZBTB16* has been previously implicated in prostate cancer tumorigenesis and androgen resistance in preclinical models (Cao et al., 2013; Kikugawa et al., 2006), with loss of *ZBTB16* upregulating the MAPK signaling pathway (Hsieh et al., 2015).

New PI3K Pathway Discoveries

The PI3K pathway was also commonly altered, with somatic alterations in 73/150 (49%) of mCRPC affected individuals (Figure 5A). This included biallelic loss of *PTEN*, as well as hotspot mutations, amplifications and activating fusions in *PIK3CA*, and p.E17K activating mutations in *AKT1* (Figure S2). Of note, *PIK3CA* amplifications resulted in overexpression compared to the remaining cohort (Figure S3).

Interestingly, mutations in another member of the PI3K catalytic subunit, *PIK3CB*, were observed in this cohort for the first time, at equivalent positions to canonical activating mutations in PIK3CA (Figure 5B). PIK3CB mutations appeared in the context of PTEN-deficient cases, which is consistent with a previous report demonstrating that some PTEN-deficient cancers are dependent on PIK3CB, rather than PIK3CA (Wee et al., 2008). Furthermore, two affected individuals harbored fusions involving PIK3CA/B, with these events resulting in overexpression of the gene relative to other tumors in the cohort (Figures 5C and 5D).

New Wnt Pathway Discoveries

27/150 (18%) of our cases harbored alterations in the Wnt signaling pathway (Figure 6A). Hotspot activating mutations in *CTNNB1* were seen (Figure 6B), as previously described (Voeller et al., 1998). Notably, recurrent alterations in *APC* were also observed, which have not been previously described in clinical mCRPC affected individuals. This prompted a broader examination of Wnt signaling genes (Figure 6B). Through integrative analysis, we identified alterations in *RNF43* and *ZNRF3*, which were recently described in colorectal, endometrial, and adrenocortical cancers (Assié et al., 2014; Giannakis et al., 2014) and were mutually exclusive with *APC* alterations (Figure 6A). Moreover, we also discovered R-spondin fusions involving *RSPO2*, as previously observed in colorectal carcinoma (Seshagiri et al., 2012) in association with RSPO2 overexpression in these cases (Figure 6C). RSPO2 is a key factor in prostate cancer organoid methodology (Gao et al., 2014). Affected individuals s with aberrations in *RNF43*, *ZNRF3*, or *RSPO2* (overall 6% of affected individuals) are predicted to respond to porcupine inhibitors (Liu et al., 2013).

Cell-Cycle Pathway

We observed *RB1* loss in 21% of cases (Figure S4). Expanding the scope of cell-cycle genes implicated in mCRPC, we noted focal amplifications involving *CCND1* in 9% of cases, as well as less common (< 5%) events in *CDKN2A/B*, *CDKN1B*, and *CDK4* (Figure S4). Cell-cycle derangement, such as through CCND1 amplification or CDKN2A/B loss, may result in enhanced response to CDK4 inhibitors in other tumor types (Finn et al., 2015), and preclinical mCRPC models predict similar activity in prostate cancer (Comstock et al., 2013).

DNA Repair Pathway

Integrative analysis of both the somatic and pathogenic germline alterations in *BRCA2* identified 19/150 (12.7%) of cases with loss of BRCA2, of which ~90% exhibited biallelic loss (Figure 7A). This was commonly a result of somatic point mutation and loss of heterozygosity, as well as homozygous deletion. One of the clinical trials in our consortium is evaluating poly(-ADP-ribose) polymerase (PARP) inhibition in unselected mCRPC affected individuals. Importantly, multiple affected individuals in this trial who experienced clinical benefit harbored biallelic *BRCA2* loss, providing further evidence of clinical actionability (Mateo et al., 2014). Eight affected individuals (5.3%) harbored pathogenic germline *BRCA2* mutations (Figure 7B) with a subsequent somatic event that resulted in biallelic loss, revealing a surprisingly high frequency relative to primary prostate cancer.

We therefore expanded the focus to other DNA repair/recombination genes and identified alterations in at least 34/150 (22.7%) of cases. These include recurrent biallelic loss of *ATM* (Figure 7B), including multiple cases with germline pathogenic alterations. ATM mutations were also observed in affected individuals who achieved clinical responses to PARP inhibition (Mateo et al., 2014). In addition, we noted events in *BRCA1*, *CDK12*, *FANCA*, *RAD51B*, and *RAD51C*. If aberrations of *BRCA2*, *BRCA1*, and *ATM* all confer enhanced sensitivity to PARP inhibitors, 29/150 (19.3%) of mCRPC affected individuals would be predicted to benefit from this therapy. Interestingly, three out of four mCRPC tumors exhibited hypermutation and harbored alterations in the mismatch repair pathway genes *MLH1* or *MSH2* (Figures 2 and 7C), corroborating a recent report identifying structural alterations in *MSH2* and *MSH6* mismatch repair genes in hypermutated prostate cancers (Pritchard et al., 2014).

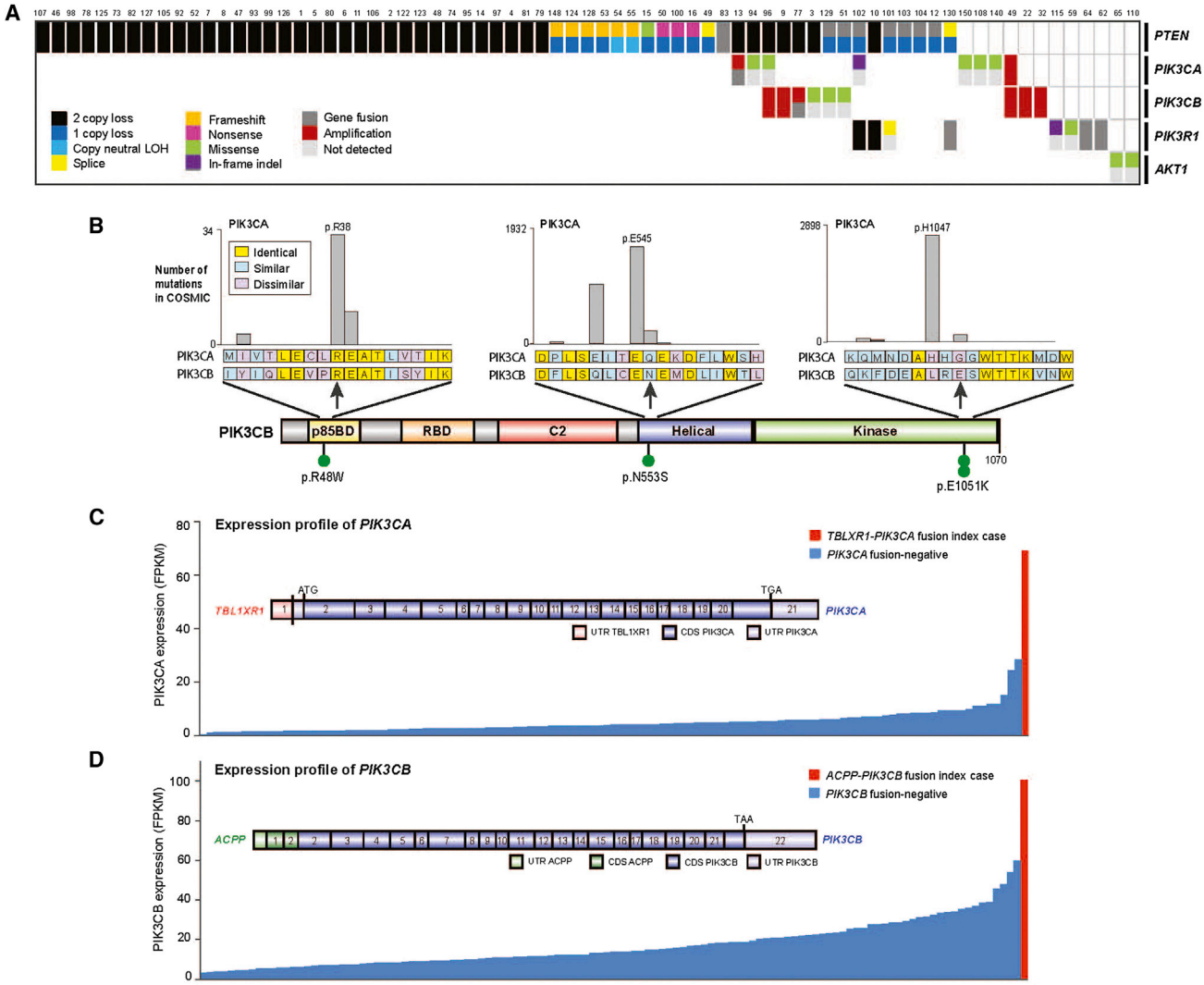

Figure 5. Aberrations in the PI(3)K Pathway Found in mCRPC

(A) Cases with aberrations in the PIK3 pathway. Case numbering as in Figure 2.

(B) Point mutations identified in PIK3CB. Amino acids altered are indicated. Analogous, recurrent COSMIC mutations in PIK3CA are shown as expansion views.

(C) Outlier expression of PK3CA in CRPC case harboring the TBL1XR1-PIK3CA gene fusion. Structure of the gene fusion is inset. UTR, untranslated region. CDS, coding sequence.

(D) As in (C), except for PIK3CB and the ACPP-PIK3CB gene fusion.

DISCUSSION

To effectively implement precision cancer medicine, prospective identification of predictive biomarkers should be performed with information derived from the most contemporary tumor assessments that reflect the affected individual's prior therapies and treatment opportunities. In mCRPC, precision cancer medicine activities have been limited by difficulties obtaining clinical samples from mCRPC affected individuals and a lack of comprehensive genomic data for potentially actionable alterations. By demonstrating the feasibility of prospective genomics in mCRPC and defining the mutational landscape in a focused metastatic clinical cohort, this report may inform multiple genomically driven clinical trials and biological investigations into key mediators of mCRPC. In nearly all of the mCRPC analyzed in this study, we identified biologically informative alterations; almost all harbored at least one driver SNV/indel, and approximately half harbored a driver gene fusion, amplification, or homozygous deletion. Remarkably, in nearly 90% of mCRPC affected individuals, we identified a potentially actionable somatic or germline event.

The high frequency of AR pathway alterations in this cohort strongly implies that the vast majority of mCRPC affected individuals remain dependent on AR signaling for viability. The "second-generation" AR-directed therapies (e.g., abiraterone acetate and enzalutamide) may select for distinct phenotypes that may be indifferent to AR signaling, and prospective

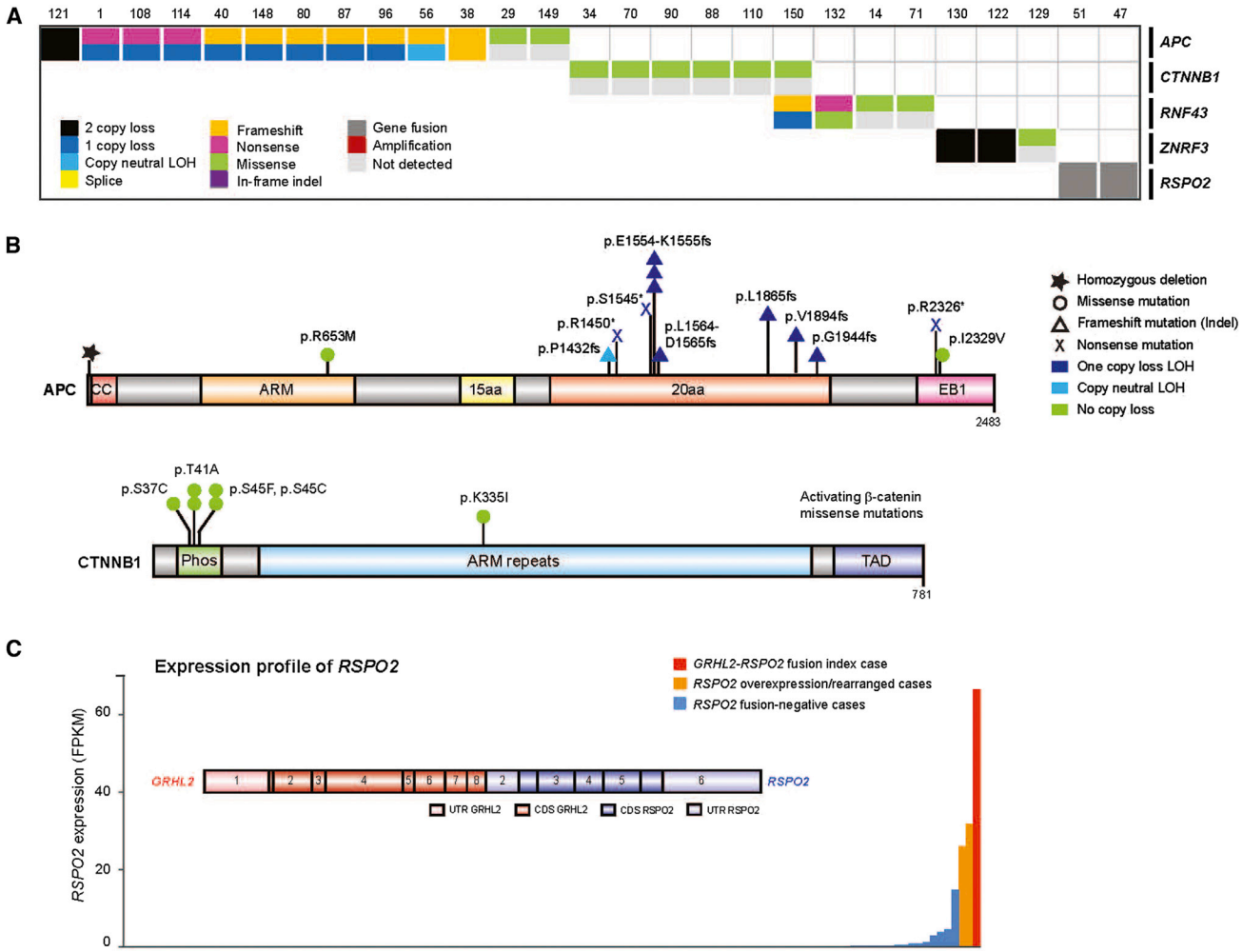

Figure 6. Aberrations in the WNT Pathway Found in mCRPC

(A) Cases with aberrations in the WNT pathway. Case numbering as in Figure 2.

(B) Aberrations identified in APC and CTNNB1. Amino acids altered are indicated. ARM, armadillo repeat. Phos, phosphorylation domain. TAD, *trans*-activating domain. EB1, end binding protein-1 domain. CC, coiled coil.

(C) Outlier expression of *RSPO2* in CRPC and the *GRHL2-RSPO2* gene fusion. RNA-seq expression across our CRPC cohort. Structure of the gene fusion is inset. UTR, untranslated region. CDS, coding sequence.

characterization of such cases will be of particular interest. We hypothesize that affected individuals with acquired *AR* mutations, including new *AR* mutations discovered in this cohort, will harbor differential responses to these second-generation ADT therapies. As the number of affected individuals in this cohort with *AR* mutations increases, we will subsequently be able to link specific AR mutations with clinical phenotypes to determine which mutations confer selective response or resistance to subsequent AR-directed therapy.

Moreover, these data identify multiple therapeutic avenues warranting clinical investigation in the CRPC population. Excluding AR aberrations, 65% of mCRPC have a potentially actionable aberration that may suggest an investigational drug or approved therapy. For example, focusing on the PI3K pathway, PIK3CB-specific inhibitors may have utility in affected individuals with mutation, amplification, and/or fusion of this gene (Schwartz et al., 2015); multiple affected individuals who achieved durable (>1 year) responses to PIK3CB-specificin inhibition harbored activating mutation or amplification in *PIK3CB* (J.S. de Bono et al., 2015, 106th Annual Meeting of the American Association for Cancer Research, abstract). RAF kinase fusions in 3% of mCPRC affected individuals would suggest the use of pan-RAF inhibitors or MEK inhibitors (Palanisamy et al., 2010). In addition, the emergence of porcupine inhibitors (Liu et al., 2013) and R-spondin antibodies may warrant investigation in mCRPC tumors harboring Wnt pathway alterations or specifically R-spondin fusions, respectively. These observations will need to be prospectively assessed in the clinical trials.

Additionally, biallelic inactivation of *BRCA2*, *BRCA1*, or *ATM* was observed in nearly 20% of affected individuals. Previous work in other cancer types suggests that these affected individuals may benefit from PARP inhibitors (Fong et al., 2009;

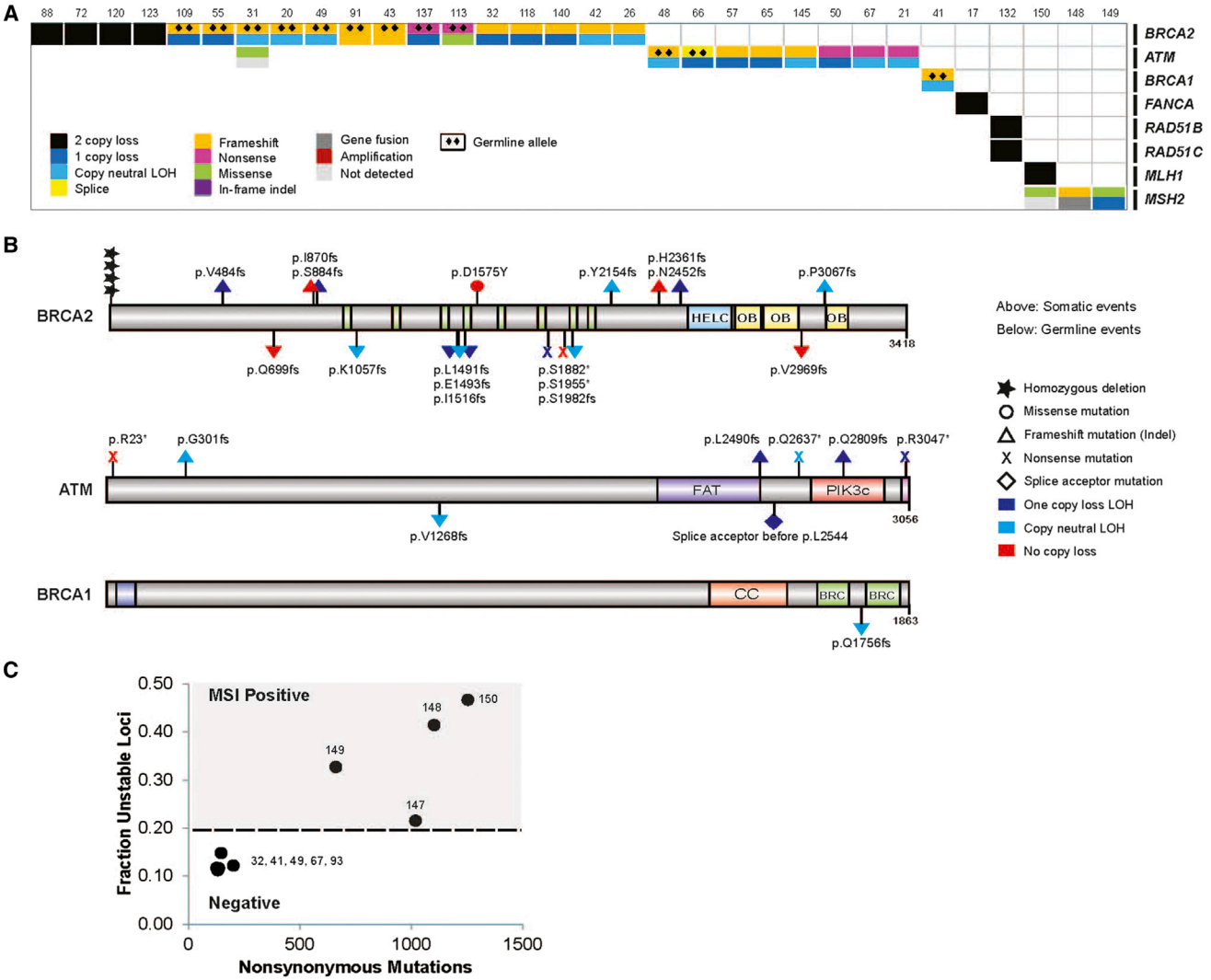

Figure 7. Aberrations in the DNA Repair Pathway Found in mCRPC

(A) Cases with aberrations in the DNA repair pathway. Case numbering as in Figure 2.

(B) Aberrations identified in BRCA2, ATM, and BRCA1. Amino acids altered are indicated. HELC, helical domain. OB, oligonucleotide binding fold. FAT, FRAP-ATM-TRRAP domain. PIK3c, PI3 kinase domain. CC, coiled coil. BRC, Brca repeat.

(C) Microsatellite instability analysis of representative hypermutated CRPC cases and non-hypermutated cases.

Kaufman et al., 2015; Weston et al., 2010) or platinum-based chemotherapy, and prior reports have implicated the presence of germline *BRCA2* alterations in primary prostate cancer with poor survival outcomes (Castro et al., 2013). Given the incidence of pathogenic germline *BRCA2* mutations in this cohort with subsequent somatic events (5%), along with enrichment for somatic *BRCA2* alterations in mCRPC (13%), germline genetic testing in mCRPC affected individuals warrants clinical consideration.

The ability to molecularly characterize mCRPC biopsy samples from affected individuals actively receiving therapy will also enable focused studies of resistance to secondary ADT therapies, including neuroendocrine-like phenotypes. This will require iterative sampling of pre-treatment and resistant tumors from matching affected individuals and may warrant multiregional biopsies from affected individuals (if feasible) given heterogeneity in mCRPC (Carreira et al., 2014; Gundem et al., 2015). Toward that end, in some affected individuals, we observed multiple *AR* mutations emerging in the same biopsy, which may indicate clonal heterogeneity within these mCRPC tumor samples. Additional genomic alterations discovered in this cohort (e.g., *ZBTB16*) warrant exploration in prostate cancer model systems, including organoid cultures (Gao et al., 2014).

Broadly, our effort demonstrates the utility of applying comprehensive genomic principles developed for primary malignancies (e.g., TCGA) to a clinically relevant metastatic tumor cohort. Our effort may also catalyze multi-institutional efforts to profile tumors from cohorts of affected individuals with metastatic, treated tumors in other clinical contexts because our results

demonstrate multiple discoveries within this advanced disease stage that have not been observed in primary tumor profiling. Moreover, this study sets the stage for epigenetic and other profiling efforts in mCRPC not taken in this study, which may enable biological discovery and have immediate therapeutic relevance in mCRPC (Asangani et al., 2014). Overall, our efforts demonstrate the feasibility of comprehensive and integrative genomics on prospective biopsies from individual mCRPC affected individuals to enable precision cancer medicine activities in this large affected individual population.

EXPERIMENTAL PROCEDURES

Affected Individual Enrollment

Affected individuals with clinical evidence of mCRPC who were being considered for abiraterone acetate or enzalutamide as standard of care, or as part of a clinical trial, were considered for enrollment. Affected individuals with metastatic disease accessible by image-guided biopsy were eligible for inclusion. All affected individuals provided written informed consent to obtain fresh tumor biopsies and to perform comprehensive molecular profiling of tumor and germline samples.

Biopsies and Pathology Review

Biopsies of soft tissue or bone metastases were obtained under radiographic guidance. Digital images of biopsy slides were centrally reviewed using schema established to distinguish usual adenocarcinoma from neuroendocrine prostate cancer (Epstein et al., 2014). All images were reviewed by genitourinary oncology pathologists (M.R., J.M.M., L.P.K., S.A.T., R.M., V.R., A.G., M.L., R.L., and M.B.).

Sequencing and Analysis

Normal DNAs from buccal swabs, buffy coats, or whole blood were isolated using the QIAGEN DNeasy Blood & Tissue Kit. Flash-frozen needle biopsies with highest tumor content for each case, as determined by pathology review, were extracted for nucleic acids. Tumor genomic DNA and total RNA were purified from the same sample using the AllPrep DNA/RNA/miRNA kit (QIAGEN) with disruption on a Tissuelyser II (QIAGEN). RNA integrity was verified on an Agilent 2100 Bioanalyzer using RNA Nano reagents (Agilent Technologies).

Whole-exome capture libraries were constructed from 100 ng to 1 μg of DNA from tumor and normal tissue after sample shearing, end repair, and phosphorylation and ligation to barcoded sequencing adaptors. Ligated DNA was size selected for lengths between 200 and 350 bp and subjected to hybrid capture using SureSelect Exome v4 baits (Agilent). Exome sequence data processing and analysis were performed using pipelines at the Broad Institute and the University of Michigan. A BAM file aligned to the hg19 human genome build was produced using Illumina sequencing reads for the tumor and normal sample and the Picard pipeline. Somatic mutation analysis was performed as described previously (Cibulskis et al., 2013; Van Allen et al., 2014c) and reviewed with Integrated Genomics Viewer (IGV) (Robinson et al., 2011).

Copy number aberrations were quantified and reported for each gene as the segmented normalized log2-transformed exon coverage ratios between each tumor sample and matched normal sample (Lonigro et al., 2011). To account for observed associations between coverage ratios and GC content across the genome, lowess normalization was used to correct per-exon coverage ratios prior to segmentation analysis. Mean GC percentage was computed for each targeted region, and a lowess curve was fit to the scatterplot of log2-coverage ratios versus mean GC content across the targeted exome using the lowess function in R (version 2.13.1) with smoothing parameter f = 0.05. The resulting copy ratios were segmented using the circular binary segmentation algorithm (Olshen et al., 2004).

Statistical analysis of recurrently mutated genes was performed using MutSig (Lawrence et al., 2013). Selective enrichment analysis (Van Allen et al., 2014b) of mutations observed in mCRPC compared to primary prostate cancer was performed by tabulating the frequency of affected-individual-normalized mutations observed in either CRPC or primary prostate cancer and performing a two-sided Fisher's exact test using allelic fraction cut off of 0.1 or greater and a set of biologically relevant cancer genes (n = 550 genes) (Futreal et al., 2004). Multiple hypothesis test correction was performed using Benjamini-Hochberg method.

Transcriptome libraries were prepared using 200–1,000 ng of total RNA. PolyA+ RNA isolation, cDNA synthesis, end-repair, A-base addition, and ligation of the Illumina indexed adapters were performed according to the TruSeq RNA protocol (Illumina). Libraries were size selected for 250–300 bp cDNA fragments on a 3% Nusieve 3:1 (Lonza) gel, recovered using QIAEX II reagents (QIAGEN), and PCR amplified using Phusion DNA polymerase (New England Biolabs). Total transcriptome libraries were prepared as above, omitting the poly A selection step and captured using Agilent SureSelect Human All Exon V4 reagents and protocols. Library quality was measured on an Agilent 2100 Bioanalyzer for product size and concentration. Paired-end libraries were sequenced with the Illumina HiSeq 2500, (2×100 nucleotide read length) with sequence coverage to 50 M paired reads and 100 M total reads.

Paired-end transcriptome sequencing reads were aligned to the human reference genome (GRCh37/hg19) using a RNA-seq spliced read mapper Tophat2 (Kim and Salzberg, 2011) (Tophat 2.0.4), with "–fusion-search" option turned on to detect potential gene fusion transcripts. Potential false-positive fusion candidates were filtered out using "Tophat-Post-Fusion" module. Further, the fusion candidates were manually examined for annotation and ligation artifacts. Gene expression, as fragments per kilobase of exon per million fragments mapped (FPKM; normalized measure of gene expression), was calculated using Cufflinks (Trapnell et al., 2012).

ACCESSION NUMBERS

The accession number for the data reported in this paper is dbGap: phs000915.v1.p1.

SUPPLEMENTAL INFORMATION

Supplemental Information includes four figures and eight tables and can be found with this article online at http://dx.doi.org/10.1016/j.cell.2015.05.001.

AUTHOR CONTRIBUTIONS

Y-M.W., N.S., R.J.L., J.-M.M., R.M., M.E.T., C.C.P., G.A., H.B., and W.A. made equal contributions. D.R., E.M.V.A., and R.J.L. coordinated overall sequencing and bioinformatics analysis. Y.M.W., D.R., E.M.V.A., R.J.L., W.A., and J.V. coordinated figures and tables. N.S. developed the SU2C-PCF IDT cBio portal. R.J.L. coordinated copy number analyses. J.-M.M. coordinated central pathology review, and L.P.K coordinated UM pathology analysis. C.C.P. coordinated hypermutation analysis and clinical germline interpretations. R.M., M.E.T, G.A., H.B., M.H., H.I.S., and E.I.H. coordinated clinical enrollment at their specific sites. R.K.B., S.P., and H.D. carried out AR splice variant analysis. J.V. managed the clinical data portal. X.C., J.S., P.F., S.M., and C.S. were involved in project management. R.M., S.A.T., V.E.R., A.G., M.L., S.P.B., R.T.L., M.B., B.D.R., J.-M.M, M.R., and L.D.T. were involved in pathology review. C.B., P.V., J.G., M.G., F.D., O.E., A. Sboner, A. Sigaras, and K.W.E. contributed to bioinformatics analysis. K.A.C., D.C.S., F.Y.F., H.I.S., D.R., S.B.S., M.J.M., R.F., Z.Z., N.T., G.G., J.C.D., J.M., D.M.N., S.T.T., E.Y.Y., Y.C., E.A.M., H.H.C., M.A.S., and K.J.P. are clinical contributors. E.M.V.A., D.R., C.L.S. and A.M.C. wrote the manuscript, which all authors reviewed. P.K., J.S.d.B., M.A.R., P.S.N., and L.A.G. are SU2C-PCF Dream Team Principals, and C.L.S. and A.M.C. are Dream Team co-Leaders.

ACKNOWLEDGMENTS

We thank the affected individuals who participated in this study to better understand the feasibility and utility of precision medicine approaches for advanced prostate cancer. Individuals at our respective institutions who helped with this study are listed by institution. University of Michigan: Karen Giles, Lynda Hodges, Erica Rabban, Ning Yu, Fengyun Su, Rui Wang, Brendan Veeneman, and Moshe Talpaz. MSKCC: Brett Carver, Kristen Curtis, and Julie

Filipenko. DFCI/Broad: Zhenwei Zhang, Daniele Depalo, and Joseph Kramkowski. University of Washington: Jina Taub, Hiep Nguyen, Colm Morrissey, and Robert Vessella. ICR/Royal Marsden: Suzanne Carreira, Ines Figueiredo, and Daniel Nava Rodrigues. This work was supported by a Stand Up To Cancer-Prostate Cancer Foundation Prostate Dream Team Translational Cancer Research Grant. Stand Up To Cancer is a program of the Entertainment Industry Foundation administered by the American Association for Cancer Research (SU2C-AACR-DT0712). The project was also supported by the following NIH awards: Clinical Sequencing Exploratory Research (CSER) UM1HG006508 (A.M.C.), Early Detection Research Network grant UO1 CA111275(A.M.C.), Prostate SPORE grants P50 CA186786 (A.M.C.), P50 CA092629 (H.I.S., C.L.S., and Y.C.), P50 CA90381 (P.K.),and P50 CA097186 (P.S.N., B.M., E.A.M., and L.D.T.), P01 CA163227 (P.S.N., S.P., R.K.B., H.D.), R01 CA116337 (M.A.R., H.B., F.D.), R01 CA155169 (C.L.S.), R01 CA092629, P50 CA092629 (H.I.S., C.L.S., and Y.C.), and R01 CA155169 (C.L.S.). This work was supported by the following DoD awards: W81XWH-09-1-0147 (PCCTC) and DOD PC121341 (H.B.). This work was also supported by the Starr Cancer Consortium (N.S., M.R., C.S., Y.C., L.A.G.). A.M.C. is an A. Alfred Taubman Scholar and an American Cancer Society Professor. H.B. is supported by Damon Runyon Cancer Research Foundation CI-67-13. C.P. is supported by a PCF Young Investigator Award and DoD PC131820. E.M.V. is supported by a NIH 1K08CA188615. E.M.V., N.S., and F.Y.F. are supported by Prostate Cancer Foundation Young Investigator Awards. The RM and ICR team is supported by the Movember Foundation and Prostate Cancer UK, PCF, the ECMC network from Cancer Research UK, the Department of Health in the UK, and BRC grant funding.

Received: March 9, 2015
Revised: April 6, 2015
Accepted: April 27, 2015
Published: May 21, 2015

REFERENCES

American Cancer Society (2015). Cancer Facts and Figures 2015. http://www.cancer.org/acs/groups/content/@editorial/documents/document/acspc-044552.pdf.

Antonarakis, E.S., Lu, C., Wang, H., Luber, B., Nakazawa, M., Roeser, J.C., Chen, Y., Mohammad, T.A., Chen, Y., Fedor, H.L., et al. (2014). AR-V7 and resistance to enzalutamide and abiraterone in prostate cancer. N. Engl. J. Med. *371*, 1028–1038.

Asangani, I.A., Dommeti, V.L., Wang, X., Malik, R., Cieslik, M., Yang, R., Escara-Wilke, J., Wilder-Romans, K., Dhanireddy, S., Engelke, C., et al. (2014). Therapeutic targeting of BET bromodomain proteins in castration-resistant prostate cancer. Nature *510*, 278–282.

Assié, G., Letouzé, E., Fassnacht, M., Jouinot, A., Luscap, W., Barreau, O., Omeiri, H., Rodriguez, S., Perlemoine, K., René-Corail, F., et al. (2014). Integrated genomic characterization of adrenocortical carcinoma. Nat. Genet. *46*, 607–612.

Baca, S.C., Prandi, D., Lawrence, M.S., Mosquera, J.M., Romanel, A., Drier, Y., Park, K., Kitabayashi, N., MacDonald, T.Y., Ghandi, M., et al. (2013). Punctuated evolution of prostate cancer genomes. Cell *153*, 666–677.

Barbieri, C.E., Baca, S.C., Lawrence, M.S., Demichelis, F., Blattner, M., Theurillat, J.P., White, T.A., Stojanov, P., Van Allen, E., Stransky, N., et al. (2012). Exome sequencing identifies recurrent SPOP, FOXA1 and MED12 mutations in prostate cancer. Nat. Genet. *44*, 685–689.

Beer, T.M., Armstrong, A.J., Rathkopf, D.E., Loriot, Y., Sternberg, C.N., Higano, C.S., Iversen, P., Bhattacharya, S., Carles, J., Chowdhury, S., et al.; PREVAIL Investigators (2014). Enzalutamide in metastatic prostate cancer before chemotherapy. N. Engl. J. Med. *371*, 424–433.

Beltran, H., Yelensky, R., Frampton, G.M., Park, K., Downing, S.R., MacDonald, T.Y., Jarosz, M., Lipson, D., Tagawa, S.T., Nanus, D.M., et al. (2013). Targeted next-generation sequencing of advanced prostate cancer identifies potential therapeutic targets and disease heterogeneity. Eur. Urol. *63*, 920–926.

Berger, M.F., Lawrence, M.S., Demichelis, F., Drier, Y., Cibulskis, K., Sivachenko, A.Y., Sboner, A., Esgueva, R., Pflueger, D., Sougnez, C., et al. (2011). The genomic complexity of primary human prostate cancer. Nature *470*, 214–220.

Cao, J., Zhu, S., Zhou, W., Li, J., Liu, C., Xuan, H., Yan, J., Zheng, L., Zhou, L., Yu, J., et al. (2013). PLZF mediates the PTEN/AKT/FOXO3a signaling in suppression of prostate tumorigenesis. PLoS ONE *8*, e77922.

Carreira, S., Romanel, A., Goodall, J., Grist, E., Ferraldeschi, R., Miranda, S., Prandi, D., Lorente, D., Frenel, J.S., Pezaro, C., et al. (2014). Tumor clone dynamics in lethal prostate cancer. Sci. Transl. Med. *6*, 254ra125.

Castro, E., Goh, C., Olmos, D., Saunders, E., Leongamornlert, D., Tymrakiewicz, M., Mahmud, N., Dadaev, T., Govindasami, K., Guy, M., et al. (2013). Germline BRCA mutations are associated with higher risk of nodal involvement, distant metastasis, and poor survival outcomes in prostate cancer. J. Clin. Oncol. *31*, 1748–1757.

Cerami, E., Gao, J., Dogrusoz, U., Gross, B.E., Sumer, S.O., Aksoy, B.A., Jacobsen, A., Byrne, C.J., Heuer, M.L., Larsson, E., et al. (2012). The cBio cancer genomics portal: an open platform for exploring multidimensional cancer genomics data. Cancer Discov. *2*, 401–404.

Cibulskis, K., Lawrence, M.S., Carter, S.L., Sivachenko, A., Jaffe, D., Sougnez, C., Gabriel, S., Meyerson, M., Lander, E.S., and Getz, G. (2013). Sensitive detection of somatic point mutations in impure and heterogeneous cancer samples. Nat. Biotechnol. *31*, 213–219.

Comstock, C.E., Augello, M.A., Goodwin, J.F., de Leeuw, R., Schiewer, M.J., Ostrander, W.F., Jr., Burkhart, R.A., McClendon, A.K., McCue, P.A., Trabulsi, E.J., et al. (2013). Targeting cell cycle and hormone receptor pathways in cancer. Oncogene *32*, 5481–5491.

Cooper, C.S., Eeles, R., Wedge, D.C., Van Loo, P., Gundem, G., Alexandrov, L.B., Kremeyer, B., Butler, A., Lynch, A.G., Camacho, N., et al.; ICGC Prostate Group (2015). Analysis of the genetic phylogeny of multifocal prostate cancer identifies multiple independent clonal expansions in neoplastic and morphologically normal prostate tissue. Nat. Genet. *47*, 367–372.

de Bono, J.S., Logothetis, C.J., Molina, A., Fizazi, K., North, S., Chu, L., Chi, K.N., Jones, R.J., Goodman, O.B., Jr., Saad, F., et al.; COU-AA-301 Investigators (2011). Abiraterone and increased survival in metastatic prostate cancer. N. Engl. J. Med. *364*, 1995–2005.

Epstein, J.I., Amin, M.B., Beltran, H., Lotan, T.L., Mosquera, J.M., Reuter, V.E., Robinson, B.D., Troncoso, P., and Rubin, M.A. (2014). Proposed morphologic classification of prostate cancer with neuroendocrine differentiation. Am. J. Surg. Pathol. *38*, 756–767.

Finn, R.S., Crown, J.P., Lang, I., Boer, K., Bondarenko, I.M., Kulyk, S.O., Ettl, J., Patel, R., Pinter, T., Schmidt, M., et al. (2015). The cyclin-dependent kinase 4/6 inhibitor palbociclib in combination with letrozole versus letrozole alone as first-line treatment of oestrogen receptor-positive, HER2-negative, advanced breast cancer (PALOMA-1/TRIO-18): a randomised phase 2 study. Lancet Oncol. *16*, 25–35.

Fong, P.C., Boss, D.S., Yap, T.A., Tutt, A., Wu, P., Mergui-Roelvink, M., Mortimer, P., Swaisland, H., Lau, A., O'Connor, M.J., et al. (2009). Inhibition of poly(ADP-ribose) polymerase in tumors from BRCA mutation carriers. N. Engl. J. Med. *361*, 123–134.

Futreal, P.A., Coin, L., Marshall, M., Down, T., Hubbard, T., Wooster, R., Rahman, N., and Stratton, M.R. (2004). A census of human cancer genes. Nat. Rev. Cancer *4*, 177–183.

Gao, J., Aksoy, B.A., Dogrusoz, U., Dresdner, G., Gross, B., Sumer, S.O., Sun, Y., Jacobsen, A., Sinha, R., Larsson, E., et al. (2013). Integrative analysis of complex cancer genomics and clinical profiles using the cBioPortal. Sci. Signal. *6*, pl1.

Gao, D., Vela, I., Sboner, A., Iaquinta, P.J., Karthaus, W.R., Gopalan, A., Dowling, C., Wanjala, J.N., Undvall, E.A., Arora, V.K., et al. (2014). Organoid cultures derived from patients with advanced prostate cancer. Cell *159*, 176–187.

Geng, C., He, B., Xu, L., Barbieri, C.E., Eedunuri, V.K., Chew, S.A., Zimmermann, M., Bond, R., Shou, J., Li, C., et al. (2013). Prostate cancer-associated

mutations in speckle-type POZ protein (SPOP) regulate steroid receptor coactivator 3 protein turnover. Proc. Natl. Acad. Sci. USA *110*, 6997–7002.

Giannakis, M., Hodis, E., Jasmine Mu, X., Yamauchi, M., Rosenbluh, J., Cibulskis, K., Saksena, G., Lawrence, M.S., Qian, Z.R., Nishihara, R., et al. (2014). RNF43 is frequently mutated in colorectal and endometrial cancers. Nat. Genet. *46*, 1264–1266.

Grasso, C.S., Wu, Y.M., Robinson, D.R., Cao, X., Dhanasekaran, S.M., Khan, A.P., Quist, M.J., Jing, X., Lonigro, R.J., Brenner, J.C., et al. (2012). The mutational landscape of lethal castration-resistant prostate cancer. Nature *487*, 239–243.

Gundem, G., Van Loo, P., Kremeyer, B., Alexandrov, L.B., Tubio, J.M., Papaemmanuil, E., Brewer, D.S., Kallio, H.M., Högnäs, G., Annala, M., et al.; ICGC Prostate UK Group (2015). The evolutionary history of lethal metastatic prostate cancer. Nature *520*, 353–357.

Hieronymus, H., Schultz, N., Gopalan, A., Carver, B.S., Chang, M.T., Xiao, Y., Heguy, A., Huberman, K., Bernstein, M., Assel, M., et al. (2014). Copy number alteration burden predicts prostate cancer relapse. Proc. Natl. Acad. Sci. USA *111*, 11139–11144.

Hong, M.K., Macintyre, G., Wedge, D.C., Van Loo, P., Patel, K., Lunke, S., Alexandrov, L.B., Sloggett, C., Cmero, M., Marass, F., et al. (2015). Tracking the origins and drivers of subclonal metastatic expansion in prostate cancer. Nat. Commun. *6*, 6605.

Hsieh, C.L., Botta, G., Gao, S., Li, T., Van Allen, E.M., Treacy, D.J., Cai, C., He, H.H., Sweeney, C.J., Brown, M., et al. (2015). PLZF, a tumor suppressor genetically lost in metastatic castration-resistant prostate cancer, is a mediator of resistance to androgen deprivation therapy. Cancer Res. Published online March 25, 2015. http://dx.doi.org/10.1158/0008-5472.CAN-14-3602.

Kaufman, B., Shapira-Frommer, R., Schmutzler, R.K., Audeh, M.W., Friedlander, M., Balmaña, J., Mitchell, G., Fried, G., Stemmer, S.M., Hubert, A., et al. (2015). Olaparib monotherapy in patients with advanced cancer and a germline BRCA1/2 mutation. J. Clin. Oncol. *33*, 244–250.

Kikugawa, T., Kinugasa, Y., Shiraishi, K., Nanba, D., Nakashiro, K., Tanji, N., Yokoyama, M., and Higashiyama, S. (2006). PLZF regulates Pbx1 transcription and Pbx1-HoxC8 complex leads to androgen-independent prostate cancer proliferation. Prostate *66*, 1092–1099.

Kim, D., and Salzberg, S.L. (2011). TopHat-Fusion: an algorithm for discovery of novel fusion transcripts. Genome Biol. *12*, R72.

Lalonde, E., Ishkanian, A.S., Sykes, J., Fraser, M., Ross-Adams, H., Erho, N., Dunning, M.J., Halim, S., Lamb, A.D., Moon, N.C., et al. (2014). Tumour genomic and microenvironmental heterogeneity for integrated prediction of 5-year biochemical recurrence of prostate cancer: a retrospective cohort study. Lancet Oncol. *15*, 1521–1532.

Lawrence, M.S., Stojanov, P., Polak, P., Kryukov, G.V., Cibulskis, K., Sivachenko, A., Carter, S.L., Stewart, C., Mermel, C.H., Roberts, S.A., et al. (2013). Mutational heterogeneity in cancer and the search for new cancer-associated genes. Nature *499*, 214–218.

Lawrence, M.S., Stojanov, P., Mermel, C.H., Robinson, J.T., Garraway, L.A., Golub, T.R., Meyerson, M., Gabriel, S.B., Lander, E.S., and Getz, G. (2014). Discovery and saturation analysis of cancer genes across 21 tumour types. Nature *505*, 495–501.

Liu, J., Pan, S., Hsieh, M.H., Ng, N., Sun, F., Wang, T., Kasibhatla, S., Schuller, A.G., Li, A.G., Cheng, D., et al. (2013). Targeting Wnt-driven cancer through the inhibition of Porcupine by LGK974. Proc. Natl. Acad. Sci. USA *110*, 20224–20229.

Lonigro, R.J., Grasso, C.S., Robinson, D.R., Jing, X., Wu, Y.M., Cao, X., Quist, M.J., Tomlins, S.A., Pienta, K.J., and Chinnaiyan, A.M. (2011). Detection of somatic copy number alterations in cancer using targeted exome capture sequencing. Neoplasia *13*, 1019–1025.

Mateo, J., Hall, E., Sandhu, S., Omlin, A., Miranda, S., Carreira, S., Goodall, J., Gillman, A., Mossop, H., Ralph, C., et al. (2014). Antitumour activity of the PARP inhibitor olaparib in unselected sporadic castration-resistant prostate cancer (CRPC) in the TOPARP trial. Annals Oncol. *25*, 1–41.

Mehra, R., Kumar-Sinha, C., Shankar, S., Lonigro, R.J., Jing, X., Philips, N.E., Siddiqui, J., Han, B., Cao, X., Smith, D.C., et al. (2011). Characterization of bone metastases from rapid autopsies of prostate cancer patients. Clin. Cancer Res. *17*, 3924–3932.

Olshen, A.B., Venkatraman, E.S., Lucito, R., and Wigler, M. (2004). Circular binary segmentation for the analysis of array-based DNA copy number data. Biostatistics *5*, 557–572.

Palanisamy, N., Ateeq, B., Kalyana-Sundaram, S., Pflueger, D., Ramnarayanan, K., Shankar, S., Han, B., Cao, Q., Cao, X., Suleman, K., et al. (2010). Rearrangements of the RAF kinase pathway in prostate cancer, gastric cancer and melanoma. Nat. Med. *16*, 793–798.

Pflueger, D., Terry, S., Sboner, A., Habegger, L., Esgueva, R., Lin, P.C., Svensson, M.A., Kitabayashi, N., Moss, B.J., MacDonald, T.Y., et al. (2011). Discovery of non-ETS gene fusions in human prostate cancer using next-generation RNA sequencing. Genome Res. *21*, 56–67.

Pritchard, C.C., Morrissey, C., Kumar, A., Zhang, X., Smith, C., Coleman, I., Salipante, S.J., Milbank, J., Yu, M., Grady, W.M., et al. (2014). Complex MSH2 and MSH6 mutations in hypermutated microsatellite unstable advanced prostate cancer. Nat. Commun. *5*, 4988.

Robinson, J.T., Thorvaldsdóttir, H., Winckler, W., Guttman, M., Lander, E.S., Getz, G., and Mesirov, J.P. (2011). Integrative genomics viewer. Nat. Biotechnol. *29*, 24–26.

Roychowdhury, S., Iyer, M.K., Robinson, D.R., Lonigro, R.J., Wu, Y.M., Cao, X., Kalyana-Sundaram, S., Sam, L., Balbin, O.A., Quist, M.J., et al. (2011). Personalized oncology through integrative high-throughput sequencing: a pilot study. Sci. Transl. Med. *3*, 111ra121.

Ryan, C.J., Smith, M.R., de Bono, J.S., Molina, A., Logothetis, C.J., de Souza, P., Fizazi, K., Mainwaring, P., Piulats, J.M., Ng, S., et al.; COU-AA-302 Investigators (2013). Abiraterone in metastatic prostate cancer without previous chemotherapy. N. Engl. J. Med. *368*, 138–148.

Scher, H.I., Fizazi, K., Saad, F., Taplin, M.E., Sternberg, C.N., Miller, K., de Wit, R., Mulders, P., Chi, K.N., Shore, N.D., et al.; AFFIRM Investigators (2012). Increased survival with enzalutamide in prostate cancer after chemotherapy. N. Engl. J. Med. *367*, 1187–1197.

Schwartz, S., Wongvipat, J., Trigwell, C.B., Hancox, U., Carver, B.S., Rodrik-Outmezguine, V., Will, M., Yellen, P., de Stanchina, E., Baselga, J., et al. (2015). Feedback suppression of PI3Kα signaling in PTEN-mutated tumors is relieved by selective inhibition of PI3Kβ. Cancer Cell *27*, 109–122.

Seshagiri, S., Stawiski, E.W., Durinck, S., Modrusan, Z., Storm, E.E., Conboy, C.B., Chaudhuri, S., Guan, Y., Janakiraman, V., Jaiswal, B.S., et al. (2012). Recurrent R-spondin fusions in colon cancer. Nature *488*, 660–664.

Taplin, M.E., Bubley, G.J., Shuster, T.D., Frantz, M.E., Spooner, A.E., Ogata, G.K., Keer, H.N., and Balk, S.P. (1995). Mutation of the androgen-receptor gene in metastatic androgen-independent prostate cancer. N. Engl. J. Med. *332*, 1393–1398.

Taylor, B.S., Schultz, N., Hieronymus, H., Gopalan, A., Xiao, Y., Carver, B.S., Arora, V.K., Kaushik, P., Cerami, E., Reva, B., et al. (2010). Integrative genomic profiling of human prostate cancer. Cancer Cell *18*, 11–22.

The Cancer Genome Atlas. (2015). The molecular taxonomy of primary prostate cancer. http://www.cbioportal.org/study.do?cancer_study_id=prad_tcga_pub.

Thorvaldsdóttir, H., Robinson, J.T., and Mesirov, J.P. (2013). Integrative Genomics Viewer (IGV): high-performance genomics data visualization and exploration. Brief. Bioinform. *14*, 178–192.

Tomlins, S.A., Rhodes, D.R., Perner, S., Dhanasekaran, S.M., Mehra, R., Sun, X.W., Varambally, S., Cao, X., Tchinda, J., Kuefer, R., et al. (2005). Recurrent fusion of TMPRSS2 and ETS transcription factor genes in prostate cancer. Science *310*, 644–648.

Tomlins, S.A., Laxman, B., Dhanasekaran, S.M., Helgeson, B.E., Cao, X., Morris, D.S., Menon, A., Jing, X., Cao, Q., Han, B., et al. (2007). Distinct classes of chromosomal rearrangements create oncogenic ETS gene fusions in prostate cancer. Nature *448*, 595–599.

Trapnell, C., Roberts, A., Goff, L., Pertea, G., Kim, D., Kelley, D.R., Pimentel, H., Salzberg, S.L., Rinn, J.L., and Pachter, L. (2012). Differential gene and

transcript expression analysis of RNA-seq experiments with TopHat and Cufflinks. Nat. Protoc. *7*, 562–578.

Van Allen, E.M., Foye, A., Wagle, N., Kim, W., Carter, S.L., McKenna, A., Simko, J.P., Garraway, L.A., and Febbo, P.G. (2014a). Successful whole-exome sequencing from a prostate cancer bone metastasis biopsy. Prostate Cancer Prostatic Dis. *17*, 23–27.

Van Allen, E.M., Mouw, K.W., Kim, P., Iyer, G., Wagle, N., Al-Ahmadie, H., Zhu, C., Ostrovnaya, I., Kryukov, G.V., O'Connor, K.W., et al. (2014b). Somatic ERCC2 mutations correlate with cisplatin sensitivity in muscle-invasive urothelial carcinoma. Cancer Discov. *4*, 1140–1153.

Van Allen, E.M., Wagle, N., Stojanov, P., Perrin, D.L., Cibulskis, K., Marlow, S., Jane-Valbuena, J., Friedrich, D.C., Kryukov, G., Carter, S.L., et al. (2014c). Whole-exome sequencing and clinical interpretation of formalin-fixed, paraffin-embedded tumor samples to guide precision cancer medicine. Nat. Med. *20*, 682–688.

Voeller, H.J., Truica, C.I., and Gelmann, E.P. (1998). Beta-catenin mutations in human prostate cancer. Cancer Res. *58*, 2520–2523.

Wang, X.S., Shankar, S., Dhanasekaran, S.M., Ateeq, B., Sasaki, A.T., Jing, X., Robinson, D., Cao, Q., Prensner, J.R., Yocum, A.K., et al. (2011). Characterization of KRAS rearrangements in metastatic prostate cancer. Cancer Discov. *1*, 35–43.

Wee, S., Wiederschain, D., Maira, S.M., Loo, A., Miller, C., deBeaumont, R., Stegmeier, F., Yao, Y.M., and Lengauer, C. (2008). PTEN-deficient cancers depend on PIK3CB. Proc. Natl. Acad. Sci. USA *105*, 13057–13062.

Weston, V.J., Oldreive, C.E., Skowronska, A., Oscier, D.G., Pratt, G., Dyer, M.J., Smith, G., Powell, J.E., Rudzki, Z., Kearns, P., et al. (2010). The PARP inhibitor olaparib induces significant killing of ATM-deficient lymphoid tumor cells in vitro and in vivo. Blood *116*, 4578–4587.

The Journal of Molecular Diagnostics, Vol. 17, No. 6, November 2015

ELSEVIER

the Journal of Molecular Diagnostics
jmd.amjpathol.org

MSIplus for Integrated Colorectal Cancer Molecular Testing by Next-Generation Sequencing

Jennifer A. Hempelmann, Sheena M. Scroggins, Colin C. Pritchard, and Stephen J. Salipante

From the Department of Laboratory Medicine, University of Washington, Seattle, Washington

Accepted for publication May 26, 2015.

Address correspondence to Stephen J. Salipante, M.D., Ph.D., University of Washington, 1959 NE Pacific St, Room NW120, Box 357110, Seattle, WA 98195-7110. E-mail: stevesal@uw.edu.

Molecular analysis of colon cancers currently requires multiphasic testing that uses various assays with different performance characteristics, adding cost and time to patient care. We have developed a single, next-generation sequencing assay to simultaneously evaluate colorectal cancers for mutations in relevant cancer genes (*KRAS*, *NRAS*, and *BRAF*) and for tumor microsatellite instability (MSI). In a sample set of 61 cases, the assay demonstrated overall sensitivity of 100% and specificity of 100% for identifying cancer-associated mutations, with a practical limit of detection at 2% mutant allele fraction. MSIplus was 97% sensitive (34 of 35 MSI-positive cases) and 100% specific (42 of 42 MSI-negative cases) for ascertaining MSI phenotype in a cohort of 78 tumor specimens. These performance characteristics were slightly better than for conventional multiplex PCR MSI testing (97% sensitivity and 95% specificity), which is based on comparison of microsatellite loci amplified from tumor and matched normal material, applied to the same specimen cohort. Because the assay uses an amplicon sequencing approach, it is rapid and appropriate for specimens with limited available material or fragmented DNA. This integrated testing strategy offers several advantages over existing methods, including a lack of need for matched normal material, sensitive and unbiased detection of variants in target genes, and an automated analysis pipeline enabling principled and reproducible identification of cancer-associated mutations and MSI status simultaneously. *(J Mol Diagn 2015, 17: 705–714; http://dx.doi.org/10.1016/j.jmoldx.2015.05.008)*

After initial diagnosis, the molecular characterization of colorectal cancers may require several separate clinical tests. Evaluation of microsatellite instability (MSI) status is recommended testing on all primary colon cancers from patients 50 years or younger (and in older patients if specific pathological features are present[1]) to serve as a screening test for Lynch syndrome, a disease of hereditary cancer predisposition.[2,3] Moreover, MSI status provides diagnostic information about disease prognosis and predicted treatment response to fluorouracil,[3–6] and can, therefore, directly inform patient care. In the case of metastatic disease, additional molecular testing beyond MSI status is indicated. Recently updated guidelines from the National Comprehensive Cancer Network recommend that extended *NRAS* and *KRAS* testing is performed on all stage IV cancers[7] to identify mutations conferring resistance to epidermal growth factor receptor inhibitors.[8–10] If *RAS* gene mutational status is negative, testing for *BRAF* mutations is then also advised, given the poor response of *BRAF*-mutated tumors to cetuximab plus irinotecan, fluorouracil, and leucovorin combination therapy,[11] and also to epidermal growth factor receptor inhibitors used beyond first-line treatment.[12,13]

Independent molecular assays are currently used to test tumor specimens for MSI status and gene mutations. Molecular diagnosis of MSI is implemented using multiplexed PCR-based MSI testing (MSI-PCR), wherein a limited number of informative microsatellite markers[14,15] are PCR amplified from tumor and matched normal material, products are resolved using capillary gel electrophoresis, and the presence of additional alleles, which are the hallmark of the MSI

Supported by Congressionally Directed Medical Research Programs award PC131820 (C.C.P.) and a Prostate Cancer Foundation 2013 Young Investigator Award (C.C.P.).

Disclosures: None declared.

http://dx.doi.org/10.1016/j.jmoldx.2015.05.008

phenotype, is qualitatively ascertained.[5,6,16] In some cases, immunohistochemical (IHC) detection of mismatch repair-pathway protein loss may additionally or alternatively be performed,[17–19] although some studies suggest that IHC does not sensitively identify all MSI-positive tumors.[17,20] In contrast, clinical testing for *NRAS*, *KRAS*, and *BRAF* gene mutations is commonly achieved using single-gene assays using melting curve analysis,[21,22] real-time PCR,[23,24] or conventional Sanger sequencing.[24] Peptide nucleic acid clamping[25] or selective amplification of mutant alleles is sometimes used to improve sensitivity.[26–28]

Next-generation sequencing (NGS) is becoming increasingly used by clinical laboratories as a cost-effective and scalable method to interrogate multiple genetic targets in parallel,[29–32] and could be adapted for the focused purpose of characterizing colorectal cancers for molecular workup. Although integrating colorectal cancer testing into an NGS diagnostic would offer practical advantages in eliminating the need for multiple, separate diagnostic tests, the unique analytic properties of NGS could also translate to performance advantages over existing testing methods. Such benefits include the following: i) The ability of the technology to detect low-prevalence, cancer-associated mutations is greater than that of conventional methods,[31–34] because each DNA molecule is examined independently by NGS, potentially providing increased sensitivity for detecting relevant cancer-associated mutations. ii) Our group[35] and others[36–38] have developed methods to computationally infer MSI status from NGS data on the basis of the quantification and distribution of observed allele lengths at microsatellite loci. This offers a standardized, statistical approach for interpreting MSI testing results, in contrast to the current practice of subjective interpretation of MSI-PCR electropherogram traces.[35] iii) Owing to the digital nature of NGS data, primary analysis can be readily automated,[31,35,39] ensuring consistency in test interpretation.

Herein, we describe the clinical validation of a novel NGS assay, MSIplus, for simultaneously evaluating tumor MSI status and mutational hotspots in *KRAS*, *NRAS*, and *BRAF* genes, and provide interpretive guidelines for its diagnostic use. In contrast to earlier research work, which has used NGS to evaluate MSI status from exome and targeted gene capture designs, our assay uses an amplicon sequencing approach, which enables effective targeting and high depth of coverage for the loci of interest. The assay is suitable for molecular characterization of colorectal cancers, does not require matched normal material for inference of MSI status, and is rapid, cost-effective, sensitive, and specific.

Materials and Methods

Selection of Target Sequences and Primer Design

For the purpose of inferring MSI status, we selected a panel of 11 microsatellite markers from our earlier analysis of colorectal cancer exome data[35] that were empirically found to be both most discriminatory for MSI and most frequently unstable in MSI-positive tumors (Table 1). We also incorporated the mononucleotide A/T tract of HSPH1,[40] the instability of which predicts sensitivity to particular anticancer agents, and the five microsatellite markers (MONO-27, BAT-25, BAT-26, NR-21, and NR-24) that compose a performance-enhanced derivative of the Bethesda panel[15] used in current clinical MSI-PCR assays.[16] Separate primers were designed to span exons containing relevant mutational hotspots in *KRAS* (exons 2, 3, and 4; codons 12, 13, 61, 117, and 147), *NRAS* (exons 2, 3, and 4; codons 12, 13, 61, 117, and 147), and *BRAF* (exon 15; codons 599, 600, and 601).

Multiplexed primer design was performed using MPprimer version 1.4[41] (*https://code.google.com/p/mpprimer*, last accessed October 15, 2013) with some manual curation. Genomic coordinates for each locus (human genome hg19/GRCh37) and PCR primer sequences are provided in Table 1. Primers were concatenated at the 5′ end to partial Illumina sequencing adaptors, which were extended in downstream steps. All oligonucleotides were synthesized by Integrated DNA Technologies (Coralville, IA).

Tumor Specimens and Clinical Testing

DNA from tumor specimens, which were predominantly colorectal cancers, but included a small subset of endometrial cancers, lung cancers, ovarian cancers, melanoma, and additional tumor types, was extracted from fresh-frozen tissue or formalin-fixed, paraffin-embedded tissue blocks. All tumors had >10% neoplastic cellularity, as estimated by review of hematoxylin and eosin–stained slides. Clinical specimens were obtained in accordance with the Declaration of Helsinki and the ethics guidelines of the human subjects division of the University of Washington (Seattle, WA).

Our study design is summarized in Figure 1. Clinical testing for mutations in *BRAF*, *KRAS*, and *NRAS* was performed in 61 specimens by the University of Washington Clinical Molecular Genetics Laboratory. Variants were identified using either the UW-OncoPlex NGS oncology assay[31] (*http://tests.labmed.washington.edu/UW-OncoPlex*, last accessed June 4, 2014) or PCR-amplification and melting curve analysis assays for each individual gene target.[21,22,26]

Clinical MSI-PCR testing of 81 colorectal tumor specimens was performed by the University of Washington Clinical Molecular Genetics Laboratory using the MSI analysis kit (Promega, Fitchburg, WI). Samples demonstrating instability at two or more of the five mononucleotide markers included in this panel were considered MSI positive [MSI high (MSI-H); diagnosis, 44 specimens]. All other specimens analyzed in this study did not demonstrate any unstable loci by MSI-PCR, and were considered MSI negative (microsatellite stable; diagnosis, 37 specimens). IHC staining for MLH1, MSH2, MSH6, and PMS2 was performed using standard diagnostic techniques.

Table 1 Loci and Primer Sequences

Assay stage	Target locus	Primer coordinates	Repeat type	Forward primer sequence	Reverse primer sequence
Stage 1 PCR	Bat-25	Chr4: 55598177-55598271	(A)22	5′-ACACTCTTTCCCTACACGACGCTCTTCCG-ATCTGGAGGATGACGAGTTGGCCCTAGAC-3′	5′-CGGTCTCGGCATTCCTGCTGAACCGCTCTTGTG-TTTCCCAAAGAGACAGCAGTTGGAACATGA-3′
Stage 1 PCR	Bat-26	Chr2: 47641524-47641622	(T)19	5′-ACACTCTTTCCCTACACGACGCTCTTCCG ATCTAGTGGAGTGGAGGAGGGGAGAGAAA-3′	5′-CGGTCTCGGCATTCCTGCTGAACCGCTCTTGTG-TTTCTTGCAGTTTCATCACTGTCTGCGGT-3′
Stage 1 PCR	MONO-27	Chr2: 39564859-39564957	(T)28	5′-ACACTCTTTCCCTACACGACGCTCTTCCG-ATCTCTACTGTCCTACTGTGCCTGGCTCC-3′	5′-CGGTCTCGGCATTCCTGCTGAACCGCTCTTGTG-TTTCCAGCCTGGGCAAGATAATGAGACCC-3′
Stage 1 PCR	NR-21	Chr14: 23652311-23652403	(A)22	5′-ACACTCTTTCCCTACACGACGCTCTTCCG-ATCTCTGGTGCACAGAGCAGAACCATCCT-3′	5′-CGGTCTCGGCATTCCTGCTGAACCGCTCTTGTG-TTTCGCAACCTCAAAAGCTGCCTCCCTTT-3′
Stage 1 PCR	NR-24	Chr2: 95849327-95849419	(T)24	5′-ACACTCTTTCCCTACACGACGCTCTTCCG-ATCTCTGTAGTCCCAGCTATTCGGGAGGC-3′	5′-CGGTCTCGGCATTCCTGCTGAACCGCTCTTGTG-TTTCAAATGACCCCTTCCTGCCCATCACT-3′
Stage 1 PCR	MSI-01	Chr1: 201754376-201754446	(T)17	5′-ACACTCTTTCCCTACACGACGCTCTTCCG-ATCTTTGATGTCCTGCGTCTAGGGTCTGC-3′	5′-CGGTCTCGGCATTCCTGCTGAACCGCTCTTGTG-TTTCGACTGGAGCCTTGGACAGGTTGAGA-3′
Stage 1 PCR	MSI-03	Chr2: 62063059-62063129	(A)17	5′-ACACTCTTTCCCTACACGACGCTCTTCCG-ATCTGCCACTGCTATTTGAAAGAGTTGCTC-3′	5′-CGGTCTCGGCATTCCTGCTGAACCGCTCTTGTG-TTTCGCCACTGCTATTTGAAAGAGTTGCTC-3′
Stage 1 PCR	MSI-04	Chr2: 108479588-108479658	(T)18	5′-ACACTCTTTCCCTACACGACGCTCTTCCG-ATCTTCCAAGATTCCTTCCCTGGCCACTC-3′	5′-CGGTCTCGGCATTCCTGCTGAACCGCTCTTGTG-TTTCACTGTCTGTAGTCCTGGCTTCGTGG-3′
Stage 1 PCR	MSI-06	Chr5: 172421726-172421796	(T)15	5′-ACACTCTTTCCCTACACGACGCTCTTCCG-ATCTAGCAGCAAACTGAACAGGTCACCAAC-3′	5′-CGGTCTCGGCATTCCTGCTGAACCGCTCTTGTG-TTTCAGCAGCAAACTGAACAGGTCACCAAC-3′
Stage 1 PCR	MSI-07	Chr6: 142691916-142691986	(T)17	5′-ACACTCTTTCCCTACACGACGCTCTTCCG-ATCTGCTGAAAGCAACCTAAGCTGTGGTGA-3′	5′-CGGTCTCGGCATTCCTGCTGAACCGCTCTTGTG-TTTCTGCTATAAGAGCTGAGCAGACGACA-3′
Stage 1 PCR	MSI-08	Chr7: 1787485-1787555	(A)17	5′-ACACTCTTTCCCTACACGACGCTCTTCCG-ATCTCCAGCCCCCATGTACACTGTAGTCG-3′	5′-CGGTCTCGGCATTCCTGCTGAACCGCTCTTGTG-TTTCCCCACCCCAAGGCCAAAATCAGTAA-3′
Stage 1 PCR	MSI-09	Chr7: 74608706-74608776	(T)13	5′-ACACTCTTTCCCTACACGACGCTCTTCCG-ATCTGTCTCGGCTACTTGGGAGGCTTAGG-3′	5′-CGGTCTCGGCATTCCTGCTGAACCGCTCTTGTG-TTTCCCGACTAAAGAGGTCATTCACTTGT-3′
Stage 1 PCR	MSI-11	Chr11: 106695477-106695550	(T)12	5′-ACACTCTTTCCCTACACGACGCTCTTCCG-ATCTAGCATGTTTGCAGCCTTCTTCTGGA-3′	5′-CGGTCTCGGCATTCCTGCTGAACCGCTCTTGTG-TTTCAGCATGTTTGCAGCCTTCTTCTGGA-3′
Stage 1 PCR	MSI-12	Chr15: 45897737-45897807	(T)14	5′-ACACTCTTTCCCTACACGACGCTCTTCCG-ATCTGCTGAGGCTAAACACTATCATGCCA-3′	5′-CGGTCTCGGCATTCCTGCTGAACCGCTCTTGTG-TTTCCAGAGGTTGCAGTGAGCCGAGATTG-3′
Stage 1 PCR	MSI-13	Chr16: 18882625-18882695	(A)15	5′-ACACTCTTTCCCTACACGACGCTCTTCCG-ATCTACATCTTCAGGTCAGGAAAACAGCTCG-3′	5′-CGGTCTCGGCATTCCTGCTGAACCGCTCTTGTG-TTTCTAATGACTTGGGCTTTGGAAGCAGC-3′
Stage 1 PCR	MSI-14	Chr17: 19314883-19314953	(T)18	5′-ACACTCTTTCCCTACACGACGCTCTTCCG-ATCTCATTTCAACTGACCTGCCTGGCCTC-3′	5′-CGGTCTCGGCATTCCTGCTGAACCGCTCTTGTG-TTTCCTTGGCAAACGGGCAAGTCTTCAGT-3′
Stage 1 PCR	*HSPH1*-T17	Chr13: 31722570-31722746	(A)17	5′-ACACTCTTTCCCTACACGACGCTCTTCCG-ATCTTGGAAAAGGAACTGCATCTGTGACGG-3′	5′-CGGTCTCGGCATTCCTGCTGAACCGCTCTTGTG-TTTCTTTTCCTAATCCCCTGTGAAACCTGT-3′
Stage 1 PCR	*BRAF* exon 15	Chr7: 140453095-140453431	NA	5′-ACACTCTTTCCCTACACGACGCTCTTCCG-ATCTACAACTGTTCAAACTGATGGGACC-3′	5′-CGGTCTCGGCATTCCTGCTGAACCGCTCTTGTG-TTTCCCTCATCCTAACACATTTCAAGCCCCA-3′
Stage 1 PCR	*KRAS* exon 4	Chr12: 25378395-25378686	NA	5′-ACACTCTTTCCCTACACGACGCTCTTCCG-ATCTTTTCAGTGTTACTTACCTGTCTTGTC-3′	5′-CGGTCTCGGCATTCCTGCTGAACCGCTCTTGTG-TTTCTGACAAAAGTTGTGGACAGGT-3′
Stage 1 PCR	*KRAS* exon 3	Chr12: 25380233-25380491	NA	5′-ACACTCTTTCCCTACACGACGCTCTTCCG-ATCTCCCAGTCCTCATGTACTGGTCCCT-3′	5′-CGGTCTCGGCATTCCTGCTGAACCGCTCTTGTG-TTTCCCGTCATCTTTGGAGCAGGAACA-3′
Stage 1 PCR	*KRAS* exon 2	Chr12: 25398245-25398504	NA	5′-ACACTCTTTCCCTACACGACGCTCTTCCG-ATCTTGAATTAGCTGTATCGTCAAGGCACTC-3′	5′-CGGTCTCGGCATTCCTGCTGAACCGCTCTTGTG-TTTCACACGTCTGCAGTCAACTGGAATTT-3′
Stage 1 PCR	*NRAS* exon 4	Chr1: 115252168-115252401	NA	5′-ACACTCTTTCCCTACACGACGCTCTTCCG-ATCTAATGCTGAAAGCTGTACCATACC-3′	5′-CGGTCTCGGCATTCCTGCTGAACCGCTCTTGTG-TTTCCCCAGCCTAATCTTGTTTTTCTT-3′
Stage 1 PCR	*NRAS* exon 3	Chr1: 115258629-115258838	NA	5′-ACACTCTTTCCCTACACGACGCTCTTCCG-ATCTTGTGGCTCGCCAATTAACCCTG-3′	5′-CGGTCTCGGCATTCCTGCTGAACCGCTCTTGTG-TTTCTGAGAGACAGGATCAGGTCAGCGG-3′
Stage 1 PCR	*NRAS* exon 2	Chr1: 115256475-115256731	NA	5′-ACACTCTTTCCCTACACGACGCTCTTCCG-ATCTAGGAAGCCTTCGCCTGTCCTCA-3′	5′-CGGTCTCGGCATTCCTGCTGAACCGCTCTTGTG-TTTCACCAGATAGGCAGAAATGGGCTTGA-3′
Stage 2 PCR	NA	NA	NA	5′-AATGATACGGCGACCACCGAGATCTAC-ACTCTTTCCCTACACGACGC-3′	5′-CAAGCAGAAGACGGCATACGAGATXXXXXXXXCG-GTCTCGGCATTCCTGCTGAACCG-3′*
Index read	NA	NA	NA	5′-AGATCGGAAGAGCGGTTCAGCAGGA-ATGCCGCGCCCG-3′	NA

*X indicates the presence of an 8-bp sample-specific index sequence.
NA, not applicable.

Determination of mSINGS Baseline Reference Values

Determining MSI status by mSINGS analysis of NGS data[35] entails comparing experimental results against baseline reference values at each microsatellite locus to assess its instability. Because amplifying microsatellite loci by PCR generates a distribution of alternate fragments (stutter artifact) that results from template slippage during cycling,[42,43] it is necessary to establish assay-specific baseline values for each locus. To establish baseline reference values, we extracted DNA from 42 peripheral blood specimens and analyzed them using the MSIplus assay.

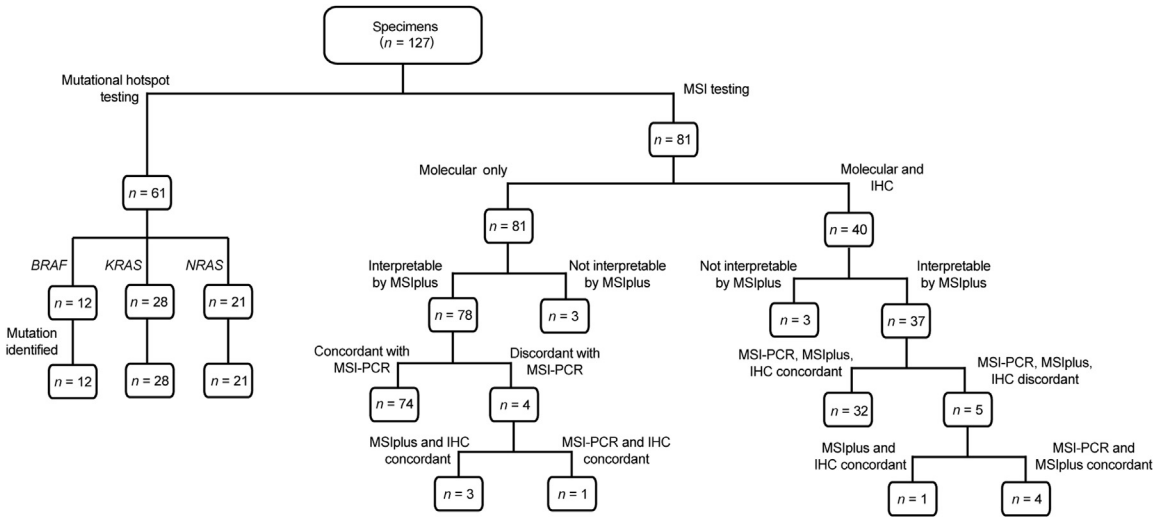

Figure 1 Study design and summary of results. Diagnostic testing algorithm and results are depicted. The number of specimens at each stage is indicated numerically at corresponding nodes. Fifteen specimens were tested for both microsatellite instability (MSI) status and mutational hotspots; thus, inclusion in these categories is not mutually exclusive. IHC, immunohistochemistry.

Library Preparation and Sequencing

Sequencing libraries were generated by PCR amplification in two separate stages. The purpose of the first stage was to simultaneously amplify the loci of interest from the genome and to incorporate partial Illumina sequencing adaptors into the amplification product. The second stage of PCR fully extended the sequencing adaptors and incorporated unique 8-bp, sample-specific index sequences (Table 1), which enabled the multiplexing of multiple specimens together onto the same sequencing run. In addition to the tumor samples, control DNA from HapMap individual NA12878 (Coriell Institute, Camden, NJ) was included with each library preparation and sequencing run, and served as a negative control for both MSI status and *RAS* and *BRAF* mutations, as was a nontemplate amplification control.

The first stage of PCR was performed in two separate reactions, one using an equimolar pool of the microsatellite primers, and the other using primers targeting mutational hotspots. In the latter primer pool, primers were combined in equimolar amounts, except for the primer pairs amplifying *NRAS* exon 2 (included at 0.5× concentration) and *NRAS* exon 4 (included at 1.5× concentration). Both first-stage PCRs were performed in a 25-μL volume using the Qiagen Multiplex PCR Kit (Qiagen, Valencia, CA), and incorporating 50-ng template DNA, 0.25 μmol/L of the appropriate primer pool, and 1× Qiagen Q-solution. PCR cycling for both primer pools was as follows: 5 minutes' incubation at 95°C; 30 cycles of 94°C for 30 seconds, 60°C for 90 seconds, and 72°C for 60 seconds; and a final extension at 72°C for 10 minutes. Before the second stage of PCR, amplification products were purified using a 0.8× volume of Agencourt AMPure XP magnetic beads (Beckman-Coulter, Indianapolis, IN), according to the manufacturer's instructions.

The second stage of PCR was performed using 5 ng of amplification products from the first stage of PCR as template. PCR was performed in a 25-μL volume using KAPA HiFi HotStart ReadyMix PCR Kit (KAPABiosystems, Wilmington, MA), and 0.3 μmol/L of each of the second-stage primers (Table 1). This phase incorporated a reverse primer carrying a sample-specific index sequence; however, the same reverse primer was used in separately amplifying the microsatellite and mutational hotspot amplicons derived from the same specimen. PCR cycling conditions were as follows: 3 minutes' incubation at 95°C; five cycles of 98°C for 20 seconds, 65°C for 15 seconds, and 72°C for 60 seconds; and a final extension at 72°C for 5 minutes. PCRs were purified using a 1.8× volume of Agencourt AMPure XP magnetic beads.

Amplicons derived from the same specimen were pooled in an 8:1 volumetric ratio of microsatellite PCR product/mutational hotspot PCR product before sequencing. Sequencing was performed on an Illumina MiSeq (San Diego, CA) using 200-bp, single-ended reads and an 8-bp index read, with the addition of a custom index read primer (Supplemental Table S1). A 5% concentration of PhiX Control version 3 (Illumina) was included in each sequencing run. Sequencing used a Micro or Nano MiSeq Reagent version 2 300-cycle kit (Illumina), depending on the number of samples pooled for sequencing (up to 32 samples and up to 9 samples, respectively).

Data Analysis

Single-ended sequence reads were initially aligned to the human genome (hg19/GRCh37) using bwa version 0.6.1-r104[44] (*http://sourceforge.net/projects/bio-bwa*, last accessed October 28, 2013) and SAMtools version 0.1.18 (*http://sourceforge.net/projects/samtools*, last accessed October 28, 2013).[45] Sample-level, fully local indel realignment was then

performed using Genome Analysis Toolkit version 3.2 (*https://www.broadinstitute.org/gatk*, last accessed May 28, 2014),[39,46] followed by quality score recalibration, to generate a final, realigned, and recalibrated alignment, which was used for subsequent analyses.

Identification of single-nucleotide variants, insertions, and deletions in *KRAS*, *NRAS*, and *BRAF* was performed using VarScan version 2.3.7 (*http://varscan.sourceforge.net*, last accessed May 16, 2014),[47] with the minimum variant frequency set to 0.005 reads, the minimum number of variant reads set to 2, and strand filtering disabled. In addition to primary variant calls, we also tabulated the absolute number of sequence reads matching specific variants of clinical actionability (Supplemental Table S2) using the VarScan readcounts function.

MSI status was determined using the mSINGS package (*https://bitbucket.org/uwlabmed/msings*, last accessed April 27, 2015)[35] with multiplier set to 1.75, msi_min_threshold set to 0.27, and msi_max_threshold set to 0.54.

Results

Sensitivity and Specificity for *KRAS*, *NRAS*, and *BRAF* Mutations

We evaluated the ability of MSIplus to detect mutations in *KRAS*, *NRAS*, and *BRAF* for a panel of 61 formalin-fixed, paraffin-embedded tumor specimens known to be positive for mutations in these genes on the basis of prior clinical testing (Table 2). We first estimated the frequency of false-positive sequence reads at each clinically significant site in *KRAS*, *NRAS*, and *BRAF* by tallying mutant reads (Supplemental Table S1) at known wild-type sites, on the basis of prior clinical testing. Of a total of 517,062 sequence reads examined from a subset of 27 specimens, 2127 sequence reads (0.4%) carried a false-positive mutation. Regardless, multiple reads must carry the same artifact mutation for a variant to be called; thus, this analysis overestimates false-positivity rate. We, therefore, considered each of the mutant calls independently, which yielded an average allele fraction of 0.07% (SD, 0.17%) for false-positive calls of any particular mutation. We set a minimum threshold of 2% allele fraction for calling mutations using MSIplus, a threshold that should exclude virtually all false-positive variant calls (z-score $= 1.5 \times 10^{-25}$) and that defines the practical limit of detection for this assay.

We next evaluated the assay's ability to detect clinically relevant mutations within the three target genes for each of 61 positive control specimens (Figure 1 and Table 2). Average read depth across the seven separate amplicons covering mutational hotspots was 1652 reads (interquartile range, 225 to 2306 reads). We achieved 100% sensitivity [61 of 61 expected variants recovered; 95% CI, 94.1%–100% by the Clopper-Pearson (exact binomial) method].

No specimen demonstrated a false-positive variant call occurring at or above a 2% allele fraction for any of the 44 possible nucleotide sequence variants encoding a clinically relevant mutation (Supplemental Table S1). These results equate to a specificity of 100% (2684 of 2684 true-negative variant calls; 95% CI, >99.3% to 100%). In addition, we observed a high degree of correlation ($R^2 = 0.84$) between the allele fraction of mutations detected by MSIplus and the estimated mutant allele fraction from previous clinical testing using targeted gene-capture NGS methods[31] (subset of 55 specimens) (Figure 2 and Supplemental Table S2). Approximate linearity between these estimates was observed over a range of 2.0% to 59.2% estimated variant allele fraction. This finding suggests that the amplification bias or other artifacts potentially affecting the calculated allele fraction are not pronounced in the MSIplus assay. Furthermore, variants in two specimens with 2.0% mutant allele frequencies were successfully identified, supporting the assay's theoretical limit of detection.

To evaluate the reproducibility of mutation detection, we examined a subset of eight control specimens across three or more independent batches of library preparation and sequencing (Supplemental Table S3). The expected mutations were recovered in all 36 independent technical replicates. The CV for the estimated allele fraction was 0.06 (range, 0.03 to 0.15).

Table 2 Detection of *KRAS*, *NRAS*, and *BRAF* Mutations

Mutation	No. of samples	No. detected
KRAS p.G12S	1	1
KRAS p.G12D	5	5
KRAS p.G12C	2	2
KRAS p.G12V	6	6
KRAS p.G13C	1	1
KRAS p.G13D	8	8
KRAS p.Q61H	3	3
KRAS p.K117N	1	1
KRAS p.A146V	1	1
NRAS p.G13V	1	1
NRAS p.G13R	1	1
NRAS p.G12S	1	1
NRAS p.G12D	6	6
NRAS p.Q61R	8	8
NRAS p.Q61L	2	2
NRAS p.Q61K	1	1
NRAS p.Q61H	1	1
BRAF p.V600K	1	1
BRAF p.V600E	11	11
Total	61	61

Determination of MSI Status

We separately assessed the assay's ability to detect the MSI-positive phenotype on the basis of mSINGS analysis of targeted microsatellite loci.[35] By using MSIplus, we typed a collection of 81 specimens (Figure 1) previously subjected to MSI-PCR testing in our laboratory (44 microsatellite unstable, or MSI-H, results and 37 microsatellite stable results). We first evaluated the reproducibility of mSINGS score determination (corresponding to the total

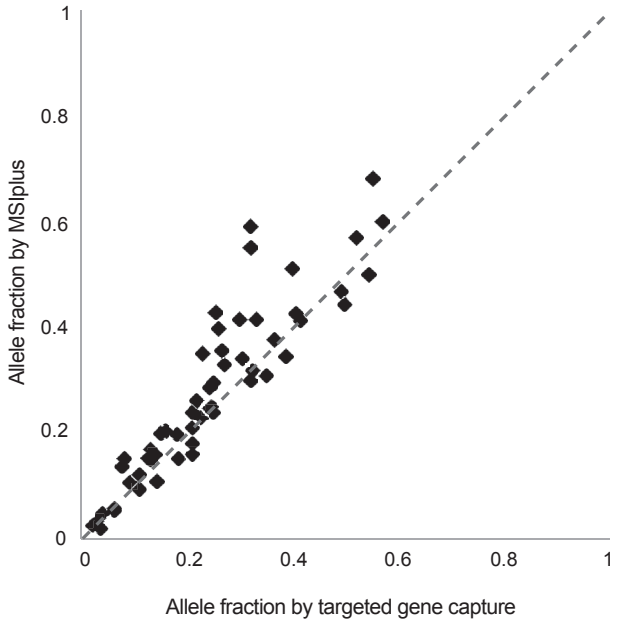

Figure 2 Correlation of allele fraction by MSIplus and targeted gene-capture next-generation sequencing. Allele fractions are estimated by either the MSIplus assay or the UW-OncoPlex targeted gene-capture sequencing panel. The subset of 55 specimens for which data from both assays were available is shown. Dashed gray line indicates a theoretical perfect correlation between the two estimations.

fraction of typed microsatellite loci that are unstable) by examining at least two separately prepared and sequenced technical replicates each for a subset of 48 specimens (Supplemental Table S4). Because several specimens had mSINGS scores of 0, calculating the CV was not meaningful. On average, the SD observed among technical replicates was 0.07 mSINGS units, and the SD of values around this mean was 0.03.

On the basis of the qualitative separation of microsatellite stable from MSI-H groups[35] (Figure 3), we initially set an empirical threshold of a 0.40 mSINGS score for differentiating MSI-positive from MSI-negative tumors. However, in light of mSINGS score variability, specimens with scores falling close to this threshold could be assigned the wrong MSI status by chance alone. To prevent improper MSI classifications resulting from assay variability, specimens with mSINGS values falling between 0.27 and 0.54 [threshold ± (average mSINGS variability + standard deviation of mSINGS variability × 2)] were consequently considered uninterpretable. In contrast, specimens with mSINGS scores lower or higher than those values could be confidently classified as MSI negative or MSI positive, respectively. Seventy-seven specimens had interpretable mSINGS scores, and we repeated library preparation for the remaining four samples that did not. On retyping, mSINGS scores for one of the four specimens became interpretable, whereas the remaining three results remained ambiguous. Thus, the MSI status of 95% of all specimens was initially interpretable, and on repeat typing, this proportion increased only modestly, to 96%.

Most MSI-negative specimens were readily distinguished from MSI-positive specimens on the basis of mSINGS score, and mSINGS interpretations were fully concordant with MSI-PCR interpretations in most cases (Figure 3 and Supplemental Table S5). However, four samples had discordant results between the two methods, which warranted further investigation.

One specimen was classified as MSI negative by MSI-PCR, but had a high mSINGS score (0.63) and was, therefore, interpreted as MSI positive by the MSIplus assay. Review of laboratory records indicated that, on subsequent workup, the tumor was found to have deficient MHS6 expression by IHC and that gene sequencing identified a germline MSH6 mutation in the patient, establishing a diagnosis of Lynch syndrome. We conclude that this instance represents a false-negative MSI-PCR result, and that the correct diagnosis was achieved by MSIplus. The other three discrepancies corresponded to specimens typed as MSI positive by MSI-PCR but classified as MSI negative using MSIplus. In two cases, clinical IHC testing was performed and did not reveal loss of expression in any mismatch repair proteins. Although MSI positivity has been observed in a background of normal MMR protein expression in approximately 5% of cases,[16] these cases are most consistent with false-positive MSI-PCR results. Conversely, the remaining discrepant case likely represents a false negative by MSIplus because loss of MSH2 and MSH6 expression was seen by IHC and a germline *MSH6* mutation was identified by genetic testing.

Accounting for these additional clinical data, and assuming that all specimens receiving a concordant

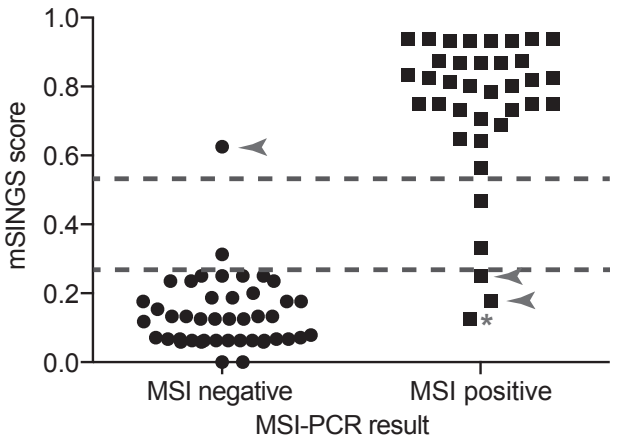

Figure 3 Inferring microsatellite instability (MSI) status by MSIplus. Data are stratified according to testing results by MSI-PCR. The mSINGS score (the fraction of interrogated microsatellite loci that are unstable) is plotted for each specimen. The dashed lines at mSINGS scores of 0.27 and 0.54 indicate the cutoffs for delineating MSI-positive and MSI-negative specimens by MSIplus: mSINGS scores falling below these values were interpreted as negative, scores above those values were interpreted as positive, and scores falling between the values could not be reliably interpreted. **Arrowheads** indicate specimens misclassified by MSI-PCR; **asterisk** indicates specimen misclassified by MSIplus, as resolved by alternative clinical testing results (immunohistochemical and/or genetic testing). For specimens that were typed multiple times, one representative mSINGS score is displayed.

diagnosis by MSI-PCR and MSIplus were correctly assigned an MSI status, we conclude that the validation set used in our study comprised a total of 36 MSI-positive cases and 42 MSI-negative cases. We calculate that MSIplus has an overall sensitivity of 97.1% (34 of 35 MSI-positive cases identified; 95% CI, 85.1%–99.9%) and a specificity of 100% (42 of 42 MSI-negative cases identified; 95% CI, 91.6%–100%) for determining tumor MSI status. The positive predictive value and negative predictive value for MSIplus were 97.1% and 97.7%, respectively. For the same panel of test specimens, MSI-PCR demonstrated a sensitivity of 97.1% (34 of 35 MSI-positive cases identified; 95% CI, 85.1%–99.9%), a specificity of 95.2% (40 of 42 MSI-negative cases identified; 95% CI, 83.8%–99.4%), a positive predictive value of 94.6%, and a negative predictive value of 95.6% for the same set of validation specimens.

Correlation of MSIplus, MSI-PCR, and IHC

Although our primary objective was to compare the results of molecular MSI testing by MSI-PCR and MSIplus, we additionally correlated our findings with IHC for 40 cases where this information was available (Figure 1 and Supplemental Table S5). The diagnosis rendered by each of the three approaches (IHC, MSI-PCR, and MSIplus) was fully concordant in 32 of 37 cases where MSIplus was interpretable. One discrepant case, discussed above, evidenced isolated loss of MSH6 by IHC, and was negative by MSI-PCR but positive by MSIplus, suggesting that MSIplus and IHC obtained the proper diagnosis. Three additional cases receiving a MSI-positive diagnosis by both MSI-PCR and MSIplus showed no loss of MMR protein expression by IHC, suggesting a MSI-positive status without loss of MMR protein expression.[20] One specimen was negative by MSI-PCR and MSIplus, but demonstrated reduction of MLH1 and PMS2 expression by IHC: it is possible that this latter case represents either a false-negative molecular result or a false-positive result by IHC.[20]

Quantitative Correlation of MSIplus and Conventional MSI-PCR

Last, we examined whether there was a correlation between the fraction of unstable markers characterized by MSIplus (ie, the mSINGS score) and the fraction of unstable microsatellite loci detected by MSI-PCR (Figure 4). We excluded from analysis specimens with discordant results between the two assays and those three having non-interpretable mSINGS scores.

Overall, the two measurements of MSI demonstrated a strong, positive correlation ($R^2 = 0.89$). Of 42 specimens with no unstable loci detectable by MSI-PCR, 20 demonstrated nonzero mSINGS scores; nevertheless, a trend of mSINGS overestimating the fraction of unstable loci was

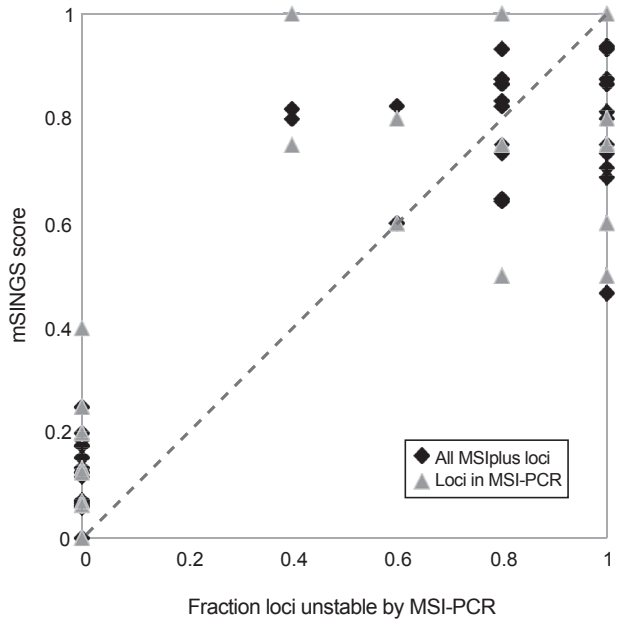

Figure 4 Correlation of locus instability measured by microsatellite instability (MSI)-PCR and MSIplus. The mSINGS score (the fraction of interrogated microsatellite loci that are unstable) is plotted against the fraction of unstable loci determined by MSI-PCR. Overall mSINGS score for the MSIplus assay is shown separately from mSINGS score calculated for the five loci in common with MSI-PCR. Dashed gray line indicates a theoretical perfect correlation between the two measures of instability.

not consistent across all specimens deemed MSI positive by MSI-PCR. We noted that if MSI-negative MSI-PCR results were removed from consideration, the correlation of mSINGS score and the fraction of unstable loci observed for MSI-H specimens was not statistically meaningful ($R^2 = 9.1 \times 10^{-3}$). This finding suggests that, above the threshold for delineating an MSI-positive phenotype, the fraction of unstable markers identified by MSI-PCR cannot be generalized to infer the degree of overall genomic instability.

We separately evaluated correlation between the fraction of unstable loci identified by either MSI-PCR or MSIplus for the subset of five loci that are represented in both assays. Again, a strong positive correlation was observed between these two metrics ($R^2 = 0.80$), although the lack of identity between them indicates subtle differences in individual loci being scored as stable or unstable between the two assays.

Discussion

Because the number of single-gene molecular tests needed to adequately characterize tumors continues to increase, the practical consequences of increased health care costs, increased test turnaround times, and the potential to deplete available tissue material during the course of testing become an increasing concern.[31] The use of highly scalable NGS technologies has proved a means to overcome this challenge, in many cases improving the quality and capabilities

of molecular testing.[30–33] In light of these considerations, we developed MSIplus, an NGS assay for characterizing colorectal tumor specimens that integrates extended *RAS* and *BRAF* gene testing with MSI analysis and, therefore, encompasses recommended molecular testing guidelines in a single assay.[7]

MSIplus had an overall sensitivity of 100% and a specificity of 100% for identifying cancer-associated mutations in *BRAF*, *KRAS,* and *NRAS* genes, as calculated from a panel of 61 specimens carrying a spectrum of known mutations (Table 2). The ability of a molecular assay to detect mutations present in a tumor specimen is dependent, in part, on the proportion of neoplastic cells in the sample and the fraction of total tumor cells that carry the mutation of interest.[31] The limit of detection for MSIplus is a 2% mutant allele fraction, lower than other prevalent clinical diagnostic methods.[21,22] Because the limit of detection in this assay partially reflects the rate of false-positive sequence reads, the sensitivity of MSIplus for low-prevalence mutations could potentially be improved in future iterations through practices such as incorporating molecular tagging-mediated sequencing error correction.[34,48,49] However, such methods present technical challenges and could negatively affect other aspects of the assay's performance.

Because it is a sequencing-based approach, MSIplus should be able to identify most single-nucleotide polymorphisms or small insertions or deletions occurring within the selected target regions. Compared with real-time PCR or melt-curve assays, which are designed to detect only a specific subset of actionable mutations,[23,24] MSIplus is capable of identifying variants without prior knowledge or expectation of the underlying genetic change. This property greatly improves the ability of MSIplus to identify rare or unusual clinically significant nucleotide alterations.

MSIplus had 97.1% sensitivity and 100% specificity for characterizing the MSI phenotype in a test set of 78 tumors, performance characteristics that were similar to those reported for MSI-PCR in other studies[5,16] and slightly better than the performance of MSI-PCR for the same set of specimens. Although MSIplus does not substantially improve sensitivity or specificity compared with MSI-PCR, it has important advantages over existing assays. Evaluation of MSI by mSINGS analysis eliminates the need for matched normal patient material,[35] which is typically required for conventional MSI-PCR, thereby expanding the scope of available patient specimens that can be successfully typed using MSIplus. The interpretation of MSIplus uses an automated analysis pipeline that is based on quantitative, descriptive statistics. This feature may improve the consistency of MSI diagnosis and reduce interlaboratory and intralaboratory variation.

We were unable to confidently call MSI status using MSIplus for a small subset of specimens (95% of specimens were interpretable with the first round of testing, whereas only 5% were not). Three of the four specimens with indeterminate mSINGS scores again yielded uninterpretable results after repeated testing, suggesting that the assay cannot confidently type MSI status for a small fraction of samples. Although the biological significance of these persistently indeterminate mSINGS scores, if any, is unclear,[50,51] studies examining larger numbers of microsatellite markers have suggested that such cases do not represent a distinct disease category of subtype of MSI.[35,38] These indeterminate specimens could potentially be resolved by increasing the number of microsatellite loci examined in the assay to enable more accurate assessment of the mSINGS score.[35]

Our study identified several cases where IHC and molecular testing were discordant, as expected.[17,20] It is known that isolated MSH6 deficiencies may result in false-negative MSI-PCR results,[52] and our sample cohort contained one such case. Unlike MSI-PCR, MSIplus identified this MSH6-deficient specimen as MSI positive, rendering a proper molecular diagnosis. Moreover, all indeterminate MSIplus results occurred in cases where IHC indicated reduced MMR protein expression, including two testing negative by MSI-PCR. Although anecdotal, these findings suggest an improved ability of MSIplus to identify MSH6-mutated specimens and improved sensitivity for detecting MMR pathway deficiencies compared with MSI-PCR. With further refinement, the MSIplus assay may offer significant performance advantages over MSI-PCR for such cases.

We anticipate that MSIplus will prove useful in characterizing colorectal cancers while potentially reducing operating costs and standardizing the interpretation of testing results. The assay is rapid, and compatible with a 2- or 3-day turnaround time: library preparation, approximately 8 hours; sequencer setup, approximately 1 hour; sequencing, approximately 8 hours; data analysis, approximately 2 hours per specimen on a four-processor machine, but scalable on larger computing systems to process multiple specimens simultaneously. Because the assay uses PCR-mediated library preparation, it requires minimal input DNA (50 ng) and should function even for partially degraded specimens. The modular nature of the multiplexed primer design will enable relatively straightforward expansion of the assay to additional molecular targets, as necessary, in response to future diagnostic requirements. The approach of focused, integrated NGS testing, tailored to a specific tumor type or diagnostic workflow, is a powerful paradigm that can be adapted to other clinical scenarios, and will become more common as NGS technologies are increasingly integrated into clinical laboratories.

Acknowledgments

We thank the Molecular Diagnostics laboratory staff for their help in identifying and obtaining specimens and Tina Lockwood (Seattle, WA) for helpful conversations.

Supplemental Data

Supplemental material for this article can be found at *http://dx.doi.org/10.1016/j.jmoldx.2015.05.008*.

References

1. Jenkins MA, Hayashi S, O'Shea AM, Burgart LJ, Smyrk TC, Shimizu D, Waring PM, Ruszkiewicz AR, Pollett AF, Redston M, Barker MA, Baron JA, Casey GR, Dowty JG, Giles GG, Limburg P, Newcomb P, Young JP, Walsh MD, Thibodeau SN, Lindor NM, Lemarchand L, Gallinger S, Haile RW, Potter JD, Hopper JL, Jass JR; Colon Cancer Family Registry: Pathology features in Bethesda guidelines predict colorectal cancer microsatellite instability: a population-based study. Gastroenterology 2007, 133:48–56
2. Beamer LC, Grant ML, Espenschied CR, Blazer KR, Hampel HL, Weitzel JN, MacDonald DJ: Reflex immunohistochemistry and microsatellite instability testing of colorectal tumors for Lynch syndrome among US cancer programs and follow-up of abnormal results. J Clin Oncol 2012, 30:1058–1063
3. Vilar E, Gruber SB: Microsatellite instability in colorectal cancer: the stable evidence. Nat Rev Clin Oncol 2010, 7:153–162
4. Ribic CM, Sargent DJ, Moore MJ, Thibodeau SN, French AJ, Goldberg RM, Hamilton SR, Laurent-Puig P, Gryfe R, Shepherd LE, Tu D, Redston M, Gallinger S: Tumor microsatellite-instability status as a predictor of benefit from fluorouracil-based adjuvant chemotherapy for colon cancer. N Engl J Med 2003, 349:247–257
5. Goel A, Nagasaka T, Hamelin R, Boland CR: An optimized pentaplex PCR for detecting DNA mismatch repair-deficient colorectal cancers. PLoS One 2010, 5:e9393
6. de la Chapelle A, Hampel H: Clinical relevance of microsatellite instability in colorectal cancer. J Clin Oncol 2010, 28:3380–3387
7. NCCN Guidelines(R) Updates. J Natl Compr Canc Netw 2013, 11: xxxii–xxxvi
8. Plesec TP, Hunt JL: KRAS mutation testing in colorectal cancer. Adv Anat Pathol 2009, 16:196–203
9. De Roock W, Claes B, Bernasconi D, De Schutter J, Biesmans B, Fountzilas G, et al: Effects of KRAS, BRAF, NRAS, and PIK3CA mutations on the efficacy of cetuximab plus chemotherapy in chemotherapy-refractory metastatic colorectal cancer: a retrospective consortium analysis. Lancet Oncol 2010, 11:753–762
10. Douillard JY, Oliner KS, Siena S, Tabernero J, Burkes R, Barugel M, Humblet Y, Bodoky G, Cunningham D, Jassem J, Rivera F, Kocakova I, Ruff P, Blasinska-Morawiec M, Smakal M, Canon JL, Rother M, Williams R, Rong A, Wiezorek J, Sidhu R, Patterson SD: Panitumumab-FOLFOX4 treatment and RAS mutations in colorectal cancer. N Engl J Med 2013, 369:1023–1034
11. Van Cutsem E, Kohne CH, Lang I, Folprecht G, Nowacki MP, Cascinu S, Shchepotin I, Maurel J, Cunningham D, Tejpar S, Schlichting M, Zubel A, Celik I, Rougier P, Ciardiello F: Cetuximab plus irinotecan, fluorouracil, and leucovorin as first-line treatment for metastatic colorectal cancer: updated analysis of overall survival according to tumor KRAS and BRAF mutation status. J Clin Oncol 2011, 29:2011–2019
12. Di Nicolantonio F, Martini M, Molinari F, Sartore-Bianchi A, Arena S, Saletti P, De Dosso S, Mazzucchelli L, Frattini M, Siena S, Bardelli A: Wild-type BRAF is required for response to panitumumab or cetuximab in metastatic colorectal cancer. J Clin Oncol 2008, 26: 5705–5712
13. Bokemeyer C, Van Cutsem E, Rougier P, Ciardiello F, Heeger S, Schlichting M, Celik I, Kohne CH: Addition of cetuximab to chemotherapy as first-line treatment for KRAS wild-type metastatic colorectal cancer: pooled analysis of the CRYSTAL and OPUS randomised clinical trials. Eur J Cancer 2012, 48:1466–1475
14. Boland CR, Thibodeau SN, Hamilton SR, Sidransky D, Eshleman JR, Burt RW, Meltzer SJ, Rodriguez-Bigas MA, Fodde R, Ranzani GN, Srivastava S: A National Cancer Institute Workshop on Microsatellite Instability for cancer detection and familial predisposition: development of international criteria for the determination of microsatellite instability in colorectal cancer. Cancer Res 1998, 58:5248–5257
15. Umar A, Boland CR, Terdiman JP, Syngal S, de la Chapelle A, Ruschoff J, Fishel R, Lindor NM, Burgart LJ, Hamelin R, Hamilton SR, Hiatt RA, Jass J, Lindblom A, Lynch HT, Peltomaki P, Ramsey SD, Rodriguez-Bigas MA, Vasen HF, Hawk ET, Barrett JC, Freedman AN, Srivastava S: Revised Bethesda Guidelines for hereditary nonpolyposis colorectal cancer (Lynch syndrome) and microsatellite instability. J Natl Cancer Inst 2004, 96:261–268
16. Bacher JW, Flanagan LA, Smalley RL, Nassif NA, Burgart LJ, Halberg RB, Megid WM, Thibodeau SN: Development of a fluorescent multiplex assay for detection of MSI-High tumors. Dis Markers 2004, 20:237–250
17. Lindor NM, Burgart LJ, Leontovich O, Goldberg RM, Cunningham JM, Sargent DJ, Walsh-Vockley C, Petersen GM, Walsh MD, Leggett BA, Young JP, Barker MA, Jass JR, Hopper J, Gallinger S, Bapat B, Redston M, Thibodeau SN: Immunohistochemistry versus microsatellite instability testing in phenotyping colorectal tumors. J Clin Oncol 2002, 20:1043–1048
18. Shia J: Immunohistochemistry versus microsatellite instability testing for screening colorectal cancer patients at risk for hereditary nonpolyposis colorectal cancer syndrome, part I: the utility of immunohistochemistry. J Mol Diagn 2008, 10:293–300
19. Zhang L: Immunohistochemistry versus microsatellite instability testing for screening colorectal cancer patients at risk for hereditary nonpolyposis colorectal cancer syndrome, part II: the utility of microsatellite instability testing. J Mol Diagn 2008, 10:301–307
20. Müller A, Giuffre G, Edmonston TB, Mathiak M, Roggendorf B, Heinmöller E, Brodegger T, Tuccari G, Mangold E, Buettner R, Rüschoff J; German HNPCC Consortium German Cancer Aid (Deutsche Krebshife): Challenges and pitfalls in HNPCC screening by microsatellite analysis and immunohistochemistry. J Mol Diagn 2004, 6:308–315
21. Ikenoue T, Hikiba Y, Kanai F, Ijichi H, Togo G, Ohta M, Watabe H, Yamaji Y, Okamoto M, Aragaki J, Matsumura M, Kawabe T, Omata M: Rapid detection of mutations in the BRAF gene using real-time polymerase chain reaction and melting curve analysis. Cancer Genet Cytogenet 2004, 149:68–71
22. Nikiforova MN, Lynch RA, Biddinger PW, Alexander EK, Dorn GW 2nd, Tallini G, Kroll TG, Nikiforov YE: RAS point mutations and PAX8-PPAR gamma rearrangement in thyroid tumors: evidence for distinct molecular pathways in thyroid follicular carcinoma. J Clin Endocrinol Metab 2003, 88:2318–2326
23. Sakai K, Yoneshige A, Ito A, Ueda Y, Kondo S, Nobumasa H, Fujita Y, Togashi Y, Terashima M, De Velasco MA, Tomida S, Nishio K: Performance of a novel KRAS mutation assay for formalin-fixed paraffin embedded tissues of colorectal cancer. Springerplus 2015, 4:7
24. Qu K, Pan Q, Zhang X, Rodriguez L, Zhang K, Li H, Ho A, Sanders H, Sferruzza A, Cheng SM, Nguyen D, Jones D, Waldman F: Detection of BRAF V600 mutations in metastatic melanoma: comparison of the Cobas 4800 and Sanger sequencing assays. J Mol Diagn 2013, 15:790–795
25. Oh JE, Lim HS, An CH, Jeong EG, Han JY, Lee SH, Yoo NJ: Detection of low-level KRAS mutations using PNA-mediated asymmetric PCR clamping and melting curve analysis with unlabeled probes. J Mol Diagn 2010, 12:418–424
26. Pritchard CC, Akagi L, Reddy PL, Joseph L, Tait JF: COLD-PCR enhanced melting curve analysis improves diagnostic accuracy for KRAS mutations in colorectal carcinoma. BMC Clin Pathol 2010, 10:6
27. Li J, Wang L, Mamon H, Kulke MH, Berbeco R, Makrigiorgos GM: Replacing PCR with COLD-PCR enriches variant DNA sequences and redefines the sensitivity of genetic testing. Nat Med 2008, 14: 579–584

28. Westwood M, van Asselt T, Ramaekers B, Whiting P, Joore M, Armstrong N, Noake C, Ross J, Severens J, Kleijnen J: KRAS mutation testing of tumours in adults with metastatic colorectal cancer: a systematic review and cost-effectiveness analysis. Health Technol Assess 2014, 18:1−132
29. Pritchard CC, Smith C, Salipante SJ, Lee MK, Thornton AM, Nord AS, Gulden C, Kupfer SS, Swisher EM, Bennett RL, Novetsky AP, Jarvik GP, Olopade OI, Goodfellow PJ, King MC, Tait JF, Walsh T: ColoSeq provides comprehensive lynch and polyposis syndrome mutational analysis using massively parallel sequencing. J Mol Diagn 2012, 14:357−366
30. Frampton GM, Fichtenholtz A, Otto GA, Wang K, Downing SR, He J, et al: Development and validation of a clinical cancer genomic profiling test based on massively parallel DNA sequencing. Nat Biotechnol 2013, 31:1023−1031
31. Pritchard CC, Salipante SJ, Koehler K, Smith C, Scroggins S, Wood B, Wu D, Lee MK, Dintzis S, Adey A, Liu Y, Eaton KD, Martins R, Stricker K, Margolin KA, Hoffman N, Churpek JE, Tait JF, King MC, Walsh T: Validation and implementation of targeted capture and sequencing for the detection of actionable mutation, copy number variation, and gene rearrangement in clinical cancer specimens. J Mol Diagn 2014, 16:56−67
32. Cottrell CE, Al-Kateb H, Bredemeyer AJ, Duncavage EJ, Spencer DH, Abel HJ, Lockwood CM, Hagemann IS, O'Guin SM, Burcea LC, Sawyer CS, Oschwald DM, Stratman JL, Sher DA, Johnson MR, Brown JT, Cliften PF, George B, McIntosh LD, Shrivastava S, Nguyen TT, Payton JE, Watson MA, Crosby SD, Head RD, Mitra RD, Nagarajan R, Kulkarni S, Seibert K, Virgin HW 4th, Milbrandt J, Pfeifer JD: Validation of a next-generation sequencing assay for clinical molecular oncology. J Mol Diagn 2014, 16:89−105
33. Harismendy O, Schwab RB, Bao L, Olson J, Rozenzhak S, Kotsopoulos SK, Pond S, Crain B, Chee MS, Messer K, Link DR, Frazer KA: Detection of low prevalence somatic mutations in solid tumors with ultra-deep targeted sequencing. Genome Biol 2011, 12:R124
34. Hiatt JB, Pritchard CC, Salipante SJ, O'Roak BJ, Shendure J: Single molecule molecular inversion probes for targeted, high-accuracy detection of low-frequency variation. Genome Res 2013, 23:843−854
35. Salipante SJ, Scroggins SM, Hampel HL, Turner EH, Pritchard CC: Microsatellite instability detection by next generation sequencing. Clin Chem 2014, 60:1192−1199
36. Lu Y, Soong TD, Elemento O: A novel approach for characterizing microsatellite instability in cancer cells. PLoS One 2013, 8:e63056
37. Niu B, Ye K, Zhang Q, Lu C, Xie M, McLellan MD, Wendl MC, Ding L: MSIsensor: microsatellite instability detection using paired tumor-normal sequence data. Bioinformatics 2014, 30:1015−1016
38. Kim TM, Laird PW, Park PJ: The landscape of microsatellite instability in colorectal and endometrial cancer genomes. Cell 2013, 155:858−868
39. McKenna A, Hanna M, Banks E, Sivachenko A, Cibulskis K, Kernytsky A, Garimella K, Altshuler D, Gabriel S, Daly M, DePristo MA: The Genome Analysis Toolkit: a MapReduce framework for analyzing next-generation DNA sequencing data. Genome Res 2010, 20:1297−1303
40. Dorard C, de Thonel A, Collura A, Marisa L, Svrcek M, Lagrange A, Jego G, Wanherdrick K, Joly AL, Buhard O, Gobbo J, Penard-Lacronique V, Zouali H, Tubacher E, Kirzin S, Selves J, Milano G, Etienne-Grimaldi MC, Bengrine-Lefevre L, Louvet C, Tournigand C, Lefevre JH, Parc Y, Tiret E, Flejou JF, Gaub MP, Garrido C, Duval A: Expression of a mutant HSP110 sensitizes colorectal cancer cells to chemotherapy and improves disease prognosis. Nat Med 2011, 17:1283−1289
41. Shen Z, Qu W, Wang W, Lu Y, Wu Y, Li Z, Hang X, Wang X, Zhao D, Zhang C: MPprimer: a program for reliable multiplex PCR primer design. BMC Bioinformatics 2010, 11:143
42. Clarke LA, Rebelo CS, Goncalves J, Boavida MG, Jordan P: PCR amplification introduces errors into mononucleotide and dinucleotide repeat sequences. Mol Pathol 2001, 54:351−353
43. Salipante SJ, Horwitz MS: Phylogenetic fate mapping. Proc Natl Acad Sci U S A 2006, 103:5448−5453
44. Li H, Durbin R: Fast and accurate short read alignment with Burrows-Wheeler transform. Bioinformatics 2009, 25:1754−1760
45. Li H, Handsaker B, Wysoker A, Fennell T, Ruan J, Homer N, Marth G, Abecasis G, Durbin R; 1000 Genomes Project Data Processing Subgroup: The Sequence Alignment/Map format and SAMtools. Bioinformatics 2009, 25:2078−2079
46. DePristo MA, Banks E, Poplin R, Garimella KV, Maguire JR, Hartl C, Philippakis AA, del Angel G, Rivas MA, Hanna M, McKenna A, Fennell TJ, Kernytsky AM, Sivachenko AY, Cibulskis K, Gabriel SB, Altshuler D, Daly MJ: A framework for variation discovery and genotyping using next-generation DNA sequencing data. Nat Genet 2011, 43:491−498
47. Koboldt DC, Zhang Q, Larson DE, Shen D, McLellan MD, Lin L, Miller CA, Mardis ER, Ding L, Wilson RK: VarScan 2: somatic mutation and copy number alteration discovery in cancer by exome sequencing. Genome Res 2012, 22:568−576
48. Kinde I, Wu J, Papadopoulos N, Kinzler KW, Vogelstein B: Detection and quantification of rare mutations with massively parallel sequencing. Proc Natl Acad Sci U S A 2011, 108:9530−9535
49. Schmitt MW, Kennedy SR, Salk JJ, Fox EJ, Hiatt JB, Loeb LA: Detection of ultra-rare mutations by next-generation sequencing. Proc Natl Acad Sci U S A 2012, 109:14508−14513
50. Pawlik TM, Raut CP, Rodriguez-Bigas MA: Colorectal carcinogenesis: MSI-H versus MSI-L. Dis Markers 2004, 20:199−206
51. Tomlinson I, Halford S, Aaltonen L, Hawkins N, Ward R: Does MSI-low exist? J Pathol 2002, 197:6−13
52. Hampel H, Frankel W, Panescu J, Lockman J, Sotamaa K, Fix D, Comeras I, La Jeunesse J, Nakagawa H, Westman JA, Prior TW, Clendenning M, Penzone P, Lombardi J, Dunn P, Cohn DE, Copeland L, Eaton L, Fowler J, Lewandowski G, Vaccarello L, Bell J, Reid G, de la Chapelle A: Screening for Lynch syndrome (hereditary nonpolyposis colorectal cancer) among endometrial cancer patients. Cancer Res 2006, 66:7810−7817

available at www.sciencedirect.com
journal homepage: www.europeanurology.com

European Association of Urology

Platinum Priority – Case Series of the Month

Editorial by Helen E. Bryant on pp. 996–997 of this issue

Biallelic Inactivation of *BRCA2* in Platinum-sensitive Metastatic Castration-resistant Prostate Cancer

Heather H. Cheng [a,b], ***Colin C. Pritchard*** [c], ***Thomas Boyd*** [d], ***Peter S. Nelson*** [e], ***Bruce Montgomery*** [a,*]

[a] *Department of Medicine, Division of Oncology, University of Washington, Seattle, WA, USA;* [b] *Clinical Research Division, Fred Hutchinson Cancer Research Center, Seattle, WA, USA;* [c] *Department of Laboratory Medicine, University of Washington, Seattle, WA, USA;* [d] *Northstar Lodge Cancer Center, Yakima, WA, USA;* [e] *Human Biology Division, Fred Hutchinson Cancer Research Center, Seattle, WA, USA*

Article info

Article history:
Accepted November 19, 2015

Associate Editor:
James Catto

Keywords:
BRCA2
Platinum
Carboplatin
Prostate cancer
mCRPC
DNA repair

Abstract

Understanding the molecular underpinnings of sensitivity to specific therapies will advance the goal of precision medicine in prostate cancer (PCa). We identified three patients with metastatic castration-resistant PCa (mCRPC) who achieved an exceptional response to platinum chemotherapy (not first-line treatment for PCa), despite disease progression on prior standard therapies. Using targeted next-generation sequencing on the primary and metastatic tumors, we found that all three patients had biallelic inactivation of *BRCA2*, a tumor suppressor gene critical for homologous DNA repair. Notably, two had germline *BRCA2* mutations, including a patient without compelling family history who was diagnosed at age 66 yr. The third patient had somatic *BRCA2* homozygous copy loss. Biallelic *BRCA2* inactivation in mCRPC warrants further exploration as a predictive biomarker for sensitivity to platinum chemotherapy.

* Corresponding author. Department of Medicine, Division of Oncology, University of Washington Medical Center, 1959 NE Pacific Street, Seattle, WA, 98195, USA.
E-mail address: rbmontgo@uw.edu (B. Montgomery).

1. Case report

Treatment for metastatic castration-resistant prostate cancer (mCRPC) now includes taxanes, androgen receptor pathway inhibitors, active cellular therapy, and a bone-targeting radiopharmaceutical [1]. Predictive biomarkers are needed to guide treatment selection and sequence. Reports describing the mutational landscape of mCRPC hold great promise for precision medicine, but actionable treatment decisions remain unclear [2–4].

Platinum chemotherapy is infrequently used for prostate cancer (PCa) except in cases of neuroendocrine differentiation [5]. We identified three patients with non-neuroendocrine mCRPC with an exceptional response to platinum, defined as patients with advanced cancer who attain a complete or partial response lasting at least 6 mo when expected response is $\leq$20%. To identify molecular changes associated with exceptional response, we retrospectively performed clinical targeted next-generation sequencing on tumor DNA. Surprisingly, the common finding between all three was biallelic inactivation of *BRCA2*, the homologous recombination DNA repair gene.

Patient 1 was diagnosed at age 66 yr with prostate-specific antigen (PSA) of 24.8 ng/ml and Gleason 4 + 4 prostate

http://dx.doi.org/10.1016/j.eururo.2015.11.022
0302-2838/

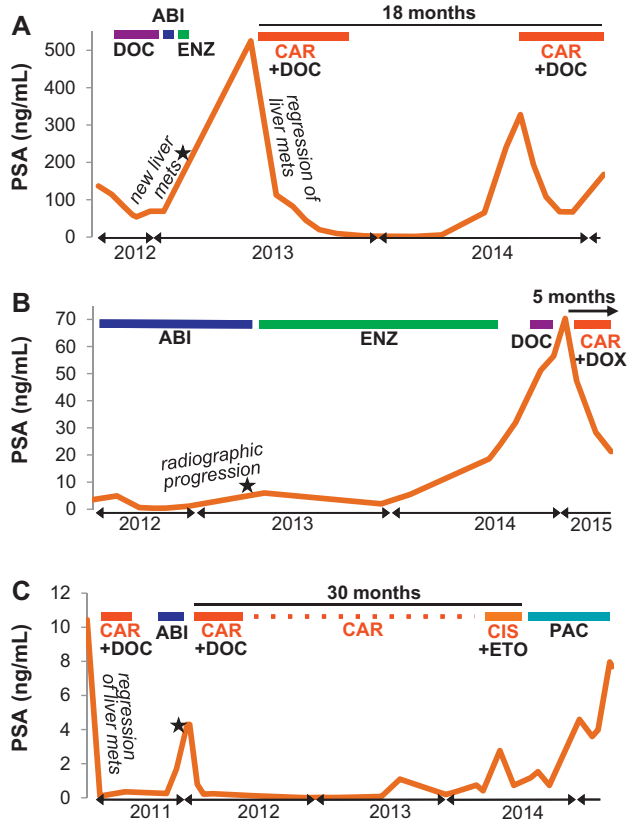

Fig. 1 – Clinical treatment course and prostate-specific antigen response. (A) Patient 1, (B) patient 2, (C) patient 3. Platinum chemotherapies are in bold red type. Stars denote time of metastatic biopsies. ABI = abiraterone; CAR = carboplatin; CIS = cisplatin; DOC = docetaxel; DOX = doxorubicin; ENZ = enzalutamide; ETO = etoposide; mets = metastases; PAC = paclitaxel; PSA = prostate-specific antigen.

adenocarcinoma and underwent neoadjuvant androgen deprivation therapy (ADT) on a clinical study followed by radical prostatectomy and salvage radiotherapy. After 4 yr, he was found to have metastases to the liver, lymph nodes, and bone. Biopsy of liver metastases revealed adenocarcinoma without evidence of neuroendocrine differentiation.

He received docetaxel with a PSA decline from 136 to 59 ng/ml, followed by PSA rise and then treatment with abiraterone followed by enzalutamide, both resulting in PSA and radiographic progression. Given earlier progression on docetaxel alone, he then received docetaxel and carboplatin with a PSA decline (Fig. 1A) and radiographic response (not shown). After a 6-mo break from treatment, he resumed docetaxel/carboplatin, again, with PSA decline. Unfortunately, he developed worsening malignant pleural effusions and ascites and ultimately elected to transition to hospice.

DNA sequencing of the metastatic liver biopsy revealed two *BRCA2* mutations, p.Q3066X and an exon 11 partial deletion on separate alleles (Table 1).

Patient 1 did not have a significant family history of cancer despite clear evidence of an inherited deleterious *BRCA2* mutation on germline testing. In light of these findings, he was referred to the medical genetics department, and mutation was confirmed.

Patient 2 was diagnosed at age 53 yr with PSA of 6.8 ng/ml and Gleason 5 + 4 prostate adenocarcinoma and underwent radical prostatectomy followed by salvage radiotherapy with ADT. After 5 yr, his PSA had risen to 12.0 ng/ml, and bone metastases were identified. He received 3 yr of intermittent ADT. On developing castration resistance, he was treated with abiraterone and then enzalutamide; both resulted in transient control and then PSA rise (Fig. 1B) and progressive disease. He then received docetaxel with no response, followed by carboplatin/doxorubicin for 6 mo with PSA and clinical response. Sequencing of a metastatic biopsy identified two deleterious *BRCA2* frameshift mutations including one that was germline (Table 1).

Patient 2 had a family history suggestive of a high-penetrance germline mutation with both father and paternal grandfather with PCa and a paternal aunt with breast cancer. He was referred to the medical genetics department, and mutation was confirmed.

Patient 3 was diagnosed at age 70 yr with PSA of 4.9 ng/ml and Gleason 5 + 5 prostate adenocarcinoma metastatic to pelvic and retroperitoneal lymph nodes. He developed castration resistance 6 mo after initiating ADT and was found to have liver metastases when PSA reached 10.0 ng/ml. Metastatic liver biopsy was obtained to assess for neuroendocrine differentiation, which was ruled out with immunohistochemistry. He was treated with docetaxel/carboplatin with a near-complete radiographic and PSA response (Fig. 1C). He was subsequently treated with abiraterone with disease progression and went on to receive a second course of docetaxel/carboplatin with another near-complete radiographic and PSA response. He then received "maintenance" carboplatin for >2 yr of progression-free survival. Sequencing of the previously obtained liver biopsy revealed somatic homozygous *BRCA2* copy loss in the metastasis (Table 1, Fig. 2). We were unable to confirm the

Table 1 – *BRCA2* mutations identified

		BRCA2 mutations[†]	Mutation type	Germline	Primary	Metastases
Patient 1	Allele 1	**c.9196C>T; p.Q3066X**	Premature stop	X	X	X
	Allele 2	**127bp del in exon 11**	Frameshift deletion		X	X
Patient 2	Allele 1	**c.8904delC; p.V2969Cfs*7**	Frameshift deletion	X	X	X
	Allele 2	**c.2611delT; p.S871Qfs*3**	Frameshift deletion		[‡]	X
Patient 3	Allele 1	**Homozygous copy loss**	Copy loss		X	X
	Allele 2	**Homozygous copy loss**	Copy loss		X	X

[†] Mutations are reported using reference transcript NM 000059.3.
[‡] Low tumor purity limited detection of somatic mutations.

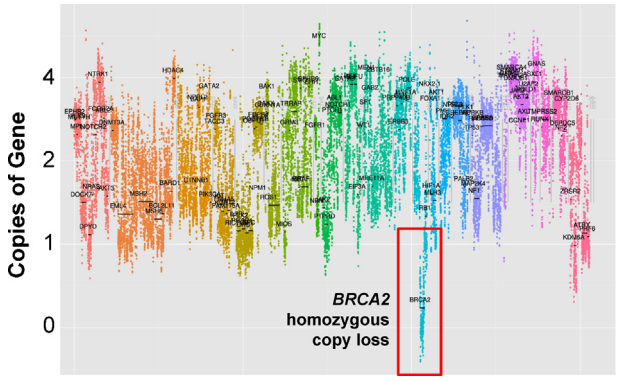

Fig. 2 – Copy number variation plot for metastatic tumor from patient 3. Changes in number of copies of genes within tumor cells were identified directly by UW-OncoPlex sequencing: (*x*-axis, left to right) each chromosome (1–22, x) is depicted in a different color; (*y*-axis) copies of genes. Selected genes are labeled.

presence of biallelic *BRCA2* copy loss in the primary tumor due to insufficient tumor.

2. Discussion

This case series documents three patients with mCRPC who achieved exceptional clinical response to platinum-based therapy after failure or progression on first-line therapies. Using a targeted next-generation sequencing clinical assay, we identified that all three had biallelic *BRCA2* inactivation in their tumors through either homozygous copy loss or germline deleterious mutation and somatic loss of function in the second allele in their metastases. By selecting for tumors with hypersensitivity to DNA damage induced by platinum chemotherapies, it is biologically plausible that defects in DNA repair would be revealed, particularly in light of observed platinum sensitivity in *BRCA1/2* germline mutation carriers in other cancer types, notably ovarian and breast cancers [6].

The prevalence of inactivation of *BRCA2* and other DNA damage repair genes in mCRPC is higher than previously thought and will require further validation. In one report, 7 of 50 (14%) patients with lethal PCa were found to have alterations in *BRCA2* [2]. The whole-exome sequencing results of the initial 150 mCRPC metastases from the SU2C Prostate International Dream Team demonstrated that 19% had aberrations in DNA repair genes (a combination of somatic and germline) including *BRCA1*, *BRCA2*, and *ATM* [4].

Inheritance of deleterious *BRCA2* mutations is well established to increase the risk of developing PCa in addition to breast, ovarian, pancreas, and other malignancies. Male *BRCA2* mutation carriers with localized PCa are at substantially higher risk of dying from PCa than their non–mutation-carrying counterparts [7]. Together with the SU2C data, this suggests that biallelic inactivation (germline and somatic) of *BRCA2* and related homologous recombination genes may be enriched among patients with aggressive mCRPC, especially when compared with the broader population of all (mostly indolent) PCa.

Our case series provides evidence that homozygous inactivation of *BRCA2* in mCRPC may confer sensitivity to platinum agents. Our series is limited by its small numbers and retrospective nature, but it suggests that inactivation of *BRCA2* and other DNA repair genes could be clinically useful as predictive biomarkers of platinum response. Whether other patients with hemizygous or homozygous inactivation of *BRCA2* or those with inactivation of other DNA repair pathway genes will be sensitive to DNA-damaging agents can only be addressed in prospective studies.

To our knowledge, this report is the first to associate dramatic response to platinum in men who had mCRPC and who were unselected for *a priori* mutation carriage with biallelic loss of *BRCA2*. Our report adds substantively to prior case reports that known *BRCA2* mutation carriers with mCRPC may respond particularly well to platinum chemotherapies. This mirrors breast and ovarian cancers, in which platinum chemotherapies are commonly used, and evidence suggests that germline and somatic mutations in homologous recombination genes such as *BRCA2* are associated with response to platinum and overall survival [8].

BRCA1/2 mutation carriers have also been effectively treated with a poly (ADP-ribose) polymerase inhibitor (PARPi) that renders synthetic lethality in cells with defective homologous DNA repair. Dramatic responses to PARPi have been reported very recently by Mateo et al [9]. Among men with mCRPC no longer responding to standard therapies whose tumors had evidence of DNA repair defects (including *BRCA2, ATM*, Fanconi anemia genes, and *CHEK2*), treatment with the PARPi olaparib resulted in a response rate of 88% (14 of 16) [9]. Clinical studies testing platinum agents, in combination and/or in sequence with PARPi, should also be explored for the subset of mCRPC patients whose tumors have biallelic inactivation of *BRCA2* and related homologous recombination repair pathway genes.

In the context of emerging data that *BRCA1/2* mutations may be present in up to 20% of mCRPC [4] and that *BRCA2* mutation–associated PCa is more aggressive [7], we are heartened by the dramatic platinum responses in these three patients whose tumors carried biallelic inactivation of *BRCA2*. Collectively, recent findings present a strong case for larger studies evaluating the tumors of all men who develop metastatic PCa for biallelic inactivation of *BRCA2* and related homologous DNA repair genes. These appear to be likely predictive biomarkers for treatment response to DNA-damaging therapy such as PARP inhibition and the widely available platinum chemotherapies.

3. Methods

We identified 14 patients with mCRPC treated with docetaxel and carboplatin between 2010 and the present. Although there was no standard institutional approach to treating patients with docetaxel and carboplatin, none had evidence of neuroendocrine differentiation, and most had aggressive features such as visceral involvement. Overall, 5 of 14 patients (36%) achieved treatment response, defined as PSA decline by 50% or radiographic partial response. Three patients had tumors available for analysis and are reported here. All three patients provided written informed consent for review of their medical record and sequencing

of their primary and metastatic PCa tissue. Research was conducted with University of Washington institutional review board approval.

DNA was extracted from formalin-fixed paraffin-embedded (FFPE) samples, as previously described [10]. Slides stained with hematoxylin and eosin were reviewed before DNA extraction for all FFPE samples, and when feasible, macrodissection of tumor areas was performed to enrich tumor cellularity. We performed sequencing with UW-OncoPlex (University of Washington, Seattle, WA, USA), a validated clinical molecular diagnostic assay that collects simultaneous deep-sequencing information, based on >500 times average coverage, for all classes of mutations in 194 targeted clinically relevant genes, as previously reported [10]. At the time of this writing, 31 patients with PCa have undergone tumor sequencing with UW-OncoPlex at our institution. Four of 31 (13%) were identified to have biallelic *BRCA2* inactivation, 1 of whom died before results became available and without receiving platinum chemotherapy. The cases of the three others were reported in this paper.

Conflicts of interest: The authors have nothing to disclose.

Funding/Support and role of the sponsor: This work was supported by generous funding from the Institute for Prostate Cancer Research, the Pacific Northwest Prostate Cancer SPORE CA097186, 2013 Young Investigator Award from the Prostate Cancer Foundation (CCP), and Congressional Designated Medical Research Program (CDMRP) award PC131820 (CCP).

EU-ACME question

Please visit www.eu-acme.org/europeanurology to answer the following EU-ACME question online (the EU-ACME credits will be attributed automatically).

Question:

In addition to the potential association of biallelic inactivation of *BRCA2* with sensitivity of metastatic castration-resistant prostate cancer to platinum chemotherapy reported in this case series, there is evidence in the literature to support the following statements:

A. When an inactivating *BRCA2* mutation is identified in germline DNA, there may be an increased risk of prostate cancer in addition to breast, ovarian, and pancreatic cancers.
B. There is a higher risk of prostate cancer–associated death among prostate cancer patients who are *BRCA2* mutation carriers compared with noncarriers.
C. Recent data suggest that up to 20% of metastatic castration-resistant prostate cancers may contain biallelic inactivation of DNA damage repair genes such as *BRCA2*.
D. All of the above.

References

[1] Basch E, Loblaw DA, Oliver TK, et al. Systemic therapy in men with metastatic castration-resistant prostate cancer. American Society of Clinical Oncology and Cancer Care Ontario clinical practice guideline. J Clin Oncol 2014;32:3436–48.
[2] Grasso CS, Wu YM, Robinson DR, et al. The mutational landscape of lethal castration-resistant prostate cancer. Nature 2012;487:239–43.
[3] Beltran H, Yelensky R, Frampton GM, et al. Targeted next-generation sequencing of advanced prostate cancer identifies potential therapeutic targets and disease heterogeneity. Eur Urol 2013;63:920–6.
[4] Robinson D, Van Allen EM, Wu YM, et al. Integrative clinical genomics of advanced prostate cancer. Cell 2015;161:1215–28.
[5] Beltran H, Tomlins S, Aparicio A, et al. Aggressive variants of castration-resistant prostate cancer. Clin Cancer Res 2014;20:2846–50.
[6] Tan DS, Rothermundt C, Thomas K, et al. "BRCAness" syndrome in ovarian cancer: a case-control study describing the clinical features and outcome of patients with epithelial ovarian cancer associated with BRCA1 and BRCA2 mutations. J Clin Oncol 2008;26:5530–6.
[7] Castro E, Goh C, Leongamornlert D, et al. Effect of BRCA mutations on metastatic relapse and cause-specific survival after radical treatment for localised prostate cancer. Eur Urol 2015;68:186–93.
[8] Scott CL, Swisher EM, Kaufmann SH. Poly (ADP-ribose) polymerase inhibitors: recent advances and future development. J Clin Oncol 2015;33:1397–406.
[9] Mateo J, Carreira S, Sandhu S, et al. DNA-repair defects and olaparib in metastatic prostate cancer. N Engl J Med 2015;373:1697–708.
[10] Pritchard CC, Salipante SJ, Koehler K, et al. Validation and implementation of targeted capture and sequencing for the detection of actionable mutation, copy number variation, and gene rearrangement in clinical cancer specimens. J Mol Diagn 2014;16:56–67.

A Pilot Study of Clinical Targeted Next Generation Sequencing for Prostate Cancer: Consequences for Treatment and Genetic Counseling

Heather H. Cheng,[1,2]* Nola Klemfuss,[3] Bruce Montgomery,[1,2] Celestia S. Higano,[1] Michael T. Schweizer,[1,2] Elahe A. Mostaghel,[1,2] Lisa G. McFerrin,[3] Evan Y. Yu,[1,2] Peter S. Nelson,[1,3] and Colin C. Pritchard[4]

[1]*Division of Oncology, Department of Medicine, University of Washington, Seattle, Washington*
[2]*Clinical Research Division, Fred Hutchinson Cancer Research Center, Seattle, Washington*
[3]*Human Biology Division, Fred Hutchinson Cancer Research Center, Seattle, Washington*
[4]*Department of Laboratory Medicine, University of Washington, Seattle, Washington*

BACKGROUND. Targeted next generation sequencing (tNGS) is increasingly used in oncology for therapeutic decision-making, but is not yet widely used for prostate cancer. The objective of this study was to determine current clinical utility of tNGS for prostate cancer management.
METHODS. Seven academic genitourinary medical oncologists recruited and consented patients with prostate cancer, largely with unusual clinical and/or pathologic features, from 2013 to 2015. UW-OncoPlex was performed on formalin-fixed, paraffin-embedded (FFPE) primary tumors and/or metastatic biopsies. Results were discussed at a multidisciplinary precision tumor board prior to communicating to patients. FFPE tumor DNA was extracted for tNGS analysis of 194 cancer-associated genes. Results, multidisciplinary discussion, and treatment changes were recorded.
RESULTS. Forty-five patients consented and 42 had reportable results. Findings included mutations in genes frequently observed in prostate cancer. We also found alterations in genes where targeted treatments were available and/or in clinical trials. 4/42 (10%) cases, change in treatment directly resulted from tNGS and multidisciplinary discussion. In 30/42 (71%) cases additional options were available but not pursued and/or were pending. Notably, 10/42 (24%) of patients harbored suspected germline mutations in moderate or high-penetrance cancer risk genes, including *BRCA2*, *TP53*, *ATM*, and *CHEK2*. One patient's tumor had bi-allelic *MSH6* mutation and microsatellite instability. In total, 34/42 (81%) cases resulted in some measure of treatment actionability. Limitations include small size and limited clinical outcomes.
CONCLUSIONS. Targeted NGS tumor sequencing may help guide immediate and future treatment options for men with prostate cancer. A substantial subset had germline mutations in cancer predisposition genes with potential clinical management implications for men and their relatives. *Prostate 9999: 1–9, 2016.* © 2016 Wiley Periodicals, Inc.

KEY WORDS: **targeted next generation sequencing; panel testing; NGS; prostate cancer; precision tumor board**

Grant sponsor: Institute for Prostate Cancer Research; Grant sponsor: Pacific Northwest Prostate Cancer SPORE; Grant number: CA097186; Grant sponsor: Young Investigator Awards from the Prostate Cancer Foundation (HHC, MTS, CCP); Grant sponsor: Congressional Designated Medical Research Program (CDMRP); Grant number: PC131820 (CCP).

The authors declare no potential conflicts of interest.

*Correspondence to: Heather H. Cheng, MD, PhD, Division of Oncology, Department of Medicine, University of Washington, 825 Eastlake Ave E, Seattle, WA 98109. E-mail: hhcheng@uw.edu
Received 28 April 2016; Accepted 1 June 2016
DOI 10.1002/pros.23219
Published online in Wiley Online Library
(wileyonlinelibrary.com).

INTRODUCTION

Prostate cancer is the most commonly diagnosed cancer and the second most common cause of cancer death among men in the U.S. Many treatments are now available for advanced disease including docetaxel, sipuleucel-T, cabazitaxel, abiraterone, enzalutamide, and radium-223 with more in pre-clinical and clinical development [1]. With the growing number of effective treatments with survival benefit, the need for predictive biomarkers—both host and/or tumor features that indicate a high likelihood of response or resistance to a therapy—are urgently needed.

Targeted next generation sequencing DNA assays (tNGS) can identify actionable mutations in DNA from tumors that associate with responses to targeted therapeutics and are used in routine clinical practice in the management of lung cancer, colorectal cancer, and melanoma [2,3]. Although tNGS is not yet in widespread clinical use for prostate cancer, largely due to the paucity of well-defined targets predictive of drug sensitivity, a number of recent studies have indicated potential actionable targets, most notably platinum chemotherapy and poly-ADP ribose polymerase inhibitors (PARPi) for tumors with DNA repair defects [4–8]. Further, an ever-increasing number of clinical trials evaluating targeted agents are underway. UW-OncoPlex is a clinical tNGS panel assay of 194 genes with actionable or potentially actionable mutations [9], and has been extensively used in hematologic malignancies as well as solid tumors such as colorectal, lung, melanoma, sarcoma, and other cancers.

We report our initial experience in a pilot study evaluating UW-OncoPlex in tumors from men undergoing active prostate cancer treatment. The goal of the study was to demonstrate the utility of tNGS testing as applied to prostate cancer patients selected by medical oncologists for unusual clinical and pathologic features, as might occur in real-world clinical practice.

MATERIALS AND METHODS

Patients

Participants were men with prostate cancer receiving care at the genitourinary cancer clinics at the University of Washington and Seattle Cancer Care Alliance (Seattle, WA). Seven medical oncologists identified and recruited men with prostate cancer who were deemed as likely to benefit from tNGS (see additional details below) between the calendar years 2013 and 2015. Forty-five patients signed informed consent to have their tumor material tested using the Clinical Laboratory Improvement Amendments (CLIA)- and College of American Pathologists (CAP)-certified clinical UW-OncoPlex assay. Schema of study flow is shown in Figure 1. Reasons for testing are summarized in Supplementary Table SI.

Ethics Statement

All clinical samples were obtained from subjects who provided written informed consent. The study was performed in accordance with the declaration of Helsinki guidelines and with ethics approval from the Institutional Review Board at the University of Washington.

Target Next-Generation Sequencing Testing

DNA was extracted from fresh or archived FFPE samples, as previously described [9]. H&E-stained slides were reviewed before DNA extraction for all FFPE samples to ensure tumor content, and when feasible, macrodissection of tumor areas was performed to enrich tumor cellularity. UW-OncoPlex is a validated, clinical molecular diagnostic assay that collects simultaneous deep-sequencing information, based on $>500\times$ average coverage, for all classes of mutations in 194 targeted, clinically relevant genes, as previously reported [9]. A clinical report was generated for each tumor sequenced, listing somatic aberrations, potentially actionable findings, along with references from the literature.

Precision Tumor Board

A monthly multidisciplinary precision tumor board was led by a clinical pathologist and attended by medical oncologists, anatomic pathologists, urologists, genetic counselors, research staff, residents, and

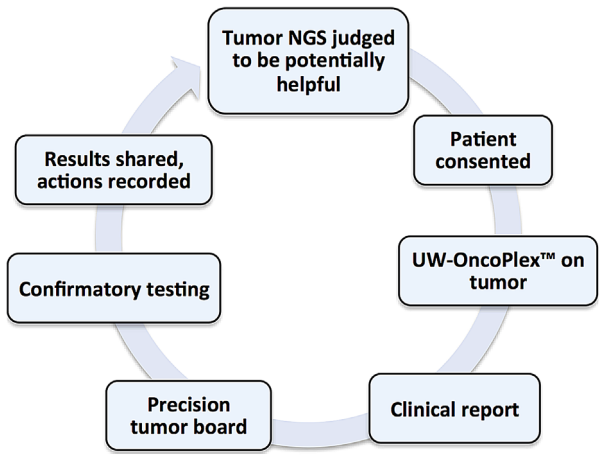

Fig. 1. Schema of pilot study flow.

fellows. Results described in this pilot study were discussed between 4/25/2013 and 2/25/2016. The treating oncologist presented the clinical and family history. The clinical pathologist reviewed and discussed the data analysis and interpretation, and reviewed potentially actionable findings. The group discussed implications for treatment, including clinical trial options, as well as the potential need for referral for genetic counseling. Possible treatments and actions were recorded.

RESULTS

Clinical Features

Of the 45 patients who consented, tumors from 42 patients were sufficient to be evaluated, including 27 primary tumors, 14 metastatic tumors, and 2 salvage surgical specimens. Patient characteristics are summarized in Table I.

In general, UW-OncoPlex was ordered for patients with: (i) an unusual clinical course (i.e., exceptional response to prior therapy); (ii) concern for cancer predisposition (i.e., young age at diagnosis, strong family history of cancers, second primary cancer); and/or (iii) atypical histology. Reasons for testing were varied and listed in detail for each patient in Supplementary Table SI. Testing was done on 11 patients with unusual histologic features, 3 exceptional responders, 23 men diagnosed at $\leq$55 years of age, 12 and 19 men with a family history of prostate or other cancers, respectively, and three with a second primary cancer, with many patients in more than one group.

TABLE I. Clinical Features at Diagnosis and at UW-OncoPlex

Age at diagnosis	
Median (range)–years	57 (45–71)
$\geq$70 years	4 (10%)
$\leq$55 years	20 (48%)
Self-reported race	
White	31 (74%)
African American	7 (17%)
Asian	2 (5%)
Unknown	2 (5%)
Gleason grade sum	
$</=6$	1 (2%)
7	12 (28%)
>7	25 (60%)
Unknown[a]	3 (7%)
Not applicable[b]	1 (3%)
Serum prostate specific antigen at diagnosis	
<4	6 (14%)
4–20	22 (52%)
21–100	7 (17%)
101–1,000	3 (7%)
>1,000	3 (7%)
Unknown	1 (2%)
Localized vs. metastatic at diagnosis	
Localized	29 (69%)
Metastatic	13 (31%)
Disease state at time of UW-OncoPlex	
Localized	14 (33%)
Biochemically recurrent	6 (14%)
Metastatic hormone-sensitive	11 (26%)
Metastatic castration-resistant	9 (21%)
Other metastatic (e.g., squamous cell carcinoma)	2 (5%)

[a]Unknown Gleason score: one received prior ADT, two did not undergo biopsy due to high PSA.
[b]Gleason scoring not applicable due to pure squamous carcinoma histology.

Identification of Somatic Mutations and Clinical Implications

Key findings and actions are shown for the group of patients with non-metastatic and metastatic prostate cancer in Tables II and III, respectively (additional details are available in the corresponding supplementary Tables SII and SIII). Summary integrative analysis is shown in Figure 2. We identified alterations in genes previously reported [4,10], for example: 10/42 (24%), of cases had alterations in genes involved in DNA repair genes (including *BRCA2*, *ATM*, and *CDK12*) similar to recent published reports [7,8]. These patients could be considered for platinum-based chemotherapy [6] or poly-ADP ribose polymerase inhibitor (PARPi) therapy [5]. We have developed a pilot study for such patients using docetaxel/carboplatin for patients with *BRCA1/2* defects (NCT02598895). Another clinical trial option is the pilot study of the PARPi BMN 673 for advanced solid tumors and deleterious BRCA mutations (NCT01989546, available at other institutions) that would not have otherwise been considered.

Other findings with treatment implications included suspected resistance mutations to androgen-receptor pathway inhibitors (such as *AR* amplification, *AR* p.T878A and *AR* p.L702H) observed following treatment with AR-directed agents such as abiraterone and enzalutamide [11,12]. Interestingly, patient 31 was found to have *AR* p.T878A following treatment with just leuprolide and bicalutamide. The presence of this alteration suggests his prostate cancer may not respond to future AR-directed therapies.

Patients with PI3K pathway alterations (including *PIK3R1* insertion, *PIK3R1* mutations, *PIK3CB* mutation and copy gain, and *PIK3CA* mutations) were considered for PI3K-AKT-mTOR inhibitor therapy, including the Phase I trial of AZD8186 (NCT01884285), which was open at our institution. Some cohorts of this study

TABLE II. Key Findings and Resulting Discussion and Actions (Non-Metastatic)

Pt	Key findings	Treatment considerations	Actual therapy change due to UW-OncoPlex	Future therapy	Genetic counseling
		Localized			
26	TMPRSS2-ERG, CHEK2 c.1100delC	Genetic counseling, PARPi, CHEK2 mutation associated with platinum response in ovarian cancer		X	X
38	ATM p.W2960X and ATM p.E2444K, TMPRSS2-ERG	Genetic counseling, consider PARPi and/or platinum		X	X
5	TMPRSS2-ERG	PARPI (TMPRSS2-ERG),		X	
7	MET p.R1327H (R1345H), PTEN p.C296X, TMPRSS2-ERG, TP53 p.G108S with LOH	MET inhibitor (cabozantinib), PI3K-AKT-mTOR inhibitor (PTEN mutation) NCT01884285		X	
13	TMPRSS2-ERG, IKZF1 p.E35K, ABL2 c.347-1G>T	Elected for adjuvant radiation therapy, PARPI (TMPRSS2-ERG)		X	
14	TMPRSS2-ERG	Elected against adjuvant radiation; consider PARPI (TMPRSS2-ERG),		X	
19	KDM6A del exon 17, MEN1 p.V190A, FGFR1 copy loss, AURKA p.V310L, FOXA1 variant	Consider HDAC chromatin remodeling agents (KDM6A), AURKA inhibitor		X	
25	Hypermutation, MSH6 c.1900_1901del with LOH, PTEN c.917_918del, PTEN c.968dup, PTEN c.302T>C, dozens of additional mutations in the context of hypermutation	Consider immune checkpoint inhibitors (Le, et al NEJM, PMID: 26028255); Pembrolizumab for MSI-high, NCT02628067		X	
30	TMPRSS2-ERG, PTEN c.635-1G>C	PARPi (TMPRSS2-ERG)		X	
33	CHD1 p.K1352Vfs*18				
16	(Limited due to low tumor purity) NF1 p. S1380C				
39	Indeterminate				
		Biochemical recurrence			
20	FOXA1 p.N252_G257delinsR, TP53 p.R273H, MYC and FGFR1 copy number gains, TSC1 p.R811Q	Genetic counseling to determine if TP53 p.R273H is germline, mTOR inhibitor (TSC1 variant)		X	X
40	PIK3CA p.A1006V	Consider PI3K-AKT-mTOR inhibitors		X	
23	No actionable findings				
10	(Limited due to poor quality DNA) CDH1 p.R281W				
18	(Limited due to low tumor purity) TP53 p. Y205D, SHH copy gain, FGFR3 copy gain, NOTCH1 copy gain, FOXA1 copy gain				
4	(Limited due to low sequence depth coverage) no actionable findings				

Future therapy defined as current treatment options and/or targeted clinical trials open, pending or expected. Gray text denotes limited study due to low tumor content or poor DNA quality.

required demonstration that the PI3K pathway was altered so the UW-OncoPlex findings both directed therapy and provided clinically useful information for study eligibility.

We also observed RAF fusions (such as *BRAF)*, and mutations in chromatin modifiers (such as *CHD1* and *KDM6A*) that could have implications for therapeutic options, such as enrollment in basket or umbrella trials that are based on specific targets, for example, NCI-Molecular Analysis for Therapy Choice (NCI-MATCH; NCT02465060).

Identification of Suspected Germline Findings

Although UW-OncoPlex is designed to identify somatic mutations, we found a number of gene

TABLE III. Key Findings and Resulting Discussion and Actions (Metastatic)

Pt	Key findings	Treatment considerations	Actual therapy change due to UW-OncoPlex	Future therapy	Genetic counseling
		Metastatic hormone sensitive			
6	ATM p.K2756X and LOH	Based on ATM mutations, genetic counseling, consider future platinum (NCT02598895), consider future PARPi	Enrolled in NCT01576172 (abiraterone +/− veliparib)	X	X
22	FOXA1 p.F254_G257del, AR amplification, RB1 copy loss (likely biallelic loss), APC copy loss (likely biallelic loss), BRAF copy gain, JAK3 p.R175X (possible germline)	Based on JAK3 mutation, genetic counseling. Based on RB1 loss, consider chemotherapy sooner because tumor may behave like AR-null		X	X
34	BRCA2 c.1929delG with LOH, TMPRSS2-ERG, TP53 p.G245C	Based on BRCA2 mutations, genetic counseling, continue future platinum (NCT02598895), consider future PARPi		X	X
1	TMPRSS2-ERG, PTEN copy loss, PIK3R1 in-frame insertion	Based on PTEN loss and PIK3R1 mutation, consider PI3K-AKT-mTOR inhibitors (NCT01884285)		X	
2	TMPRSS2-ERG, TP53 p.G245S	Based on TP53 mutation, consider future Wee1 inhibitor trials		X	
3	BRAF p.K601E, FOXA1 p.F224L, TP53 p.G105_G108del	Based on BRAF mutation, consider BRAF inhibitor or MEK inhibitors		X	
12	TMPRSS2-ERG, CHD1 deletion, RB1 p.R251X with LOH	Based on RB1 loss, consider chemotherapy sooner because tumor may behave like AR-null.		X	
24	TP53 p.R273C, TMPRSS2-ERG, copy number loss chr 2 (including MSH2), chr 6, chr 9; copy gains on portions of chr 1,2,6,17	Based on TP53 mutation, consider future Wee1 inhibitor trials		X	
27	SPOP p.W131R, biallelic inactivation of APC p.R1450X with LOH due to copy loss, CDKN2A homozygous copy loss	CDKN2A loss observed in exceptional responses to taxanes; more confidence in early docetaxel (was already under consideration)		X	
36	PTEN copy loss, PIK3R1 p.W597*, TMPRSS2-ERG	Based on PTEN loss and PIK3R1 mutation, consider PI3K-AKT-mTOR inhibitors (NCT01884285)		X	
		Squamous histology			
28	PIK3R1 m582fs*3 may be gain of function, TP53 p.N29Tfs*15, MYC copy gain, TMPRSS2-ERG fusion and RB exon 4-27 loss and rearrangement	May be more responsive to chemotherapy due to similarities with AR-null tumors	Treated with docetaxel/ carboplatin over AR-directed therapy	X	
8	TP53 c.11101-2A>G, PTEN copy loss, FGFR1 copy gain, NTRK1 p.H772R	Based on suspected germline TP53 mutation, genetic counseling. Based on PTEN loss, consider PI3K-AKT-mTOR inhibitors (NCT01884285). Based on NTRK1 mutation, consider NTRK1 inhibitor trial (NCT02097810). Based on TP53 mutation, consider future Wee1 inhibitor trials		X	X

(Continued)

TABLE III. Continued.

Pt	Key findings	Treatment considerations	Actual therapy change due to UW-OncoPlex	Future therapy	Genetic counseling
		Metastatic castration resistant prostate cancer			
31	AR p.T878A, biallelic inactivation CDK12 c.2495delC AND p.C924G, FOXA1 p.R261C, ABL1 p.F1066L, p. C1067R	Avoid abiraterone (AR p.T878A). Based on CDK12 mutations, consider future platinum (NCT02598895) or PARPi	Avoided abiraterone due to resistance mutation	X	
35	AR p.T878A, PTEN copy loss, MRE11A p.L56W AND p.K633Tfs*45	Based on MRE11A mutations, treat with DNA damaging agent (radium-223), consider future platinum (NCT02598895) or PARPi	Treated with radium-223	X	
11	BRCA2 p.Q3066X, BRCA2 127bp del in exon 11, CHEK2 1100delC, TSC2 c.3883+6G>A	Based on BRCA2 mutations, continue platinum, consider future PARPi. Based on suspected germline BRCA2 mutation, refer to genetic counseling		X	X
17	BRCA2 p.V2969Cfs*7, BRCA2 somatic frame shift deletion, TP53 p.R175H, MLLp.E4650*, AR amplification, APC copy loss	Based on BRCA2 mutations, consider future platinum (NCT02598895) or PARPi. Based on suspected germline BRCA2 mutation, refer to genetic counseling		X	X
15	BRCA2 p.Q2530X and LOH, FOXA1 p. H247R, PTEN copy loss,	Based on BRCA2 mutations, consider future platinum (NCT02598895) or PARPi. Based on suspected germline BRCA2 mutation, refer to genetic counseling. Based on PTEN loss, consider PI3K-AKT-mTOR inhibitor (NCT01884285)		X	X
9	BRCA2 bi-allelic loss, MAP2K1 (MEK1) in-frame del, AR p.W742C, FLT3 p. R387Q, MYC high copy gain	Based on BRCA2 loss, consider future platinum (NCT02598895) or PARPi. May be resistant to anti-androgens.		X	
21	AR amplification, TMPRSS2-ERG fusion, PTEN biallelic inactivation due to large focal deletion	Implications for anti-AR inhibitor resistance. Based on PTEN loss, consider PI3K-AKT-mTOR inhibitors (NCT01884285)		X	
32	PIK3CB p. E1051K mutation, PIK3CB copy gain, PTEN copy loss	Based on PIK3CB mutations, consider PI3K-AKT-mTOR inhibitors (NCT01884285)		X	
29	AR p.L702H, AR high copy gain, SPOP p.F133L, CHD1 homozygous copy loss, APC homozygous copy loss	Consistent with resistance to AR-directed therapies		X	
42	CDK12 c.2963+1G>T and p. H194Kfs*133	Based on CDK12 mutations, consider future platinum (NCT02598895) or PARPi		X	
41	AR partial tandem duplication including exon 3, PTEN homozygous copy loss, BRCA2 copy loss, RB1 copy loss, TP53 mutations	Based on PTEN loss, consider PI3K-AKT-mTOR inhibitors (NCT01884285)		X	
37	MED12 p.L1224F, SF3B1 p.D781G				

ADT, androgen deprivation therapy; TURP, transurethral resection of prostate.
Future therapy defined as current treatment or clinical trial options that were not pursued and/or targeted clinical trials that were pending or anticipated.

Fig. 2. Integrative analysis of genetic aberrations identified through targeted next generation sequencing. Columns represent individual affected individuals, and rows represent specific genes grouped in pathways. Color legend of the aberrations represented including amplification, gain, deep deletion, shallow deletion, missense, inframe/frameshift, truncated, and intronic. Cased with more aberrations in a gene are represented by split colors. Confirmed germline mutations are indicated with a gray box.

alterations that were suspected to be germline mutations in high-penetrance cancer risk genes, such as in *BRCA2* in 4/42 (10%) cases and *TP53* in 2/42 (5%) cases. We also found mutations in moderate-penetrance cancer risk genes, such as *CHEK2* 2/42 (5%) [13]. Other mutations were found in genes conferring risk for other cancers such as breast and ovarian, but are not yet well established as prostate cancer risk genes, such as *ATM* in 2/42 (5%). Overall, 10/42 (24%) had suspected deleterious germline mutations genes with potential implications for inherited cancer predisposition. These patients were informed that the tumor sequencing results suggested the possibility of an inherited cancer risk gene and were referred for genetic evaluation, of which seven patients were confirmed. In two cases, results were not available until after death, but families were notified of the findings and offered referral to genetic counseling.

DISCUSSION

The molecular characterization of cancers using tNGS assays has the potential to enhance the outcomes of cancer patients by efficiently identifying patients with specific tumor features that confer drug susceptibility and/or drug resistance, resulting in personalized cancer treatment strategies. In prostate cancer there is not yet routine use of tNGS testing, in part because targets linked to treatment options have not yet been as well-defined and validated as in colorectal cancer, lung cancer, and melanoma [2,3]. The past several years have brought not only better understanding of the molecular profiles of prostate cancer, but also increasing availability and ease of access to tNGS testing platforms, including and FoundationOne, even to community providers. We conducted this pilot study to assess the feasibility and utility of integrating a tNGS in the setting of a real-world prostate cancer clinical practice using the UW-OncoPlex platform.

One observation that became apparent in the precision tumor board discussions is a lack of standard criteria for defining clinical actionability, which varies widely depending on the stringency of criteria used and including the level of evidence and the disease context. Here, we found it useful to delineate three categories of action at the time of results reporting (shown in Tables II and III): First, actual therapy change, rigorously defined as a direct change in treatment that would not have occurred were it not for the UW-OncoPlex results. Second, future therapy implications, which we defined as treatment options or clinical trials that were suggested by UW-OncoPlex results, but were not immediately chosen and/or were pending or anticipated. For example, patients whose results pointed toward a target for which a clinical trial of a targeted agent existed but was not yet open at our institution, or patients with localized disease or biochemical recurrence with no need for immediate treatment, but who might need treatment options down the line. Third, immediate genetic counseling implications, defined as results from tumor testing suggesting possible germline mutation in a cancer predisposition gene (irrespective of family history of cancer).

We found a high proportion of findings that were suspected to be germline based on tumor-only testing, not entirely surprising given that a majority (but not all) had a positive family history of cancer. In such cases, referral for genetic counseling was recommended. Several groups including American Society of Clinical Oncology and National Cancer Institute have recently published thoughtful discussions and guiding recommendations regarding germline implications of tumor testing [14,15]. A report describing NGS testing of 1566 solid tumors tested found that 13% had mutations in genes associated with inherited cancer susceptibility [16]. A study of 1,915 ovarian cancers determined that 18% carried germline mutations associated with ovarian cancer risk [17]. For prostate cancer, as with other tumors that undergo somatic profiling, managing the information and its implications is an important consideration for ordering providers. Secondary findings such as suspected

germline mutations come with complex decision-making dilemmas, but also offer another avenue for significant potential medical benefit to patients and their families.

Our pilot study was initiated with the goal of evaluating the feasibility and utility of integrating NGS testing into clinical practice in our dedicated prostate cancer clinics. We intentionally allowed flexibility of patient selection criteria so that medical oncologists could have the freedom to explore what tNGS could offer in terms of illuminating treatment options. Because oncologists selected patients considered "high risk" for significant somatic and germline genetic alterations, it was not surprising that we found a relatively high frequency of mutations associated with more aggressive disease and germline mutations. For example, this pilot cohort has a high rate of actionable findings as well as a higher estimated rate of potential germline findings compared to recent estimates [7] (Pritchard, et al. NEJM, in press).

Although UW-OncoPlex testing in the localized or biochemical relapse settings yielded numerous findings, we observed that there were no clinical trials of targeted agents that were available and appropriate for our patients in the non-metastatic setting. However, this is likely to change over time as the recent observation that DNA repair mutations may predict response to platinum chemotherapy and PARP inhibition may lead to trials of these agents in the earlier disease settings in selected patients whose cancers bear these mutations.

Limitations to our study are the small numbers inherent to a pilot study. We did not set strict entry criteria, but rather allowed treating oncologists to determine when they felt testing might be useful. As a consequence, the patient population is heterogeneous. In addition, we do not have extensive follow-up data to demonstrate that tNGS-directed therapy leads to better outcomes compared to empiric therapy choices. Future studies will be needed to further investigate these measures.

In summary, this pilot study suggests a role for tNGS of prostate cancer in guiding therapy planning including treatment and clinical trial selection. In addition, the possibility that tumor sequencing may suggest and indicate the presence of inherited mutations in cancer predisposition genes is important to counsel and prepare patients for, and may have far-reaching implications for genetic counseling, screening, and prevention in family members. Medical providers caring for prostate cancer patients should be alert to and prepared for the possibility that tumor testing may uncover potential germline findings with implications for genetic counseling.

CONCLUSIONS

Targeted next generation sequencing of prostate cancers in the context of a prostate cancer precision tumor board is feasible, and has the potential to guide and prioritize timely discussions around the identification of consequential variants.

ACKNOWLEDGMENTS

We are especially grateful to the patients who generously volunteered to participate in this study. In addition, we thank: Bob Livingston, University of Washington; and Hiep Nguyen University of Washington, for their help with this study.

REFERENCES

1. Basch E, Loblaw DA, Oliver TK, Carducci M, Chen RC, Frame JN, Garrels K, Hotte S, Kattan MW, Raghavan D, Saad F, Taplin ME, Walker-Dilks C, Williams J, Winquist E, Bennett CL, Wootton T, Rumble RB, Dusetzina SB, Virgo KS. Systemic therapy in men with metastatic castration-resistant prostate cancer: American Society of Clinical Oncology and Cancer Care Ontario clinical practice guideline. J Clin Oncol 2014; 32(30):3436–3448.
2. Hagemann IS, Devarakonda S, Lockwood CM, Spencer DH, Guebert K, Bredemeyer AJ, Al-Kateb H, Nguyen TT, Duncavage EJ, Cottrell CE, Kulkarni S, Nagarajan R, Seibert K, Baggstrom M, Waqar SN, Pfeifer JD, Morgensztern D, Govindan R. Clinical next-generation sequencing in patients with non-small cell lung cancer. Cancer 2015;121(4):631–639.
3. Fisher KE, Zhang L, Wang J, Smith GH, Newman S, Schneider TM, Pillai RN, Kudchadkar RR, Owonikoko TK, Ramalingam SS, Lawson DH, Delman KA, El-Rayes BF, Wilson MM, Sullivan HC, Morrison AS, Balci S, Adsay NV, Gal AA, Sica GL, Saxe DF, Mann KP, Hill CE, Khuri FR, Rossi MR. Clinical validation and implementation of a targeted next-generation sequencing assay to detect somatic variants in non-small cell lung, melanoma, and gastrointestinal malignancies. J Mol Diagn 2016;18(2):299–315.
4. Beltran H, Yelensky R, Frampton GM, Park K, Downing SR, MacDonald TY, Jarosz M, Lipson D, Tagawa ST, Nanus DM, Stephens PJ, Mosquera JM, Cronin MT, Rubin MA. Targeted next-generation sequencing of advanced prostate cancer identifies potential therapeutic targets and disease heterogeneity. Eur Urol 2013;63(5):920–926.
5. Mateo J, Carreira S, Sandhu S, Miranda S, Mossop H, Perez-Lopez R, Nava Rodrigues D, Robinson D, Omlin A, Tunariu N, Boysen G, Porta N, Flohr P, Gillman A, Figueiredo I, Paulding C, Seed G, Jain S, Ralph C, Protheroe A, Hussain S, Jones R, Elliott T, McGovern U, Bianchini D, Goodall J, Zafeiriou Z, Williamson CT, Ferraldeschi R, Riisnaes R, Ebbs B, Fowler G, Roda D, Yuan W, Wu YM, Cao X, Brough R, Pemberton H, A'Hern R, Swain A, Kunju LP, Eeles R, Attard G, Lord CJ, Ashworth A, Rubin MA, Knudsen KE, Feng FY, Chinnaiyan AM, Hall E, de Bono JS. DNA-repair defects and olaparib in metastatic prostate cancer. N Engl J Med 2015;373(18): 1697–1708.
6. Cheng HH, Pritchard CC, Boyd T, Nelson PS, Montgomery B. Biallelic inactivation of BRCA2 in pplatinum-sensitive metastatic castration-resistant prostate cancer. Eur Urol 2016; 69(6):996–997.

7. Robinson D, Van Allen EM, Wu YM, Schultz N, Lonigro RJ, Mosquera JM, Montgomery B, Taplin ME, Pritchard CC, Attard G, Beltran H, Abida W, Bradley RK, Vinson J, Cao X, Vats P, Kunju LP, Hussain M, Feng FY, Tomlins SA, Cooney KA, Smith DC, Brennan C, Siddiqui J, Mehra R, Chen Y, Rathkopf DE, Morris MJ, Solomon SB, Durack JC, Reuter VE, Gopalan A, Gao J, Loda M, Lis RT, Bowden M, Balk SP, Gaviola G, Sougnez C, Gupta M, Yu EY, Mostaghel EA, Cheng HH, Mulcahy H, True LD, Plymate SR, Dvinge H, Ferraldeschi R, Flohr P, Miranda S, Zafeiriou Z, Tunariu N, Mateo J, Perez-Lopez R, Demichelis F, Robinson BD, Schiffman M, Nanus DM, Tagawa ST, Sigaras A, Eng KW, Elemento O, Sboner A, Heath EI, Scher HI, Pienta KJ, Kantoff P, de Bono JS, Rubin MA, Nelson PS, Garraway LA, Sawyers CL, Chinnaiyan AM. Integrative clinical genomics of advanced prostate cancer. Cell 2015;161(5):1215–1228.
8. Cancer Genome Atlas Research. The molecular taxonomy of primary prostate cancer. Cell 2015;163(4):1011–1025.
9. Pritchard CC, Salipante SJ, Koehler K, Smith C, Scroggins S, Wood B, Wu D, Lee MK, Dintzis S, Adey A, Liu Y, Eaton KD, Martins R, Stricker K, Margolin KA, Hoffman N, Churpek JE, Tait JF, King MC, Walsh T. Validation and implementation of targeted capture and sequencing for the detection of actionable mutation, copy number variation, and gene rearrangement in clinical cancer specimens. J Mol Diagn 2014;16(1):56–67.
10. Grasso CS, Wu YM, Robinson DR, Cao X, Dhanasekaran SM, Khan AP, Quist MJ, Jing X, Lonigro RJ, Brenner JC, Asangani IA, Ateeq B, Chun SY, Siddiqui J, Sam L, Anstett M, Mehra R, Prensner JR, Palanisamy N, Ryslik GA, Vandin F, Raphael BJ, Kunju LP, Rhodes DR, Pienta KJ, Chinnaiyan AM, Tomlins SA. The mutational landscape of lethal castration-resistant prostate cancer. Nature 2012;487(7406):239–243.
11. Chen EJ, Sowalsky AG, Gao S, Cai C, Voznesensky O, Schaefer R, Loda M, True LD, Ye H, Troncoso P, Lis RL, Kantoff PW, Montgomery RB, Nelson PS, Bubley GJ, Balk SP, Taplin ME. Abiraterone treatment in castration-resistant prostate cancer selects for progesterone responsive mutant androgen receptors. Clin Cancer Res 2015;21(6):1273–1280.
12. Romanel A, Gasi Tandefelt D, Conteduca V, Jayaram A, Casiraghi N, Wetterskog D, Salvi S, Amadori D, Zafeiriou Z, Rescigno P, Bianchini D, Gurioli G, Casadio V, Carreira S, Goodall J, Wingate A, Ferraldeschi R, Tunariu N, Flohr P, De Giorgi U, de Bono JS, Demichelis F, Attard G. Plasma AR and abiraterone-resistant prostate cancer. Sci Transl Med 2015; 7(312):312re10.
13. Naslund-Koch C, Nordestgaard BG, Bojesen SE. Increased risk for other cancers in addition to breast cancer for CHEK2*1100delC heterozygotes estimated from the Copenhagen General Population Study. J Clin Oncol 2016;34(11): 1208–1216.
14. Raymond VM, Gray SW, Roychowdhury S, Joffe S, Chinnaiyan AM, Parsons DW, Plon SE, G. Clinical Sequencing Exploratory Research Consortium Tumor Working. Germline findings in tumor-only sequencing: Points to consider for clinicians and laboratories. J Natl Cancer Inst 2016;108(4): djv351.
15. Robson ME, Bradbury AR, Arun B, Domchek SM, Ford JM, Hampel HL, Lipkin SM, Syngal S, Wollins DS, Lindor NM. American Society of Clinical Oncology Policy Statement Update: Genetic and genomic testing for cancer susceptibility. J Clin Oncol 2015;33(31):3660–3667.
16. Schrader KA, Cheng DT, Joseph V, Prasad M, Walsh M, Zehir A, Ni A, Thomas T, Benayed R, Ashraf A, Lincoln A, Arcila M, Stadler Z, Solit D, Hyman D, Zhang L, Klimstra D, Ladanyi M, Offit K, Berger M, Robson M. Germline variants in targeted tumor sequencing using matched normal DNA. JAMA Oncol 2016;2(1):104–111.
17. Norquist BM, Harrell MI, Brady MF, Walsh T, Lee MK, Gulsuner S, Bernards SS, Casadei S, Yi Q, Burger RA, Chan JK, Davidson SA, Mannel RS, DiSilvestro PA, Lankes HA, Ramirez NC, King MC, Swisher EM, Birrer MJ. Inherited mutations in women with ovarian carcinoma. JAMA Oncol 2016;2(4): 482–490.

SUPPORTING INFORMATION

Additional supporting information may be found in the online version of this article at the publisher's web-site.

available at www.sciencedirect.com
journal homepage: www.europeanurology.com

European Association of Urology

Platinum Priority – Review – Prostate Cancer

Editorial by XXX on pp. x–y of this issue

DNA Repair in Prostate Cancer: Biology and Clinical Implications

Joaquin Mateo [a,b], *Gunther Boysen* [a], *Christopher E. Barbieri* [c,d,e], *Helen E. Bryant* [f], *Elena Castro* [g], *Pete S. Nelson* [h,i], *David Olmos* [g,j], *Colin C. Pritchard* [h], *Mark A. Rubin* [d,e,k], *Johann S. de Bono* [a,b,*]

[a] *Division of Cancer Therapeutics and Division of Clinical Studies, The Institute of Cancer Research, London, UK;* [b] *Drug Development Unit, The Royal Marsden NHS Foundation Trust, London, UK;* [c] *Department of Urology, Weill Cornell Medicine, New York, NY, USA;* [d] *Caryl and Israel Englander Institute for Precision Medicine, New York Presbyterian Hospital-Weill Cornell Medicine. New York, NY, USA;* [e] *Sandra and Edward Meyer Cancer Center, Weill Cornell Medicine, New York, NY, USA;* [f] *Sheffield Institute for Nucleic Acids, Department of Oncology and Metabolism, University of Sheffield, Sheffield, UK;* [g] *Prostate Cancer Unit, Spanish National Cancer Research Centre, Madrid, Spain;* [h] *Department of Laboratory Medicine, University of Washington, Seattle, WA, USA;* [i] *Divisions of Human Biology and Clinical Research, Fred Hutchinson Cancer Research Center, University of Washington, Seattle, WA, USA;* [j] *Medical Oncology Department, CNIO-IBIMA Genitourinary Cancer Unit, Hospital Virgen de la Victoria and Hospital Regional de Malaga, Malaga, Spain;* [k] *Department of Pathology and Laboratory Medicine, Weill Cornell Medicine, New York, NY, USA*

Article info

Article history:
Accepted August 12, 2016

Associate Editor:
James Catto

Keywords:
Prostate cancer
DNA repair
PARP
BRCA
Personalized medicine
DNA damage

Abstract

Context: For more precise, personalized care in prostate cancer (PC), a new classification based on molecular features relevant for prognostication and treatment stratification is needed. Genomic aberrations in the DNA damage repair pathway are common in PC, particularly in late-stage disease, and may be relevant for treatment stratification.
Objective: To review current knowledge on the prevalence and clinical significance of aberrations in DNA repair genes in PC, particularly in metastatic disease.
Evidence acquisition: A literature search up to July 2016 was conducted, including clinical trials and preclinical basic research studies. Keywords included *DNA repair, BRCA, ATM, CRPC, prostate cancer, PARP, platinum, predictive biomarkers*, and *hereditary cancer*.
Evidence synthesis: We review how the DNA repair pathway is relevant to prostate carcinogenesis and progression. Data on how this may be relevant to hereditary cancer and genetic counseling are included, as well as data from clinical trials of PARP inhibitors and platinum therapeutics in PC.
Conclusions: Relevant studies have identified genomic defects in DNA repair in PCs in 20–30% of advanced castration-resistant PC cases, a proportion of which are germline aberrations and heritable. Phase 1/2 clinical trial data, and other supporting clinical data, support the development of PARP inhibitors and DNA-damaging agents in this molecularly defined subgroup of PC following success in other cancer types. These studies may be an opportunity to improve patient care with personalized therapeutic strategies.
Patient summary: Key literature on how genomic defects in the DNA damage repair pathway are relevant for prostate cancer biology and clinical management is reviewed. Potential implications for future changes in patient care are discussed.

* Corresponding author. Division of Clinical Studies, The Institute of Cancer Research Drug Development Unit, The Royal Marsden NHS Foundation Trust, Downs Road, Sutton SM2 5PT, UK. Tel. +44 208 7224028; Fax: +44 208 6427979.
E-mail address: johann.de-bono@icr.ac.uk (J.S. de Bono).

http://dx.doi.org/10.1016/j.eururo.2016.08.037
0302-2838/

Please cite this article in press as: Mateo J, et al. DNA Repair in Prostate Cancer: Biology and Clinical Implications. Eur Urol (2016), http://dx.doi.org/10.1016/j.eururo.2016.08.037

1. Introduction

While therapeutic options for patients with advanced prostate cancer (PC) have improved over the last decade, castration-resistant PC (CRPC) remains a lethal disease [1]. Recently, relevant studies have identified genomic defects in DNA repair in advanced and primary PC. This has led to clinical studies that provide a strong rationale for developing PARP inhibitors and DNA-damaging agents in this molecularly defined PC subgroup. Following the successful development of targeted agents for molecularly defined subpopulations in other cancer types [2,3], there may be an opportunity to potentially improve patient care in PC via personalized therapeutic strategies. In this article, we review the biology and clinical implications of deleterious inherited or acquired DNA repair pathway aberrations in PC.

2. Evidence acquisition

A literature search for clinical trials and preclinical basic research studies up to July 2016 was conducted. Keywords for the included "DNA repair", "BRCA", "ATM", "CRPC", "prostate cancer", "PARP", "platinum", "predictive biomarkers", and "hereditary cancer".

3. Evidence synthesis

3.1. The molecular landscape of primary and advanced PC

Advances in genomics have permitted the identification of putative drivers of carcinogenesis and cancer progression. These genomic data provide for precise molecular tumor subclassification that extends beyond traditional histologic descriptions. For optimal utility, molecular clusters should provide prognostic or predictive information relevant for patient care [4].

Several studies have depicted the genomic landscape of primary prostate tumors [5–7]. Recently, The Cancer Genome Atlas Research Network (TCGA) reported on whole-exome sequencing of a series of 333 localized PCs [8]. Seven subgroups were defined on the basis of certain gene fusions involving the ERG/ETS transcription factor family (ERG, ETV1/4, and FLI1) or recurrent mutations in specific genes (*SPOP*, *FOXA1*, and *IDH1*); these subgroups differ with regard to androgen receptor (AR) signaling activity, DNA methylation, and microRNA expression.

In the TCGA study, in which Gleason ≥8 tumors represented 26% of the cohort, 62/333 (19%) tumors had deleterious germline or somatic aberrations in genes key to the DNA damage repair pathway (*BRCA2*, *BRCA1*, *CDK12*, *ATM*, *FANCD2*, *RAD51C*). Six of these aberrations involved a *BRCA2* K3326* nonsense germline variant, which arguably does not greatly impact protein function despite a modest association with risk of cancer [9], and 23 cases had heterozygous deletions of *FANCD2* or *RAD51* without evidence of biallelic inactivation; consequently, the proportion of localized PCs with impaired DNA repair function is probably less than 19%.

Next-generation sequencing studies of metastatic tumors identified enrichment of mutations in DNA repair genes among patients with lethal disease [10,11]. To provide a systematic analysis of the genomic landscape of CRPC and its potential relevance for patient care, the Stand Up To Cancer (SU2C)-Prostate Cancer Foundation (PCF) International Dream Team pursued whole-exome and transcriptome sequencing of 150 biopsies from metastatic CRPC (mCRPC) [12]. Higher prevalence of aberrations in key DNA repair genes (23%), *TP53* (53%), *RB1* (21%), the PTEN-PI3K pathway (49%), and *AR* (63%) in mCRPC than in localized disease was confirmed. It is not yet clear if this enrichment is secondary to a tumor evolution process in response to therapy exposure, or purely suggests markers of more aggressive PCs (Table 1).

Table 1 – Prevalence of DNA repair gene mutations and deletions described in studies on localized and metastatic prostate cancer

Study	Disease status	Samples	Gene frequency							
		(*n*)	Homologous recombination				MMR		NER	
SU2C-PCF CRPC genomic landscape [12]	CRPC metastasis	150	*BRCA1*	0.7%	*CDK12*	4.7%	*MLH1*	1.3%	*ERCC2*	1.3%
			BRCA2	13.3%	*CHEK2*	3.0%	*MSH2*	3.0%	*ERCC5*	1.3%
			ATM	7.3%	*PALB2*	2.0%	*MSH6*	2.0%		
UM PC genomics [11]	CRPC metastasis	50	*BRCA1*	0%	*CDK12*	6.0%	*MLH1*	2.0%	*ERCC2*	2.0%
			BRCA2	12.0%	*CHEK2*		*MSH2*	2.0%	*ERCC5*	12.0%
			ATM	6.0%	*PALB2*	0%	*MSH6*	2.0%		
UM PC genomics [11]	Treatment-naïve tumors	11	*BRCA1*	0%	*CDK12*	0	*MLH1*	0	*ERCC2*	0
			BRCA2	1/11	*CHEK2*	0	*MSH2*	1/11	*ERCC5*	0
			ATM	1/11	*PALB2*	0	*MSH6*	1/11		
Weill Cornell/Broad [6]	Prostatectomy for localized or locally advanced PC (somatic only)	109	*BRCA1*	1.8%	*CDK12*	0	*MLH1*	0	*ERCC2*	0
			BRCA2	0%	*CHEK2*	0	*MSH2*	0	*ERCC5*	0
			ATM	2.8%	*PALB2*	1.8%	*MSH6*	0.9%		
TCGA localized PC [8]	Localized PC	333	*BRCA1*	1.0%	*CDK12*	2.0%	*MLH1*	0.3%	*ERCC2*	0.6%
			BRCA2	3.0%*	*CHEK2*	0%	*MSH2*	0.3%	*ERCC5*	0.3%
			ATM	4.0%	*PALB2*	0%	*MSH6*	1.5%		

MMR = mismatch repair; NER = nucleotide-excision repair; PC = prostate cancer; CRPC = castration-resistant PC; SU2C-PCF = Stand Up To Cancer-Prostate Cancer Foundation; UM = University of Michigan; TCGA = The Cancer Genome Atlas.

Please cite this article in press as: Mateo J, et al. DNA Repair in Prostate Cancer: Biology and Clinical Implications. Eur Urol (2016), http://dx.doi.org/10.1016/j.eururo.2016.08.037

With regard to DNA repair genes, the SU2C-PCF study identified inactivation of key DNA repair genes in at least 23% of cases, including homologous recombination (HR)–mediated repair genes (most commonly *BRCA2* and *ATM*) and mismatch repair (MMR) genes (*MLH1*, *MSH2*). Other DNA repair mechanisms are also likely to be impacted because of known influences of the AR in nonhomologous end-joining (NHEJ), and possibly aberrations in nucleotide excision repair (NER) and base excision repair (BER).

Intrapatient tumor heterogeneity represents a challenge for genomic stratification of PC in the clinic. Several studies have comprehensively observed an overall higher degree of heterogeneity within primary prostate tumors than in advanced disease [13–15]. This is likely to be related to: (1) bottlenecks in the metastatic process that limit metastatic spread and growth; (2) the capacity of metastatic tumor cells to seed other metastasis and even reseed the primary tumor; and (3) the selection of resistant clones driven by treatment exposures. Alterations in DNA repair genes have been related to increased mutational burden and may generate increased intrapatient heterogeneity; specific studies addressing the impact of genomic instability on treating the diverse subtypes of this common disease are now needed.

3.2. The DNA damage response pathway: a general overview

At any time, the DNA in human cells is constantly being damaged. If there is a deficient repair of this damage, genome stability is compromised, which can contribute to tumorigenesis. Damage can occur endogenously (due to spontaneous hydrolysis of bases or reaction of DNA with naturally occurring reactive oxygen species or alkylating agents) or can be induced by exogenous agents (eg, radiation and toxins). To protect their genome integrity, cells have evolved a complex signaling machinery for recognizing and repairing damage that includes several pathways with complementary and partially overlapping functions. Different forms of DNA damage trigger a response from different branches of this complex system. The main workflow is as follows; when genomic insults are detected, cell-cycle checkpoints are activated to halt the cell cycle and allow the cellular machinery to repair the DNA damage. If the repair is successful, the cell can continue its normal cycle; otherwise, programmed cell death or senescence programs are triggered. If the DNA repair mechanisms are dysfunctional, genomic instability, which is one of the hallmarks of carcinogenesis, ensues.

When damage is limited to one of the DNA strands (single-strand breaks or base modifications), different repair mechanisms can be deployed. These include BER, single-strand break repair (SSBR), NER, and MMR. Each of these pathways uses the complementary undamaged strand as a template to ensure fidelity of repair. BER is mainly activated to repair endogenous oxidative or alkylated base damage [16]. PARP1 and PARP2 are involved in detecting single-strand breaks, which are formed either directly or as intermediates in BER, and help to coordinate the SSBR response. The NER machinery is responsible for repairing bulky adducts such as those induced by UV light, for which the ERCC family of proteins are key mediators. The MMR pathway corrects mutations formed during DNA replication and recombination. The MSH and MLH family of genes are, among others, critical for MMR. The primary mechanisms involved in DNA double-strand break (DSB) repair comprise the HR system and NHEJ. HR requires a sister chromatid as template and is therefore restricted to the S/G2 phases of the cell cycle. It restores the original DNA code error-free. Key mediators of this pathway include BRCA1, BRCA2, PALB2, ATM, ATR, RAD51, MRE11, CHEK2, and XRCC2/3. In contrast, NHEJ functions by ligating broken DNA ends without the use of a template and is therefore functional throughout the cell cycle. The error-prone mode of NHEJ action leads to errors that are permanent and can drive genomic instability (Fig. 1). SSBs that are not repaired before DNA replication takes place will collapse replication forks, leading to formation of DSBs, which then require HR for repair and continued replication [17].

3.3. DNA repair defects play a relevant role in carcinogenesis and PC progression

Prostate carcinogenesis is mediated, as in other cancers, by the accumulation of genetic and epigenetic aberrations; these molecular changes can be inherited or be the result of altered AR transcriptional activity, changes in chromatin architecture, oncogenic replication, error-prone DNA repair, or defective cell division. The sum of these processes confers survival and growth advantage to the transformed cell. Many of these alterations are induced by factors of the microenvironment, particularly the immune system. Chronic inflammation with continued oxidative stress contributes to carcinogenesis of the prostate epithelium by inducing genomic damage. Deficient DNA repair response and defective apoptotic checkpoint control can then lead to permanent incorporation of these genome abnormalities.

AR signaling is critical not only for normal development of the prostate gland but also for prostate carcinogenesis. Genomic instability is related to AR transcriptional activity, and the cross-regulation between AR signaling and DNA damage response pathways appears to be relevant for PC progression [18]. Nevertheless, the role of AR in genome instability is only partly understood [19,20].

Rearrangements between the androgen-regulated *TMPRSS2* gene and the ETS genes *ERG*, *ETV1*, and *ETV4* are common in PC; these appear to be early events contributing to, but not sufficient on their own, prostate carcinogenesis, and are at least partly lineage-specific [5]. AR-driven transcription can result in increased DNA DSB generation at transcriptional hubs, probably as a result of topoisomerase-IIβ enzyme activity, leading to complex structural rearrangements across the genome [21,22]. Mechanistically, this is supported by AR binding to specific chromosomal sites creating a proximity to otherwise distant chromatin loci [20]. *TMPRSS2-ERG* translocation is probably the commonest example of such processes [23,24].

Interestingly, some PCs are characterized by high numbers of rearrangements. Many of these tumors have

Please cite this article in press as: Mateo J, et al. DNA Repair in Prostate Cancer: Biology and Clinical Implications. Eur Urol (2016), http://dx.doi.org/10.1016/j.eururo.2016.08.037

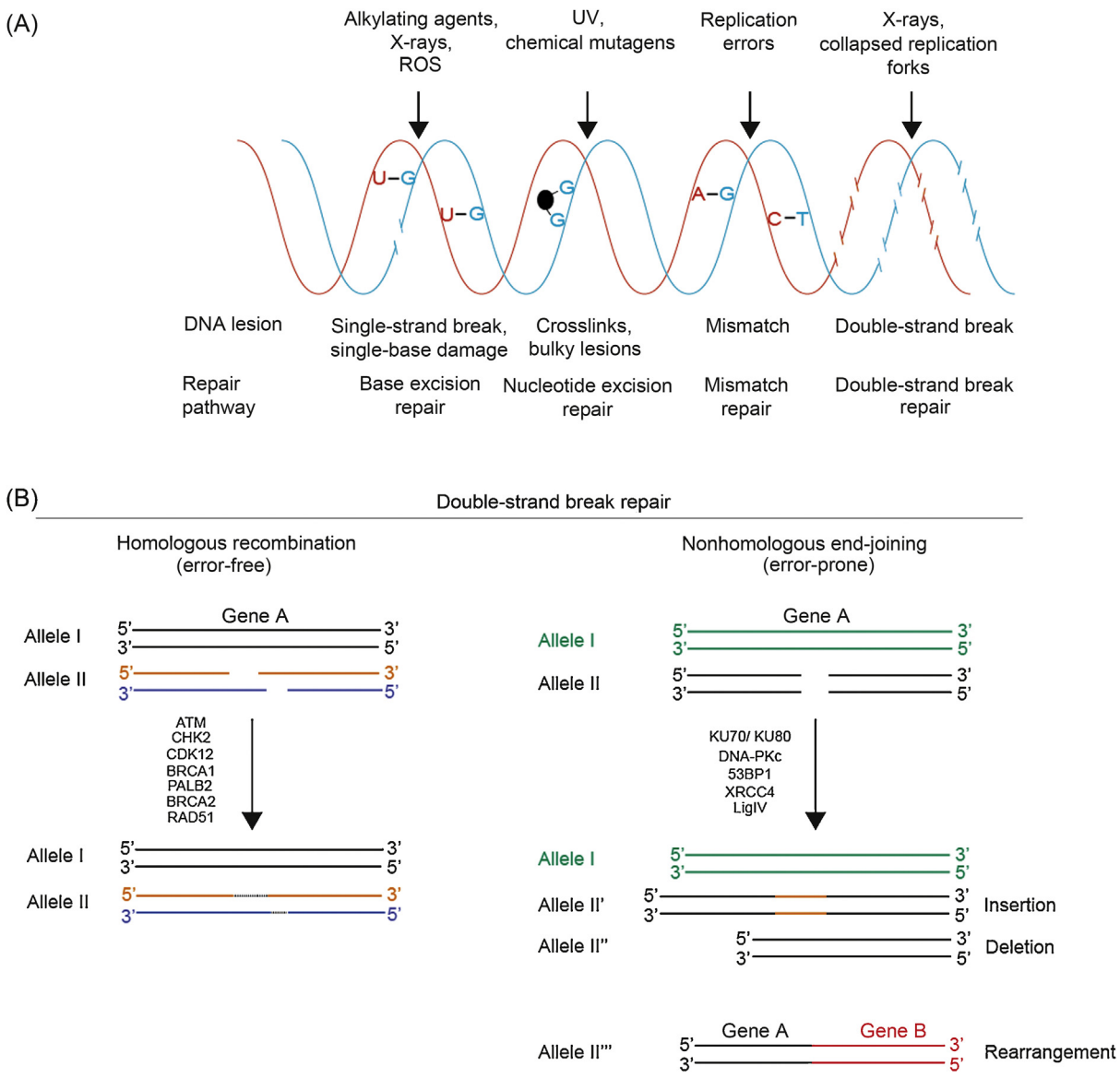

Fig. 1 – An overview of the most important DNA damage–inducing stresses and the corresponding molecular pathways that eukaryotic cells established to repair these. Diverse environmental and endogenous stresses can damage DNA, causing either single-strand (lilac) or double-strand (red box) DNA breaks. Eukaryotic cells developed various molecular mechanisms that repair such damage. DNA double-strand breaks are the most toxic DNA damage, and can be lethal for a cell if not properly repaired. The two most common and best-studied DNA double-strand repair pathways are homologous recombination (HR; error-free) and nonhomologous end-joining (NHEJ; error-prone). HR is limited to the S/G2 phases of the cell cycle and requires a sister chromatid as repair template. Key pathway components are highlighted. NHEJ is active mostly during the G1 phase of the cell cycle and can lead to structural genomic alterations (rearrangements), loss of genomic material (deletion), or insertion of additional nucleotides as a consequence of its imprecise nature. Key pathway components are highlighted.

oncogenic mutations in the *SPOP* gene that stabilize proteins including AR and its transcriptional regulators. Mechanistically, *SPOP* mutant tumors rely predominantly on NHEJ-based DSB repair (while reducing error-free HR-mediated DSB repair activity) [25].

The pattern of genomic aberrations may partly depend on deficiencies in specific DNA repair pathway branches. It has been shown that loss of MMR function induces a hypermutated microsatellite unstable genotype [12]. Somatic complex rearrangements in *MSH2* and *MSH6*, as well as somatic and germline truncating mutations in these two genes, have been described as the most common mechanism for MMR-deficient prostate tumors [26,27]. BRCA2-deficient PCs also present specific mutation signatures enriched in deletions and with higher mutational burden than wild-type–BRCA2 tumors [28,29].

3.4. *Inherited mutations in DNA repair genes and PC risk*

Hereditary germline mutations in DNA repair genes are associated with a higher risk of PC. This results in one gene allele being dysfunctional in every cell, with the second

allele commonly lost by a second hit (mutation, deletion, epigenetic silencing) [30]. Germline mutations in *BRCA2* increase the risk of developing PC (relative risk 8.6 in men <65 yr) [31,32]; their role in the development and progression of breast, ovarian, and pancreatic cancers is also well established. Moreover, inherited mutations in other DNA repair genes such as *PALB2*, *MLH1*, *MSH2*, and *PMS2* also appear to be associated with PC risk [33]. While the proportion of patients carrying a germline *BRCA1/2* mutation is low (1–2%) among the general population of primary PC patients, a multicenter study lead by the SU2C-PCF consortium in metastatic PC patients estimated the prevalence of germline *BRCA2* mutations as 5.3% in the setting of advanced disease; when a panel of 20 DNA repair genes was considered, 82/692 (11.8%) of patients with metastatic disease carried an underlying germline mutation [34]. Interestingly, age at diagnosis and family history of PC did not identify the mutation carriers, although there was enrichment among patients with a family history of cancer. It is therefore now critical to reconsider current guidelines for germline DNA testing; this could be relevant not only for treatment stratification but also in triggering cascade genetic testing for relatives who may be candidates for targeted cancer screening programs.

At present there is no consensus on how to manage this high-risk population with regard to screening for PC. To address this issue, the IMPACT study is evaluating targeted PC screening in men with germline *BRCA1/2* (gBRCA1/2) mutations. Annual prostate-specific antigen (PSA) tests are performed, and a biopsy is triggered if PSA >3ng/ml. A total of 1522 gBRCA1/2 mutation carriers and 959 controls had been recruited at last reporting. Preliminary results have revealed a higher incidence of PC in g*BRCA2* mutation carriers (3.3% vs 2.6% in g*BRCA1* mutation carriers, <2% for controls), who also have a higher likelihood of intermediate/high risk. Final results from these studies are awaited to ascertain the optimal screening strategies for this population [35].

Inherited mutations impairing the MMR function (Lynch syndrome) have been associated with an almost fivefold higher risk of PC, although additional work is needed to determine precise risks [36].

3.5. Impact of DNA repair defects on clinical outcome and response to treatment in PC

The relevance of somatic loss of function of DNA repair genes in the treatment of CRPC is still not clear, as neither the TCGA (primary tumors) nor the SU2C/PCF (metastatic disease) landscape studies reported follow-up clinical outcome data. Prospective studies looking at whether this molecular classification results in clinically relevant stratification for prognosis and treatment response are needed [8,12]. There are data on clinical outcome according to gBRCA1/2 in localized disease. In a series of more than 2000 patients with localized PC, including 61 *BRCA2* and 18 *BRCA1* mutation carriers, 23% of gBRCA1/2 mutation carriers developed metastasis after 5 yr of radical treatment, compared to 7% of noncarriers ($p = 0.001$). Cause-specific survival was significantly shorter among carriers (8.6 yr) compared to noncarriers (15.7 yr; $p = 9 \times 10^{-8}$). Subgroup analysis confirmed g*BRCA2* mutations as independent factor for poor prognosis [37]. The poorer outcome for g*BRCA2* mutation carriers seems to be particularly relevant for patients treated with radical radiotherapy in comparison to surgery, although the patient numbers evaluated were too small to support a robust claim [38]. The exact biological reasons underlying this poorer outcome remain to be fully elucidated; data from small series suggest that these tumors remain sensitive to taxanes [39,40].

3.6. Using DNA repair defects as a therapeutic target: PARP inhibitors

Over the last decade, exploitation of the vulnerabilities of tumor cells with DNA repair gene defects has been pursued in different tumor types, most successfully in ovarian and breast cancers. The identification of a subgroup of mCRPC with DNA repair defects with a similar genomic profile provides a strong rationale for developing the same therapeutic strategies for this molecular subtype of PC [10].

Poly (ADP-ribose) polymerases (PARP) are a family of enzymes involved, primarily, in transcriptional regulation and in detecting and localizing other DNA repair proteins to DNA single strand breaks. Activation of PARP1 and PARP2 triggers the damage response and recruits of key effectors of repair.

The fundamental basis for inhibiting PARP as anticancer therapy is the established biological concept called synthetic lethality: two genomic events that are each relatively innocuous individually become lethal when occurring together [41]. When PARP1/2 are pharmacologically inhibited, SSBs cannot be repaired and eventually progress to toxic DSBs. If a cell is competent in repairing damage, it will be able to fix the DSB. However, if a cell is lacking HR repair capacity (eg, *BRCA1*, *BRCA2*, *PALB2* or *ATM* is dysfunctional or lost), then PARP inhibiton would become lethal.

Two landmark studies demonstrated in 2005 specific killing of cell lines in which BRCA1/2 had been silenced or lost by the PARP inhibitor (PARPi) KU-0059436 (later named AZD2281, olaparib) [42,43]. In these studies, PARP inhibition led to γH2AX accumulation and the absence of RAD51 foci formation in BRCA-deficient models. Subsequent studies have revealed similar effects for other PARP inhibitors now in clinical development, and demonstrated that sensitivity to PARP inhibition also appears when other HR proteins besides BRCA1/2 are nonfunctional or lost [44,45].

This mechanistic interpretation of PARPi-associated synthetic lethality may, however, be a simplification of the underlying biological effect. It is now clear that PARP1 is involved in other DNA damage responses as well as SSBR, with reported functions in DNA replication and repair of stalled replication forks [46,47]. Moreover, certain PARP inhibitors may also have a direct cytotoxic effect by trapping PARP at DNA SSBs. These trapped PARP enzymes eventually induce replication fork stalling, which results in cell cycle arrest and apoptosis [48].

Lastly, of particular relevance to PC, PARP1 is involved in transcriptional regulation and has been implicated in AR

Please cite this article in press as: Mateo J, et al. DNA Repair in Prostate Cancer: Biology and Clinical Implications. Eur Urol (2016), http://dx.doi.org/10.1016/j.eururo.2016.08.037

signaling and ERG function [49,50]. This direct interaction between PARP1 and ERG, as well as an interaction between PI3K/PTEN pathway aberrations and HR DNA repair [51,52], also raised hopes for a wider target population. However, these mechanisms have not been confirmed in human clinical trials to date [53,54].

3.7. Clinical development of PARP inhibitors in PC

A first-in-man clinical trial of olaparib among a cohort of patients with advanced solid tumors enriched in gBRCA1/2 mutation carriers provided critical proof of concept and clinical data on the exquisite antitumor activity of this drug in BRCA-deficient tumors [55]. Since then, olaparib has been evaluated in several phase II/III studies, mainly in ovarian cancer as a single agent, until granted US Food and Drug Administration and European Medicines Agency approval in 2014 for advanced ovarian cancer associated with *BRCA1/2* mutations [56–59].

With regard to mCRPC patients, a few carriers of deleterious gBRCA1/2 mutations were enrolled in the initial trials of olaparib, and showed promising tumor responses. In a phase 2 basket trial including 298 g*BRCA1/2* mutation carriers with different tumor types, eight mCRPC patients were enrolled (1 *BRCA1* mutant carrier, 7 *BRCA2* cases) [60]. Half (4/8) of the mCRPC patients experienced a radiologic partial response; the median progression-free survival for all eight patients was 7.2 mo, with two patients responding for over 1 yr. Of note, 4/8 patients had prior treatment with platinum-based chemotherapy before receiving olaparib. In line with data suggesting some degree of secondary cross-resistance [61], only 1/4 patients who were exposed to platinum responded to olaparib, compared to 3/4 of those who were platinum-naïve.

Other PARP inhibitors are in clinical development; data for PC patients are primarily from g*BRCA1/2* mutation carriers with PC who participated in early clinical trials of these compounds. Preclinical studies of BMN673 (Biomarin/Medivation) demonstrated high potency in inhibiting PARP [62], and tumor responses were seen in *BRCA1/2* mutation carriers across tumor types in a phase 1 clinical trial [63]. Rucaparib (AG-014699/CO-338, Pfizer/Clovis Oncology) and veliparib (ABT-888, Abbott Laboratories) have mainly been developed so far in combination with chemotherapies or other targeted agents [64,65].

The antitumor activity of PARP inhibitors as single agents in patients besides g*BRCA1/2* mutation carriers has been investigated in two studies. During the first-in-man trial of niraparib (MK-4827, Merck/Tesaro), an expansion cohort for "sporadic" CRPC patients was pursued. Eighteen patients received niraparib at the recommended phase 2 dose (300 mg QD). One patient achieved a >50% decrease in PSA, remaining on treatment for 10 mo [54]. Three more patients had significant declines in circulating tumor cell (CTC) counts for >6 mo. The trial was unable to associate responses with either PTEN or ERG expression.

More recently, results from the first stage of a phase 2 investigator-initiated adaptive study of olaparib in mCRPC have been reported, raising interest in developing PARP inhibitors for this disease. The TOPARP study conducted in the UK included a first stage (TOPARP-A) aimed at testing the antitumor activity of olaparib in a "sporadic" mCRPC population (not known to be g*BRCA1/2* mutation carriers and not selected based on any prior knowledge of the genomic background) [66]. The primary endpoint of the study was the response rate, using a composite definition of response: radiologic response according to RECIST 1.1 and/or PSA declines >50% and/or conversion in CTC count from poor (>5 CTC/7.5 ml of blood) to positive prognostic profile (≤5 CTC/7.5 ml of blood), confirmed in at least two readings 4 wk apart. Progression-free and overall survival were explored as secondary endpoints. Response to olaparib was evaluated in 49/50 patients who received at least one dose of olaparib. These were all mCRPC patients progressing on docetaxel and, for all but one, on abiraterone and/or enzalutamide. Some 58% of patients also progressed on cabazitaxel before participating in the study. Of the 49 patients, 16 fulfilled at least one of the response criteria, including 11 cases with a PSA decline >50% and 6/32 with radiologic partial responses among the patients with measurable disease. The antitumor activity observed was strongly associated with the presence of mutations or homozygous deletions in DNA repair genes, evaluated by next-generation sequencing for metastatic biopsies collected at trial entry. Seven patients were found to have biallelic loss of *BRCA2*, either by germline or somatic mutations and deletions, with all seven responding to therapy. In five cases, mutations impacting *ATM* function were found; 4/5 responded to olaparib, including patients with germline and somatic mutations, and two patients with a single-allele mutation in the ATM kinase domain and no evidence of biallelic loss. Moreover, four cases with biallelic events in other genes involved in DNA damage response, including *PALB2*, *FANCA*, and *BRCA1*, showed benefit, primarily involving prolonged CTC conversions. Only two patients responding to olaparib did not have a clear DNA repair defect according to genomic analysis. Several long response durations were observed, including four patients benefiting for >1 yr. Patients with defects in DNA repair genes exhibited improved progression-free and overall survival from treatment initiation, although the preliminary survival data reported will need to be re-evaluated after longer follow-up.

The promising results in this first stage of the TOPARP study led to initiation of a second trial (TOPARP-B) with prospective selection of patients with aberrations in DNA repair genes; the objectives are to validate the antitumor activity seen in patients with the most common mutations (*BRCA2*, *ATM*) and to acquire critical data on sensitivity to olaparib for patients with mutations or deletions in less commonly affected genes.

The tolerability profile of PARP inhibitors is manageable, with anemia, thrombocytopenia, fatigue, and gastrointestinal toxicities (primarily nausea) the most frequent. In the TOPARP-A trial, anemia (20%) and fatigue (12%) were the most common grade ≥3 adverse events; gastrointestinal toxicities were less relevant than reported for ovarian cancer [67]. Hematologic toxicities and fatigue were also

Please cite this article in press as: Mateo J, et al. DNA Repair in Prostate Cancer: Biology and Clinical Implications. Eur Urol (2016), http://dx.doi.org/10.1016/j.eururo.2016.08.037

the dose-limiting events determining the recommended dose for other PARP inhibitors such as BMN673 and niraparib [54,63].

PARP inhibitors are also being evaluated in combination trials in mCRPC. An obvious strategy is to combine PARPi with DNA-damaging agents, mostly chemotherapy agents, to achieve a synergistic effect by blocking the response to chemotherapy-induced DNA damage. In a trial of veliparib and the alkylating agent temozolamide [65], 2/26 treated patients experienced PSA declines of >30%; the rate of grade 3–4 anemia and thrombocytopenia was 15% and 23% respectively. Overlapping hematologic toxicities also represent a major hurdle for combining platinum chemotherapies and PARPi.

An alternative approach would be to aim for a synthetic lethal interaction rather than a synergistic effect. Preclinical data demonstrating enhanced death of prostate tumor cells when combining HDAC and PARPi exemplify an opportunity for clinical development [68].

Lastly, trials combining PARPi with AR-targeting agents may be of interest on the basis of the crossregulation of both pathways and the central role of hormonal therapy in PC. Preliminary results from a randomized trial combining veliparib and abiraterone determined that 27% of patients had aberrations in DNA repair genes; this subgroup experienced high response rates to the combination and, remarkably, to abiraterone alone [53]. Data from a randomized trial combining abiraterone and olaparib are also expected. However, interpretation of putative predictive biomarkers of response in combination trials may be challenging.

3.8. *DNA damaging agents: should they be reconsidered for PC?*

Platinum salts are part of standard management for other tumor types, but their use in PC has been limited since phase 3 trials of the orally available platinum derivative satraplatin failed to meet the primary endpoint of overall survival (OS) improvement [69]. However, some antitumor activity has been described for carboplatin, cisplatin, and satraplatin in mCRPC. This, together with the possibility now of identifying DNA repair–defective tumors and data on DNA repair mutations and response to platinum from ovarian cancer studies, has raised interest in re-evaluating the role of platinum agents in this disease.

Recently, Kumar et al reported longer benefit from carboplatin for cases with HR defects in a retrospective series of patients ($p = 0.002$ for duration of treatment, $n = 21$). Small case series have reported tumor responses to carboplatin in mCRPC patients with biallelic *BRCA2* loss [70]. Nonetheless, the mechanisms involved in sensitivity to platinum and PARPi may be similar but not identical, and further investigation of cross-sensitivity and cross-resistance between agents is now needed following data from ovarian cancer studies. For example, the predominance of NER in repairing platinum-generated adducts warrants specific clinical trials [71,72].

A few clinical trials have explored combinations of carboplatin and taxanes for PC. One of the most relevant was a phase 2 study of carboplatin and docetaxel, followed by cisplatin and etoposide on progression. The study recruited 120 patients with mCRPC with prespecified clinicopathologic characteristics suggestive of more aggressive, arguably less AR-dependent disease [73]. With median OS of 16 mo, the radiological response rate was ~30% for both first- and second-line combinations. The tolerability was relatively acceptable, with only three cases of febrile neutropenia.

Use of the topoisomerase inhibitor mitoxantrone in PC has declined as several other therapies became available over the last decade. However, the main mechanism in the cytotoxicity of mitoxantrone is disruption of DNA synthesis and repair, so re-evaluation of its activity in molecularly defined populations may be of interest.

4. Conclusions

The identification of a subgroup of PCs with lethal disease with genomic deleterious aberrations of DNA repair genes supports further evaluation of this biomarker-driven treatment stratification of advanced PC in registration studies. If the efficacy of this strategy is, it might also be possible to apply it to earlier disease stages, including high-risk locally advanced disease.

Further studies are now needed to clinically qualify multiplex predictive biomarkers of DNA repair–defective PCs, particularly for the less common genomic aberrations that cause this phenotype. On the basis of recent studies indicating that these aberrations are common in the germline DNA of patients with metastatic PC, somatic and germline DNA testing for patients with advanced PC should be considered in view not only of the therapeutic consequences for the patient but also the possibility of pursuing targeted screening in this population. A major limitation at present for adoption of this strategy is the implementation and standardization of genomic testing in the community setting, but the decreasing costs of next-generation sequencing and lessons learned from stratified therapies in other diseases will help us to pursue more precise care for PC patients.

Author contributions: Johann S. de Bono had full access to all the data in the study and takes responsibility for the integrity of the data and the accuracy of the data analysis.

Study concept and design: Mateo, Boysen, de Bono.
Acquisition of data: Mateo, Boysen, de Bono.
Analysis and interpretation of data: All authors.
Drafting of the manuscript: Mateo, Boysen.
Critical revision of the manuscript for important intellectual content: All authors.
Statistical analysis: None.
Obtaining funding: None.
Administrative, technical, or material support: None.
Supervision: Barbieri, Bryant, Castro, Nelson, Olmos, Pritchard, Rubin, de Bono.
Other: None.

Financial disclosures: Johann S. de Bono certifies that all conflicts of interest, including specific financial interests and relationships and

Please cite this article in press as: Mateo J, et al. DNA Repair in Prostate Cancer: Biology and Clinical Implications. Eur Urol (2016), http://dx.doi.org/10.1016/j.eururo.2016.08.037

affiliations relevant to the subject matter or materials discussed in the manuscript (eg, employment/affiliation, grants or funding, consultancies, honoraria, stock ownership or options, expert testimony, royalties, or patents filed, received, or pending), are the following: None.

Funding/Support and role of the sponsor: None.

Acknowledgments: J. Mateo and J.S. de Bono acknowledge funding from an Experimental Cancer Medical Centre grant, Cancer Research UK, Prostate Cancer Foundation, Prostate Cancer UK, a Biomedical Research Centre grant to the ICR/Royal Marsden, and a Medical Research Council - Prostate Cancer UK - Movember Fellowship to J. Mateo. G. Boysen was supported by a Marie Sklodowska-Curie International Individual Postdoctoral Fellowship (CDELP) and Prostate Cancer UK (PG13-036). C.E. Barbieri is a Damon Runyon Clinical Investigator supported (in part) by the Damon Runyon Cancer Research Foundation, and supported by the US National Cancer Institute (K08CA187417-02), the Prostate Cancer Foundation, and the Urology Care Foundation (Rising Star in Urology Research Award). H. Bryant is supported by Yorkshire Cancer Research (SS012PHD). C.C. Pritchard is supported by a CDMRP award (PC131820). The Prostate Cancer Unit at CNIO is supported by CRIS Fundación contra el cancer. E. Castro is the recipient of a Juan de la Cierva Grant from Ministerio de Economía y Competitividad (Spain). D. Olmos is also supported by Fundación Científica de la Asociación Española Contra el Cáncer. The Prostate Cancer Foundation provided support to the following authors through Young Investigator Awards: J. Mateo, C.E. Barbieri, D. Olmos, and C.C. Pritchard.

References

[1] Lorente D, Mateo J, Perez-Lopez R, de Bono JS, Attard G. Sequencing of agents in castration-resistant prostate cancer. Lancet Oncol 2015;16:e279–92.
[2] Slamon DJ, Leyland-Jones B, Shak S, et al. Use of chemotherapy plus a monoclonal antibody against HER2 for metastatic breast cancer that overexpresses HER2. N Engl J Med 2001;344:783–92.
[3] Flaherty KT, Robert C, Hersey P, et al. Improved survival with MEK inhibition in BRAF-mutated melanoma. N Engl J Med 2012;367:107–14.
[4] Rubin MA, Girelli G, Demichelis F. Genomic correlates to the newly proposed grading prognostic groups for prostate cancer. Eur Urol 2015;69:2–5.
[5] Baca SC, Prandi D, Lawrence MS, et al. Punctuated evolution of prostate cancer genomes. Cell 2013;153:666–77.
[6] Barbieri CE, Baca SC, Lawrence MS, et al. Exome sequencing identifies recurrent SPOP, FOXA1 and MED12 mutations in prostate cancer. Nat Genet 2012;44:685–9.
[7] Berger MF, Lawrence MS, Demichelis F, et al. The genomic complexity of primary human prostate cancer. Nature 2011;470:214–20.
[8] Abeshouse A, Ahn J, Akbani R, et al. The molecular taxonomy of primary prostate cancer. Cell 2015;163:1011–25.
[9] Meeks HD, Song H, Michailidou K, et al. BRCA2 polymorphic stop codon K3326X and the risk of breast, prostate, and ovarian cancers. J Natl Cancer Inst 2016;108, djv315.
[10] Beltran H, Yelensky R, Frampton GM, et al. Targeted next-generation sequencing of advanced prostate cancer identifies potential therapeutic targets and disease heterogeneity. Eur Urol 2013;63:920–6.
[11] Grasso CS, Wu Y-M, Robinson DR, et al. The mutational landscape of lethal castration-resistant prostate cancer. Nature 2012;487:239–43.
[12] Robinson D, Van Allen EM, Wu Y-M, et al. Integrative clinical genomics of advanced prostate cancer. Cell 2015;161:1215–28.
[13] Kumar A, Coleman I, Morrissey C, et al. Substantial interindividual and limited intraindividual genomic diversity among tumors from men with metastatic prostate cancer. Nat Med 2016;22:369–78.
[14] Beltran H, Prandi D, Mosquera JM, et al. Divergent clonal evolution of castration-resistant neuroendocrine prostate cancer. Nat Med 2016;22:298–305.
[15] Gundem G, Van Loo P, Kremeyer B, et al. The evolutionary history of lethal metastatic prostate cancer. Nature 2015;520:353–7.
[16] Wood RD, Wood RD, Mitchell M, Sgouros J, Lindahl T. Human DNA repair genes. Science 2011;1284:241–83.
[17] Saleh-Gohari N, Bryant HE, Schultz N, Parker KM, Cassel TN, Helleday T. Spontaneous homologous recombination is induced by collapsed replication forks that are caused by endogenous DNA single-strand breaks. Mol Cell Biol 2005;25:7158–69.
[18] Goodwin JF, Schiewer MJ, Dean JL, et al. A hormone-DNA repair circuit governs the response to genotoxic insult. Cancer Discov 2013;3:1254–71.
[19] Polkinghorn WR, Parker JS, Lee MX, et al. Androgen receptor signaling regulates DNA repair in prostate cancers. Cancer Discov 2013;3:1245–53.
[20] Lin C, Yang L, Tanasa B, et al. Nuclear receptor-induced chromosomal proximity and DNA breaks underlie specific translocations in cancer. Cell 2009;139:1069–83.
[21] Ju B-G, Lunyak VV, Perissi V, et al. A topoisomerase IIβ-mediated dsDNA break required for regulated transcription. Science 2006;312:1798–802.
[22] Wu C, Wyatt AW, McPherson A, et al. Poly-gene fusion transcripts and chromothripsis in prostate cancer. Genes Chromosomes Cancer 2012;51:1144–53.
[23] Tomlins SA, Rhodes DR, Perner S, et al. Recurrent fusion of TMPRSS2 and ETS transcription factor genes in prostate cancer. Science 2005;310:644–8.
[24] Mani R, Tomlins SA, Callahan K, et al. Induced chromosomal proximity and the genesis of gene fusions in prostate cancer. Science 2010;326:2009–11.
[25] Boysen G, Barbieri CE, Prandi D, et al. SPOP mutation leads to genomic instability in prostate cancer. Elife 2015;4:e09207.
[26] Pritchard CC, Morrissey C, Kumar A, et al. Complex MSH2 and MSH6 mutations in hypermutated microsatellite unstable advanced prostate cancer. Nat Commun 2014;5:4988.
[27] Chen Y, Wang J, Fraig MM, et al. Defects of DNA mismatch repair in human prostate cancer. Cancer Res 2001;61:4112–21.
[28] Decker B, Karyadi DM, Davis BW, et al. Biallelic BRCA2 mutations shape the somatic mutational landscape of aggressive prostate tumors. Am J Hum Genet 2016;98:1–12.
[29] Castro E, Jugurnauth-Little S, Karlsson Q, et al. High burden of copy number alterations and c-MYC amplification in prostate cancer from BRCA2 germline mutation carriers. Ann Oncol 2015;26:2293–300.
[30] Carter BS, Beaty TH, Steinberg GD, Childs B, Walsh PC. Mendelian inheritance of familial prostate cancer. Proc Natl Acad Sci U S A 1992;89:3367–71.
[31] Kote-Jarai Z, Leongamornlert D, Saunders E, et al. BRCA2 is a moderate penetrance gene contributing to young-onset prostate cancer: implications for genetic testing in prostate cancer patients. Br J Cancer 2011;105:1230–4.
[32] Leongamornlert D, Mahmud N, Tymrakiewicz M, et al. Germline BRCA1 mutations increase prostate cancer risk. Br J Cancer 2012;106:1697–701.
[33] Eeles R, Goh C, Castro E, et al. The genetic epidemiology of prostate cancer and its clinical implications. Nat Rev Urol 2014;11:18–31.
[34] Pritchard CC, Mateo J, Walsh MF, et al. Inherited DNA repair gene mutations in men with metastatic prostate cancer. N Engl J Med 2016;375:443–5. http://dx.doi.org/10.1056/NEJMoa1603144.
[35] Bancroft EK, Page EC, Castro E, et al. Targeted prostate cancer screening in BRCA1 and BRCA2 mutation carriers: results from the initial screening round of the IMPACT study. Eur Urol 2014;66:489–99.

[36] Haraldsdottir S, Hampel H, Wei L, et al. Prostate cancer incidence in males with Lynch syndrome. Genet Med 2014;16:553–7.
[37] Castro E, Goh C, Olmos D, et al. Germline BRCA mutations are associated with higher risk of nodal involvement, distant metastasis, and poor survival outcomes in prostate cancer. J Clin Oncol 2013;31:1748–57.
[38] Castro E, Goh C, Leongamornlert D, et al. Effect of BRCA mutations on metastatic relapse and cause-specific survival after radical treatment for localised prostate cancer. Eur Urol 2015;68:186–93.
[39] Gallagher DJ, Cronin AM, Milowsky MI, et al. Germline BRCA mutation does not prevent response to taxane-based therapy for the treatment of castration-resistant prostate cancer. BJU Int 2012;109:713–9.
[40] Gallagher DJ, Gaudet MM, Pal P, et al. Germline BRCA mutations denote a clinicopathologic subset of prostate cancer. Clin Cancer Res 2010;16:2115–21.
[41] Dobzhansky T. Genetics of natural populations. Xiii. Recombination and variability in populations of Drosophila pseudoobscura. Genetics 1946;31:269–90.
[42] Farmer H, McCabe N, Lord CJ, et al. Targeting the DNA repair defect in BRCA mutant cells as a therapeutic strategy. Nature 2005;434:917–21.
[43] Bryant HE, Schultz N, Thomas HD, et al. Specific killing of BRCA2-deficient tumours with inhibitors of poly(ADP-ribose) polymerase. Nature 2005;434:913–7.
[44] McCabe N, Turner NC, Lord CJ, et al. Deficiency in the repair of DNA damage by homologous recombination and sensitivity to poly(-ADP-ribose) polymerase inhibition. Cancer Res 2006;66:8109–15.
[45] Murai J, Huang S-YN, Renaud A, et al. Stereospecific PARP trapping by BMN 673 and comparison with olaparib and rucaparib. Mol Cancer Ther 2014;13:433–43.
[46] Patel AG, Sarkaria JN, Kaufmann SH. Nonhomologous end joining drives poly(ADP-ribose) polymerase (PARP) inhibitor lethality in homologous recombination-deficient cells. Proc Natl Acad Sci U S A 2011;108:3406–11.
[47] Bryant HE, Petermann E, Schultz N, et al. PARP is activated at stalled forks to mediate Mre11-dependent replication restart and recombination. EMBO J 2009;28:2601–15.
[48] Murai J, Huang SN, Das BB. Trapping of PARP1 and PARP2 by clinical PARP inhibitors. Cancer Res 2012;72:5588–99.
[49] Schiewer MJ, Goodwin JF, Han S, et al. Dual roles of PARP-1 promote cancer growth and progression. Cancer Discov 2012;2:1134–49.
[50] Brenner JC, Ateeq B, Li Y, et al. Mechanistic rationale for inhibition of poly(ADP-ribose) polymerase in ETS gene fusion-positive prostate cancer. Cancer Cell 2011;19:664–78.
[51] Kumar A, Fernandez-Capetillo O, Carrera AC. Nuclear phosphoinositide 3-kinase controls double-strand break DNA repair. Proc Natl Acad Sci U S A 2010;107:7491–6.
[52] McCabe N, Hanna C, Walker SM, et al. Mechanistic rationale to target PTEN-deficient tumor cells with inhibitors of the DNA damage response kinase ATM. Cancer Res 2015;75:2159–65.
[53] Hussain M, Daignault S, Twardowski P, et al. Co-targeting androgen receptor (AR) and DNA repair: a randomized ETS gene fusion-stratified trial of abiraterone + prednisone (Abi) +/− the PARP1 inhibitor veliparib for metastatic castration-resistant prostate cancer (mCRPC) patients (pts) (NCI9012). J Clin Oncol 2016;34(Suppl):5010.
[54] Sandhu SK, Schelman WR, Wilding G, et al. The poly(ADP-ribose) polymerase inhibitor niraparib (MK4827) in BRCA mutation carriers and patients with sporadic cancer: a phase 1 dose-escalation trial. Lancet Oncol 2013;2045:1–11.
[55] Fong PCP, Boss DDS, Yap T, et al. Inhibition of poly (ADP-ribose) polymerase in tumors from BRCA mutation carriers. N Engl J Med 2009;361:123–34.
[56] Ledermann J, Harter P, Gourley C, et al. Olaparib maintenance therapy in platinum-sensitive relapsed ovarian cancer. N Engl J Med 2012;366:1382–92.
[57] Tutt A, Robson M, Garber JE, et al. Oral poly(ADP-ribose) polymerase inhibitor olaparib in patients with BRCA1 or BRCA2 mutations and advanced breast cancer: a proof-of-concept trial. Lancet 2010;376:235–44.
[58] Ledermann J, Harter P, Gourley C, et al. Olaparib maintenance therapy in patients with platinum-sensitive relapsed serous ovarian cancer: a preplanned retrospective analysis of outcomes by BRCA status in a randomised phase 2 trial. Lancet Oncol 2014;15:852–61.
[59] Audeh MW, Carmichael J, Penson RT, et al. Oral poly(ADP-ribose) polymerase inhibitor olaparib in patients with BRCA1 or BRCA2 mutations and recurrent ovarian cancer: a proof-of-concept trial. Lancet 2010;376:245–51.
[60] Kaufman B, Shapira-Frommer R, Schmutzler RK, et al. Olaparib monotherapy in patients with advanced cancer and a germline BRCA1/2 mutation. J Clin Oncol 2015;33:244–50.
[61] Fong PC, Yap T, Boss DS, et al. Poly(ADP)-ribose polymerase inhibition: frequent durable responses in BRCA carrier ovarian cancer correlating with platinum-free interval. J Clin Oncol 2010;28:2512–9.
[62] Shen Y, Rehman FL, Feng Y, et al. BMN 673, a novel and highly potent PARP1/2 inhibitor for the treatment of human cancers with DNA repair deficiency. Clin Cancer Res 2013;19:5003–15.
[63] de Bono JS, Mina L, Gonzalez M, et al. First-in-human trial of novel oral PARP inhibitor BMN 673 in patients with solid tumors. J Clin Oncol 2013;31(Suppl):2580.
[64] Ihnen M, zu Eulenburg C, Kolarova T, et al. Therapeutic potential of the poly(ADP-ribose) polymerase inhibitor rucaparib for the treatment of sporadic human ovarian cancer. Mol Cancer Ther 2013;12:1002–15.
[65] Hussain M, Carducci MA, Slovin S, et al. Targeting DNA repair with combination veliparib (ABT-888) and temozolomide in patients with metastatic castration-resistant prostate cancer. Invest New Drugs 2014;32:904–12.
[66] Mateo J, Carreira S, Sandhu S, et al. DNA-repair defects and olaparib in metastatic prostate cancer. N Engl J Med 2015;373:1697–708.
[67] Mateo J, Moreno V, Gupta A, et al. An adaptive study to determine the optimal dose of the tablet formulation of the PARP inhibitor olaparib. Target Oncol 2016;11:401–15.
[68] Chao OS, Goodman OB. Synergistic loss of prostate cancer cell viability by coinhibition of HDAC and PARP. Mol Cancer Res 2014;12:1755–66.
[69] Sternberg CN, Petrylak DP, Sartor O, et al. Multinational, double-blind, phase III study of prednisone and either satraplatin or placebo in patients with castrate-refractory prostate cancer progressing after prior chemotherapy: the SPARC trial. J Clin Oncol 2009;27:5431–8.
[70] Cheng HH, Pritchard CC, Boyd T, Nelson PS, Montgomery B. Biallelic inactivation of BRCA2 in platinum-sensitive metastatic castration-resistant prostate cancer. Eur Urol 2016;69:992–5.
[71] Ang JE, Gourley C, Powell B. Efficacy of chemotherapy in BRCA1/2 mutation carrier ovarian cancer in the setting of poly(ADP-ribose) polymerase inhibitor resistance: a multi-institutional study. Clin Cancer Res 2013;44:1–31.
[72] Ceccaldi R, O'Connor KW, Mouw KW, et al. A unique subset of epithelial ovarian cancers with platinum sensitivity and PARP inhibitor resistance. Cancer Res 2015;75:1–8.
[73] Aparicio AM, Harzstark AL, Corn PG, et al. Platinum-based chemotherapy for variant castrate-resistant prostate cancer. Clin Cancer Res 2013;19:3621–30.

Please cite this article in press as: Mateo J, et al. DNA Repair in Prostate Cancer: Biology and Clinical Implications. Eur Urol (2016), http://dx.doi.org/10.1016/j.eururo.2016.08.037

ORIGINAL ARTICLE

Inherited DNA-Repair Gene Mutations in Men with Metastatic Prostate Cancer

C.C. Pritchard, J. Mateo, M.F. Walsh, N. De Sarkar, W. Abida, H. Beltran, A. Garofalo, R. Gulati, S. Carreira, R. Eeles, O. Elemento, M.A. Rubin, D. Robinson, R. Lonigro, M. Hussain, A. Chinnaiyan, J. Vinson, J. Filipenko, L. Garraway, M.-E. Taplin, S. AlDubayan, G.C. Han, M. Beightol, C. Morrissey, B. Nghiem, H.H. Cheng, B. Montgomery, T. Walsh, S. Casadei, M. Berger, L. Zhang, A. Zehir, J. Vijai, H.I. Scher, C. Sawyers, N. Schultz, P.W. Kantoff, D. Solit, M. Robson, E.M. Van Allen, K. Offit, J. de Bono, and P.S. Nelson

ABSTRACT

BACKGROUND

Inherited mutations in DNA-repair genes such as *BRCA2* are associated with increased risks of lethal prostate cancer. Although the prevalence of germline mutations in DNA-repair genes among men with localized prostate cancer who are unselected for family predisposition is insufficient to warrant routine testing, the frequency of such mutations in patients with metastatic prostate cancer has not been established.

METHODS

We recruited 692 men with documented metastatic prostate cancer who were unselected for family history of cancer or age at diagnosis. We isolated germline DNA and used multiplex sequencing assays to assess mutations in 20 DNA-repair genes associated with autosomal dominant cancer-predisposition syndromes.

RESULTS

A total of 84 germline DNA-repair gene mutations that were presumed to be deleterious were identified in 82 men (11.8%); mutations were found in 16 genes, including *BRCA2* (37 men [5.3%]), *ATM* (11 [1.6%]), *CHEK2* (10 [1.9% of 534 men with data]), *BRCA1* (6 [0.9%]), *RAD51D* (3 [0.4%]), and *PALB2* (3 [0.4%]). Mutation frequencies did not differ according to whether a family history of prostate cancer was present or according to age at diagnosis. Overall, the frequency of germline mutations in DNA-repair genes among men with metastatic prostate cancer significantly exceeded the prevalence of 4.6% among 499 men with localized prostate cancer ($P<0.001$), including men with high-risk disease, and the prevalence of 2.7% in the Exome Aggregation Consortium, which includes 53,105 persons without a known cancer diagnosis ($P<0.001$).

CONCLUSIONS

In our multicenter study, the incidence of germline mutations in genes mediating DNA-repair processes among men with metastatic prostate cancer was 11.8%, which was significantly higher than the incidence among men with localized prostate cancer. The frequencies of germline mutations in DNA-repair genes among men with metastatic disease did not differ significantly according to age at diagnosis or family history of prostate cancer. (Funded by Stand Up To Cancer and others.)

The authors' full names, academic degrees, and affiliations are listed in the Appendix. Address reprint requests to Dr. Nelson at the Division of Human Biology, Fred Hutchinson Cancer Research Center, 1100 Fairview Ave., Mailstop D4-100, Seattle, WA 98109, or at pnelson@fhcrc.org.

Drs. Pritchard, Mateo, and Walsh and Drs. Offit, de Bono, and Nelson contributed equally to this article.

This article was published on July 6, 2016, at NEJM.org.

DOI: 10.1056/NEJMoa1603144

Carcinoma of the prostate is a common cancer with a wide spectrum of clinical behavior that ranges from decades of indolence to rapid metastatic progression and lethality.[1,2] Prostate cancer is also among the most heritable of human cancers, with 57% (95% confidence interval [CI], 51 to 63) of the interindividual variation in risk attributed to genetic factors.[3] Thus far, genomewide association studies have identified more than 100 common variants that account for approximately 33% of the excess familial prostate cancer risk.[4-7] Mutations in other genes, including *BRCA1*, *BRCA2*, *MSH2*,[8-10] and *HOXB13*,[11] account for a small proportion of familial cases, with *BRCA2* mutations associated with 1.2 to 1.8% of prostate cancer overall.[9,12]

Thus far, only mutations that disrupt the function of genes involved in repairing DNA damage through homologous recombination have been shown to be associated with the aggressive clinical behavior of localized prostate cancer and with cancer-specific mortality.[9,12-14] The need for genetic prognostic markers is critical, because the clinicopathological diversity of prostate cancer has confounded efforts to develop effective screening strategies that avoid overdetection and overtreatment yet capture cancers that are destined to affect survival.[15] Persons who are shown to have cancer-predisposition mutations in the germline may serve as sentinels for the identification of families at high risk. It should be noted that men with metastatic prostate cancer and DNA-repair gene mutations have been reported to have sustained responses to poly-ADP ribose polymerase (PARP) inhibitors and platinum-based chemotherapy.[16,17]

Although the prevalence of germline DNA-repair gene mutations is low among men with localized prostate cancer who are unselected for family predisposition, the frequency of such mutations among men with metastatic prostate cancer has not been established. We recently reported an analysis of the spectrum of somatic aberrations that occur in metastatic prostate cancer, using whole-exome sequencing of metastatic tumors.[18] For comparison purposes, we also sequenced germline DNA exomes from these men and unexpectedly found that 8% carried pathogenic germline mutations in DNA-repair genes. This finding suggested that men with metastatic prostate cancer represent a population that is enriched for heritable defects in DNA repair. To confirm this finding and to further ascertain the spectrum and prevalence of germline DNA-repair gene mutations in metastatic prostate cancer, we recruited 542 additional men with a confirmed prostate cancer metastasis and used next-generation sequencing to analyze DNA-repair genes associated with autosomal dominant cancer-predisposition syndromes.

METHODS

STUDY POPULATIONS

Seven case series of men with metastatic prostate cancer across multiple institutions in the United States and United Kingdom, including a total of 692 patients, were analyzed. All the patients had a diagnosis of metastatic prostate cancer and were not selected on the basis of family history, age, or any knowledge of genetic background. The demographic characteristics of the men in each series are summarized in Table 1. Detailed information on the specific germline mutations and on clinical features of mutation carriers in each series is provided in Tables S1, S2, and S3 in the Supplementary Appendix, available with the full text of this article at NEJM.org.

Case Series 1, the Stand Up to Cancer–Prostate Cancer Foundation (SU2C-PCF) International Prostate Cancer Dream Team discovery series, was made up of 150 patients for whom data were previously reported in the SU2C-PCF study of molecular stratification of metastatic prostate cancer.[18] Case Series 2, the SU2C-PCF validation series, was made up of 84 patients who were newly enrolled in the SU2C-PCF study and for whom data had not been reported previously. Case Series 3, Royal Marsden Prostate Cancer Genomics series, included 131 patients who were considered for enrollment in clinical trials at the Royal Marsden Hospital from January 2013 through July 2015. Case Series 4 consisted of 91 consecutive patients included in the University of Washington rapid autopsy program from 1997 through 2013. Case Series 5 included 69 consecutive patients who were enrolled in the Weill Cornell Medical College precision medicine program. Case Series 6 was made up of 43 consecutive patients from the University of Michigan rapid autopsy program. Case Series 7, from the Memorial Sloan Kettering Cancer Center,

included 124 consecutive patients who were enrolled through the Memorial Sloan Kettering Integrated Mutation Profiling of Actionable Cancer Targets (MSK-IMPACT) study.

The protocols for these case series were approved by the local institutional review boards, and written informed consent was obtained from all patients at the local sites before enrollment. Correlative clinical data were collected at each site with the use of electronic patient records and were entered into deidentified databases. The study was designed by the Stand Up To Cancer–Prostate Cancer Foundation International Prostate Cancer Dream Team investigators. The study sponsors had no role in the design of the study, the collection or analysis of the data, or the preparation of the manuscript. The manuscript was written by four of the authors. All authors reviewed the manuscript, agreed to submit the manuscript for publication, and vouch for the accuracy and completeness of the data and for the fidelity of the study to the protocol.

SEQUENCING AND BIOINFORMATICS ANALYSIS

For the analysis involving Case Series 1, 2, and 6, whole-exome sequencing of germline and tumor DNA was performed as described previously.[18] Germline DNA from buccal swabs, buffy coats, or whole blood was isolated with the use of the QIAGEN DNeasy Blood and Tissue Kit. Whole-exome sequencing was performed on the Illumina HiSeq 2500 in paired-end mode.

For the analysis of Case Series 3, germline DNA was extracted from saliva or buccal swab samples with the use of the Oragene kit (DNA Genotek). Libraries for targeted sequencing were constructed with a customized GeneRead DNaseq Panel (Qiagen) covering 53 genes and run on the Illumina MiSeq sequencer, as described previously.[16]

For the analyses of Case Series 4 and 5, germline DNA was extracted from peripheral blood or nontumor tissue and from matched tumor DNA, as described previously.[19] Targeted deep sequencing was performed with the BROCA panel of 53 DNA-repair pathway genes. The bioinformatics pipeline has been described previously.[20,21] For tumors from Case Series 5, analyses were performed by means of exome sequencing, as described previously.[22] For Case Series 7, tumor and germline genomic sequencing was performed as described previously, with the use of the MSK-IMPACT hybrid capture-based next-generation sequencing assay.[23,24]

The mean sequencing depth of coverage was more than 100× for all case series, with the exception of sequencing of *BAP1*, *BARD1*, *BRIP1*, and *FAM175A*, which were not included on the Royal Marsden Hospital panel, and *GEN1*, which was not included on the Royal Marsden Hospital or Memorial Sloan Kettering panel. Data from the Royal Marsden Hospital and Memorial Sloan Kettering cases were censored for analyses of these genes. In addition, data were censored for *CHEK2* in 158 cases for which exon sequencing coverage was incomplete. The depth of coverage for each gene according to site is provided in Table S4 in the Supplementary Appendix.

To compare our results with data from a large series of patients with localized prostate cancer, we analyzed public data from the Cancer Genome Atlas prostate cancer study.[25] Paired-end reads (100 bp) were aligned to the hg19 reference human genome with the use of the Burrows–Wheeler Aligner. Annotations were defined with ANNOVAR (http://annovar.openbioinformatics.org/en/latest). Population allele frequencies were extracted from the Exome Aggregation Consortium ExAC Browser (http://exac.broadinstitute.org/), 1000 Genomes (www.1000genomes.org), and the single-nucleotide polymorphism database of the National Center for Biotechnology Information (dbSNP), version 138 (www.ncbi.nlm.nih.gov/projects/SNP).

INTERPRETATION OF VARIANTS

Our analysis focused on variants identified among 20 genes associated with autosomal dominant cancer-predisposition syndromes that involve maintenance of DNA integrity (Table 2). The pathogenicity of germline variants was determined according to established American College of Medical Genetics and Genomics and Association for Molecular Pathology consensus criteria and International Agency for Research on Cancer guidelines.[24,26] At least two independent expert reviewers evaluated all variants against published literature and public databases, including ClinVar and variant-specific databases, in addition to population frequency databases, including 1000 Genomes and the Exome Aggregation Consortium. Expected high-penetrance or moderate-penetrance variants classified as mutations that are pathogenic or likely

Table 1. Demographic Characteristics of the Patients with Prostate Cancer.*

Characteristic	Case Series 1 (N=150)		Case Series 2 (N=84)		Case Series 3 (N=131)		Case Series 4 (N=91)		Case Series 5 (N=69)		Case Series 6 (N=43)		Case Series 7 (N=124)		All Case Series (N=692)		TCGA Cohort with Primary Prostate Cancer (N=499)†			
																	L-I Risk		High Risk	
	M	NM	M	NM	M	NM	M	NM	M	NM	M	NM	M	NM	M	NM	M	NM	M	NM
	number of patients																			
Total	15	135	9	75	16	115	8	83	7	62	4	39	23	101	82	610	4	158	19	318
Age																				
<50 yr	2	16	0	2	1	6	1	5	1	2	0	3	2	9	7	43	0	15	1	11
50–59 yr	6	40	4	30	3	37	2	18	2	15	0	6	9	47	26	193	3	63	8	103
60–69 yr	6	63	3	24	11	56	3	38	3	20	2	25	11	36	39	262	1	67	8	167
70–79 yr	1	15	1	11	1	15	2	19	1	11	2	5	1	9	9	85	0	13	2	37
≥80 yr	0	1	0	2	0	1	0	1	0	8	0	0	0	0	0	13	0	0	0	0
Unknown	0	0	1	6	0	0	0	2	0	6	0	0	0	0	1	14	0	0	0	0
Race or ethnic background‡																				
Non-Hispanic white	12	116	8	60	16	103	5	70	3	37	4	30	22	90	70	506	2	118	16	270
Hispanic	0	1	1	0	0	0	0	0	2	7	0	0	0	0	3	8	0	1	1	5
Non-Hispanic black	1	8	0	4	0	12	2	0	1	5	0	2	0	5	4	36	2	27	2	27
Asian or Pacific Islander	1	2	0	2	0	0	0	0	0	5	0	1	0	1	1	11	0	3	0	9
Other or unknown	1	8	0	9	0	0	1	13	1	8	0	6	1	5	4	49	0	9	0	7
History of cancer in a first-degree relative																				
Prostate cancer	4	31	3	11	2	16	0	14	2	12	0	4	5	29	16	117	NA	NA	NA	NA
Other cancer	10	55	4	35	8	53	6	30	3	14	1	19	19	64	51	270	NA	NA	NA	NA
No cancer	2	46	2	27	5	35	1	25	3	29	1	12	4	25	18	199	NA	NA	NA	NA
Unknown	2	15	1	5	2	17	1	21	1	9	2	6	0	0	9	73	NA	NA	NA	NA
Gleason score§																				

≤6	0	8	0	3	0	11	1	9	1	3	0	2	0	4	2	40	1	32	1	11
3+4	0	19	1	9	0	10	1	6	1	3	0	2	2	11	5	60	3	94	1	50
4+3	1	18	2	7	1	11	0	15	2	7	0	4	4	20	10	82	0	32	5	64
8–10	11	70	3	44	12	65	6	39	3	28	4	16	17	64	56	326	0	0	12	193
Unknown	3	20	3	12	3	18	0	14	0	21	0	15	0	2	9	102	0	0	0	0

* The studies included in each case series were as follows: 1, Stand Up To Cancer–Prostate Cancer Foundation discovery series; 2, Stand Up To Cancer–Prostate Cancer Foundation validation series; 3, Royal Marsden Hospital; 4, University of Washington; 5, Weill Cornell Medical College; 6, University of Michigan; and 7, Memorial Sloan Kettering Cancer Center. L-I denotes low to intermediate, M mutation present, NA not applicable, and NM no mutation present.
† The Cancer Genome Atlas (TCGA) cohort includes a series of patients with localized prostate cancer.
‡ Race and ethnic background were self-reported.
§ The Gleason score is a measure of the differentiation state of prostate cancer; scores range from 2 to 10, with higher scores associated with worse clinical outcomes. When two grades are given (e.g., 3+4), the first indicates the more common grade found in the tumor.

to be pathogenic are reported here. Low-penetrance variants, such as *CHEK2* p.I157T, were excluded.

STATISTICAL ANALYSIS

Associations between DNA-repair gene mutation status and age, race, or Gleason score strata were evaluated with the use of two-sided Fisher's exact tests. The frequencies of DNA-repair gene mutations among the 692 patients with metastatic prostate cancer were evaluated relative to the expected frequencies from the Exome Aggregation Consortium (53,105 persons) or the Cancer Genome Atlas cohort (499 persons) with the use of two-sided exact binomial tests. We also performed analyses in which the 150 men from the previously reported Case Series 1 were excluded[18] (Table S5 in the Supplementary Appendix). No adjustments were made for multiple comparisons; P values of less than 0.05 were considered to indicate statistical significance.

RESULTS

PATIENT CHARACTERISTICS

All 692 men in our analysis had documented metastatic prostate cancer, as determined by histologic evaluation of a tumor-biopsy specimen or surgical-resection specimen. The demographic characteristics of the men from each case series are shown in Table 1.

GERMLINE DNA-REPAIR GENE MUTATIONS

We assessed 20 genes that maintain DNA integrity and have been associated with autosomal dominant cancer-predisposition syndromes (Table 2), using whole-exome sequencing or targeted next-generation sequencing assays designed to interrogate the status of DNA-repair genes.[27] Of the 692 men evaluated, 82 (11.8%) had at least one presumed pathogenic germline mutation in a gene involved in DNA-repair processes (Table 2). Mutation frequencies were similar across independent case series (Table 3). The 84 germline mutations that were presumed to be pathogenic (2 men had mutations in 2 genes) included 79 truncating mutations and 5 known deleterious missense mutations (Fig. 1, and Table S1 in the Supplementary Appendix). Mutations were identified in 16 different genes, including *BRCA2* (37 mutations [44% of total mutations]), *ATM* (11 [13%]), *CHEK2* (10 [12%]), *BRCA1* (6 [7%]), *RAD51D*

Table 2. Germline Mutations in Metastatic Cases as Compared with the General Population and Primary Cases.

Gene	Metastatic Prostate Cancer (N=692)*	Exome Aggregation Consortium (N=53,105)†	TCGA Cohort with Primary Prostate Cancer (N=499)	Metastatic Prostate Cancer vs. Exome Aggregation Consortium		Metastatic Prostate Cancer vs. TCGA Cohort	
	No. of Mutations (% of Men)			Relative Risk (95% CI)	P Value	Relative Risk (95% CI)	P Value
ATM	11 (1.59)	133 (0.25)	5 (1.00)	6.3 (3.2–11.3)	<0.001	1.6 (0.8–2.8)	0.12
ATR	2 (0.29)	43 (0.08)	0	3.6 (0.4–12.8)	0.11	—	—
BAP1‡	0	1	0	—	—	—	—
BARD1‡	0	38 (0.07)	1 (0.20)	—	—	—	—
BRCA1	6 (0.87)	104 (0.22)	3 (0.60)	3.9 (1.4–8.5)	0.005	1.4 (0.5–3.1)	0.32
BRCA2	37 (5.35)	153 (0.29)	1 (0.20)	18.6 (13.2–25.3)	<0.001	26.7 (18.9–36.4)	<0.001
BRIP1‡	1 (0.18)	100 (0.19)	1 (0.20)	0.9 (0.02–5.3)	1.0	0.9 (0.0–4.9)	1.0
CHEK2‡	10 (1.87)	314 (0.61)	2 (0.40)	3.1 (1.5–5.6)	0.002	4.7 (2.2–8.5)	<0.001
FAM175A‡	1 (0.18)	52 (0.10)	0	1.8 (0.05–10.1)	0.42	—	—
GEN1‡	2 (0.46)	42 (0.08)	0	5.8 (0.7–20.8)	0.048	—	—
MLH1	0	11 (0.02)	0	—	—	—	—
MRE11A	1 (0.14)	36 (0.07)	1 (0.20)	2.1 (0.1–11.8)	0.38	0.7 (0.0–4.0)	1.0
MSH2	1 (0.14)	23 (0.04)	1 (0.20)	3.3 (0.1–18.5)	0.26	0.7 (0.0–4.0)	1.0
MSH6	1 (0.14)	41 (0.08)	1 (0.20)	1.9 (0.05–10.4)	0.41	0.7 (0.0–4.0)	1.0
NBN	2 (0.29)	61 (0.11)	1 (0.20)	2.5 (0.3–9.1)	0.19	1.4 (0.2–5.2)	0.40
PALB2	3 (0.43)	65 (0.12)	2 (0.40)	3.5 (0.7–10.3)	0.05	1.1 (0.2–3.1)	0.76
PMS2	2 (0.29)	56 (0.11)	1 (0.20)	2.7 (0.3–9.8)	0.17	1.4 (0.2–5.2)	0.40
RAD51C	1 (0.14)	59 (0.11)	2 (0.40)	1.3 (0.03–7.2)	0.54	0.4 (0.0–2.0)	0.54
RAD51D	3 (0.43)	40 (0.08)	1 (0.20)	5.7 (1.2–16.7)	0.02	2.2 (0.4–6.3)	0.16
XRCC2	0	23 (0.04)	0	—	—	—	—

* The denominators for genes for which data were censored were 561 (*BAP1*, *BARD1*, *BRIP1*, and *FAM175A*), 437 (*GEN1*), and 534 (*CHEK2*).
† Data are for the persons in the Exome Aggregation Consortium, minus the patients included in the TCGA studies. The percent with a mutation was calculated on the basis of the total number of persons for whom sequence coverage was adequate for the given allele, which differed slightly from the total of 53,105 persons, depending on the specific mutation.
‡ Data for metastatic cases with inadequate sequencing for this gene were censored.

(3 [4%]), and *PALB2* (3 [4%]) (Fig. 2). Four genes had no clearly detrimental aberrations. One man had mutations in *ATM* and *CHEK2*, and one man had mutations in *BRCA2* and *CHEK2*. The majority of men with DNA-repair gene mutations for whom the Gleason score was available (73 men) had primary tumors with high scores (Gleason scores range from 2 to 10, with higher scores associated with worse clinical outcomes): 56 men (77%) had a Gleason score of 8 through 10, 15 men (21%) had a score of 7, and 2 men (3%) had a score of 6. We found no association between the presence of a germline DNA-repair gene mutation and an age at diagnosis of younger than 60 years versus 60 years or older (P=0.90) or non-Hispanic white versus other race (P=0.84). There was marginal evidence that the presence of a germline DNA-repair gene mutation was associated with a Gleason score of 8 through 10 versus 7 or lower (odds ratio, 1.8; 95% confidence interval [CI], 1.0 to 3.5; P=0.04).

FAMILY CANCER HISTORY

Information regarding family history was available for 72 of 82 men (88%) with presumed pathogenic mutations in DNA-repair genes and for 537 of 610 men (88%) without DNA-repair gene mutations. In both groups, 22% of the men (16 of 72 men with DNA-repair gene mutations and 117 of 537 men without such mutations) had

a first-degree relative with prostate cancer (P=1.0). However, 51 of the 72 patients with DNA-repair gene mutations (71%) had a first-degree relative with cancer other than prostate cancer, whereas 270 of the 537 patients without DNA-repair gene mutations (50%) had a first-degree relative with cancer other than prostate cancer (odds ratio, 2.4; 95% CI, 1.4 to 4.3; P=0.001). Inspection of extended pedigree information of probands with DNA-repair gene mutations revealed affected relatives with breast cancer (24 probands), ovarian cancer (10), leukemia and lymphoma (6), pancreatic cancer (7), or other gastrointestinal cancers (18).

Table 3. Germline DNA-Repair Gene Mutations in Seven Metastatic Prostate Cancer Case Series.

Case Series	Description	Patients	Patients with Mutations
		no.	*no. (%)*
1	Stand Up To Cancer–Prostate Cancer Foundation discovery series	150	15 (10.0)
2	Stand Up To Cancer–Prostate Cancer Foundation validation series	84	9 (10.7)
3	Royal Marsden Hospital	131	16 (12.2)
4	University of Washington	91	8 (8.8)
5	Weill Cornell Medical College	69	7 (10.1)
6	University of Michigan	43	4 (9.3)
7	Memorial Sloan Kettering Cancer Center	124	23 (18.5)
Total		692	82 (11.8)

SOMATIC MUTATIONS IN DNA-REPAIR GENES

Tumor sequencing data were available for 61 of the men with germline DNA-repair gene mutations. For 36 (59%) of these men, the second allele was clearly aberrant, in that either a second loss-of-function mutation or a gene-copy loss was present (Table S1 in the Supplementary Appendix). A study of cancer-predisposition genes in children with cancer showed that 66% of children with a presumed pathogenic gene mutation had a second "hit" somatic aberration within the tumor genome,[28] and a study involving patients with advanced cancer showed that 21.4% of patients with a presumed pathogenic gene mutation had a somatic second-allele aberration.[23] Although a subset of germline loss-of-function mutations may not represent the causal event in the genesis of a given tumor, inactivation of the remaining allele may occur through epigenetic mechanisms or other processes.[29]

GERMLINE MUTATIONS IN DNA-REPAIR GENES IN LOCALIZED PROSTATE CARCINOMAS

We compared the frequency of germline DNA-repair gene mutations among men with metastatic prostate cancer with the frequency of such mutations among men with localized prostate cancer. In the Cancer Genome Atlas prostate cancer study,[25] which included 499 men for whom germline whole-exome sequencing data were available, 23 men (4.6%) had germline mutations in DNA-repair genes (P<0.001 for the comparison with metastatic disease). In addition, 6 men harbored the *BRCA2* K3326* polymorphism, a C-terminal truncating variant that is unlikely to be associated with a predisposition to prostate cancer.[30] It should be noted that to accommodate Cancer Genome Atlas requirements, the majority of tumors had high-risk characteristics: 90% were clinical stage T2c or greater, and 91% of the carcinomas had a Gleason score higher than 6, which far exceeds the approximately 30% of cancers with a Gleason score higher than 6 that was reported among men whose cancer was diagnosed by screening.[31-33] Presumed pathogenic mutations in DNA-repair genes were identified in 2 of 45 men (4%) who had cancer with a Gleason score of 6, in 9 of 249 men (4%) who had cancer with a Gleason score of 7, and in 12 of 205 men (6%) who had cancer with a Gleason score of 8, 9, or 10 (P=0.37 for trend). Four of 162 men (2%) with localized low-to-intermediate–risk tumors and 19 of 337 men (6%) with localized high-risk tumors, as categorized according to National Comprehensive Cancer Network risk criteria,[34] had germline DNA-repair gene mutations (Table 1). The odds of DNA-repair gene mutations being present among men with metastatic prostate cancer differed significantly from the odds among men with localized low-to-intermediate–risk tumors (odds ratio, 5.3; 95% CI, 1.9 to 20.2; P<0.001) or among those with high-risk tumors (odds ratio, 2.2; 95% CI, 1.3 to 4.0; P=0.002) (Table S6 in the Supplementary Appendix). As observed in men with metastatic prostate cancer, there was no association between the presence of a germline mutation in a DNA-repair gene and an age at diagnosis of younger than

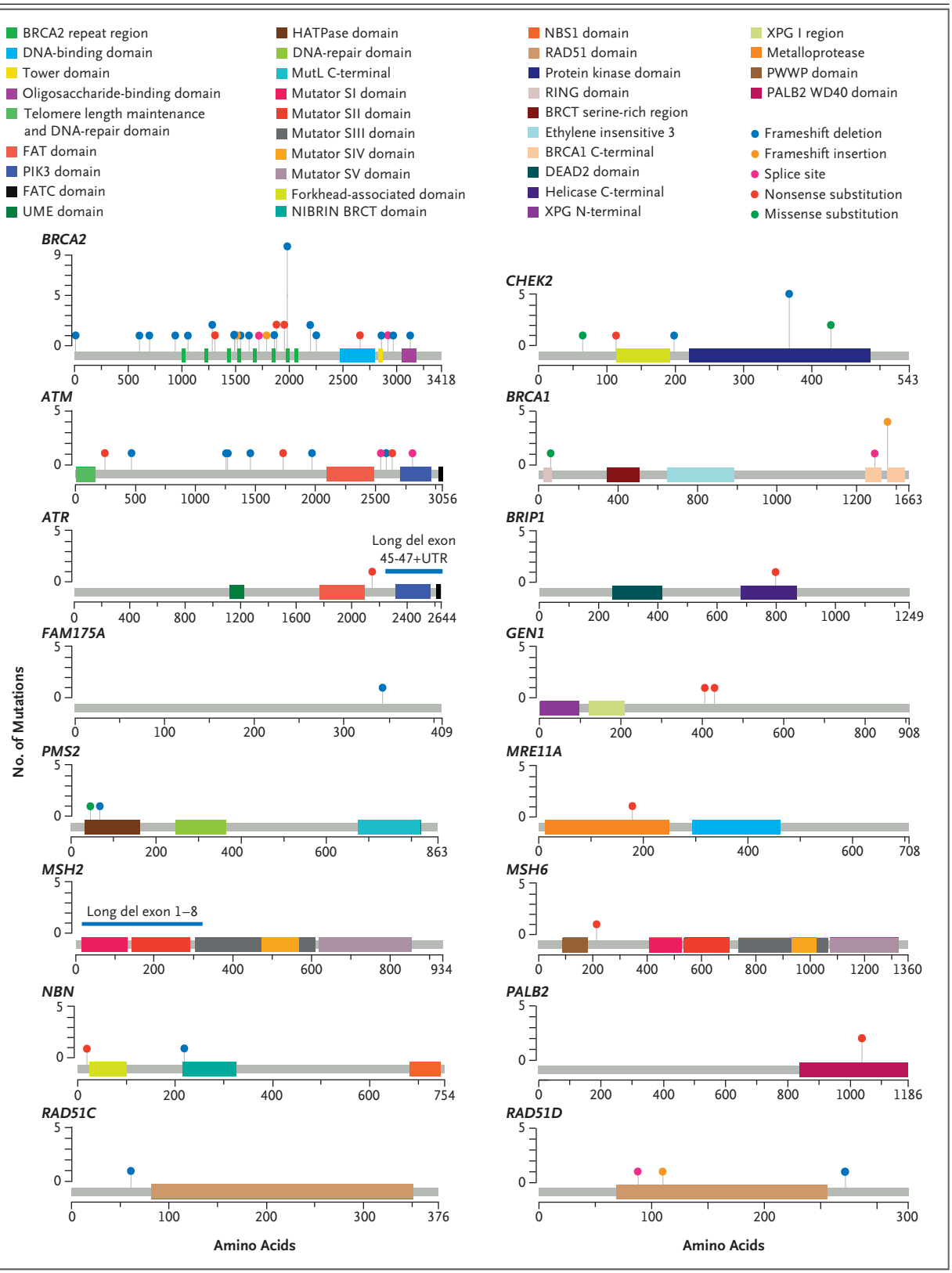

Figure 1 (facing page). Presumed Pathogenic Germline Mutations.

Locations of mutations and domains in proteins encoded by 16 predisposition genes are shown by lollipop structures, with the mutation type indicated by color. Protein domains are also distinguished by color. On the graph of each gene, the x axis reflects the number of amino acid residues, and the y axis represents the total number of mutations identified. Of the 20 genes analyzed, 4 (*BAP1*, *BARD1*, *MLH1*, and *XRCC2*) had no presumed pathogenic germline mutations.

60 versus 60 years of age or older (P=0.28) or non-Hispanic white versus other race (P=0.39).

GERMLINE MUTATIONS IN DNA-REPAIR GENES IN THE POPULATION

To estimate the population frequencies of germline mutations in DNA-repair genes, we analyzed exome data compiled from 53,105 persons included in the Exome Aggregation Consortium. We excluded data from persons with cancer who had been included in the Cancer Genome Atlas studies, the inclusion of which could have biased the comparisons with men with prostate cancer. The odds of any deleterious DNA-repair gene mutation being present in men with metastatic prostate cancer differed significantly from the odds in the Exome Aggregation Consortium population (odds ratio, 5.0; 95% CI, 3.9 to 6.3; P<0.001); a similar result was obtained when men from the previously reported Case Series 1 were excluded (odds ratio, 5.2; 95% CI, 4.0 to 6.8; P<0.001) (Table S5 in the Supplementary Appendix). The relative risk of mutations in individual DNA-repair genes among men with metastatic prostate cancer, as compared with men in the Exome Aggregation Consortium population, was substantial, ranging from 18.6 (95% CI, 13.2 to 25.3; P<0.001) for *BRCA2* to 3.1 (95% CI, 1.5 to 5.6; P=0.002) for *CHEK2* (Table 2).

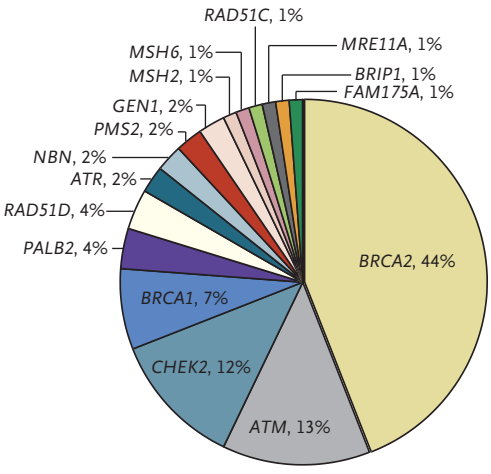

Figure 2. Distribution of Presumed Pathogenic Germline Mutations.

Shown are mutations involving 16 DNA-repair genes. Four genes did not have any pathogenic mutations identified and are not included in the distribution.

DISCUSSION

Inherited and acquired defects in DNA damage repair are key mechanisms in the genesis of malignant tumors. The detection of mutations in DNA-repair genes identifies persons and families who have a predisposition to cancer and defines cancer subtypes that have distinct vulnerabilities to specific therapeutics.[35] The ascertainment of germline mutations in DNA-repair genes in men with prostate cancer has several important clinical implications. First, the recent finding that pharmacologic inhibitors of PARP1 induce substantial objective responses in patients with metastatic prostate cancer expressing homologous recombination DNA-repair defects provides a clear treatment pathway in accordance with precision medicine strategies.[16] These tumors also appear to be responsive to platinum-based chemotherapy,[17] as has been documented for cancers of the ovary and breast in carriers of *BRCA1* and *BRCA2* mutations.[36,37] Second, the identification of a germline mutation in a DNA-repair gene provides information that is key to relatives, both male and female, and that can prompt "cascade" counseling to identify cancer predisposition and deploy risk-reduction strategies. Prospective studies assessing the prognostic and predictive significance of mutations in DNA-repair genes with regard to clinical outcomes are now needed to inform personalized care.

The significant family history of nonprostate cancers among men with mutations in DNA-repair genes was largely accounted for by breast, ovarian, and pancreatic cancers, in which mutations in DNA-repair pathways are known. The possible association between mutations in DNA-repair genes and familial hematologic and gas-

trointestinal cancers requires further analysis of cosegregation in affected kindreds. As observed for *BRCA1* and *BRCA2* in breast cancer, mutations may be found in persons who do not have a known syndromic history.[38,39] Thus, broader testing of patients with metastatic prostate cancer without regard to family history will increase the yield of actionable mutations identified, in a manner parallel to the recent inclusion of all patients with epithelial ovarian cancers for germline testing regardless of family history.[40]

This study has several limitations. First, although efforts were made to standardize DNA-sequencing analyses, direct comparability across institutions and with public data is not guaranteed. Second, we focused on clearly deleterious mutations in a selected set of DNA-repair genes; consequently, our findings may underestimate the true frequency of pathogenic events that influence the development of metastatic prostate cancer. Third, although patients across institutions and in the control populations were unselected for family history, possible bias cannot be ruled out. Finally, our case series and the Cancer Genome Atlas study include few persons who were older than 70 years of age at diagnosis, and the incidence of germline DNA-repair gene mutations may differ in this older age group.

In conclusion, the 11.8% overall frequency of germline aberrations in genes responsible for maintaining DNA integrity in men with metastatic prostate cancer is substantially higher than the 1.2 to 1.8% incidence of *BRCA2* mutations alone in localized prostate cancer[9,12] or the 7.3% incidence of mutations in 22 tumor-suppressor genes in familial prostate cancer.[14] Because the high frequency of DNA-repair gene mutations is not exclusive to an early-onset phenotype and is associated with clinically and histologically aggressive disease, with compelling evidence for therapeutic relevance, it may be of interest to routinely examine all men with metastatic prostate cancer for the presence of germline mutations in DNA-repair genes.

Supported by a Stand Up To Cancer–Prostate Cancer Foundation (SU2C-PCF) International Prostate Cancer Dream Team Translational Cancer Research Grant. Stand Up To Cancer is a program of the Entertainment Industry Foundation administered by the American Association for Cancer Research (SU2C-AACR-DT0712). The project was also supported by the following National Institutes of Health and Department of Defense awards: Prostate SPORE (grants P50CA097186 and P50CA92629, P30CA008748, PC131820, PC140799, R01CA116337, and 1K08CA188615) and the Prostate Cancer Foundation (Movember Challenge Awards). Drs. Beltran and Van Allen are supported by Damon Runyon Clinical Investigator Awards. Drs. Pritchard, Abida, Cheng, Schultz, and Van Allen are supported by Prostate Cancer Foundation Young Investigator Awards. Drs. Chinnaiyan and Sawyers are supported by the Howard Hughes Medical Research Institute. We also acknowledge funding from the Richard M. Lucas Foundation, the Institute for Prostate Cancer Research, Prostate Cancer UK and Movember to the London Prostate Cancer Centre of Excellence, the Starr Cancer Consortium (support to Drs. Beltran and Rubin), a Medical Research Council-Prostate Cancer UK Fellowship (to Dr. Mateo), an Experimental Cancer Medical Centre grant, a Biomedical Research Centre grant to the Institute of Cancer Research–Royal Marsden, the Andrew Sabin Family Foundation, the Marie-Josée and Henry R. Kravis Center for Molecular Oncology, and the Robert and Kate Niehaus Center for Inherited Cancer Genomics at Memorial Sloan Kettering Cancer Center.

Disclosure forms provided by the authors are available with the full text of this article at NEJM.org.

We thank the men who participated in this study for helping us to gain a better understand the role of genetic predisposition in advanced prostate cancer, the investigators and staff participating in the Stand Up to Cancer–Prostate Cancer Foundation International Prostate Cancer Dream Team, and the following persons at our respective institutions who helped with this study: Hiep Nguyen, Mary-Claire King, Barbara Norquist, Celestia Higano, Lawrence True, and Robert Vessella (University of Washington); Claudia Bertan, Susana Miranda, Penny Flohr, Roberta Ferraldeschi, Zsofia Kote-Jarai, Bindu Raobaikady, Ajit Sarvadikar, Dionne Alleyne, Lucy Hamilton, Sheena Vadgama, and Ada Balasopoulou (Institute for Cancer Research); Jacob Musinsky, Josh Armenia, Diana Mandelker, Maria Arcila, and David Hyman (Memorial Sloan Kettering Cancer Center); Xuhong Cao, Yi-Mi Wu, and Felix Feng (University of Michigan); Elizabeth Heath (Wayne State University); and Tuo Zhang (Weill Cornell Medical College). We also thank the Exome Aggregation Consortium and the groups that provided exome variant data for comparison; a full list of groups contributing to the Exome Aggregation Consortium can be found at http://exac.broadinstitute.org/about.

APPENDIX

The authors' full names and academic degrees are as follows: Colin C. Pritchard, M.D., Ph.D., Joaquin Mateo, M.D., Michael F. Walsh, M.D., Navonil De Sarkar, Ph.D., Wassim Abida, M.D., Ph.D., Himisha Beltran, M.D., Andrea Garofalo, B.Sc., Roman Gulati, M.Sc., Suzanne Carreira, Ph.D., Rosalind Eeles, M.D., Ph.D., Olivier Elemento, Ph.D., Mark A. Rubin, M.D., Dan Robinson, Ph.D., Robert Lonigro, Ph.D., Maha Hussain, M.D., Arul Chinnaiyan, M.D., Ph.D., Jake Vinson, B.Sc., Julie Filipenko, M.Sc., Levi Garraway, M.D., Ph.D., Mary-Ellen Taplin, M.D., Saud AlDubayan, M.D., G. Celine Han, Ph.D., Mallory Beightol, B.Sc., Colm Morrissey, Ph.D., Belinda Nghiem, B.Sc., Heather H. Cheng, M.D., Ph.D., Bruce Montgomery, M.D., Tom Walsh, Ph.D., Silvia Casadei, Ph.D., Michael Berger, Ph.D., Liying Zhang, M.D., Ph.D., Ahmet Zehir, Ph.D., Joseph Vijai, Ph.D., Howard I. Scher, M.D., Charles Sawyers, M.D., Nikolaus Schultz, Ph.D., Philip W. Kantoff, M.D., David Solit, M.D., Mark Robson, M.D., Eliezer M. Van Allen, M.D., Kenneth Offit, M.D., Johann de Bono, M.B., Ch.B., Ph.D., and Peter S. Nelson, M.D.

The authors' affiliations are as follows: the University of Washington (C.C.P., M. Beightol, C.M., B.N., H.H.C., B.M., T.W., S. Casadei, P.S.N.) and Fred Hutchinson Cancer Research Center (N.D.S., R.G., P.S.N.) — both in Seattle; the Institute of Cancer Research and Royal Marsden Hospital, London (J.M., S. Carreira, R.E., J.B.); Memorial Sloan Kettering Cancer Center (M.F.W., W.A., M. Berger, L.Z., A.Z.,

J. Vijai, H.I.S., C.S., N.S., P.W.K., D.S., M.R., K.O.), Weill Cornell Medical College (H.B., O.E., M.A.R.), and the Prostate Cancer Clinical Trials Consortium (J. Vinson, J.F.) — all in New York; the University of Michigan, Ann Arbor (D.R., R.L., M.H., A.C.); Howard Hughes Medical Institute, Chevy Chase, MD (A.C., C.S.); and Dana–Farber Cancer Institute, Boston (A.G., L.G., M.-E.T., S.A., G.C.H., E.M.V.A.).

REFERENCES

1. Albertsen PC, Hanley JA, Fine J. 20-Year outcomes following conservative management of clinically localized prostate cancer. JAMA 2005;293:2095-101.
2. Siegel RL, Miller KD, Jemal A. Cancer statistics, 2016. CA Cancer J Clin 2016;66:7-30.
3. Mucci LA, Hjelmborg JB, Harris JR, et al. Familial risk and heritability of cancer among twins in Nordic countries. JAMA 2016;315:68-76.
4. Amin Al Olama A, Kote-Jarai Z, Schumacher FR, et al. A meta-analysis of genome-wide association studies to identify prostate cancer susceptibility loci associated with aggressive and non-aggressive disease. Hum Mol Genet 2013;22:408-15.
5. Szulkin R, Karlsson R, Whitington T, et al. Genome-wide association study of prostate cancer-specific survival. Cancer Epidemiol Biomarkers Prev 2015;24:1796-800.
6. Helfand BT, Roehl KA, Cooper PR, et al. Associations of prostate cancer risk variants with disease aggressiveness: results of the NCI-SPORE Genetics Working Group analysis of 18,343 cases. Hum Genet 2015;134:439-50.
7. Berndt SI, Wang Z, Yeager M, et al. Two susceptibility loci identified for prostate cancer aggressiveness. Nat Commun 2015;6:6889.
8. Haraldsdottir S, Hampel H, Wei L, et al. Prostate cancer incidence in males with Lynch syndrome. Genet Med 2014;16:553-7.
9. Kote-Jarai Z, Leongamornlert D, Saunders E, et al. BRCA2 is a moderate penetrance gene contributing to young-onset prostate cancer: implications for genetic testing in prostate cancer patients. Br J Cancer 2011;105:1230-4.
10. Leongamornlert D, Mahmud N, Tymrakiewicz M, et al. Germline BRCA1 mutations increase prostate cancer risk. Br J Cancer 2012;106:1697-701.
11. Xu J, Lange EM, Lu L, et al. HOXB13 is a susceptibility gene for prostate cancer: results from the International Consortium for Prostate Cancer Genetics (ICPCG). Hum Genet 2013;132:5-14.
12. Gallagher DJ, Gaudet MM, Pal P, et al. Germline BRCA mutations denote a clinicopathologic subset of prostate cancer. Clin Cancer Res 2010;16:2115-21.
13. Castro E, Goh C, Olmos D, et al. Germline BRCA mutations are associated with higher risk of nodal involvement, distant metastasis, and poor survival outcomes in prostate cancer. J Clin Oncol 2013;31:1748-57.
14. Leongamornlert D, Saunders E, Dadaev T, et al. Frequent germline deleterious mutations in DNA repair genes in familial prostate cancer cases are associated with advanced disease. Br J Cancer 2014;110:1663-72.
15. Loeb S, Bjurlin MA, Nicholson J, et al. Overdiagnosis and overtreatment of prostate cancer. Eur Urol 2014;65:1046-55.
16. Mateo J, Carreira S, Sandhu S, et al. DNA-repair defects and olaparib in metastatic prostate cancer. N Engl J Med 2015;373:1697-708.
17. Cheng HH, Pritchard CC, Boyd T, Nelson PS, Montgomery B. Biallelic inactivation of BRCA2 in platinum-sensitive metastatic castration-resistant prostate cancer. Eur Urol 2016;69:992-5.
18. Robinson D, Van Allen EM, Wu YM, et al. Integrative clinical genomics of advanced prostate cancer. Cell 2015;161:1215-28.
19. Pritchard CC, Morrissey C, Kumar A, et al. Complex MSH2 and MSH6 mutations in hypermutated microsatellite unstable advanced prostate cancer. Nat Commun 2014;5:4988.
20. Pritchard CC, Smith C, Salipante SJ, et al. ColoSeq provides comprehensive Lynch and polyposis syndrome mutational analysis using massively parallel sequencing. J Mol Diagn 2012;14:357-66.
21. Pritchard CC, Salipante SJ, Koehler K, et al. Validation and implementation of targeted capture and sequencing for the detection of actionable mutation, copy number variation, and gene rearrangement in clinical cancer specimens. J Mol Diagn 2014;16:56-67.
22. Beltran H, Eng K, Mosquera JM, et al. Whole-exome sequencing of metastatic cancer and biomarkers of treatment response. JAMA Oncol 2015;1:466-74.
23. Schrader KA, Cheng DT, Joseph V, et al. Germline variants in targeted tumor sequencing using matched normal DNA. JAMA Oncol 2016;2:104-11.
24. Richards S, Aziz N, Bale S, et al. Standards and guidelines for the interpretation of sequence variants: a joint consensus recommendation of the American College of Medical Genetics and Genomics and the Association for Molecular Pathology. Genet Med 2015;17:405-24.
25. Cancer Genome Atlas Research Network. The molecular taxonomy of primary prostate cancer. Cell 2015;163:1011-25.
26. Shirts BH, Casadei S, Jacobson AL, et al. Improving performance of multigene panels for genomic analysis of cancer predisposition. Genet Med 2016 February 4 (Epub ahead of print).
27. Walsh T, Lee MK, Casadei S, et al. Detection of inherited mutations for breast and ovarian cancer using genomic capture and massively parallel sequencing. Proc Natl Acad Sci USA 2010;107:12629-33.
28. Zhang J, Walsh MF, Wu G, et al. Germline mutations in predisposition genes in pediatric cancer. N Engl J Med 2015;373:2336-46.
29. Tapia T, Smalley SV, Kohen P, et al. Promoter hypermethylation of BRCA1 correlates with absence of expression in hereditary breast cancer tumors. Epigenetics 2008;3:157-63.
30. Meeks HD, Song H, Michailidou K, et al. BRCA2 polymorphic stop codon K3326X and the risk of breast, prostate, and ovarian cancers. J Natl Cancer Inst 2016;108:108.
31. Wilt TJ, Brawer MK, Jones KM, et al. Radical prostatectomy versus observation for localized prostate cancer. N Engl J Med 2012;367:203-13.
32. Schröder FH, Hugosson J, Roobol MJ, et al. Screening and prostate-cancer mortality in a randomized European study. N Engl J Med 2009;360:1320-8.
33. Schröder FH, Hugosson J, Carlsson S, et al. Screening for prostate cancer decreases the risk of developing metastatic disease: findings from the European Randomized Study of Screening for Prostate Cancer (ERSPC). Eur Urol 2012;62:745-52.
34. Mohler JL, Armstrong AJ, Bahnson RR, et al. Prostate cancer, version 1.2016. J Natl Compr Canc Netw 2016;14:19-30.
35. Jeggo PA, Pearl LH, Carr AM. DNA repair, genome stability and cancer: a historical perspective. Nat Rev Cancer 2016;16:35-42.
36. Isakoff SJ, Mayer EL, He L, et al. TBCRC009: a multicenter phase II clinical trial of platinum monotherapy with biomarker assessment in metastatic triple-negative breast cancer. J Clin Oncol 2015;33:1902-9.
37. Alsop K, Fereday S, Meldrum C, et al. BRCA mutation frequency and patterns of treatment response in BRCA mutation-positive women with ovarian cancer: a report from the Australian Ovarian Cancer Study Group. J Clin Oncol 2012;30:2654-63.
38. King MC, Marks JH, Mandell JB. Breast and ovarian cancer risks due to inherited mutations in BRCA1 and BRCA2. Science 2003;302:643-6.
39. Weitzel JN, Lagos VI, Cullinane CA, et al. Limited family structure and BRCA gene mutation status in single cases of breast cancer. JAMA 2007;297:2587-95.
40. National Comprehensive Cancer Network. Genetic/familial high-risk assessment: breast and ovarian, version 2.2016. (https://www.nccn.org/professionals/physician_gls/pdf/genetics_screening.pdf).

nature medicine

Classification and characterization of microsatellite instability across 18 cancer types

Ronald J Hause[1], Colin C Pritchard[2], Jay Shendure[1,3] & Stephen J Salipante[2]

Microsatellite instability (MSI), the spontaneous loss or gain of nucleotides from repetitive DNA tracts, is a diagnostic phenotype for gastrointestinal, endometrial, and colorectal tumors, yet the landscape of instability events across a wider variety of cancer types remains poorly understood. To explore MSI across malignancies, we examined 5,930 cancer exomes from 18 cancer types at more than 200,000 microsatellite loci and constructed a genomic classifier for MSI. We identified MSI-positive tumors in 14 of the 18 cancer types. We also identified loci that were more likely to be unstable in particular cancer types, resulting in specific instability signatures that involved cancer-associated genes, suggesting that instability patterns reflect selective pressures and can potentially identify novel cancer drivers. We also observed a correlation between survival outcomes and the overall burden of unstable microsatellites, suggesting that MSI may be a continuous, rather than discrete, phenotype that is informative across cancer types. These analyses offer insight into conserved and cancer-specific properties of MSI and reveal opportunities for improved methods of clinical MSI diagnosis and cancer gene discovery.

MSI is a molecular tumor phenotype resulting from genomic hypermutability. The gain or loss of nucleotides from microsatellite tracts—DNA elements composed of short repeating motifs—is the diagnostic hallmark of MSI[1] and manifests as novel alleles of varying length[2]. These changes can arise from impairments in the mismatch repair (MMR) system, which limits correction of spontaneous mutations in repetitive DNA sequences[3,4]. MSI-affected tumors may, accordingly, result from mutational inactivation or epigenetic silencing of genes in the MMR pathway[2,3]. MSI is classically associated with colorectal cancers, for which it holds well-defined clinical implications[3]. However, MSI has been reported in diverse cancer types including endometrial, ovarian, gastric, and prostate cancer and glioblastoma[3,5,6]. Recent work suggests that MSI may be an actionable marker for immune-checkpoint-blockade therapy; clinical trials have demonstrated improved outcomes for patients with MSI-positive tumors treated with inhibitors of programmed cell death 1 (PD-1), presumably as a result of T lymphocyte recognition of neoantigens produced by somatic mutations[7,8]. However, mutations resulting from MSI can also drive oncogenesis, by inactivating tumor suppressor genes, for example[9]. These observations underscore the need for a more complete understanding of MSI.

MSI signatures may differ among cancer types; disparate loci may be preferentially unstable[5,10–14], MSI positivity may carry different prognostic values[11], and MSI may occur at different frequencies[5] across malignancies. However, these observations come from examination of dozens of loci in cohorts no larger than 100 individuals. Beyond limited studies restricted to four cancer types with established MSI phenotypes[10,15,16], variation in MSI among malignancies has not yet been evaluated systematically or on a genomic scale.

Molecular diagnosis of MSI is currently achieved by examining PCR products from a few (typically 5–7) informative microsatellite markers (MSI–PCR)[1,17]. Recently, our group and others[10,18–22] developed methods to infer MSI using massively parallel DNA-sequencing technologies, enabling interrogation of MSI with a breadth and quantitative precision not previously achievable. Here, we describe a robust approach for predicting MSI status independently of cancer type and use tumor exomes from the Cancer Genome Atlas (TCGA) Research Network to more comprehensively examine MSI across tumor types.

RESULTS

MSI classifier

From a total of 19,075,236 microsatellites computationally identified across the human genome, we included a subset of 516,876 loci (2.7%) that were within or adjacent to the exome capture baits used by TCGA, representing 95.9% of all coding microsatellites and 98.4% of microsatellites occupying splice sites (**Fig. 1a**,**b** and **Supplementary Table 1**). These loci were primarily mononucleotide repeats (**Supplementary Table 2**) and, as expected from our study design, fell disproportionately into intronic and coding regions compared to distributions observed genome-wide (**Fig. 1b** and **Supplementary Table 3**). Insufficient sequencing read depth precluded interrogation of all microsatellites for every specimen: 223,082 loci (43%) had sufficient coverage (≥30 reads) in both tumor and normal tissue for instability status to be inferred in at least half of the 5,930 total specimens.

For each locus we catalogued microsatellite allele lengths in tumor and patient-matched normal exomes (**Fig. 1c**, **Supplementary Fig. 1**, and **Supplementary Tables 4** and **5**) to identify and quantify MSI events. Using these instability calls, we designed a classifier to

[1]Department of Genome Sciences, University of Washington, Seattle, Washington, USA. [2]Department of Laboratory Medicine, University of Washington, Seattle, Washington, USA. [3]Howard Hughes Medical Institute, Seattle, Washington, USA. Correspondence should be addressed to S.J.S. (stevesal@uw.edu) or J.S. (shendure@uw.edu).

Received 3 May; accepted 29 August; published online 3 October 2016; doi:10.1038/nm.4191

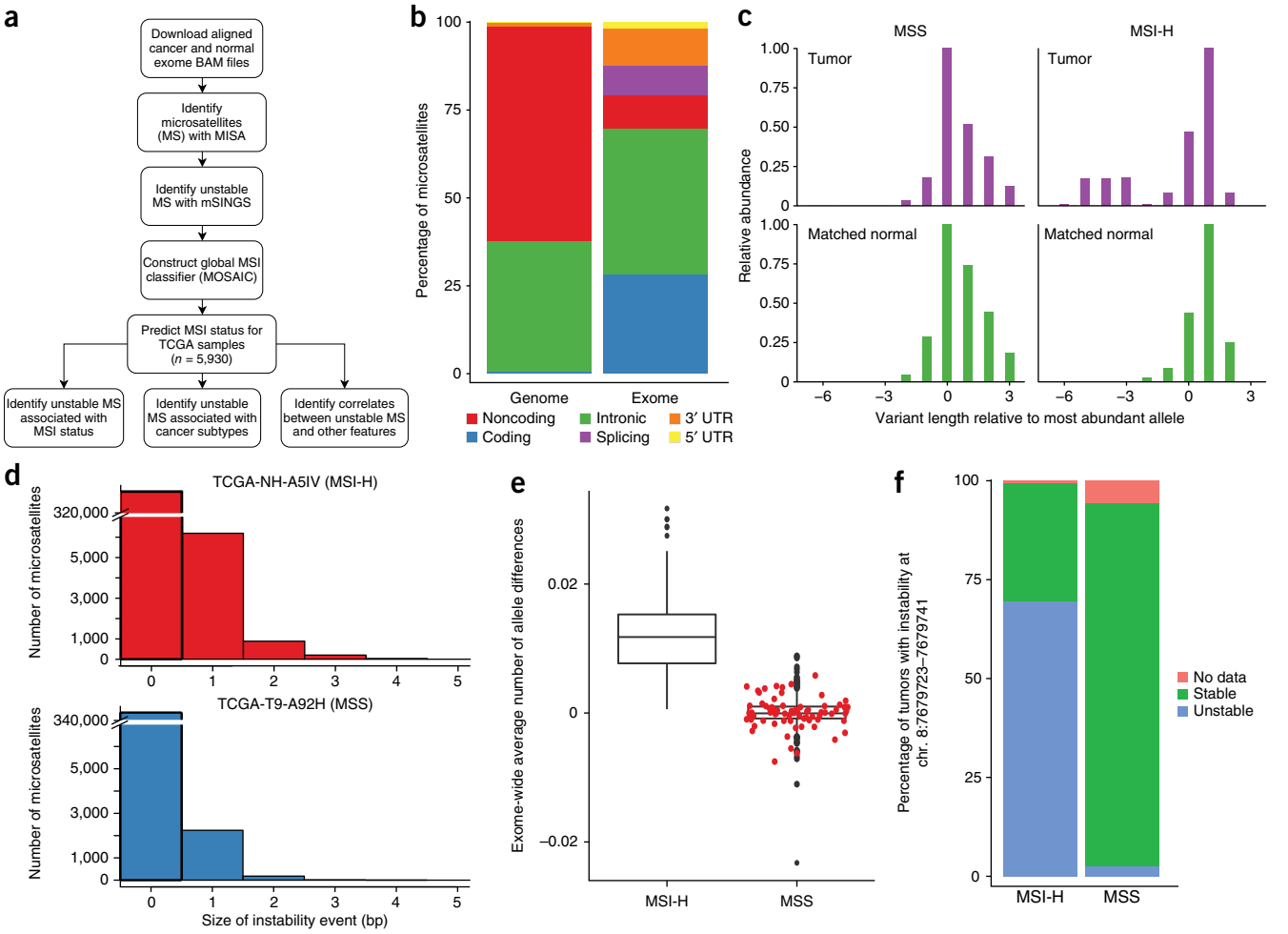

Figure 1 Evaluating MSI using exome-sequencing data. (**a**) Schematic of the approach used for analyzing MSI across TCGA exomes. MISA, microsatellite identification tool, mSINGS, microsatellite instability by next-generation sequencing. (**b**) Relative proportions of microsatellite loci within indicated genomic annotations across the whole genome and regions targeted by exome capture. Data represent computational identification and annotation of all microsatellites in the human reference genome and the subset within or immediately adjacent to TCGA exome capture baits. (**c**) Detection of MSI events from sequencing data. Representative virtual electropherograms[21] of a compound repeat at chr. 1:33145935–33145982 are illustrated for MSS and MSI-H cases, comparing the length and relative abundance of microsatellite alleles between tumors and patient-matched normal material. (**d**) Size of MSI events in representative MSI-H and MSS colon cancers. TCGA patient identifiers are indicated. (**e**) Correlation between MSI status (diagnosed using conventional clinical methods; MSI-H $n = 171$, MSS $n = 446$) and differences in global measurements of locus instability in tumor and paired normal specimens. Box boundaries indicate the interquartile range; center lines, medians; whiskers, values within 1.5 interquartile ranges of median; circles, extreme outliers. Red points represent MSI-L cancers ($n = 73$). (**f**) Proportion of MSI-H and MSS tumors with instability in a microsatellite locus located at chr. 8:7679723–7679741, within *DEFB105A/B*. This locus was the most significantly unstable microsatellite in MSI-H ($n = 171$) relative to MSS tumors ($n = 446$, $P = 2 \times 10^{-61}$, Fisher's exact test).

distinguish MSI-positive (MSI-high (MSI-H)) from MSI-negative (MSI-stable (MSS)) specimens independently of cancer type. Of all covariates tested across a cohort of colon, rectal, endometrial, and gastric tumors with available MSI–PCR results, the average total gain in the number of microsatellite alleles observed in a tumor relative to normal tissue across all microsatellite loci was the most significant feature separating MSI-H from MSS cancers (**Fig. 1d**,**e**; MSI-H median = 0.012, MSS median = -5.4×10^{-5}, $P = 9.4 \times 10^{-80}$, two-sided Wilcoxon rank-sum test). Related metrics, including the overall numbers of unstable microsatellites and variances in the allele number gain between tumor and normal, were also significantly different between MSI status groups (**Supplementary Fig. 2**; $P < 10^{-72}$, two-sided Wilcoxon rank-sum test). We also tested all microsatellite loci for discriminatory power to differentiate MSI-H from MSS samples and identified a locus within *DEFB105A* or *DEFB105B* (*DEFB105A/B*), chr. 8:7679723–7679741, as the most significantly unstable microsatellite in MSI-H tumors, as compared to MSS tumors (**Fig. 1f**; unstable in 119 of 171 MSI-H and 11 of 446 of MSS tumors, $P = 2 \times 10^{-61}$, two-sided Fisher's exact test). On the basis of these data, we created a parsimonious, weighted-tree microsatellite instability classifier (MOSAIC) for predicting MSI status using the most informative and independent features for classifying MSI—average gain of novel microsatellite alleles detected in a tumor specimen and, secondarily, locus instability within *DEFB105A/B* (**Supplementary Fig. 3a**). Incorporating additional covariates did not substantially improve the classifier (**Supplementary Fig. 3b**), nor did more sophisticated machine learning approaches. Compared with MSI–PCR, MOSAIC classified MSI-H from MSS cancers with 96.6% leave-one-sample-out cross-validation accuracy (95.8% sensitivity, 97.6% specificity) in a set of 617 specimens (128 MSS and 44 MSI-H for

colon; 63 MSS and 3 MSI-H for rectal; 169 MSS and 92 MSI-H for endometrial; 86 MSS and 32 MSI-H for stomach cancers). MOSAIC was discordant with clinical testing in classifying 11 of 171 MSI-H tumors (1 rectal and 10 endometrial) as MSS and 7 (1 rectal, 1 colon, and 5 endometrial) of 446 MSS cancers as MSI-H (**Supplementary Table 6**). Discordant classifications were primarily in endometrial cancers, which showed the smallest differences between MSI-H and MSS groups for all instability metrics measured. However, evidence suggests that many of these specimens were improperly classified by MSI–PCR: a review of accessory genetic and epigenetic data for somatic disruption of MSI-causative genes revealed that 7 of the 16 cases with complete metadata available were compatible with MOSAIC classifications but not MSI–PCR results (**Supplementary Table 6**). Furthermore, in terms of average number of gained microsatellite alleles and global burden of unstable microsatellites, discordant specimens were more consistent with MOSAIC classifications than with MSI–PCR testing (**Supplementary Fig. 4**).

Last, we evaluated whether differences in sequencing read depth between matched tumor and normal exomes or across microsatellite loci could confound our analysis. We observed no meaningful correlation between instability calls and these read depth metrics ($R^2 = 0.01$ and $\rho = -0.04$, respectively; **Supplementary Fig. 5**). Overall, these results demonstrate that we can accurately classify MSI status from tumor and matched-normal tissue exome-sequencing data.

Investigation of MSI-low phenotype

MSI-low (MSI-L) is a subcategory of MSI marked by instability at a minimal fraction of typed microsatellite markers. It is debated

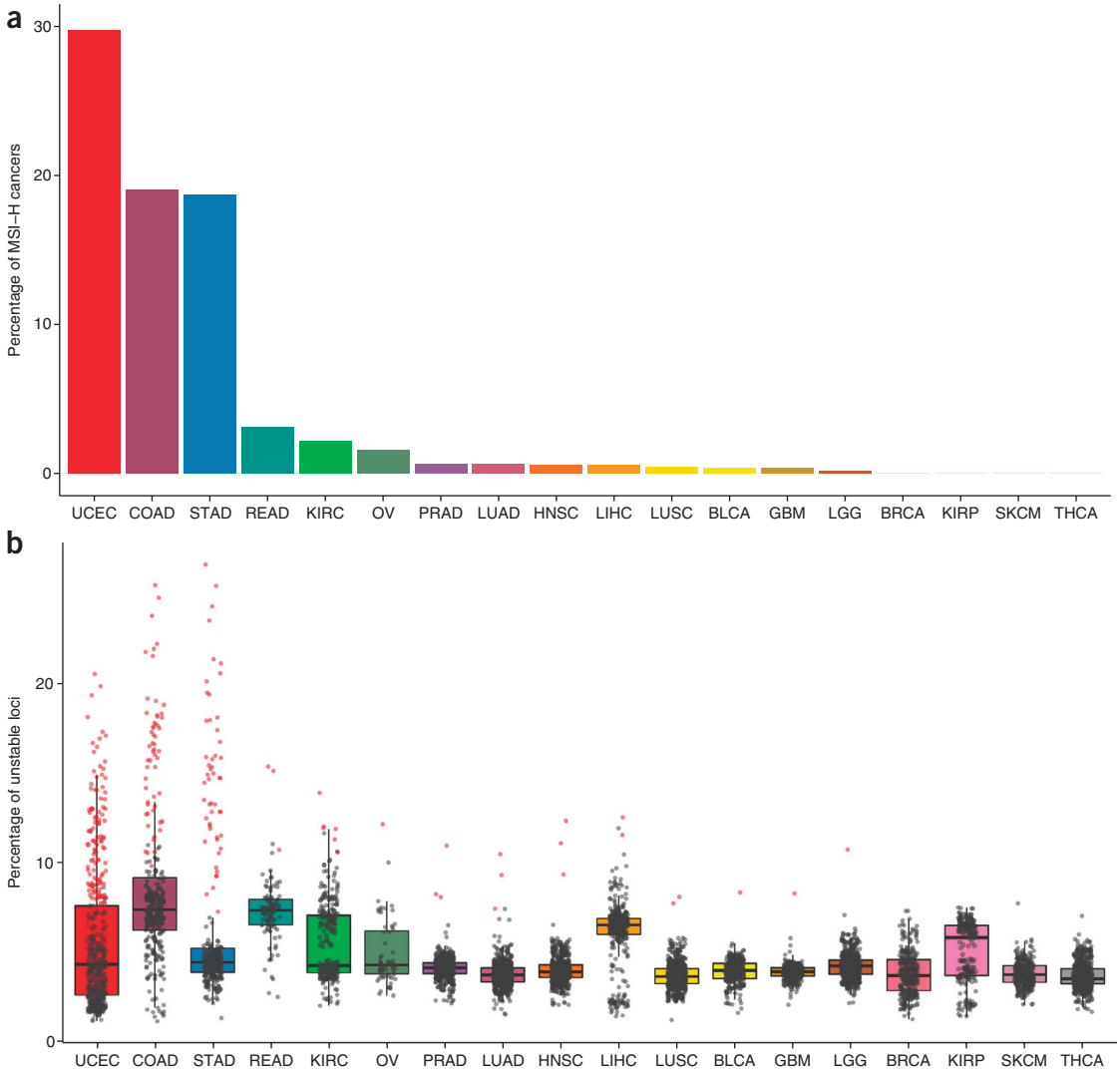

Figure 2 The landscape of MSI across TCGA exomes. (**a**) Inferred proportion of MSI-H tumors identified for each cancer cohort. (**b**) Distributions of the overall percentages of unstable microsatellite loci identified for each cancer type. Box boundaries indicate the interquartile range; center lines, medians; whiskers, values within 1.5 interquartile ranges of median. Overlaid points represent the number of unstable loci detected in individual tumor specimens; data for tumors classified as MSI-H are shown in red. UCEC, uterine corpus endometrial carcinoma ($n = 437$); COAD, colon adenocarcinoma ($n = 294$); STAD, stomach adenocarcinoma ($n = 278$); READ, rectal adenocarcinoma ($n = 96$); KIRC, kidney renal clear cell carcinoma ($n = 279$); OV, ovarian serous cystadenocarcinoma ($n = 63$); PRAD, prostate adenocarcinoma ($n = 463$); LUAD, lung adenocarcinoma ($n = 480$); HNSC, head and neck squamous cell carcinoma ($n = 506$); LIHC, liver hepatocellular carcinoma ($n = 338$); LUSC, lung squamous cell carcinoma ($n = 443$); BLCA, bladder urothelial carcinoma ($n = 253$); GBM, glioblastoma multiforme ($n = 262$); LGG, brain lower grade glioma ($n = 513$); BRCA, breast invasive carcinoma ($n = 266$); KIRP, kidney renal papillary cell carcinoma ($n = 207$); SKCM, skin cutaneous melanoma ($n = 268$); THCA, thyroid carcinoma ($n = 484$).

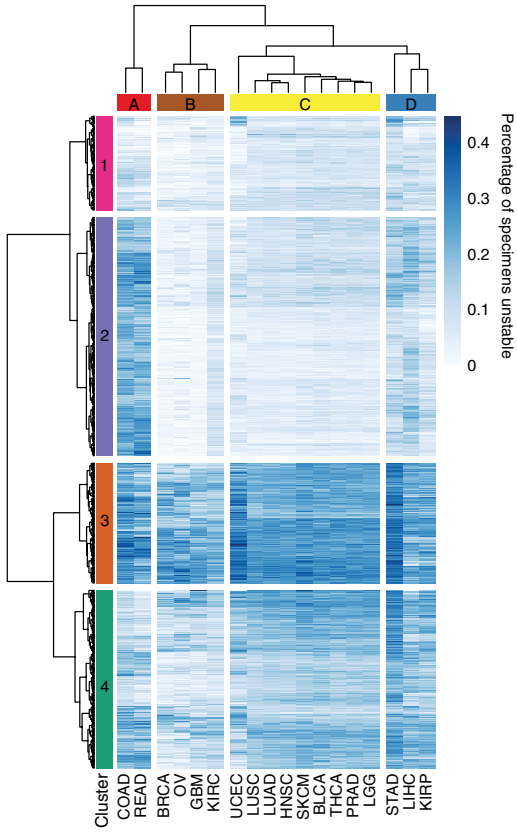

Figure 3 Cancer-specific signatures of MSI. Heatmap indicating the proportions of specimens within cancer types (columns) that were unstable at individual loci microsatellites (rows). Loci significant for differences among cancer types at FDR < 0.05 are shown. Colored microsatellite clusters (1–4, at left) denote groups of loci with similar instability trends based on Bayesian information criterion of the most likely model and number of clusters. Cancer types were also organized by hierarchical clustering into groups with similar patterns of MSI (A–D, top). UCEC, uterine corpus endometrial carcinoma; COAD, colon adenocarcinoma; STAD, stomach adenocarcinoma; READ, rectal adenocarcinoma; KIRC, kidney renal clear cell carcinoma; OV, ovarian serous cystadenocarcinoma; PRAD, prostate adenocarcinoma; LUAD, lung adenocarcinoma; HNSC, head and neck squamous cell carcinoma; LIHC, liver hepatocellular carcinoma; LUSC, lung squamous cell carcinoma; BLCA, bladder urothelial carcinoma; GBM, glioblastoma multiforme; LGG, brain lower grade glioma; BRCA, breast invasive carcinoma; KIRP, kidney renal papillary cell carcinoma; SKCM, skin cutaneous melanoma; THCA, thyroid carcinoma.

whether MSI-L is a distinct disease entity or an artifact of examining small numbers of loci through conventional MSI testing[23]. We therefore examined exome instability covariates in colon, rectal, endometrial, and stomach cancers clinically categorized as MSI-L. We observed no significant differences between MSI-L and MSS cancers in numbers of gained microsatellite alleles in tumor relative to normal tissue (P = 0.73, two-sided Wilcoxon rank-sum test), overall variation in allele number differences across all loci (P = 0.10), or total number of unstable microsatellites (P = 0.20; **Fig. 1f** and **Supplementary Fig. 2**). The lack of observable differences between these categories supports previous observations[10] and indicates that MSI-L tumors are consistent with MSS tumors in overall MSI burden. We reclassified MSI-L tumors as MSS for all subsequent analyses.

MSI status and landscape across different cancers

We broadly applied MOSAIC to assign MSI status for 5,930 tumor exomes from 18 cancer types (**Fig. 2a** and **Supplementary Tables 4** and **5**), enabling us to extend the analysis to 15 additional cancer types for which MSI status is not tested in clinical practice and to identify an additional 93 MSI-H samples. Cancer exomes contained a wide range of unstable microsatellites, from 87 to 9,032 (**Supplementary Table 5**). The average number of unstable sites varied considerably by cancer type, from a minimum of 765, for thyroid carcinomas, to a maximum of 2,315, for colon cancers. Similarly, the fraction of inferred MSI-H tumors also varied. The highest proportion of MSI-H cases occurred in cancer types that classically demonstrate MSI: endometrial (30%), colon (19%), and gastric (19%). Rectal cancers had a lower prevalence of MSI-H specimens (3%). Still lower, but detectable, frequencies of MSI-H were observed in 12 other cancer types; collectively, one or more individual MSI-H tumors were identified in 16 of the 18 cancer types examined. For several cancer types, including kidney papillary, kidney clear cell, and liver hepatocellular carcinomas, we observed a bimodal distribution in the proportion of unstable microsatellites for cancers classified as MSS (**Fig. 2b**), indicating trends in instability rates within MSI classifications.

As anticipated, we observed a strong correlation between predicted MSI status and the occurrence of somatic mutations or epigenetic silencing in MMR-pathway and DNA proofreading genes (odds ratio (OR) = 13.7 for having a somatic mutation in MSI-H malignancies compared with MSS, $P = 6 \times 10^{-64}$; **Supplementary Table 7**). Notably, these somatic alterations did not predict MSI-H status with high accuracy, suggesting contributions of additional factors to MSI. Despite the well-established role of mismatch repair gene *MLH1* silencing in MSI-H tumors[1], 8 of 98 tumors with *MLH1* silencing were classified as MSS by both MOSAIC and MSI–PCR.

To provide a more comprehensive view of the MSI landscape within and across cancer types, we next examined global patterns of microsatellite mutation using instability calls for individual loci. We included all specimens, irrespective of inferred MSI status, and restricted analysis to 92,385 microsatellites that were called in at least half of the samples across each of the 18 cancer types (**Supplementary Table 8**). No instability was observed at 57.4% of loci in any tumor. Of the sites that were unstable in at least 5% of specimens, hierarchical clustering distinguished four major groups (A–D) of cancer types having similar signatures of MSI (**Fig. 3**). Cancers that are canonically affected by MSI were distributed between three different groups: colon and rectal cancers exclusively comprised group A, whereas stomach cancers were placed in a separate category with liver hepatocellular and kidney renal carcinoma (D), and endometrial tumors were separately grouped with multiple other cancer types (C). Other malignancies, representing those with lower or no inferred incidences of MSI-H, were distributed among three groups (B, C, and D) but were disproportionately allocated to group C. All cancer types, including those entirely comprising MSS tumors, showed high frequencies of instability events at particular loci or groups of similarly mutated loci. The microsatellite loci were also partitioned by hierarchical clustering into four major divisions (1–4) that showed similar rates of instability across cancer groups (**Fig. 3**). We examined enrichment of gene ontologies and KEGG pathway annotations of factors harboring unstable microsatellites in each division and noted differences (**Supplementary Fig. 6** and **Supplementary Table 9**) but observed no obvious patterns of biological function.

Differences between MSS and MSI-H cancers

Because MSS tumors have a low baseline level of MSI[24], we examined whether MSS tumors mutate at the same loci as tissue-matched MSI-H tumors by comparing their relative frequencies of instability events at each microsatellite. For sufficient numbers, we focused on the four cancer types with the highest incidence of MSI-H samples (colon, rectal, endometrial, and stomach). Although both the frequency of instability events and the number of alternative microsatellite alleles were significantly elevated in MSI-H tumors, they tended to occur at the same loci that were unstable at lower frequencies in MSS cases (**Fig. 4a**,**b**); we observed a correlation between the frequency of MSI events in MSI-H and MSS malignancies of the same

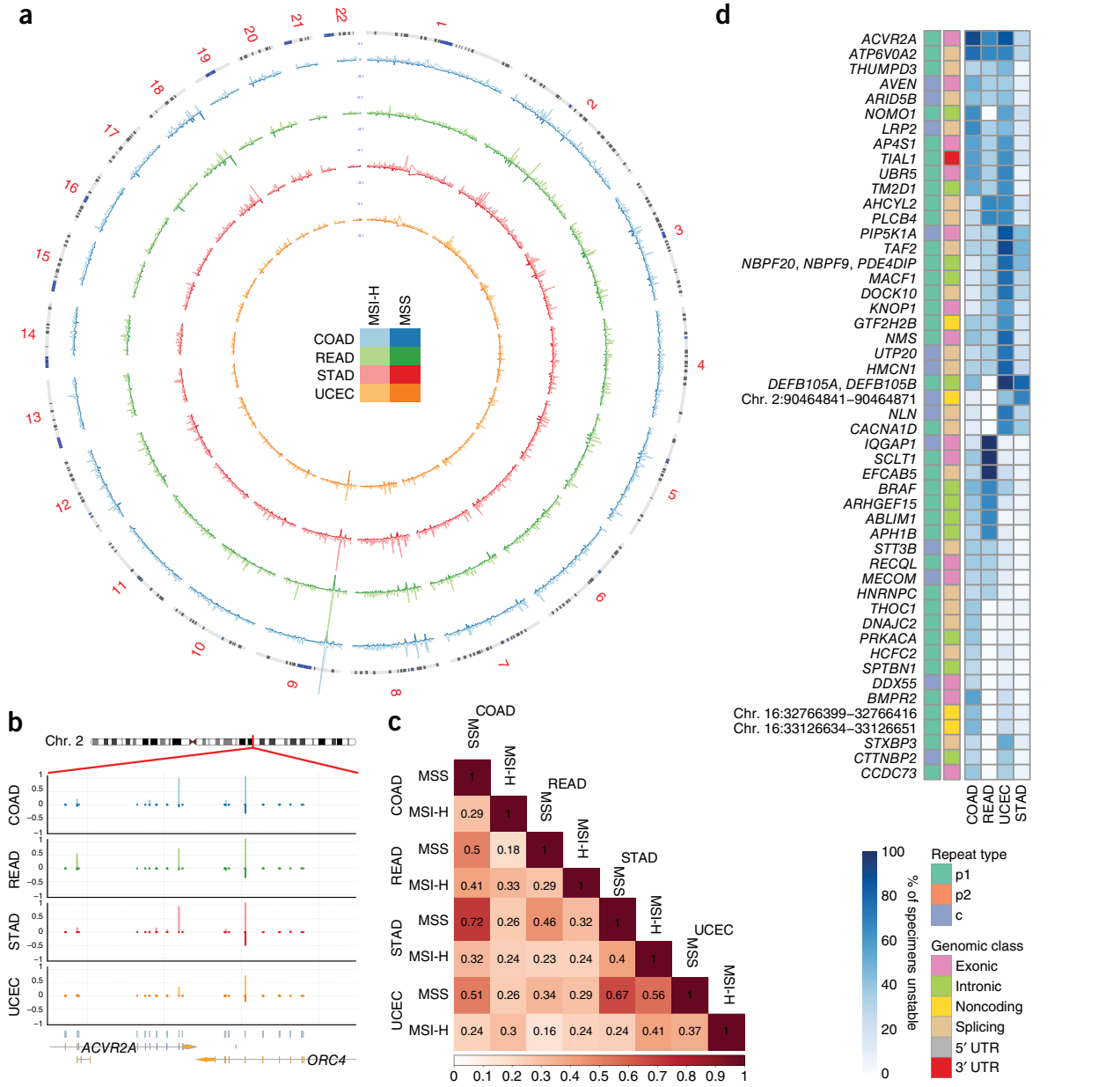

Figure 4 Signatures of MSI in MSI-H tumors. (**a**) Circos plot representing differences in the proportion of MSS and MSI-H tumors with instability at microsatellite loci across the genome. External ring denotes chromosomal position; internal rings indicate the average proportion of cancers with microsatellite locus instability for markers integrated across 1-Mb windows. For each cancer type, the proportion of tumors with instability within each window is indicated by the height of the trace, with MSI-H and MSS tumors for each cancer type plotted separately on different sides of the axis (positive and negative, respectively). The large peak on chromosome 9 reflects a single microsatellite in an intergenic region between *LINGO1* and *LOC401497* that was frequently unstable in both MSI-H and MSS cancers. (**b**) Representative region of chromosome 2 demonstrating differences in MSI profiles between MSI-H and MSS tumors and differences among MSI-H cancer types. The proportion of tumors with locus instability at each locus is indicated as in **a**. (**c**) Cosine similarity matrix comparing the sets of microsatellites unstable in at least half of tumors in each cancer subtype (stratified by MSI status and cancer type). (**d**) Heatmap indicating the proportion of specimens within MSI-H cancer types affected (columns) at the top 50 most differentially unstable microsatellite loci (rows). All loci were significant at FDR < 10^{-5}. For each microsatellite, repeat type and genomic annotation are indicated. p1, mononucleotide repeat; p2, dinucleotide repeat; c, compound repeat. UCEC, uterine corpus endometrial carcinoma (n = 437); COAD, colon adenocarcinoma (n = 294); STAD, stomach adenocarcinoma (n = 278); READ, rectal adenocarcinoma (n = 96).

Table 1 Ten most significant loci associated with MSI-H cancers

Locus coordinates	Proportion unstable (MSI-H)	Proportion unstable (MSS)	*P* value	*Q* value	OR	Genomic class	Gene(s)	Repeat sequence
Chr. 8:7679723–7679741	190/263 (72%)	173/5626 (3%)	9.19×10^{-191}	1.88×10^{-185}	81.76	Intronic	*DEFB105A*, *DEFB105B*	(A)9
Chr. 2:148683681–148683698	134/253 (52%)	30/5504 (<1%)	1.97×10^{-168}	2.02×10^{-163}	203.24	Coding	*ACVR2A*[a]	(A)8
Chr. 8:7346862–7346880	188/263 (71%)	274/5625 (4%)	3.55×10^{-161}	2.42×10^{-156}	48.849	Intronic	*DEFB105A*, *DEFB105B*	(T)9
Chr. 17:56435156–56435172	112/243 (46%)	10/5557 (<1%)	6.86×10^{-154}	3.51×10^{-149}	471.32	Coding	*RNF43*[a]	(C)7
Chr. 3:51417599–51417615	109/233 (46%)	24/4824 (<1%)	3.55×10^{-133}	1.46×10^{-128}	174.42	Coding	*DOCK3*[a]	(C)7
Chr. 7:74608736–74608758	230/257 (89%)	873/4882 (17%)	3.17×10^{-129}	1.08×10^{-124}	39.1	ncRNA Intronic	*GTF2IP1*, *LOC100093631*	(T)13
Chr. 11:120350632–120350654	104/264 (39%)	29/5579 (<1%)	1.31×10^{-121}	3.82×10^{-117}	124.15	Intronic	*ARHGEF12*[a]	(T)8(C)5
Chr. 16:14983087–14983105	100/264 (37%)	25/5643 (<1%)	5.99×10^{-119}	1.53×10^{-114}	136.12	Intronic	*NOMO1*[a]	(A)9
Chr. 1:151196698–151196722	127/264 (48%)	110/5643 (1%)	6.84×10^{-119}	1.56×10^{-114}	46.56	Coding	*PIP5K1A*[a]	(T)9(C)6
Chr. 1:200594037–200594054	98/250 (39%)	23/5249 (<1%)	2.89×10^{-117}	5.91×10^{-113}	145.57	Intergenic	*KIF14*[a] (dist. = 4,175 bp), *DDX59* (dist. = 19,111 bp)	(T)8

Dist., distance from microsatellite to indicated gene.
[a]Gene is implicated in oncogenesis (**Supplementary Table 12**).

cancer type and also across types (ρ = 0.28–0.53), indicating related instability patterns within and across malignancies. A representative example is provided by two loci in neighboring genes *ACVR2A* (chr. 2:148683681–148683698) and *ORC4* (chr. 2:148701095–148701119) (**Fig. 4b**). *ACVR2A* contains a coding mononucleotide microsatellite that is unstable in 28–90% of MSI-H samples (**Supplementary Table 10**), depending on the cancer type, but in only 0–6% of MSS cancers. *ORC4* harbors a mononucleotide repeat in a splicing region that is also unstable in 67–100% of MSI-H tumors but in only 19–44% of MSS samples.

To examine differences between MSS and MSI-H categories, we focused on microsatellites that were unstable in at least 25% of the samples within each cancer subtype and typable in all specimens. We computed cosine similarities between sets of all frequently unstable sites between each group (**Fig. 4c**). Colon, rectal, gastric, and endometrial MSI-H cancers intersected at a large fraction of their frequently unstable microsatellites, with tissue-matched MSS cancers sharing a smaller subset of those loci. MSS tumors from different tumor types showed substantially less overlap. Taken together, these findings indicate that MSI patterns in tissue-matched MSI-H and MSS cancers are related and follow consistent patterns, but MSI-H cancers share overall similarities in their most frequently unstable sites.

Differences among MSI-H cancers

To compare MSI among different MSI-H cancer types, we examined only cancer types with the highest MSI-H prevalence to lend sufficient power for statistically meaningful comparisons. As was observed for the entire collection of specimens (**Fig. 3**), separate MSI-H cancer types showed individualized signatures of instability at a subset of microsatellite loci (**Fig. 4d**). In total, 2,685 of the 3,296 microsatellites unstable in at least 5% of MSI-H cancers were differentially unstable in at least one cancer type at an FDR < 0.05 (**Supplementary Table 10**). These differentially unstable microsatellites included several in *NIPBL*, *TCF4*, and *PTEN*, among other genes reported as mutational targets of MSI[25,26]. An example is again provided by the microsatellites in *ACVR2A* and *ORC4* (**Fig. 4b**): the former was unstable in 90% of colon, 67% of rectal, and 87% of stomach MSI-H tumors, but only 28% of endometrial MSI-H tumors, and the latter was unstable in 97% of colon, 67% of endometrial, and 100% of rectal and stomach MSI-H tumors investigated.

To explore the functional consequences of different instability signatures among MSI-H cancer types, we examined factors that were uniquely unstable in one cancer type (**Supplementary Fig. 7**). Uniquely unstable factors in colon and rectal cancers shared overlap in multiple aggregated functional categories, although cancer-type-specific differences were observed among assorted cellular functions. Stomach adenocarcinomas were uniquely and highly enriched for instability in ion-binding genes while demonstrating instability in several categories frequently observed for MSI-H colon and rectal tumors. Endometrial cancers were exclusively enriched for uniquely unstable sites in protein complex binding genes, without overlap in categories identified for other cancer types, although the small number of endometrial-cancer-specific unstable sites limited our power for ascertaining such ontological enrichments.

Properties of unstable microsatellites

We investigated features associated with unstable loci by associating various intrinsic properties, annotations, and metrics with the likelihood of locus instability. After stratifying by repeat composition and MSI status, we found compound microsatellites to be more preferentially unstable than other repeat types, with 11.7% and 5.3% of those loci unstable in more than 20% of MSI-H and MSS samples, respectively (**Supplementary Fig. 8a**). Intrinsic length of the microsatellite tract had bearing on instability frequency, with a maximum occurring around 16 repeat units in length (**Supplementary Fig. 8b**). When loci were stratified by their genomic annotations (**Supplementary Fig. 8c**), microsatellites in coding regions were less likely to be unstable in at least one sample (OR = 0.87, $P = 2.3 \times 10^{-57}$). By contrast, microsatellites in splice sites were more likely to be unstable (OR = 1.37, $P = 2.2 \times 10^{-82}$). We compared primary sequence enrichments of microsatellites unstable in at least one cancer (**Supplementary Fig. 8d**) and observed no significant differences among MSI-H cancer types (**Supplementary Fig. 9a**). However, CA and GA dinucleotide repeats were the most likely to be unstable overall. We also observed variability in the likelihood of instability at CpG sites, which probably reflects their functional importance in gene regulation. We observed significant enrichments for instability at DNase hypersensitivity sites ($P = 0.01$), conserved transcription factor binding sites ($P = 3 \times 10^{-6}$), and evolutionarily conserved genomic regions ($P = 6 \times 10^{-9}$; **Supplementary Fig. 9b**). Last, we tested for a correlation between the average frequency of locus instability within 1-Mb windows across individuals and DNA replication timing[10,27] but found no significant associations (**Supplementary Fig. 9c**).

Unstable microsatellites in cancer-associated genes

To identify elements common to a generalizable MSI-H signature across cancer types, we tested for loci that were significantly more

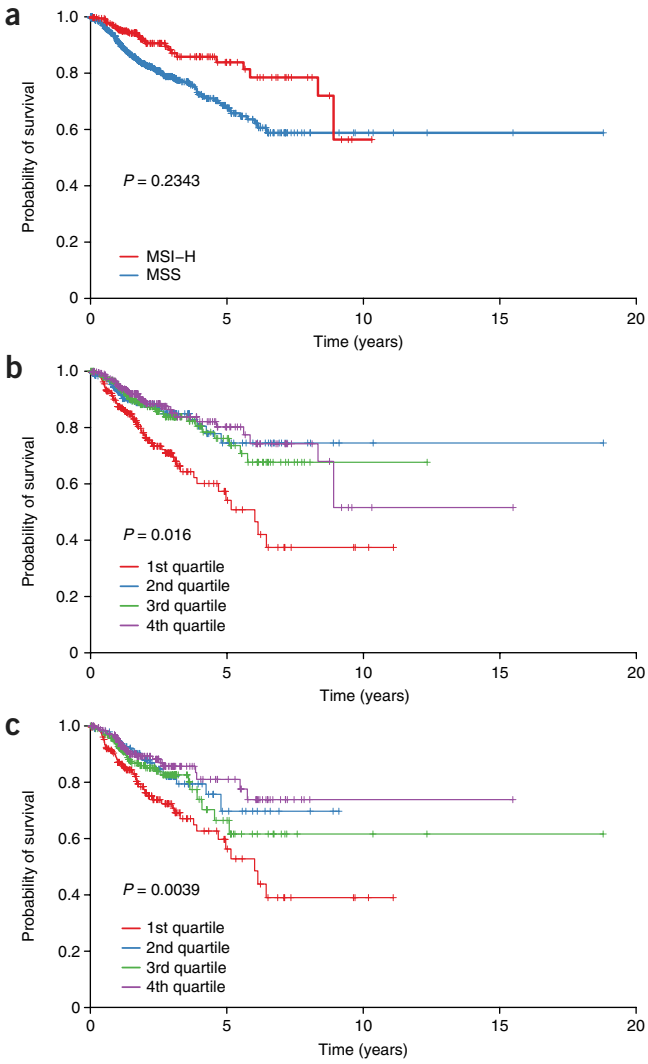

Figure 5 Global MSI load and patient survival. (**a**) Patient survival aggregated for endometrial, stomach, colon, and rectal cancers, stratified by inferred MSI status (MSS $n = 864$, MSI-H $n = 241$). (**b**) Patient survival for the same tumors in **a** as a function of the proportion of unstable microsatellites detected, grouped by quartile. (**c**) Patient survival for MSS cancers from **a**, grouped by quartile. *P* values in **b** and **c** represent the significance of the continuous variable of the proportion of unstable microsatellites per sample as determined from likelihood ratio tests. Significance in all panels was assessed after correcting for age, sex, radiation therapy status, and cancer type.

likely to be unstable in all MSI-H tumors ($n = 264$) than in all MSS cancers ($n = 5{,}666$). Of the 204,797 microsatellites with sufficient coverage to be called in at least half of MSI-H and MSS samples across cancer types, 17,564 sites within 6,882 unique genes were significant at an FDR < 0.05 (**Supplementary Fig. 8e** and **Supplementary Table 11**), indicating that a subset of markers are reliably unstable across cancer types and may represent common genomic lesions in MSI-H malignancies.

We noted that many recurrently unstable loci in MSI-H tumors (**Table 1**) involved cancer-associated genes, including coding regions in tumor suppressor genes *ACVR2A* and *RNF43*, which are frequent and validated targets of mutation in MSI-H cancers[28,29]. We explored a possible correlation of instability events with occurrence in genes participating in oncogenic pathways[9]. Using permutation testing, we tested whether recurrently unstable loci (**Supplementary Table 10**) were more likely to occur in genes registered in the COSMIC cancer gene census[30] and observed that microsatellites located in genes with known involvement in oncogenesis were significantly more likely to be unstable (**Supplementary Fig. 8f**; OR = 1.51, $P < 10^{-4}$). Moreover, a review of the literature for the genes harboring or proximal to the top 100 most significantly mutated loci in MSI-H cancers showed that 58 are in or near genes with previously established cancer-related biological functions (**Supplementary Table 12**). Furthermore, 25 of 27 known recurrent mutational targets of colorectal cancer MSI[26] examined in our study contained loci that were significantly unstable in MSI-H relative to MSS samples at an FDR < 0.05 ($P = 5 \times 10^{-9}$).

Patient survival and MSI burden

MSI-H status is associated with modestly improved patient survival in colorectal cancers[31]. We therefore examined whether there was a general correlation between MSI-H classification and survival outcome across cancer types, after correcting for covariates. We observed a weak association between MSI status and survival outcome when considering in aggregate the four cancer types with the highest incidence of MSI-H ($P = 0.23$, hazard ratio (HR) for MSI-H = 0.79; **Fig. 5a**). We next evaluated whether the global burden of unstable microsatellites would correlate with survival when treated as a continuous variable independently of MSI status and observed a stronger, more significant positive correlation with survival ($P = 0.02$, HR per increase of 100 unstable sites = 0.984; **Fig. 5b**). Given that MSI-H samples showed, on average, approximately 2,100 more unstable sites than MSS samples, this would equate to a HR of 0.72 for MSI-H. Furthermore, the association between the number of unstable sites and patient survival was more pronounced in MSS samples alone ($P = 0.004$, HR per increase of 100 unstable sites = 0.959; **Fig. 5c**). This observation led us to question whether the metric would also be prognostic of patient outcome in cancer types for which MSI is not typically evaluated. Although no significant effect was observed when cancer types were examined in aggregate, for individual cancer types we observed positive trends between prognosis and instability burden in uterine, endometrial, rectal, colon, stomach, and thyroid cancer and lower-grade glioma (**Supplementary Fig. 10**). Limited sample sizes for each cancer type restrict power for establishing the significance of these trends.

Last, we tested whether MSI was high in cancers that had progressed by quantifying instability events in primary and metastatic tumors within cancer types. We examined cancers for which multiple patient samples from metastatic disease were available, including seven patient-matched metastatic and primary breast tumors, seven patient-matched metastatic and primary thyroid tumors, and six primary and 174 metastatic melanoma cases from unrelated patients. All were MSS. The fractions of unstable loci were not significantly different between metastatic and primary tumors (median percentage unstable for each group = 0.37%, $P = 0.13$, nested ANOVA; **Supplementary Fig. 11**), which suggests that MSI is not associated with likelihood of metastasis, although additional samples will be necessary to substantiate this observation.

DISCUSSION

To explore the landscape of MSI in different cancers, we developed MOSAIC for ascertaining MSI status from tumor–normal tissue pairs examined with exome-sequencing data. Our approach leverages the observation that MSS tumors have a lower baseline level of instability

events than MSI-H tumors, which enables MSI classifications to be distinguished on the basis of global MSI calls. MOSAIC corrects for class imbalance in its cross-validation training procedure (an approximately 3:1 MSS-to-MSI-H ratio), allowing predictions in new cancer types to be made without prior assumption about the expected prevalence of MSI-H tumors. Although we noted a few discrepancies between our classifier and conventional MSI typing, genomic data suggest that these represent false positive and false negative outcomes from clinical typing[32,33] and that discordant results are more consistent with MOSAIC classifications.

Most cancer types examined (14 of 18) included one or more MSI-H representatives, suggesting that MSI may be a generalized cancer phenotype. The identification of infrequently occurring MSI-H tumors from cancer types conventionally associated with MSI confirms published reports[6,34–40]. Notably, most cancer types, even those for which there were few or no examples with the MSI-H phenotype in our cohort, showed a high frequency of MSI at restricted subsets of loci. This observation raises the possibility that findings[41] of MSI in some cancer types may reflect artifacts from typing local mutational hot spots by conventional methods rather than a global instability phenotype.

Microsatellite mutations occurring within the coding regions, introns, or untranslated regions of genes may positively or negatively influence gene expression or protein function by affecting changes in transcription or gene splicing[9,15,42–44]. We observed a depletion of unstable microsatellites in exons, transcription factor binding sites, and evolutionarily conserved genomic regions, consistent with purifying selection against mutations with biologically functional consequences[10]. Nevertheless, regulatory alterations for some targets may confer selective growth advantages to cancer cells, and unstable microsatellite loci have been speculated to fall within genes implicated in oncogenesis and to participate in the evolution of MSI-H cancers[9,13,14,16,45–47]. For unstable microsatellites observed in genic regions, our data support the idea that they preferentially accumulate in genes involved in carcinogenesis or tumor survival and therefore probably serve as drivers of cancer evolution. Differences in patterns of MSI among cancer types may consequently reflect different positive and negative selective pressures experienced during carcinogenesis. We observed that frequently unstable microsatellites in MSI-H malignancies are preferentially located in known cancer-associated genes, supporting this view and suggesting that there may be an underappreciated contribution of MSI in generating cancer-driving mutations. Moreover, roughly half of unstable microsatellites fall within genes not previously reported to be involved in cancer, including several intergenic loci, raising the possibility that these microsatellites also function as cancer drivers. Although functionally evaluating newly implicated factors is outside the scope of this work, many of the differences between MSS and MSI-H tumors are pronounced, and these data illustrate the utility of microsatellite analysis of exome-sequencing data as a primary approach for identifying cancer-relevant genes. Identification of features that are recurrently affected by MSI is complementary to methods that highlight genes on the basis of their recurrent somatic coding sequence mutations[48].

Although differences in selection during carcinogenesis may account for much of the variability in instability rates observed among microsatellite markers, we also observed significant correlations with more generalized properties of the loci themselves. We observed a weak but significant correlation between elevated MSI rates and loci occupying DNase-hypersensitivity sites, supporting earlier work[10] and indicating that instability events are enriched within euchromatic regions. Other factors, including repeat composition and locus length, affected instability[44]. It is likely that local nucleotide sequence or secondary structure surrounding repeats also define the inherent instability of a locus[44,49].

Consistent with other genomic studies[10,21], we found no evidence that tumors classified as MSI-L are a distinct disease group. This conclusion supports the view that MSI-L is a technical artifact reflecting a low background frequency of MSI in tumors with intact MMR systems[1,24]. Nevertheless, specimens in our study spanned a continuum of observed instability, and, at their extremes, tumors classified as MSI-H and MSS showed some overlap in their overall burden of unstable microsatellites. In general, we observed that the number of unstable microsatellite loci in a tumor exome correlated with patient survival when considered as a continuous metric better than conventional MSI-H or MSS classification alone. This result may reflect a link between MSI events and the production of cancer neoantigens that can be recognized as 'non-self' by the immune system[7,50]. Although the effect sizes we observed were smaller because of our limited cohort sizes, they are consistent with values reported in larger cohorts[31]. These findings suggest that, when sufficient numbers of loci are considered, the MSI phenotype may be a more continuous phenotype than previously appreciated—indeed, the global burden of MSI within MSS samples alone was prognostic of patient outcome. Because this continuous distribution of global instability is more indicative of patient survival independently of conventional MSI classification, it may prove more informative in the clinical management and treatment of cancer[7].

The existence of cancer-specific MSI landscapes and the potential predictive power of MSI as a continuous metric have implications for the molecular diagnosis of MSI in clinical practice: because current assays are optimized for the detection of MSI in colon and rectal cancers[17], they may not detect instability events effectively, or at all, in other cancer types. The behavior of any particular microsatellite locus can vary greatly across cancers, and loci that are inherently stable in one cancer type may be frequently mutated in another. Because MOSAIC for genome-scale MSI classification is more comprehensive and less prone to cancer-type-specific biases, it may serve as a better clinical strategy for pan-cancer MSI determination and ascertainment of instability burden.

Microsatellites are preferentially located in noncoding regions of the genome, and we anticipate that the future availability of more cancer whole-genome sequences will provide an improved understanding of the overall genomic landscape of MSI in different malignancies. As suggested by our study, such data may implicate novel, noncoding oncogenic motifs that affect gene regulation and will yield further insights into potentially important genomic sites involved in carcinogenesis.

METHODS

Methods and any associated references are available in the online version of the paper.

Note: Any Supplementary Information and Source Data files are available in the online version of the paper.

ACKNOWLEDGMENTS

We thank A. McKenna and other members of S.J.S. and J.S.'s laboratories for helpful advice and assistance. This work was supported in part by the Damon Runyon Cancer Research Foundation (DRG-2224-15 to R.J.H.), a Congressionally Directed Medical Research Program (PC131820 to C.C.P.), and a Young Investigator Award from the Prostate Cancer Foundation (to C.C.P.).

AUTHOR CONTRIBUTIONS

R.J.H. and S.J.S. conceived the work and designed and performed the analyses; R.J.H., S.J.S., C.C.P., and J.S. interpreted results; and R.J.H. and S.J.S. wrote the paper with input from C.C.P. and J.S.

COMPETING FINANCIAL INTERESTS

The authors declare no competing financial interests.

1. de la Chapelle, A. & Hampel, H. Clinical relevance of microsatellite instability in colorectal cancer. *J. Clin. Oncol.* **28**, 3380–3387 (2010).
2. Murphy, K.M. *et al.* Comparison of the microsatellite instability analysis system and the Bethesda panel for the determination of microsatellite instability in colorectal cancers. *J. Mol. Diagn.* **8**, 305–311 (2006).
3. Vilar, E. & Gruber, S.B. Microsatellite instability in colorectal cancer—the stable evidence. *Nat. Rev. Clin. Oncol.* **7**, 153–162 (2010).
4. Oki, E., Oda, S., Maehara, Y. & Sugimachi, K. Mutated gene-specific phenotypes of dinucleotide repeat instability in human colorectal carcinoma cell lines deficient in DNA mismatch repair. *Oncogene* **18**, 2143–2147 (1999).
5. Boland, C.R. *et al.* A National Cancer Institute Workshop on Microsatellite Instability for cancer detection and familial predisposition: development of international criteria for the determination of microsatellite instability in colorectal cancer. *Cancer Res.* **58**, 5248–5257 (1998).
6. Pritchard, C.C. *et al.* Complex MSH2 and MSH6 mutations in hypermutated microsatellite unstable advanced prostate cancer. *Nat. Commun.* **5**, 4988 (2014).
7. Le, D.T. *et al.* PD-1 blockade in tumors with mismatch-repair deficiency. *N. Engl. J. Med.* **372**, 2509–2520 (2015).
8. Timmermann, B. *et al.* Somatic mutation profiles of MSI and MSS colorectal cancer identified by whole-exome next-generation sequencing and bioinformatics analysis. *PLoS One* **5**, e15661 (2010).
9. Woerner, S.M. *et al.* SelTarbase, a database of human mononucleotide-microsatellite mutations and their potential impact to tumorigenesis and immunology. *Nucleic Acids Res.* **38**, D682–D689 (2010).
10. Kim, T.M., Laird, P.W. & Park, P.J. The landscape of microsatellite instability in colorectal and endometrial cancer genomes. *Cell* **155**, 858–868 (2013).
11. Onda, M. *et al.* Microsatellite instability in thyroid cancer: hot spots, clinicopathological implications, and prognostic significance. *Clin. Cancer Res.* **7**, 3444–3449 (2001).
12. Forgacs, E. *et al.* Searching for microsatellite mutations in coding regions in lung, breast, ovarian and colorectal cancers. *Oncogene* **20**, 1005–1009 (2001).
13. Duval, A. *et al.* Target gene mutation profile differs between gastrointestinal and endometrial tumors with mismatch repair deficiency. *Cancer Res.* **62**, 1609–1612 (2002).
14. Mori, Y. *et al.* Instabilotyping reveals unique mutational spectra in microsatellite-unstable gastric cancers. *Cancer Res.* **62**, 3641–3645 (2002).
15. Sonay, T.B., Koletou, M. & Wagner, A. A survey of tandem repeat instabilities and associated gene expression changes in 35 colorectal cancers. *BMC Genomics* **16**, 702 (2015).
16. Yoon, K. *et al.* Comprehensive genome- and transcriptome-wide analyses of mutations associated with microsatellite instability in Korean gastric cancers. *Genome Res.* **23**, 1109–1117 (2013).
17. Bacher, J.W. *et al.* Development of a fluorescent multiplex assay for detection of MSI-high tumors. *Dis. Markers* **20**, 237–250 (2004).
18. Lu, Y., Soong, T.D. & Elemento, O. A novel approach for characterizing microsatellite instability in cancer cells. *PLoS One* **8**, e63056 (2013).
19. McIver, L.J., Fonville, N.C., Karunasena, E. & Garner, H.R. Microsatellite genotyping reveals a signature in breast cancer exomes. *Breast Cancer Res. Treat.* **145**, 791–798 (2014).
20. Niu, B. *et al.* MSIsensor: microsatellite instability detection using paired tumor-normal sequence data. *Bioinformatics* **30**, 1015–1016 (2014).
21. Salipante, S.J., Scroggins, S.M., Hampel, H.L., Turner, E.H. & Pritchard, C.C. Microsatellite instability detection by next generation sequencing. *Clin. Chem.* **60**, 1192–1199 (2014).
22. Huang, M.N. *et al.* MSIseq: software for assessing microsatellite instability from catalogs of somatic mutations. *Sci. Rep.* **5**, 13321 (2015).
23. Pawlik, T.M., Raut, C.P. & Rodriguez-Bigas, M.A. Colorectal carcinogenesis: MSI-H versus MSI-L. *Dis. Markers* **20**, 199–206 (2004).
24. Laiho, P. *et al.* Low-level microsatellite instability in most colorectal carcinomas. *Cancer Res.* **62**, 1166–1170 (2002).
25. Kim, M.S., An, C.H., Chung, Y.J., Yoo, N.J. & Lee, S.H. NIPBL, a cohesion loading factor, is somatically mutated in gastric and colorectal cancers with high microsatellite instability. *Dig. Dis. Sci.* **58**, 3376–3378 (2013).
26. Boland, C.R. & Goel, A. Microsatellite instability in colorectal cancer. *Gastroenterology* **138**, 2073–2087 (2010).
27. Supek, F. & Lehner, B. Differential DNA mismatch repair underlies mutation rate variation across the human genome. *Nature* **521**, 81–84 (2015).
28. Jung, B. *et al.* Loss of activin receptor type 2 protein expression in microsatellite unstable colon cancers. *Gastroenterology* **126**, 654–659 (2004).
29. Giannakis, M. *et al.* RNF43 is frequently mutated in colorectal and endometrial cancers. *Nat. Genet.* **46**, 1264–1266 (2014).
30. Futreal, P.A. *et al.* A census of human cancer genes. *Nat. Rev. Cancer* **4**, 177–183 (2004).
31. Samowitz, W.S. *et al.* Microsatellite instability in sporadic colon cancer is associated with an improved prognosis at the population level. *Cancer Epidemiol. Biomark. Prev.* **10**, 917–923 (2001).
32. Hampel, H. *et al.* Screening for Lynch syndrome (hereditary nonpolyposis colorectal cancer) among endometrial cancer patients. *Cancer Res.* **66**, 7810–7817 (2006).
33. Goel, A., Nagasaka, T., Hamelin, R. & Boland, C.R. An optimized pentaplex PCR for detecting DNA mismatch repair–deficient colorectal cancers. *PLoS One* **5**, e9393 (2010).
34. Altavilla, G., Fassan, M., Busatto, G., Orsolan, M. & Giacomelli, L. Microsatellite instability and hMLH1 and hMSH2 expression in renal tumors. *Oncol. Rep.* **24**, 927–932 (2010).
35. Martinez, R. *et al.* Low-level microsatellite instability phenotype in sporadic glioblastoma multiforme. *J. Cancer Res. Clin. Oncol.* **131**, 87–93 (2005).
36. Jensen, K.C. *et al.* Microsatellite instability and mismatch repair protein defects in ovarian epithelial neoplasms in patients 50 years of age and younger. *Am. J. Surg. Pathol.* **32**, 1029–1037 (2008).
37. Kazachkov, Y. *et al.* Microsatellite instability in human hepatocellular carcinoma: relationship to p53 abnormalities. *Liver* **18**, 156–161 (1998).
38. Dacic, S., Lomago, D., Hunt, J.L., Sepulveda, A. & Yousem, S.A. Microsatellite instability is uncommon in lymphoepithelioma-like carcinoma of the lung. *Am. J. Clin. Pathol.* **127**, 282–286 (2007).
39. Field, J.K. *et al.* Microsatellite instability in squamous cell carcinoma of the head and neck. *Br. J. Cancer* **71**, 1065–1069 (1995).
40. Eckert, A. *et al.* Microsatellite instability in pediatric and adult high-grade gliomas. *Brain Pathol.* **17**, 146–150 (2007).
41. Amira, N. *et al.* Microsatellite instability in urothelial carcinoma of the upper urinary tract. *J. Urol.* **170**, 1151–1154 (2003).
42. Dorard, C. *et al.* Expression of a mutant HSP110 sensitizes colorectal cancer cells to chemotherapy and improves disease prognosis. *Nat. Med.* **17**, 1283–1289 (2011).
43. Shin, N. *et al.* Identification of frequently mutated genes with relevance to nonsense-mediated mRNA decay in the high microsatellite instability cancers. *Int. J. Cancer* **128**, 2872–2880 (2011).
44. Shah, S.N., Hile, S.E. & Eckert, K.A. Defective mismatch repair, microsatellite mutation bias, and variability in clinical cancer phenotypes. *Cancer Res.* **70**, 431–435 (2010).
45. Woerner, S.M. *et al.* Pathogenesis of DNA repair-deficient cancers: a statistical meta-analysis of putative Real Common Target genes. *Oncogene* **22**, 2226–2235 (2003).
46. Duval, A. *et al.* Evolution of instability at coding and non-coding repeat sequences in human MSI-H colorectal cancers. *Hum. Mol. Genet.* **10**, 513–518 (2001).
47. Imai, K. & Yamamoto, H. Carcinogenesis and microsatellite instability: the interrelationship between genetics and epigenetics. *Carcinogenesis* **29**, 673–680 (2008).
48. Lawrence, M.S. *et al.* Discovery and saturation analysis of cancer genes across 21 tumor types. *Nature* **505**, 495–501 (2014).
49. Eckert, K.A. & Hile, S.E. Every microsatellite is different: Intrinsic DNA features dictate mutagenesis of common microsatellites present in the human genome. *Mol. Carcinog.* **48**, 379–388 (2009).
50. Mlecnik, B. *et al.* Integrative analyses of colorectal cancer show immunoscore is a stronger predictor of patient survival than microsatellite instability. *Immunity* **44**, 698–711 (2016).

ONLINE METHODS

Exome microsatellite data. Exome data for all specimens (tumors and patient-matched normal blood) were obtained from the TCGA Research Network (http://cancergenome.nih.gov/; **Supplementary Table 5**) as alignments against hg19. Researchers were not blinded to the MSI status of specimens where those data were available. We identified all autosomal microsatellite tracts with repeating subunits of 1–5 bp in length and comprising 5 repeats or more in the human reference genome (GRCh37/hg19) using MISA (http://pgrc.ipk-gatersleben.de/misa/misa.html) and padded their start and stop coordinates by 5 bp. 10 bp or fewer were permitted between repeats for adjacent microsatellites to be combined into single loci, termed either 'complex' (c*) if comprised of microsatellites with different repeat subunit lengths or 'compound' (c) if comprised of disparate repeats with the same repeat length. Microsatellites directly tiled by the NimbleGen SeqCap_EZ_Exome_v3 capture design (which was used by TCGA) and those within 50 bp of a capture bait were retained. Repeat features were annotated using ANNOVAR[51] (24 February 2014 release).

Calling unstable microsatellite loci. Primary analysis of microsatellite loci was performed in each specimen to determine stability using mSINGS as previously described[21]. Briefly, we evaluated the number of sequence reads of different lengths present within each of the identified microsatellite markers, then expressed the relative abundance of individual lengths for a microsatellite as the fraction of reads supporting that length normalized to the number of reads counted for the most frequently occurring length at that locus. Microsatellite tract lengths at <5% relative abundance were discarded. Although identified length polymorphisms may include some reproducible artifacts resulting from slippage during PCR amplification, their total number is proportional to the actual number of microsatellite alleles present at a locus[21], and in comparative analysis of genetically related tumor–normal pairs such artifacts are well controlled. Instability at each locus was subsequently defined in two ways: (i) the high-sensitivity approach, in which identification was performed by comparing the absolute number of lengths identified between tumor and paired normal specimens, and the locus was considered unstable if one or more additional lengths for a microsatellite were detected from the tumor; and (ii) the high-specificity approach, in which Kolmogorov–Smirnov scores were calculated when comparing the normalized distribution of lengths for tumor and paired normal specimens, considering any difference less than $P = 0.05$ to signify locus instability[10]. We determined the latter method to be overly conservative (a median of only 5 unstable sites were called per MSI-H cancer), and therefore did not implement it in practice. Accordingly, the burden of unstable sites identified in our study was considerably higher than approximated in other work[10], probably because of the greater sensitivity-to-specificity tradeoff of our approach.

Constructing MOSAIC from sequencing-based locus instability calls. We examined data from colon, rectal, stomach, and endometrial cancer exomes (**Supplementary Tables 4** and **5**) for which clinical MSI status was available from standard diagnostic methods[17]. We observed that the average size of instability events (i.e., the length of alternate microsatellite alleles) was greater in MSI-H than MSS tumors (**Fig. 1d**,**e**; $P = 9 \times 10^{-80}$, two-sided Wilcoxon rank-sum test). Clinical MSI–PCR results (MSI-H, MSI-L, and MSS) were obtained from TCGA. The average gain in unique alleles in tumor relative to matched normal tissue across all interrogated microsatellites (peak_avg), variation in allele gain (peak_var), total number of unstable sites defined by the high-sensitivity method (num_unstable), and proportion of callable unstable sites (prop_unstable) were calculated for each sample. Furthermore, we tested for the power of each microsatellite locus to differentiate between MSI-H and MSS tumors using Fisher's exact tests and identified a locus within *DEFB105A/B*, chr. 8:7679723–7679741, as the most significantly unstable microsatellite in MSI-H relative to MSS tumors (defbsite). These features, along with the top 100 most significantly unstable microsatellites in MSI-H relative to MSS tumors, were then used to predict clinical MSI-H or MSS diagnosis by recursive partitioning classification trees or random forests implemented using the rpart v4.1-10, randomForest v4.6-12, and caret v6.0.62 packages in R v3.2.1. Leave-one-sample-out cross-validation was used to learn the optimal features and parameters for predicting MSI status, interrogating a grid search space of 0, 0.001, 0.01, 0.1, 0.45, and 0.95 complexity parameters (cp) with the minimum number of observations in any terminal node (minbucket) set to 6 and the maximum depth of any node of the final tree set to 3 for recursive partitioning, and 2 and 3 randomly sampled variables as candidates at each split (mtry) with 1,000 trees for random forests. Weights were included to correct for class imbalances in the training data (MSI-H $n = 171$, MSS $n = 446$), and the optimal parameters selected were cp = 0.001 and mtry = 2. Notably, peak_avg and debsite were selected by recursive feature selection using decision trees as the most significant two features for inclusion in the final model; incorporating more than two covariates did not significantly improve the classifier (**Supplementary Fig. 3b**). The final models achieved 96.6% (rpart) and 96.4% (randomForest) accuracy. The more accurate and parsimonious rpart model was used to predict MSI status across all remaining cancer samples.

Identifying uniquely unstable microsatellites in MSI-H cancers. For each of the 204,797 microsatellite loci called in at least half of MSI-H and MSS cancers ($n > 132$ and $n > 2{,}833$, respectively), we performed two-sided Fisher exact tests comparing the ratios of individuals for which the site was unstable in MSI-H samples to the ratio of individuals for which the site was unstable in MSS samples. FDR values were estimated using Storey's q-value method, with a q-value < 0.05 considered significant.

Determining cancer-specific microsatellite sites. Multiple proportions tests were implemented in R using the prop.test function to identify sites differentially unstable in at least one cancer type relative to the average frequency of instability observed across all other groups from the 92,385 sites called in at least half of the samples for each cancer. To determine MSI-H cancer-specific microsatellites, multiple proportions tests were performed for each site for colon, rectal, endometrial, and stomach MSI-H cancers. FDR values were estimated as described above. To compare across cancers and MSI diagnostic types, we computed cosine similarity scores. Because the number of frequently unstable sets in MSI-H cancers was an order of magnitude larger than that observed for MSS cancers, cosine similarity was less sensitive to these set inequalities than the overlap coefficient or Jaccard index, which artificially inflate or deflate the observed overlap, respectively.

Gene Ontology enrichment analyses. Gene enrichment was performed using the R package clusterProfiler version 2.2.5 (ref. 52). clusterProfiler implements a hypergeometric model to test for gene set overrepresentation relative to a background gene set. Each cluster (1–4) from the global instability results was compared with the background of all other microsatellites sequenced at sufficient depth in our study, with a Benjamini–Hochberg FDR threshold of 0.20 defined as significant enrichment. Enrichment in KEGG pathways was analyzed with the enrichKEGG function and the same parameters. Enrichment between MSI-H specific clusters was analyzed using the compareCluster function with fun = enrichGO, pvalueCutoff = 0.05, OrgDb = org.Hs.eg.db. Significantly enriched GO terms were simplified using GOSemSim to calculate the similarity of GO terms and remove highly similar terms (cutoff = 0.7) by retaining the most significant representative term. GO analyses were corrected for gene size in that enrichment analyses were performed at the microsatellite level, such that larger genes required greater numbers of unstable sites for significant enrichment relative to the background distributions of microsatellites in genes covered in our study.

Enrichment of unstable microsatellites in cancer-associated genes. After excluding microsatellites with intergenic and intronic annotations, we extracted annotations for the 252,127 microsatellites that had valid calls in MSS samples, resulting in a panel of 18,104 unique genes. We compared this full gene panel against the 17,564 loci that were unstable with significantly greater frequency in MSI-H cancers at an FDR < 0.05, comprising a set of 6,821 unique genes. We compared these data sets to the COSMIC cancer gene census (accessed 15 June 2015), which contained 573 unique cancer-associated genes. To test for enrichment against the COSMIC database, 1,000 permutations were performed, sampling 6,821 genes from all possible unique genes in the full gene panel.

Correlation of instability and DNA replication timing. We first filtered our data to 77,215 sites that were called in more than half of the samples within each

doi:10.1038/nm.4191

of the 32 (cancer type by MSI status) groups and called completely across all groups. We downloaded wavelet-smoothed Repli-Seq signals from 11 ENCODE cell lines from the UCSC Genome Browser (GEO GSE34399). We then averaged the proportions of MSI and Repli-Seq signals across 1-Mb windows throughout the genome and calculated the median Repli-Seq signal across all 11 cell lines as representative of 'general' replication timing throughout the genome, with values ranging 0–100 (higher numbers indicating earlier replication). Spearman correlation coefficients were calculated between binned, averaged instability proportions between MSI classifications and across cancer types compared with median and cell-line-specific binned Repli-Seq signals.

Survival analyses. We assessed the association of MSI with overall survival using the coxph function from the R survival package version 2.38, with significance assessed by Wald tests. Age, sex, cancer type, radiation therapy, and pathologic stage (I, II, III, IV) were included as covariates in multivariate analyses. The proportional hazards assumption for covariates in these Cox regression models was tested using the cox.zph function and violating covariates were stratified when necessary.

Statistical analyses. All statistical tests used in this study were nonparametric and therefore made no assumptions about distributions or equal variance between groups. Two-sided Fisher exact tests were used to identify differentially unstable microsatellites in MSI-H cancers and enriched or depleted genomic annotations for unstable sites. To determine unstable microsatellites unique to specific MSI-H cancers, multiple proportions tests were performed for each site across colon, rectal, endometrial, and stomach MSI-H cancers. FDR values for both analyses were estimated using Storey's q-value method, with a q-value < 0.05 considered significant. To compare instability events across cancers and MSI diagnostic types, we computed cosine similarity scores. Hypergeometric tests were implemented to test for the enrichment of genes harboring frequently unstable sites in GO terms and KEGG pathways. Permutation tests were performed to test for enrichment in MSI-affected genes against the COSMIC database. Spearman correlation coefficients were calculated to evaluate correlations between instability and DNA replication timing. Lastly, survival curves were represented with Kaplan-Meier curves, with the significance of covariate effects estimated by fitting Cox proportional-hazards regression models.

Data access. Primary sequencing data are available from TCGA Research Network (http://cancergenome.nih.gov/). Primary MSI calls from this study are available from (http://krishna.gs.washington.edu/content/members/hauser/mosaic/).

Code availability. Code for primary analysis of microsatellite loci through mSINGS (git commit e32b776) is available at https://bitbucket.org/uwlabmed/msings. Code for secondary analyses and MOSAIC are available at https://github.com/ronaldhause/mosaic.

51. Wang, K., Li, M. & Hakonarson, H. ANNOVAR: functional annotation of genetic variants from high-throughput sequencing data. *Nucleic Acids Res.* **38**, e164 (2010).
52. Yu, G., Wang, L.-G., Han, Y. & He, Q.-Y. clusterProfiler: an R package for comparing biological themes among gene clusters. *OMICS* **16**, 284–287 (2012).